Inter-Subject Variability Of The Healthy Tibiofemoral Function

By

Francesca Bucci

B.Eng. (Biomedical), M.Eng. (Biomechanical)

Supervisors: Assoc. Prof. Saulo Martelli

Prof. Mark Taylor

Dr. Rami Al-Dirini

Thesis Submitted to Flinders University

for the degree of

Doctor of Philosophy

College of Science and Engineering

16th August 2023

Keywords

(1) Tibiofemoral Function Variability; (2) Unloaded Knee Passive Motion Envelope; (3) Influence of Sex; (4) Knee Compliance Matrices; (5) Computationally Efficient Musculoskeletal Modelling; (6) Passive And Active Ligaments Role.

Abstract

Knee joint diseases, especially osteoarthritis, along with ligament injuries, constitute a major global health burden. Women are more affected than men, with a two- to three-fold risk of experiencing ligament injuries and developing knee osteoarthritis than their male counterparts. Ideally, clinical evaluation tools should be able to diagnose knee ligament injuries and pathologies, and surgical procedures to fully restore the individual joint function. However, there is a lack of baseline information concerning tibiofemoral joint function and ligament mechanics across populations affecting these outcomes. Thus, the **overall objective of this thesis** was to advance the understanding of the healthy tibiofemoral joint function and its inter-subject variability. By interacting with articular surfaces and muscles, ligaments determine tibiofemoral joint function, and yet their role remains not entirely clear; therefore, this thesis hypothesized that (1) ligaments do not significantly influence tibiofemoral paths within the passive knee motion envelope, (2) when recruited they act as constraints defining envelope boundaries, and (3) outside, their individual stiffness and combined action provide an elastic response.

A combination of novel ex vivo and in silico methodologies was developed, and population studies were undertaken to achieve this thesis aim and test the hypothesis. As approaches to quantifying tibiofemoral passive motion ex vivo examine either a singular coupled flexion path or the envelope of knee passive motion, mostly in male populations or small samples, the variability across populations, the influence of sex and the role of ligaments in knee passive motion remain unclear. Therefore, the **first study** of this thesis aimed at developing a novel ex vivo experimental assessment to quantify the envelope of knee passive motion. Analysis and quantification of the errors of this novel methodology were performed. For the first time, the medial and lateral extremes of the unloaded knee passive motion envelope were quantified in healthy intact knees, along their six coupled degrees-of-freedom paths. The **second study** of this thesis quantified the variability across a healthy adult population and sex-based differences of the unloaded envelope of knee passive motion between males and females. Medial and lateral passive motion extremes were analysed in thirty intact knee specimens. Furthermore, as currently anatomically detailed tibiofemoral models, which enable the study of active ligament contributions during normal exercise, are computationally expensive and time-consuming, the investigation of the variability of tibiofemoral elastic responses across populations is limited. Hence, in the **third study** of this thesis, a time-efficient elastic-joint musculoskeletal model was developed to provide a tool for the investigation of individual tibiofemoral elastic response, through compliance matrices.

Findings of this thesis included the medial and lateral extremes differing significantly from one another, i.e., unloaded knee passive motion envelope extent in internal-external rotation was 18° up to 29°. The significant differences between the medial and lateral extremes of knee passive

motion, combined with the substantial variations in central motion patterns reported within the knee passive motion envelope across individuals and methodologies, suggest that the observed inter-individual variability in knee joint motion may be influenced by specific captured paths and methodological inconsistencies. Therefore, standardized procedures should be developed for measuring and reporting knee passive motion across laboratories to help mitigate these sources of variability and provide more consistent and comparable results. Furthermore, this thesis suggests that a compliance matrix-based musculoskeletal-modelling approach, providing a faster computation of individual active tibiofemoral function with fewer input data, would enable the investigation of the variability of knee elasticity across populations. This could provide insight into ligament active contribution and facilitates the translation of these models into clinical applications.

Although further research is needed, according to this thesis **hypothesis** (1) ligaments do not appear to play a role in guiding the tibiofemoral joint, as they do not bind the joint to a specific coupled path, based on experimental evidence that multiple tibiofemoral paths can be captured within this envelope; (2) ligaments act as constraints on the boundary of the envelope, guiding the tibiofemoral joint along consistent and reliable medial and lateral extremes of the unloaded passive motion envelope; (3) there were only small differences between the motion patterns obtained from a gait simulation using a musculoskeletal tibiofemoral rigid model based on the experimental unloaded knee envelope (study 2) and the active tibiofemoral motion measured from an in vivo biplanar fluoroscopy study in the literature, thereby suggesting that passive soft tissues, including ligaments, provide a minor contribution towards joint elasticity, while muscles play a more dominant role.

Clinically relevant outcomes of this thesis include measurements of tibiofemoral motion variability within a healthy population and quantification of tibiofemoral motion sex-based differences between males and females. Results displayed a moderately sex-specific influence on tibiofemoral passive motion, with females reporting higher abduction in the medial extreme. However, as individual variability was higher than sex-specific variations, this thesis suggests that knee interventions should focus on personalized, rather than sex-specific solutions.

These results have led to **more research**; in particular (1) a study of the relationship between geometry and function and the influence of sex through partial least regression modelling was conducted and (2) an experimental study was performed to investigate the restoration of the individual tibiofemoral function before and after total knee replacement. Finally, this thesis has also prompted further research on (1) validating kinematic models and (2) applying these approaches and models in studying the effect of tibial osteotomy.

Table of Contents

Publications

Journal articles prepared for publication or currently under review included in this thesis and conference presentations.

Peer-Reviewed Journals Articles

Journal Articles are herein presented in order of appearance in the thesis.

1. **F. Bucci**, M. Taylor, R. Al-Dirini, S. Martelli (2023) – Comparison of the envelope of knee passive motion in males and females. Journal of Orthopaedic Research. *In preparation for submission to peer-reviewed journal.*
2. **F. Bucci**, M. Taylor, R. Al-Dirini, S. Martelli (2023) – A novel methodology to capture the envelope of knee passive motion. Technical Note. Journal of Orthopaedic Research. *In preparation for submission to peer-reviewed journal.*
3. **F. Bucci**, M. Taylor, R. Al-Dirini, S. Martelli (2023) – Elastic musculoskeletal joint model as efficient representation of the knee joint laxity. Journal of Biomechanics. Journal Article. *In preparation for submission to peer-reviewed journal.*
4. **F. Bucci**, M. Taylor, R. Al-Dirini, S. Martelli (2023) – Mapping review on in silico knee and tibiofemoral joint modelling: a cost - complexity - utility perspective. The knee. Journal Article. *In preparation for submission to peer-reviewed journal.*
5. D. O'Rourke, **F. Bucci**, M. Taylor, R. Al-Dirini, S. Martelli (2023) – Determining the relationship between tibiofemoral geometry and passive motion with partial least squares regression. Journal of Orthopaedic Research. Journal Article. https://doi.org/10.1002/jor.25526. *Manuscript Published.*
6. M. Howes, M. Bajger, G. Lee, **F. Bucci**, S. Martelli (2021) – Texture enhanced Statistical Region Merging with application to automatic knee bones segmentation from CT. In 2021 Digital Image Computing: Techniques and Applications (DICTA) (pp. 01-08). IEEE. https://doi.org/10.1109/DICTA52665.2021.9647224. *Manuscript Published.*

National And International Conference Presentations

Almost all conferences during my second year of my PhD were cancelled due to the Covid-19 pandemic. Therefore, I only participated in online conferences I was able to remotely attend during my third year. Conference attended are herein presented in chronologic order.

1. **F. Bucci**, M. Taylor, R. Al-Dirini, S. Martelli (2021) – Gender Differences Of Passive Knee Kinematics. In Proceedings of the 26th Congress of the European Society of Biomechanics (ESB). Annual Congress of the European Society of Biomechanics. Online Conference. Jul 2021. *Podium Presentation.*

2. **F. Bucci**, M. Taylor, R. Al-Dirini, S. Martelli (2021) – Does Sex Influence The Knee Passive Kinematics? In Proceedings of the 26th Congress of the Australian & New Zealand Orthopaedic Research Society (ANZORS). Annual Congress of the Australian & New Zealand Orthopaedic Research Society. Online Conference. Oct 2021. *Podium Presentation*.

3. **F. Bucci**, M. Taylor, R. Al-Dirini, S. Martelli (2021) – Differences Of Passive Knee Kinematics Between Males And Females. In Proceedings of the 12th Congress of the Australian & New Zealand Society Of Biomechanics (ABC12). Annual Congress of the Australian & New Zealand Society Of Biomechanics. Online Conference. Dec 2021. *Podium Presentation*.

4. **F. Bucci**, M. Taylor, R. Al-Dirini, S. Martelli (2022) – Does passive knee motion differ between sexes? An ex vivo investigation on healthy adults. In Proceedings of the Annual Meeting of the Orthopaedic Research Society (ORS). Annual Meeting of the Orthopaedic Research Society. Hybrid Online and In Person, Tampa Florida USA. Feb 2021. *Poster Presentation*.

5. D. O'Rourke, **F. Bucci**, W. Burton, R. Al-Dirini, M. Taylor, S. Martelli (2022) – Characterising The Relationship Between Knee Bone Geometry And Passive Kinematics. In Proceedings of the 27th Congress of the European Society of Biomechanics (ESB). Annual Congress of the European Society of Biomechanics. Online Conference. June 2022. *Poster Presentation.*

6. **F. Bucci**, M. Taylor, R. Al-Dirini, S. Martelli (2022) – An Innovative Approach To Investigate The Tibiofemoral Elasticity During Gait With 3D Compliance Matrices. In Proceedings of the 27th Congress of the European Society of Biomechanics (ESB). Annual Congress of the European Society of Biomechanics. Online Conference. June 2022. *Poster Presentation.*

7. **F. Bucci**, M. Taylor, R. Al-Dirini, S. Martelli (2022) – In vivo 3d Tibiofemoral Compliance Matrices: An Innovative Musculoskeletal Approach To Investigate The Knee Joint Elasticity During Gait. In Proceedings of the 9th World Congress Of Biomechanics (WCB9). Quadrennial Congress of the World Society Of Biomechanics. Hybrid Online – In Person Conference, Taipei Taiwan. July 2022. *Podium Presentation.*

8. **F. Bucci**, M. Taylor, R. Al-Dirini, S. Martelli (2022) – Knee Passive Motion Differences Between Sexes: An Ex vivo Investigation On Healthy Adults. In Proceedings of the 9th World Congress Of Biomechanics (WCB9). Quadrennial Congress of the World Society Of Biomechanics. Hybrid Online – In Person Conference, Taipei Taiwan. July 2022. *Poster Presentation.*

Honours And Awards

Honours and awards are herein presented in chronologic order.

1. Privately Funded Scholarship 'Australian Research Council', AUD 27084 per annum for 3.5 years.

2. Fee Waiver Scholarship PhD Flinders University for the duration of the PhD.
3. Semi-Finalist – 3 Minute Thesis Competition at Flinders University June 2019.
4. "Bake Your PhD" Judges and People's Choice Runner Up, Higher Degree Research Conference, Flinders University, Adelaide, South Australia, 2019, AUD100.
5. Travel Grant, Australian and New Zealand Orthopaedic Research Society 25th Annual Conference, Canberra, Australia, 2019, AUD250.
6. Co-investigator Zimmer Biomed Project – A cadaveric investigation of knee stability after TKR: Preliminary work to establish a radiographic method to investigate TKR stability in vivo using RSA and the preliminary investigation into the development of the concept of an intrinsically stable total knee replacement (ongoing project – 2021).
7. Conference Grant, 9th World Congress Of Biomechanics (WCB), Hybrid Online – In Person Conference, Taipei Taiwan. July 2022. AUD300.

List of Figures

List of Tables

List of Abbreviations

TF – Tibiofemoral

TFi – Tibiofibular

PF – Patellofemoral

DoF – Degree of Freedom

PROM – Passive Range of Motion

OA – Osteoarthritis

TKA/TKR – Total Knee Arthroplasty/Replacement

FEM – Finite Element Method

MSK – Musculoskeletal

CT – Computed Tomography

MRI – Magnetic Resonance Imaging

ACL – Anterior Cruciate Ligament

PCL – Posterior Cruciate Ligament

LCL – Lateral Collateral Ligament

MCL – Medial Collateral Ligament

FE – Flexion Extension

AA – Abduction Adduction

IE – Internal External

AP – Antero Posterior

IS – Infero Superior

ML – Medio Lateral

CM – Compliance Matrix

Glossary Of Terms

Knee joint function

Knee joint function encompasses both passive and active kinematics, kinetics, loading, and activities. Passive kinematics refers to the range of motion achievable by the knee joint without muscle activation. Active kinematics involves the movement produced by muscle contractions. Kinetics refers to the forces acting on the knee joint during movement. Loading refers to the distribution and magnitude of forces applied to the knee joint. Activities encompass various movements and tasks performed by individuals, such as walking, running, jumping, and climbing stairs.

Mobility

Mobility refers to the capacity of a joint or body segment, such as the knee joint, to move freely and achieve a desired range of motion. In the specific context of tibiofemoral motion, mobility is crucial for various functional activities, including walking, running, squatting, and climbing stairs. It enables dynamic stability, efficient force transmission, and shock absorption within the lower extremity, facilitating smooth and coordinated movement patterns.

Envelope of knee passive motion

The envelope of knee passive motion, as described by Blankevoort et al. (1988), represents the range of motion achievable by the knee joint without any active muscle contraction. It defines the maximum flexion, extension, and rotational capacities of the knee joint when external forces are applied.

Knee joint elasticity

Knee joint elasticity refers to the linear behaviour of the knee joint in response to external forces. It describes the ability of the joint to deform under loading and then return to its original shape when the load is removed. The linear behaviour implies that the magnitude of the deformation is directly proportional to the magnitude of the applied force, allowing the joint to absorb and distribute forces effectively during movement. This property of knee joint elasticity plays a crucial role in providing stability, shock absorption, and maintaining the overall integrity of the joint.

Declaration

I certify that this thesis does not incorporate without acknowledgment any material previously submitted for the award of a degree or diploma in any university or other tertiary institution; and that to the best of my knowledge and belief it does not contain any material previously published or written by another person except where due reference is made in the text.

Francesca Bucci

December 10th, 2022

Statement Of Ethical Conduct

Ethical approval for research undertaken in this thesis was obtained from the Flinders University Institutional Research Ethics Committee (Reference Number - SBREC 6832).

Acknowledgements

My master thesis project brought me to Australia for the first time at the end of 2017, a beautiful adventure that has changed my life and that I would have never expected would lead to this moment, writing my PhD thesis. This note is dedicated to everyone that helped me grow into the person and researcher I am today, as I reflect on the support and guidance, I received during my time at Flinders University's Medical Device Research Institute.

I would like to express my gratitude to my supervisor Associate Professor Saulo Martelli who offered me this amazing opportunity and guided me throughout this project. This endeavour would not have been possible without Professor Mark Taylor and Doctor Rami Al-Dirini, whose expertise and guidance I greatly appreciate. I would like to acknowledge the financial support provided by Australia Research Council (DP180103146). To the Medical Device Research Institute, thank you for all the support you have provided.
Words cannot express my gratitude to Associate Professor Egon Perilli, you have been my mentor and friend, a reference point in my toughest moments, conveying to me your passion for research, supporting me and encouraging me.

I would like to thank my amazing family, especially my mum Ilaria, my dad Jurgen, my brother Simone and my nonni Ebe, Anna e Berto for their immense love and support. You have always supported my dreams even when they led me far away from home. To my cuginetti Gaia e Thiago, with the hope to inspire them to always dream big and follow their hearts. This achievement belongs not only to me, but to you all.

I would like to thank all my friends. I am forever grateful for your unconditional support and encouragement. To all my friends here in Adelaide that helped me to go through all this, you have been the biggest support system. To all my fellow PhD candidates and colleagues, old and new ones, especially the ones who I can proudly call friends, there would be so much to say and to thank you for, it would have been so difficult without you, particularly to Maged, Robbie, Laura, Dhara, Marco, Sophie, Michael, and Dani. To my Italian friends in Australia, for the escapes, for the laughter and for your support Benedetta, Edoardo, Luigi and Diego. And to my friends in Italy (e non), Baby, Matte, Alessandra, Margherita, Nicole, Sara, Andrea, Martina, Lollo, even from far away I feel you are always right next to me.

Finally, to my partner Gianraffaele, for the love, for the encouragement, for the nights without sleep, the coffees, the sushis and the chocolate, for supporting me endlessly and for having made of Adelaide my home, your friends my friends, and your family my family. I feel blessed every single day to have you all in my life.

Chapter 1

INTRODUCTION

CONTENTS

1.1 Background And Motivation

Knee ligament injuries affect knee laxity and cause joint instability, leading to chronic pain, diminished function, and osteoarthritis (Fleming et al., 2005). Young Australians reported the highest anterior cruciate ligament injury rate in the world (Zbrojkiewicz et al., 2018), with a related osteoarthritis incidence increase in one in every six Australians of older age (Australian Institute of Health and Welfare-Canberra, 2020); among women, the risk is even greater (Webster et al., 2021). Australia spends every year approximately $A142 million on ligament reconstructions (Zbrojkiewicz et al., 2018) and $A24.9 billion on knee arthroplasty (Australian Institute of Health and Welfare-Canberra, 2020) aiming at restoring knee joint mobility and stability while alleviating pain. Despite the high success rates of ligament reconstructions and total knee replacement, revisions are on the rise (Leathers et al., 2015). Patients show satisfaction with ligament surgeries, with rates varying between 75% and 96% (Christiani et al., 2019), while approximately 20% of patients are unsatisfied with the outcome of replacement (Robertsson et al., 2000). Ideally, clinical evaluation tools and procedures should diagnose ligament injuries and fully restore knee function. However, studies quantifying the variability of healthy tibiofemoral joint and ligament mechanics among individuals are scarce (Noble et al., 2005; Ithurburn et al., 2019; Söderman et al., 2021) leaving the inter-subject variability of healthy tibiofemoral function not fully understood.

Diagnostic and surgical tools for treating and researching the complex individual knee function rely on the assessment of knee passive motion (Goodfellow et al., 2002; Ghosh et al., 2014; Martelli et al., 2020). For instance, comprehensive evaluations of passive motion are critical for successful total knee replacement surgeries, to achieve an evenly balanced medial-lateral gap (Bottros et al., 2006). Nevertheless, despite the crucial role of understanding individual variations in knee passive motion for personalized treatments, complication reduction, and optimized clinical outcomes, limited literature exists on quantifying such variations across populations. A variety of approaches have been used to measure knee passive motion. Clinical knee laxity tests to assess the range of passive motion in vivo provide variable accuracy and reliability (Markolf et al., 1978; Athwal et al., 2014) based on clinician experience/ability to 'feel' the resistance provided by soft tissues for manual tests (Cannon et al., 2002), or arthrometers for instrumented tests (Anderson et al., 1992; Pugh et al., 2009). More accurate ex vivo cadaveric experiments were performed using ad hoc testing rigs and robotic simulators, besides surgical navigation systems, motion capture, medical imaging, and other in vivo techniques (Athwal et al., 2014; Martelli et al, 2007; Belvedere et al., 2011; Cyr and Maletsky 2014; Roth et al., 2015); yet errors and uncertainties associated with these measurement approaches were quantified only in a few studies. Furthermore, studies in literature were often limited in sample size (Blankevoort et al., 1988; Wilson et al., 2000; Eagar et al., 2001; Victor et al., 2010; Nowakowski et al., 2012; Torzilli et al., 1994), focused on a single sex (Cyr and Maletsky 2014; Victor et al., 2010; Torzilli et al., 1994), on

selected axes of motion (Walker et al., 1988; Blankevoort et al., 1988; Wunshel et al., 2012) and restricted knee flexion ranges (Blankevoort et al., 1988; Wilson et al., 2000; Torzilli et al., 1994). A few studies have provided information on the variability of a nominal central path of passive flexion within the envelope across a healthy cohort (Victor et al., 2010; Wunshel et al., 2012; Belvedere et al., 2011), a single study investigated the variability of knee laxity in males only (Cyr and Maletsky 2014). As reported in the literature, these are the two main protocols utilized to assess knee passive motion. On one hand, laxity studies support the notion that tibial relative position to femurs can only be specified within an envelope of possible positions, not accounting for the coupling between degrees of freedom (Cyr and Maletsky 2014; Roth et al., 2015). Conversely, studies measuring the coupling in a single nominal representative path within the envelope (Belvedere et al., 2011; Victor et al., 2010; Wilson et al., 2000), showed high sensitivity to small variations in experimental setup (Wilson et al., 2000). As of yet, no consensus has been reached on which approach is most appropriate and/or accurate for investigating knee passive motion. Further, as part of total knee replacement to achieve gap balancing, associated with surgical navigation characteristic parallel tracking, stressed flexion-extension tests are performed by applying lateral and medial forces to the distal tibia (Sheth et al., 2017); as of now, these tests have not been considered or included in currently available protocols. Finally, to date, no methodology has captured multiple passive-coupled paths, nor knee passive motion coupling and envelope simultaneously.

Restoration of native tibiofemoral joint function and range of motion requires re-establishing the relationships between all underlying anatomical structures, identifying their individual and concomitant contributions and additional contributing factors (Shrive et al., 1978). A few studies explored linear relationships between the variability of both tibiofemoral anatomy, kinematic and kinetic of a singular task (Smoger et al., 2015; Fitzpatrick et al., 2011; Clouthier et al., 2019). Smoger et al. (2015) investigated a male population only, simulating squatting movements through ex vivo cadaveric testing (Smoger et al., 2015); Clouthier et al. (2019) analysed how simulated variations of bone and cartilage geometry, generated by in silico statistical modelling, affected walking (Clouthier et al., 2019). Some studies related knee kinematic variations, during passive and active motion, to specific knee bone morphological features (Lansdown et al., 2017; Martelli and Pinskerova, 2002; Parenti-Castelli et al., 2004a; Smoger et al., 2015), some others to ligament laxity (Barink et al., 2005; Myers et al., 2012) or again to sex (Bredbenner et al., 2010). For instance, tibial slope, affecting knee kinematics and ligament mechanics, was found higher in females (Shelburne et al., 2011). Literature studies, however, reveal contrasting results, some confirming (Gillespie et al., 2011) and some disproving (Asseln et al., 2018) the existence of sex-based knee anatomical differences. The results of in vivo investigations of sex-based differences in tibiofemoral joint mechanics varied considerably, some showing no differences (Tanikawa et al., 2013) and others showing statistically significant differences varying from study to study (Cronström et al., 2016).

The influence of sex on knee passive motion is still unclear as more accurate ex vivo studies of knee passive motion available only include male cohorts or have limited sample sizes.

Increasingly, experimental in vivo and ex vivo techniques have been combined and integrated with in silico modelling to overcome technical limitations and ethical issues inherent to tibiofemoral joint research. This trend is evidenced by the growing use of in silico musculoskeletal modelling, which combines data from in vivo gait analyses with joint models derived from passive motion studies and tissue materials, and mechanical properties from cadaveric tests. By estimating joint articular forces otherwise unmeasurable without compromising joint integrity, musculoskeletal models provide the means for investigating the effects of combined variation in articular surface geometry and ligaments on individual active tibiofemoral joint function. A wide body of research is dedicated to ligament representations, ranging from rigid to linear and non-linear spring bundles and geometry-based representations as their fidelity heavily impact joint predictions, leading to inconsistent report (Kiapour et al., 2014; Lenhart et al., 2015; Erdemir et al., 2019). Time and costs drastically grow with the level of fidelity and detail included, as well as computational time required to obtain the solution once the model is in use. Navacchia (Navacchia et al., 2019) presented a TF contact model with ligament elastic bundles solved with a computationally efficient approach and reported 60 hours of computational time on 13 cores for each subject, just to solve iteratively a muscle-driven simulation of activity using explicit finite element modelling of the knee. As their clinical adoption to provide subject-specific solutions depend on the time and costs, research is concentrated on finding a compromise between accuracy and efficiency (Killen et al., 2020). At present, no musculoskeletal model can provide an easier and more compact lumping representation of all the elastic structures of the tibiofemoral joint, while predicting in a computationally efficient way articular forces without solving a contact problem.

In conclusion, the function of the tibiofemoral joint within individuals, its variability across populations, and the role played by ligaments in those have not been fully understood yet. Studies in literature quantifying the variability of healthy tibiofemoral joint and ligament mechanics among individuals are scarce. Ex vivo studies on knee passive motion focus on a few subjects or male populations only, thereby leaving inter-subject variability of knee passive motion and the influence of sex still open for debate. Moreover, tibiofemoral passive motion measurement approaches currently available are either limited to a single coupled path or the envelope of knee passive motion, did not include detailed error analyses or considered stressed medial-lateral flexion-extension test inclusion. Furthermore, anatomically detailed models of the individual tibiofemoral joint, capable of predicting individual elastic response and investigating the contribution of ligaments during activities, are complex, computationally expensive, and time-consuming, thus, not allowing for population studies of the active tibiofemoral mechanics.

1.2 Objective, Aims And Significance

The flowchart below illustrates the main objective and goals of this thesis, including additional research performed by this author as part of a wider Australian Research Council-funded project (DP180103146) (Fig. 1.1).

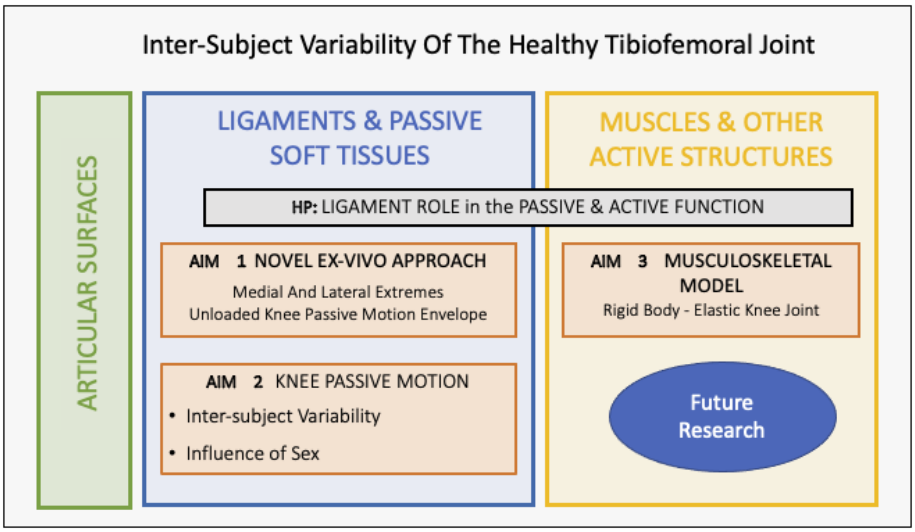

Figure 1.1 *– Schematic representation delineating the fundamental goals, objectives, hypothesis, and essential elements of the PhD thesis research.*

The overall objective of this research was to gain a better understanding of the inter-subject variability of healthy tibiofemoral joint function. A combination of novel ex vivo and in silico methodologies was developed, and population studies were undertaken to achieve this thesis aim.

- A novel ex vivo experimental assessment of the knee passive motion extremes was designed, and the analysis of the errors, accuracy and reliability conducted (AIM 1). This approach was developed to measure the two tibiofemoral coupled 'varus' and 'valgus' flexion paths, corresponding to the 'medial' and 'lateral' extremes of the unloaded knee passive motion envelope, across an adult cohort.

- Measurements of these unloaded passive motion envelope extremes in a healthy cohort of thirty specimens, both males and females, were performed using the ex vivo approach developed. Inter-subject variability was quantified along with differences between males and females, to investigate the individual variation of the native tibiofemoral function and the influence of sex (AIM2).

- Fast generation and solution of computationally efficient musculoskeletal models enable efficient population studies, enhance the feasibility of studying inter-subject variability, and reduce time and resource requirements for data analysis, contributing to understanding tibiofemoral joint function variability. A computationally efficient musculoskeletal model of

tibiofemoral mechanics was developed by accounting through compliance matrices individual passive motion and laxity variations and relating them to the active tibiofemoral function. The simulated elastic joint accounted for all anatomical elastic structures without direct representation, with the use of compliance matrices, while no contact problem was required to be solved (AIM 3).

As knee ligaments play a pivotal role in healthy active and passive tibiofemoral function, while still not fully understood and their function still debated, this thesis offers the opportunity to provide new insight into the ligament function. This thesis tested the hypothesis that:

'Within passive knee motion envelopes, ligaments do not significantly influence tibiofemoral path, when recruited act as constraints defining envelope boundaries, and outside, provide a mild elastic response through their individual stiffness and combined action'.

In Figure 1.2, a more detailed flowchart presents the structural organization of the research conducted in this Ph.D. thesis. The flowchart includes key elements such as input data, methodologies, outputs, and additional related research, contributing to the aim of the study. References to specific chapters and appendices within the thesis are provided for further exploration.

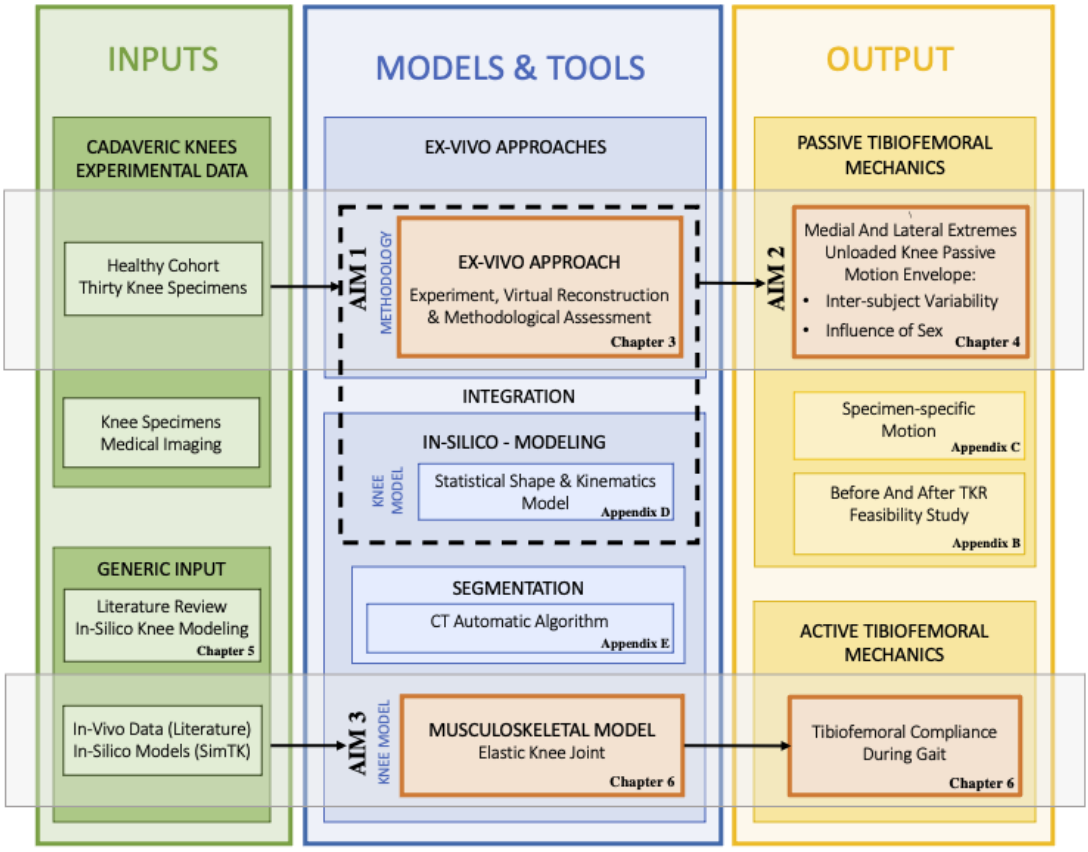

Figure 1.2 *– Comprehensive flowchart showcasing the structural organization, input data, methodologies, outputs, and supplementary research components of the PhD thesis. Includes references to specific chapters and appendices for a holistic understanding of the entire research journey.*

The significance and relevance of this research have been demonstrated by the further research prompted through this thesis: (1) a study on the relationship between geometry and function has already been conducted by integrating the experimental data in a statical shape model of the tibiofemoral joint, and it is reported in the appendices (Appendix D - Statistical Shape And Kinematics Model); (2) within a separate project investigating total knee replacement, the use of the ex vivo approach developed, has been used to investigate the restoration of the individual function before and after total knee replacement (Appendix B). Furthermore, (1) the experimental individual tibiofemoral passive motion is currently in use for validation of kinematic models; research in progress is (2) applying these models, in studying the effect of tibial osteotomy.

A deeper understanding of the interactions between ligament structures, articular surface, and muscles, within the tibiofemoral passive and active function and its variability across populations, are an important focus of current knee research (Fitzpatrick et al., 2012; Fregly et al., 2012; Lansdown et al., 2017; McGibbon et al., 2021). Research findings from this study are expected to contribute to the advancement of implant design, ligament reconstruction, rehabilitation, treatment, and prevention of knee ligament and joint injuries, and diseases, as well as to the development of training and targeted exercises (Fregly et al., 2012; DeVita et al., 2018; Asaeda et al., 2019; McGibbon et al., 2021). The generation of new knowledge and technology could predict categories more at risk, improve future knee ligament reconstruction methods, provide further insights on osteoarthritis causes, development, treatment, and knee replacements (Mukherjee et al., 2020; Alijehani et al., 2022). Finally, a growing interest is being shown in developing in silico musculoskeletal models for clinical applications, towards which this research directly contributes to making their generation easier and providing faster fruition (Taylor et al., 2013; Mukherjee et al., 2020; Curreli et al., 2021).

1.3 Outline Of The Dissertation

Chapter 1 highlights the background and motivation, and outlines the significance, aims and objectives of this research.

Chapter 2 provides an overview of the knee joint, along with a review of literature that identifies current knowledge on knee ligaments and joint mechanics, the assumptions/hypotheses behind their studies in literature and limitations.

Chapter 3 outlines the approach developed to quantify the six-coupled degrees of freedom medial and lateral extremes motion of the unloaded knee passive motion envelope, including a comprehensive methodology assessment and error analysis.

Chapter 4 quantifies (1) the variability of the medial and lateral extremes of the passive motion across a healthy adult population, and (2) the differences between males and females, investigates population variability and the influence of sex.

Chapter 5 presents a mapping literature review to evaluate a cost-complexity-utility perspective on in silico knee and tibiofemoral joint modelling.

Chapter 6 presents an efficient musculoskeletal approach to model tibiofemoral elasticity through compliance matrices.

Chapter 7 discusses the impact and significance of the findings included within this thesis, along with limitations and recommendations for future research.

Appendix A includes the statements of contribution.

Appendix B presents a feasibility study to investigate the extremes of unloaded passive knee motion before and after total knee replacement.

Appendix C provides specimen-specific extremes of the unloaded knee passive motion envelope against the percentage of cycle and flexion angle for each degree of freedom and trial.

Appendix D investigates the causality in the relationship between knee anatomical variations and two tasks of experimental knee passive kinematics across a healthy adult population, through a partial least-square regression approach and the impact of sex on this relationship.

Appendix E introduces a new algorithm for automatic CT segmentation of knee bones using texture-enhanced statistical region merging.

Chapter 2

BACKGROUND

The Native Tibiofemoral Joint

CONTENTS

Please refer to the mapping literature review in Chapter 5 for a more comprehensive exploration of knee and tibiofemoral joint modelling, which provides an in-depth discussion from a cost-complexity-utility perspective (Chapter 5).

2.1 Anatomical Structures Variability And Function

The human knee is the largest compounded synovial joint of the body and articulates femur, tibia, fibula, and patella. There are three articulations between these four bones: tibiofemoral (TF), patellofemoral (PF), and proximal tibiofibular (TFi) articulations. Each comprises bones and soft tissues, including articular cartilage, ligaments, menisci, tendons, and muscles (Gray, 1878b) (Fig. 2.1). Cartilage covers the bony surfaces involved in the articulations, while ligaments connect bones together, and tendons link these last to the muscles. Connective membranes envelop the knee, entirely and in its internal structures, such as bursae, tendon, and muscle sheets, providing nutrition and lubrification for the structures in their chambers. Finally, fat pads, blood vessels and nerves make the picture complete list of the anatomical structures of the knee.

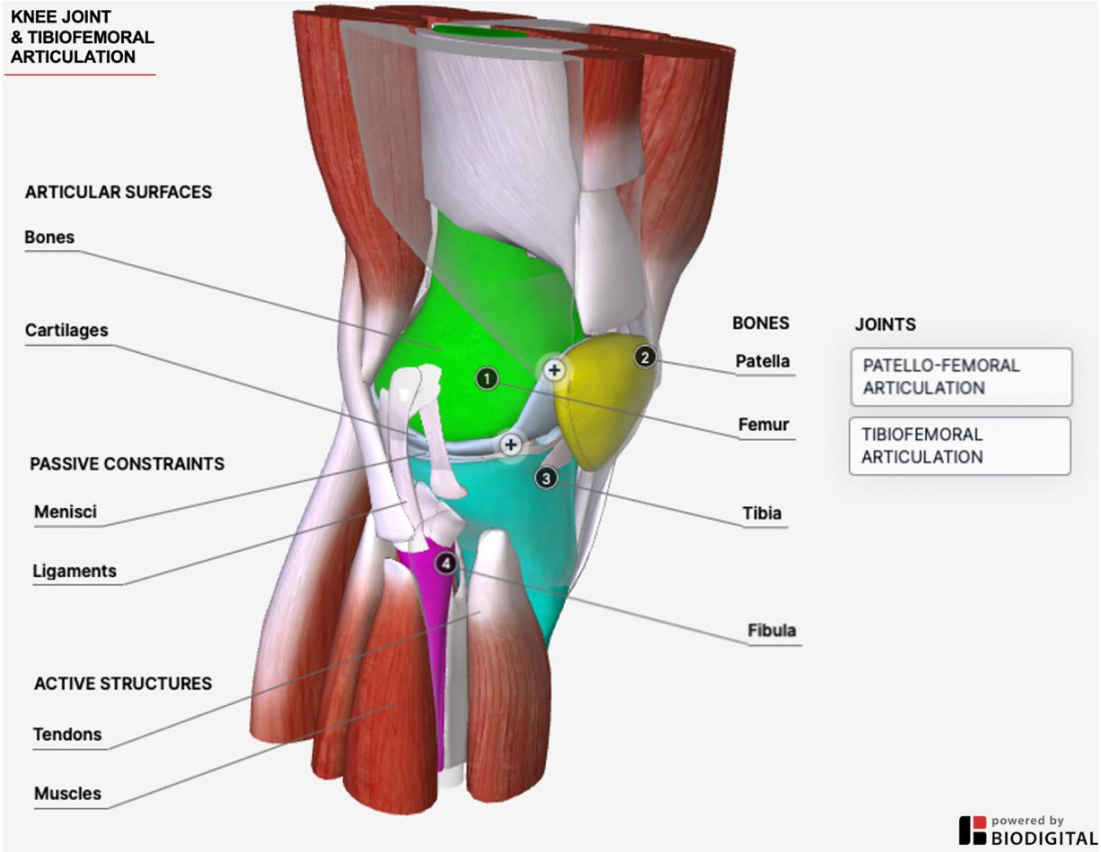

Figure 2.1 *– Antero-lateral view of the right knee joint: illustrative depiction emphasizing the complex interplay of bones, soft tissue structures, and articulations (anatomical model powered by BioDigital, image crafted by the author).*

The knee joint has two apparently contrasting and conflicting functions: ensuring stability and allowing mobility, by transmitting, absorbing and redistributing the forces, with the minimum effort (Masouros et al., 2010). The TF joint is primarily responsible for knee stability and mobility, by acting as a transmission line between the femur and the tibia. The PF articulation acts as a separate extensor mechanism, stabilizing the knee by dissipating forward momentum (Amis et al., 2004). The TFi does not appear to contribute to knee movements. For simplicity, as joint PT and TFI investigations are beyond this thesis scope, hereafter the term knee will refer to TF

articulation only unless otherwise stated. The TF joint is further divided into medial and lateral compartments, which differ greatly from one another (LaPrade et al., 2007; Sanchez et al., 2006).

As anatomy helps to perform the function, TF anatomical structures contribute to the knee joint function, through their individual and combined action.

- Passive motion, in the absence of forces/deformations, is guided by articular surfaces, bone and cartilage topography, acting as purely geometrical constraints (Amiri et al., 2006).
- Soft tissue structures, primarily ligaments, help to provide passive stability by preventing non-physiological motions (outside the normal range of motion), resulting in joint paths offering minimum resistance to motion (Parenti-Castelli et al., 2004a).
- Active structures, such as muscles and tendons, interact dynamically with passive stabilizers, to balance external forces, causing internal joint forces and a possible elastic response. During normal physical activities, active motion occurs within the passive motion envelope with no ligament interaction and loading when the force is perpendicular to hard constraints (bones); when additional non-perpendicular components are present, ligament contribution is necessary and may produce an elastic response. This is based on the understanding that during normal physical activities within the natural range of motion (i.e., within the passive motion envelope), additional ligament interaction or loading is not required when the force is perpendicular to hard constraints such as bones. This notion is supported by the work of Blankevoort et al. (1988), which discusses the passive motion envelope and the role of ligament interaction and loading during extreme or forced motions that exceed this envelope (Blankevoort et al., 1988).

The study of tibiofemoral mechanics involves assessing TF motion (kinematics) and the TF forces and moments that cause it (kinetics). TF kinematics requires the definition of the femoral and tibial local coordinate systems based on subject-specific anatomical features. Their relative movement can be described by translations and rotations with a 4x4 transformation matrix for a total of six degrees of freedom (DoFs) in three orthogonal planes - sagittal, frontal, and transverse (Grood and Suntay, 1983) (Fig. 2.2). TF joint kinetics are reported in the same planes and along the same axes.

- The sagittal plane is the vertical plane separating left and right sides of the knee, also known as medial and lateral respectively going towards the inner or outer part of the limb (this last characterized by the presence of the fibula). The rotations in this plane, around its perpendicular axis, are known as flexion-extension (FE), bringing respectively closer together and further away from each other femur and tibia; the displacements along its perpendicular axis are known as medial-lateral (ML) translations.

- The frontal plane, also known as coronal or longitudinal, is the vertical plane perpendicular to the sagittal, that divides the knee into anterior and posterior sides. The rotations in this plane, around its perpendicular axis, are known as adduction-abduction (AA), respectively rotating towards the medial or lateral side; the displacements along its perpendicular axis are known as anterior-posterior (AP) translations.

- The transverse plane is the horizontal plane, orthogonal to the other planes, that parts the superior and inferior sides. The rotations in this plane, around its perpendicular axis, are known as internal-external (IE) rotations, with the tibia rotating respectively medially and laterally; the translations along this axis are known as inferior-superior (IS) respectively for distal and proximal anatomical displacement.

The measure of the extent of TF translations and rotations is called range of motion (ROM), and in absence of muscle involvement it is typically referred to as passive ROM (p-ROM).

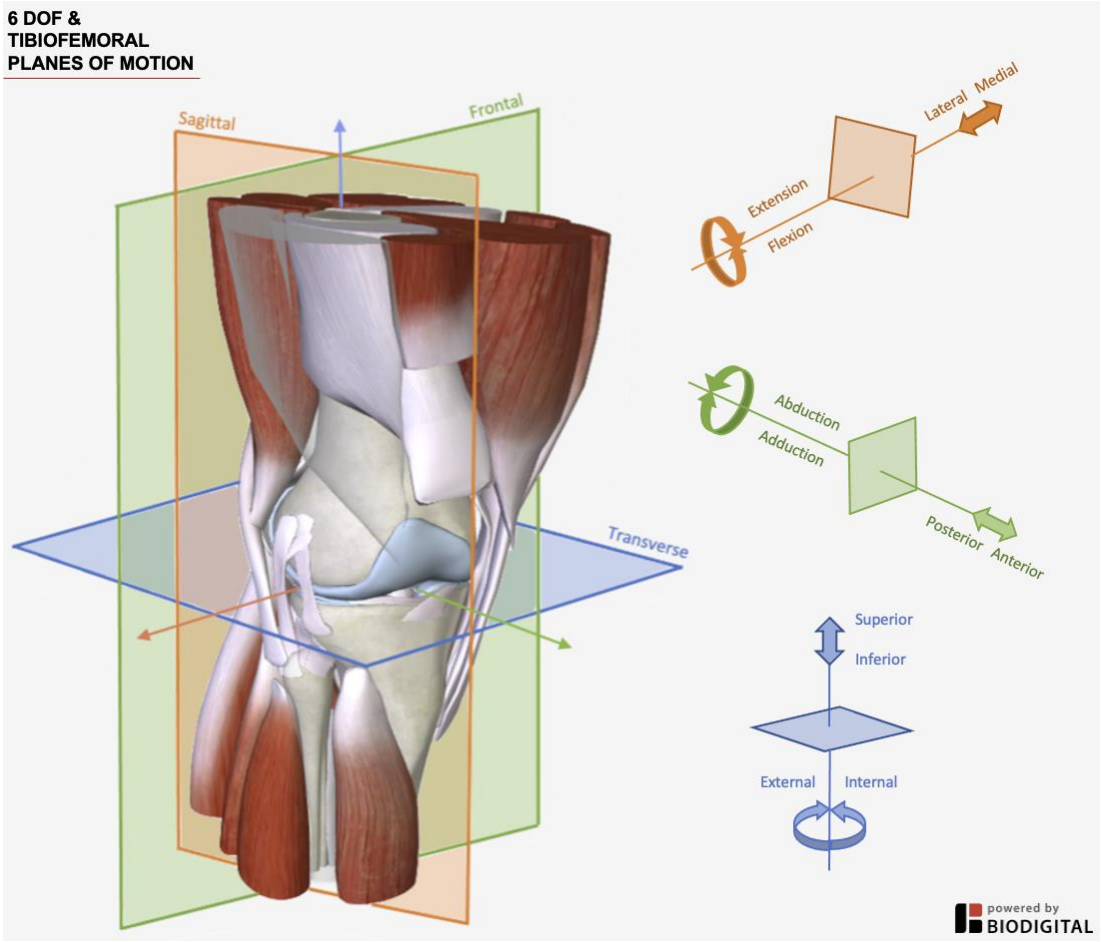

Figure 2.2 *– Depiction of Tibiofemoral planes of motion and six degrees of freedom kinematic axes in the right knee, with sagittal plane motions encompassing flexion-extension and medial-lateral translation, frontal plane motions involving abduction-adduction and anterior-posterior translation, and transverse plane motion consisting of internal-external rotations and superior-inferior translation (anatomical model powered by BioDigital, image crafted by the author).*

A key point in the understanding of TF mechanics relates to its high degree of variability in addition to its functional complexity. A variety of factors determine the variability of the

tibiofemoral anatomy, passive and active function (Fig. 2.3). Some of these factors responsible for this variability are ageing, sex, race, besides individual peculiarities (Sharma et al., 1999). A number of differences have been found between individuals in terms of bone shape, size, specific anatomical features, and material properties (Audenaert et al., 2019). Location and orientation in the space of ligament structures also greatly vary between individuals, impacting passive stability (Amiri et al., 2006). Individual variations of mobility while performing activities could be due to additional differences in muscles and tendons; in particular, shape, volume, cross-sectional area, material properties and pattern of activation can individually change (Duda et al., 1996). Possible factors that introduce variability among individuals while performing activities are personal habits, training, or clinical history. Variability exponentially grows with different activities, e.g., walking, running, or jumping, within the same person (Myers et al., 2012). The following sections will examine these points in more detail.

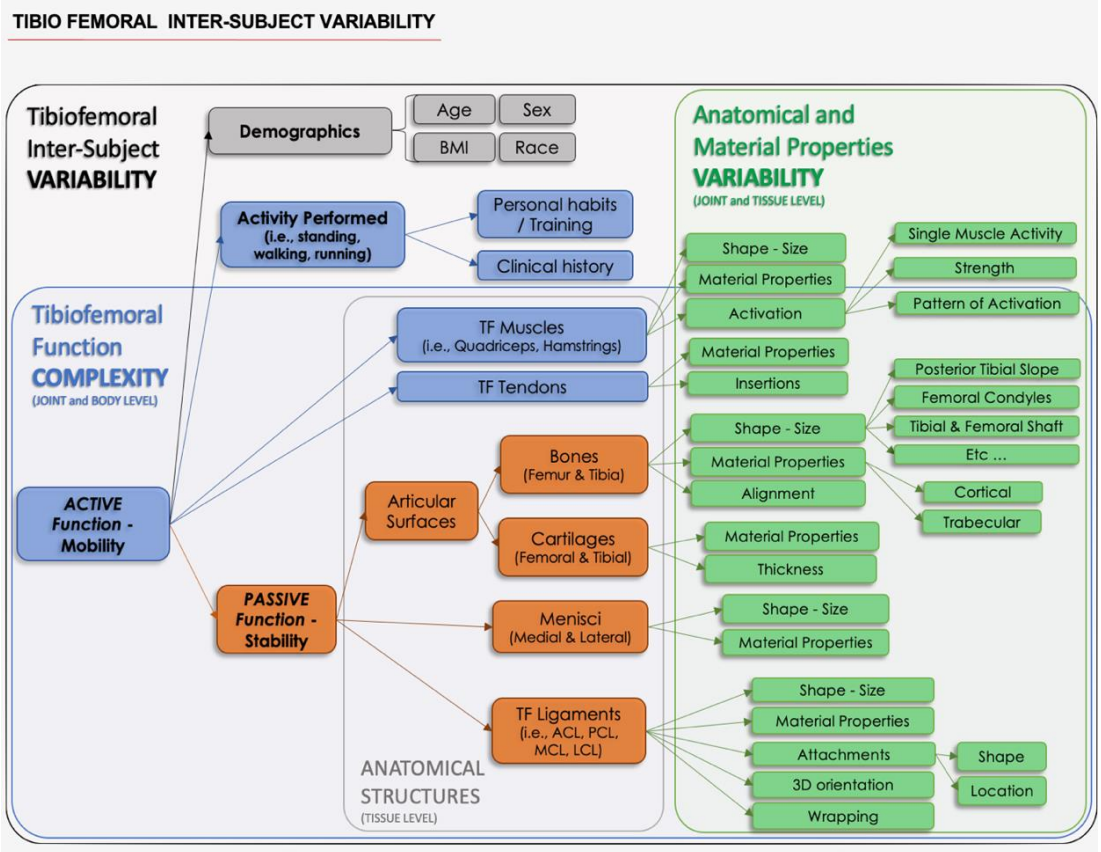

Figure 2.3 *– Comprehensive schematic depicting the multi-level factors influencing variability in passive and active human tibiofemoral joint function within individuals, encompassing inherent complexity, variations in anatomical structures, and interactions contributing to joint stability and mobility, as well as between individuals, including demographic factors and the influence of activities performed.*

2.1.1 Articular Surfaces Incongruency

The distal femur and proximal tibia, and their cartilage, define the TF articular surfaces, are characterized by incongruency, and determine the path of articulation when moving (Amiri et al., 2006; Martelli et al., 2002).

Bones

The literature reveals a range of knee anatomical variability, demonstrating variations in knee morphology across diverse individuals and populations. Some studies suggested that the knee in females is narrower than in males, regardless of their knee size (Dargel et al., 2011; Guy et al., 2012). Bellemans et al. (2010) suggested that morpho-typical variations based on the pelvis width/total leg length ratio could explain the variability within each sex (Bellemans et al., 2010). Regardless of their sex, patients with short and wide morphotype had wider knees, whereas long and narrow morphotype was associated with narrower knees. However, morphotype significantly predicted only the femoral aspect ratio, not the tibial. High variability in knee alignment was observed in relation to biological sex (Rao et al., 2013a), where knee alignment angles, defined as the angle between the femoral and tibial mechanical axes in the frontal plane, exhibited ranges such as neutral (-3° to 3°), varus (>3°), or valgus (<-3°). The figure below summarizes the main anatomical landmarks of the tibiofemoral joint, utilized for identifying those reference systems axes and facilitating comparisons (Fig. 2.4).

The femur is the strongest and longest bone of the body (Fig. 2.4). It is enlarged with a cuboid shape at the distal extremity, forming two large prominences, called medial and lateral condyles, oblong along the anteroposterior axes, the medial of which is greater than the lateral. The lateral condyle is more prominent anteriorly, whereas the medial condyle is longer and narrower. In front of the two condyles, the trochlear surface forms a smooth surface, and the inter-condyloid fossa is the depression between them. The femoral aspect ratio, which relates to anteroposterior and mediolateral distal femur lengths, varies with sex and race (Lonner et al., 2008; Kim et al., 2017). For instance, women have a larger mean aspect ratio compared with men, 0.84 and 0.81 respectively (Lonner et al., 2008). Moreover, morphology and shape differ individually with respect to the sphericity of femoral condyles, more or less pronounced anterior and posterior prominence of the condyles and intercondylar notch shape (Lansdown and Ma, 2018). The tibia, the second longest bone in the body, has a proximal extremity with a parallelepiped shape (Fig. 2.4). Despite it being called the tibial plateau, the surface of the tibia that articulates with the femur is not flat and characterized by a slope that is highly variable both between sexes and among individuals (Gray, 1878b). In the tibia, asymmetric medial and lateral plateaus complement the condyles, while not congruent. The tibial medial plateau is slightly concave and more elongated than the lateral, instead nearly circular shape, concave and with a lightly convex region backwards. Two horns, intercondyloid eminences, and an anterior and posterior intercondyloid fossa divide these compartments. The depth of the medial plateau varies among individuals, affecting articular congruence (Lansdown and Ma, 2018). As with the femur, the aspect ratio of the tibia is affected by sex and race (Lonner et al., 2008; Kim et al., 2017).

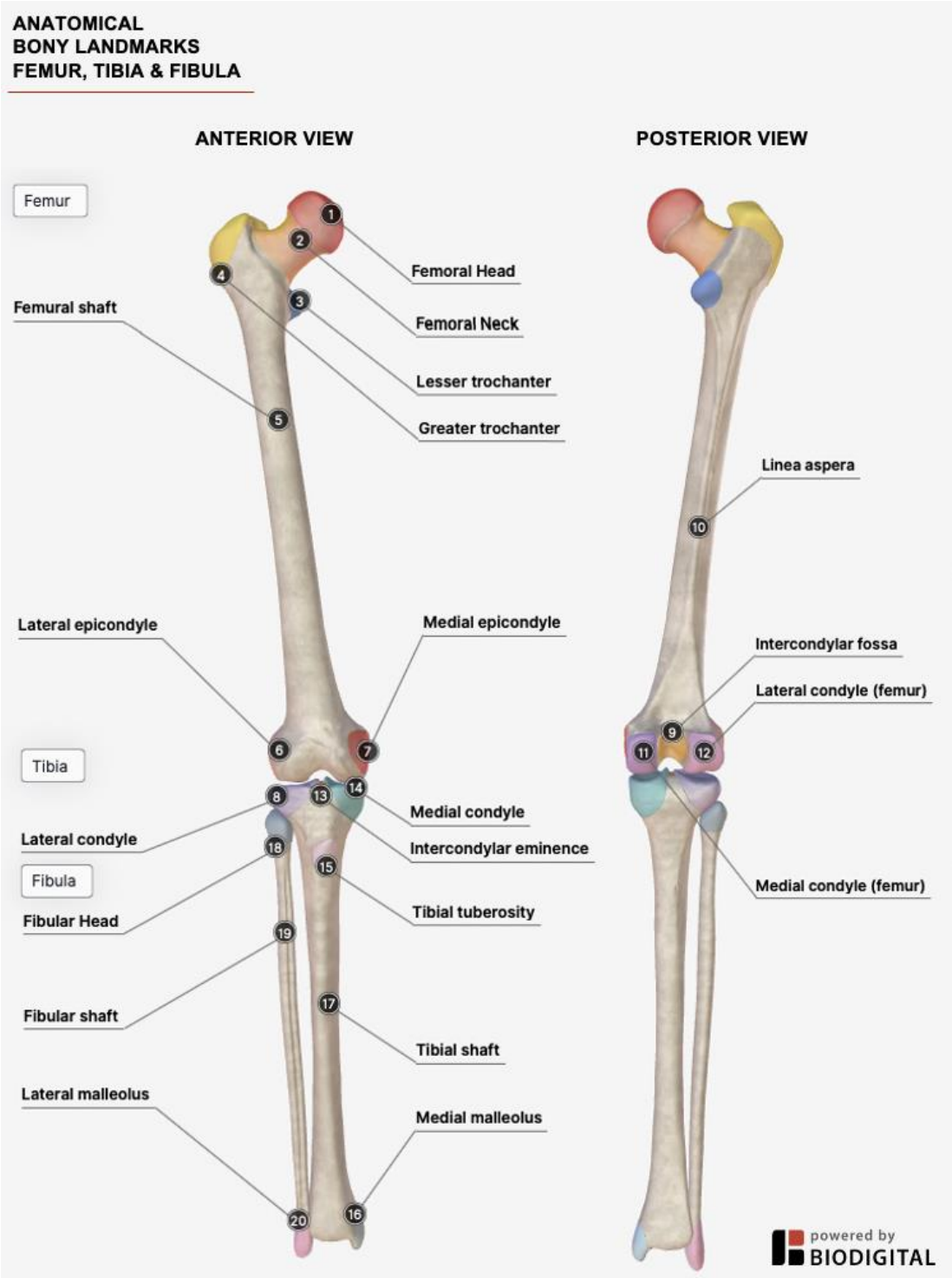

Figure 2.4 *– Anatomical bony landmarks of the femur, tibia, and fibula in the right lower limb, displayed in both anterior and posterior views, for reference system axes identification (anatomical model powered by BioDigital, image crafted by the author).*

Articular Cartilage

The tibial plateaus and femoral condyles are covered with a layer of shiny hyaline cartilage (Shepherd and Seedhom, 1999) (Fig. 2.5). The articular cartilage or hyaline cartilage is a connective non-calcified tissue characterized by a porous matrix of collagen and proteoglycans saturated with fluid (mainly water) (Pal, 2014). The cartilage are load-bearing surfaces with very low friction,

providing superior-quality lubrification and shock absorption. The porous matrix under compression prevents fluid from flowing from proteoglycans through the pores to surrounding tissues, while removal of the load restores the liquid phase into the matrix (prolonged compression makes fluid harder to return). The composition and orientation of the collagen fibres change through the different layers from parallel at the surface layer to perpendicular at the bone interface. Mechanically, cartilage is viscoelastic, inhomogeneous, and anisotropic. Additionally, they are not subjected to the regeneration of tissue in case of damage or ageing. Their properties are highly variable due to different individual features, daily life activities, and clinical/personal history.

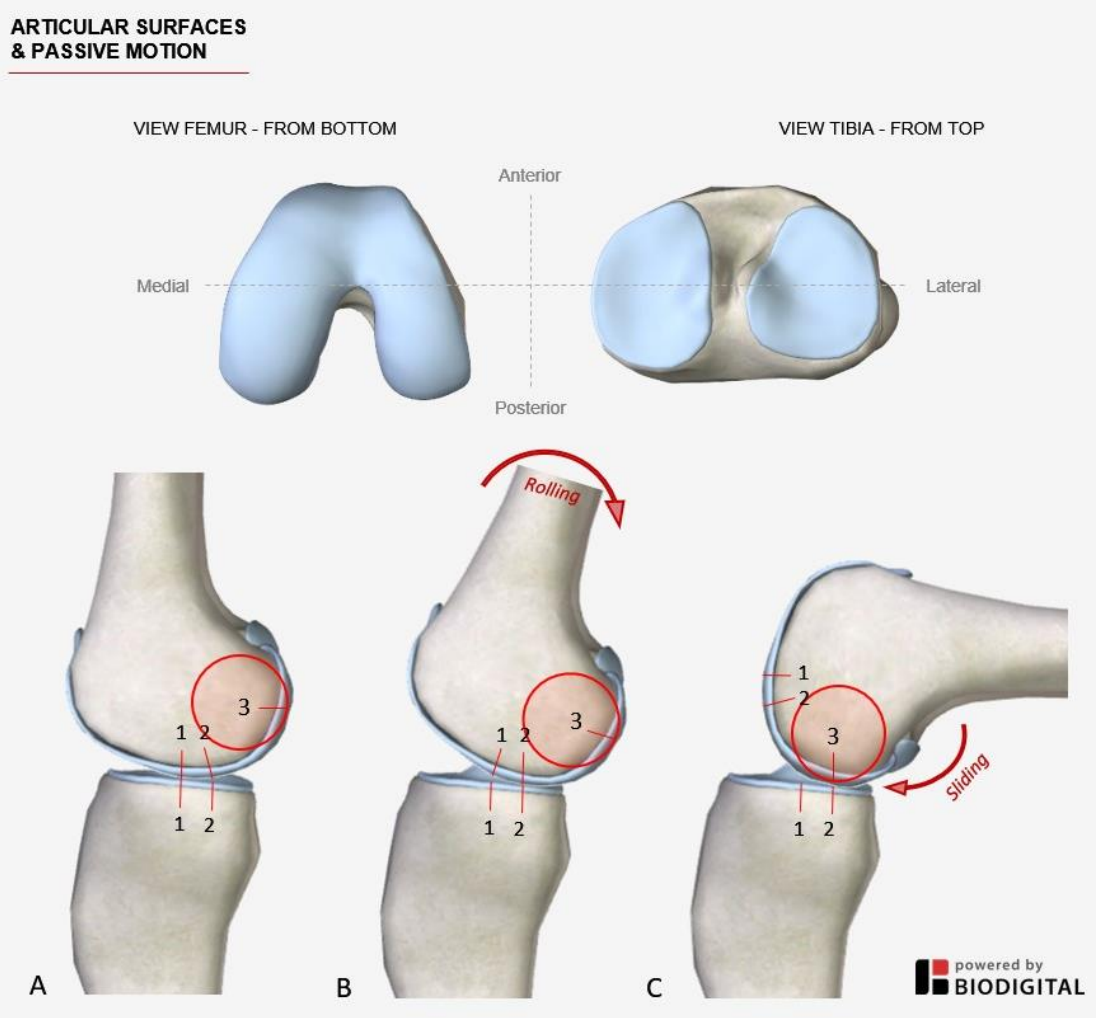

Figure 2.5 *– Articular surfaces of the femur and tibia of the right knee (top), demonstrating the dynamic changes in contact points and motion during passive flexion (bottom), with (A) Extension - central contact of the femur (f1) onto the tibia (t1), (B) Early flexion - posterior rolling occurs, shifting the contact to f2 onto t2, and (C) Deep flexion - anterior cruciate ligament restricts rolling back, causing the femur to slide on the tibia, with f3 moving onto t2 (anatomical model powered by BioDigital, image crafted by the author).*

Furthermore, articular cartilage exhibits not only variability in its material properties but also in thickness. Variability in cartilage thickness is observed among individuals, between and within populations, and within an individual along the articular surfaces (Gray, 1878b; Shah et al., 2019). Shah et al. (2019) conducted a study across a healthy population, exploring the variability of knee cartilage thickness, and they reported an average femoral cartilage thickness of 2.34 mm (Shah et

al., 2019). Specifically, the distal-medial and distal-lateral regions showed thinner cartilage, measuring -0.17 mm and -0.32 mm, respectively, compared to the posterior-medial region, which exhibited increased thickness measuring +0.21 mm. Additionally, the study found significant differences between populations, with a negative impact on cartilage thickness observed in females, with a magnitude of -0.36 mm (Shah et al., 2019).

Passive Flexion Movement

The relative movement between the tibia and femur is best described by a combination of rolling and gliding in the sagittal plane (Amiri et al., 2006) (Fig. 2.5). During passive motion, this point of contact between the femur and tibia changes. In FE, the posterior region of the medial and lateral condyles is defined by a smaller radius being in contact with the tibia (Fig. 2.5-A) (Iwaki et al., 2000). This movement of passive flexion-extension is characterized by a mobile ML axis around which motion takes place; the axis shifts forward during extension and backward during flexion. The medial condyle remains roughly in place (Fig. 2.5-B) (Amiri et al., 2006), until moving posteriorly in deep flexion (Fig. 2.5-C), whereas it is the lateral condyle that moves posteriorly throughout flexion (Amiri et al., 2006; Iwaki et al., 2000). A slight internal rotation occurs at the beginning of flexion and the end-stage of extension. Rotational freedom increases while the femur posteriorly translates, because of the sphericity of the condyles and thanks to the tibial distal and medial plateau flatness. At mid-flexion, posterior translation and IE rotation are permitted to the maximum extent.

2.1.2 The Role Of Passive Structures And Ligaments

Passive stability of TF articulation occurs as a result of complex interactions between articular surfaces and passive stabilizers, such as menisci and TF ligaments (Iwaki et al., 2000; Amiri et al., 2007). Menisci act as stabilizers by increasing articular surfaces congruency. Ligaments provide stability by connecting the femur and tibia holding them in place and preventing dislocation. However, ligament individual and combined function are still not fully clear.

Menisci

Menisci are semilunar fibrocartilage structures between the femur and tibia. Medial and lateral menisci act as stabilizers by increasing articular surfaces congruency. Size, shape, thickness, and mobility are different between the two (Gray, 1878b). Each has a concave upper surface and a flat lower surface. The medial is noticeably larger than the lateral, covering a wider portion of the tibial plateau with a saucer shape and approximate triangular thickness. Conversely, the lateral meniscus is wedge-shaped, smaller, and thinner, and it blends into the anterior cruciate ligament in front. Topography is in accordance with bone structure and therefore varies from individual to individual; like cartilage, menisci have different thicknesses across populations. The menisci are

believed to stabilize translations, guide rotations, spread contact area, absorb shocks, preserve cartilage, and lubricate the joint (Fox et al., 2012).

Ligaments

Ligaments provide stability both passively and actively, by constraining the range of motion and resisting abnormal movements. Ligaments are bands of fibrous connective non-calcified soft tissues. Ligaments have negligible mineral content while having a high-water content. Their structure is made of a proteoglycan matrix that varies according to ligament location and function, reinforced by collagen, fibres, and elastin, besides water (Weaver et al., 2000; Pal, 2014). Collagen is a fibrous component, originated by bundles of parallel fibrils, which are structured packages of parallel microfibrils, defined as agglomerates of tropocollagen. While collagen confers viscoelasticity, elastin is the protein responsible for elasticity. Material properties and tissues microstructure reflect their mechanical function (Freutel et al., 2014). In these hypocellular tissues, cells work to the maintenance of the collagen scaffold, which primary function is resisting tensile stresses (Pal, 2014). Like collagen, ligaments have a multi-dimensional scale structure (Weaver et al., 2000) and can be described as packages of parallel close collagen fibre bundles, strongly oriented in the direction of loads, and aligned in the longitudinal direction, respect the movement to provide high stiffness, consistently with their function. Typically, this is described through force-elongation (Fig. 2.6) or stress-strain curves.

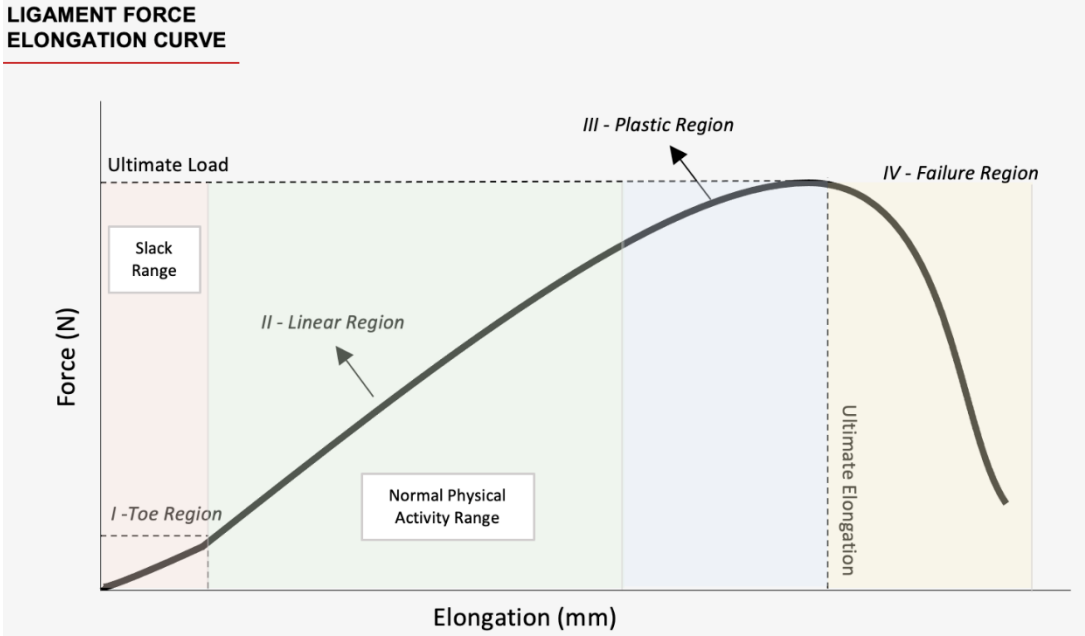

Figure 2.6 – *Representative force-elongation curve of a bone-ligament-bone specimen, illustrating ligament mechanical behavior with identifiable areas: toe, linear, plastic, and failure regions.*

The 'crimp pattern' of collagen fibres, in addition to the interaction and the elastic cross-linking, concurs in creating paths within the range of passive motion with minimal resistance to the movement (Toe Region); this region is also called slack region and is characterized by non-

linearity. Outside the 'crimp' state also known as fibres recruitment, brings the fibre to a straightened condition, preventing further elongation and dislocation with linearity (Linear Region). However, ligaments are currently defined as composite materials, characterized by anisotropy, non-linearity in time and history-dependent viscoelasticity. These curves vary based on the individual morphometry of the ligaments, such as cross-sectional area, and resting length, besides material properties and attachment sites (Amiri et al., 2006). However, they seem to be not related to individual physical characteristics, such as weight, height or BMI (Kopf et al., 2011). Stability and motion are influenced by the anatomical shape of ligaments and their attachment sites. Ligaments are under some tension even when the joint is in a neutral position, defined as the position of minimal resistance to displacements. Known as in situ or initial stress, it is responsible for much of the joint stability, especially in the absence of muscle or tendon forces. Experimentally, in situ strain has been measured in ligaments, they vary with joint position (1% up to 5% across flexion) and are non-uniform throughout individual ligaments (Adouni et al., 2020). It is especially at the bone ligament insertions that the loading patterns become complex (Momersteeg et al., 1995). Furthermore, ligaments wrap around bone surfaces (Giori et al., 1993).

Collateral ligaments are extra-capsular, while cruciate ligaments are intra-capsular (Flandry and Hommel, 2003) (Fig. 2.7). The articular knee capsule, also known as the capsular ligament, is one of the largest membranes within the musculoskeletal system, consisting of an inner synovial membrane and an outer fibrous membrane separated by a fat deposit (Gray, 1878b). While it may not be exhaustive, the following ligament overview aims to cover key ligaments and their functions.

- The Anterior Cruciate ligament (ACL) originates in the medial femoral condyle, within the depression in the posterolateral surface of the intercondylar notch (Fig. 2.7). It runs anteriorly, posteriorly, and medially to the condyle until the insertion with the tibia. It blends with the anterior margin of the lateral meniscus and fixes it to the medial and posterior side of the lateral femoral condyle. As previously mentioned, the high variability of ligaments includes ACL insertion shapes, which currently can be clinically classified as triangular, circular, and ellipsoidal. The elastic modulus of ACLs ranges from 20 to 115 MPa (Arnoux et al., 2005), with females having a 22.49% lower modulus (Chandrashekar et al., 2006). Researchers agreed to divide ACL into two bundles (Flandry and Hommel, 2003): an anteromedial, tighter during extension, while the posterolateral one is during flexion. Together, they serve as the primary restraint, preventing anterior tibial translation and hyperextension. Secondly, they participate in the control of the internal rotation and tibial abduction.

- The Posterior Cruciate ligament (PCL) originates within the posterior aspect of the intercondylar notch of the medial femur condyle and the medial meniscus's posterior margin (Gray, 1878b; Flandry and Hommel, 2003) (Fig. 2.7). It courses distally to insert on fovea centralis

of the inter-condyloid fossa of the tibia. It is shorter and the direction is less slanting than the anterior and it has a bigger cross-sectional area of all the ligaments though, which confers more strength. In experiments, PCL elastic modulus ranged from 24 to 207 MPa (Arnoux et al., 2005). Again, PCL plays a vital role with ACL in the anteroposterior rolling and sliding kinematics of TF articulations during flexion-extension. The PCL consists of two bundles: a posteromedial in tension during extension and the anterolateral during flexion. The PCL acts principally for constraining the posterior tibial translation during deep flexion, while in extension it slackens.

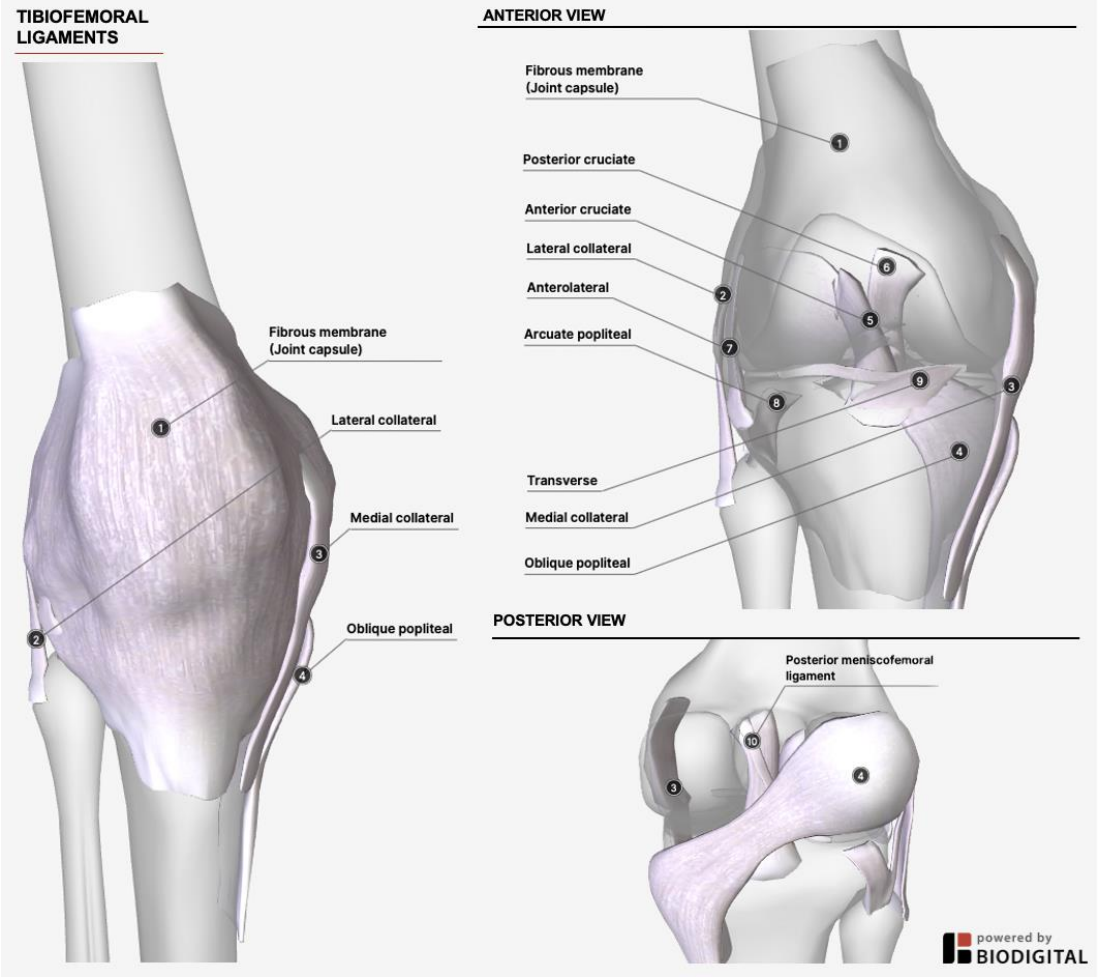

Figure 2.7 *– Depiction of the right knee ligaments in anterior view outside the joint capsule and in both anterior and posterior views within the capsule, highlighting the tibiofemoral cruciate and collateral ligaments and their insertions, along with the anterolateral, arcuate popliteal, transverse, oblique popliteal, and posterior meniscofemoral ligaments (anatomical model powered by BioDigital, image crafted by the author).*

- The Tibial or Medial Collateral ligament (MCL) includes a superficial and a deep portion (Gray, 1878b; Flandry and Hommel, 2003) (Fig. 2.7). The superficial MCL originates in the posterior-superior part of the medial femoral epicondyle and ends into the medial shaft of the tibia. The deep MCL originates from a lower epicondyle area of the distal femur, then sometimes attaches to the medial meniscus, and terminates on the proximal tibia. A Young's modulus of 11.5 to 51 MPa was calculated for MCL (Arnoux et al., 2005). MCL guides firstly the abduction and the internal tibial rotation but also restrains external rotation and anterior tibial translation.

- The Fibular or Lateral Collateral ligament (LCL) originates from the lateral femoral epicondyle, joins the bicep femoris tendon and attaches to the lateral side of the fibula's head (Flandry and Hommel, 2003) (Fig. 2.7). Young's modulus of LCL ranged from 21.5 to 32.5 MPa (Arnoux et al., 2005). LCL acts as a restraint on the lateral compartment, during knee flexion mainly for adduction and external tibial rotation; it also restrains posterior translation.

Passive Motion

In the absence of load, ligaments are highly deformable structures, whereas during activities they have the potential to undergo stretching and develop tensile forces that prevent further elongation (Masouros et al., 2010). Ligaments provide an individual and combined contribution to guide the joint and restrain movements to a physiological range. The level of contribution of ligaments to joint stability dynamically changes with joint orientations and in the presence/absence of external loads. The ligament/s optimally positioned relative to the displacement direction or line of action of forces, also called primary restraints, in the event of injury are replaced by secondary restraints. The level of contribution of ligaments to joint stability dynamically changes with joint orientations and in the presence/absence of external loads. Laxity tests are common clinical tools used to assess ligament function. During a laxity test, uniaxial displacements are applied until ligament recruitment occurs, while multiple passive stabilizers are used to maintain stability during the test. Table 2.1 presents the primary and secondary soft tissue constraints to uniaxial displacements across the passive FE range.

Table 2.1 *– Restraining function of the main soft tissues of the knee joint to applied displacements during passive flexion (adapted from Masouros et al., 2010).*

Applied Displacement	Flexion Angles (deg)	Primary Restraint	Secondary Restraint
Anterior drawer	0	ACL	MCL, LCL, Menisci
	30	ACL	Menisci, MCL
	60 - 120	ACL	
Posterior drawer	0 - 30	PCL	aPCL, LCL
	40 - 120	aPCL	pPCL
	120-140	pPCL, aPCL	
Adduction	0 - 60	LCL	PCL
Abduction	0	MCL	ACL
	30	MCL	ACL
	60	MCL	
External tibial rotation	0	LCL, PCL	Menisci, MCL
	30-90	LCL, PCL	PCL, Menisci
Internal tibial rotation	0 - 30		ACL, MCL, Menisci
	60	MCL	ACL, Menisci
Hyperextension			ACL, pPCL

As the knee moves between full flexion, extension, and hyperextension, it is possible to identify four main phases. (1) The knee passive motion mechanism in full flexion allows simple contained rolling movement while the posterior parts of the femoral condyles rest on the corresponding portions of the meniscal-tibial surfaces. (2) In the transition, until almost extension, the axis

through the inner and outer condyles of the femur gradually is shifted forward due to a superposition of gliding on the rolling movement. During this passage, most of the posterior articular surfaces of the two femoral condyles move forward equally having similar curvatures and parallel to each other. Through the last part of this phase, as the knee approaches full extension, the collateral ligaments can be approximately considered isometric (Victor et al., 2009). (3) This third phase by which all these parts are brought into accurate apposition is known as the locking movement of the joint. Ligaments play a primary role in this phase. The ACL starts to constrain the lateral condyle almost at rest, despite which it moves slightly forward and medially, and pushes the anterior part of the lateral meniscus. An increase of ACL tension allows a progressive tibial posterior translation until 90 degrees when the PCL start to reduce its tensions helping this mechanism from 120 degrees. The anterior translation is constrained by the combined effect of ACL tension and contact force on the medial meniscus. The tibial surface on the medial condyle is prolongated forward which shape is directed lateralward. Contemporarily to the movement forward of the condyles limited by the ACL, the tibia is rotating internally. In this late stage of flexion, the mutual cruciate ligaments effect is involved. The LCL operates after 30 degrees flexion jointly with the contact forces on the convex shape of the lateral tibial plateau. Upon reaching full extension, the lateral part of the lateral condyle presses against the meniscus, anteriorly, while the medial part rests on the articular margin in front of the lateral part of tibial inter-condyloid eminence. The anterior part of the medial meniscus is adapted into the groove of the medial condyle, while the forepart of the inter-condyloid fossa of the femur accommodates the ACL and the articular margin in front of the medial part of the tibial inter-condyloid eminence. Full extension of the knee is made stable due to ACL, articular geometries, and menisci. The extension is the most stable position to reach (i.e., 0° flexion) and it is also defined as the respective alignment of the long axis passing through femur and tibia (Masouros et al., 2010). To achieve full extension, the medial femoral condyle must "rock" up onto the upward-sloping tibial condyle, and the lateral femoral condyle rolls forward onto the flat tibial surface. (4) Finally, the knee passive motion can reach hyperextension, up to -10° in unloaded conditions (Masouros et al., 2010); extending further is prevented by the tension of the ACL, oblique popliteal, and collateral ligaments.

Many questions are still open regarding ligament function as passive motion studies reported contrasting findings. The coupling between DoF is still debated. Studies investigating passive unloaded knee motion highlighted a coupled mechanism of TF translations, IE, and AA rotations with the FE angle (Wilson et al., 2000), while others described an envelope of passive motion (Blankevoort et al., 1988). Several investigators have reported that IE rotations of the tibia are paired with FE of the knee, with the tibia rotating internally during flexion and reversed in extension (Meyer, 1853; Markolf et al., 1976; Trent et al., 1976; Biden et al., 1984; Fitzpatrick, 1989; Shoemaker et al., 1993). According to these observations, the tibia follows a single path

during passive flexion. On the other hand, the envelope of passive motion consists of a set of consistent and reliable paths of limit positions when the tibia is subjected to low torque. According to these studies, IE rotation is independent of the angle of flexion, and resides within a large passive knee flexion envelope, with boundaries defined by the tibial motion under moderate internal and external torques (Blankevoort et al., 1988). Nevertheless, it is still not clear how the envelope relates to the single tibiofemoral path in completely unloaded conditions, where motion was found highly susceptible to different approaches and experimental set-ups. High inter-subject variability was shown in all knee passive motion studies (Wilson et al., 2000; Victor et al., 2010; Wünshel et al., 2011; Cyr and Maletsky, 2014).

2.1.3 Active Structures And Physical Activity

Muscles

Several muscles are contributing to actuating the knee joint. Muscles are connected to the bones through tendons, fibrous structures at their extremes. In the knee, the tendons overlay the anterior and posterior aspects of the joint, transferring contractile force from the muscle groups of the upper leg and so generating motion. Muscles are divided into groups based on the movement they are responsible for. Biceps femoris, Semitendinosus and Semimembranosus are known as knee flexor muscles, assisted by Gracilis and Sartorius. The Quadriceps femoris is an extensor group of muscles, assisted by tensor Fasciae Latae. Medial rotation is actuated by Popliteus, Semimembranosus, and Semitendinosus, assisted by Sartorius and Gracilis, while lateral rotation is by Biceps Femoris. The Quadriceps femoris is a group of four muscles in the front of the thigh, which includes Rectus femoris, Vastus lateralis, medialis and intermedius (Gray, 1878b) (Fig. 2.8). Biceps femoris, Semitendinosus and Semimembranosus, with their tendons, can be gathered in a singular muscle group called Hamstrings (Fig. 2.8).

Situated on the lateral and posterior aspect of the thigh, the Hamstrings (also known as Biceps Femoris) are antagonist muscles to the Quadriceps femoris, allowing the knee to reach full flexion. As the name suggests, the Biceps Femoris muscle has two heads of origin (short and long). These heads share a tendon with the Semitendinosus muscle, and the tendon of the Biceps Femoris is divided into two portions by the LCL (Gray, 1878b). While Semitendinosus and Semimembranosus allow the knee to reach a low range of internal rotation, the Biceps is necessary to achieve higher ranges of internal rotation and external rotation. The Semitendinosus is located at the posterior and medial aspect of the thigh, while the Semimembranosus is located at the back and medial side of the thigh (Gray, 1878b). Both originate from a tendon of the Biceps femoris (Gray, 1878b). Other antagonists of the Quadriceps muscle are the Gracilis and Sartorius, involved in flexion and internal rotation (Gray, 1878b) (Fig. 2.7). Finally, the Gastrocnemius consists of two heads connected by flat strong tendons to the medial and lateral condyles of the

femur and plays a minor role in knee flexion (Gray, 1878b) (Fig. 2.8). Muscles, like ligaments, exhibit high inter-subject variability. Muscle insertions, origins, size, and shape, as well as cross-sectional area and volume, vary across populations and between individuals (Duda et al., 1996).

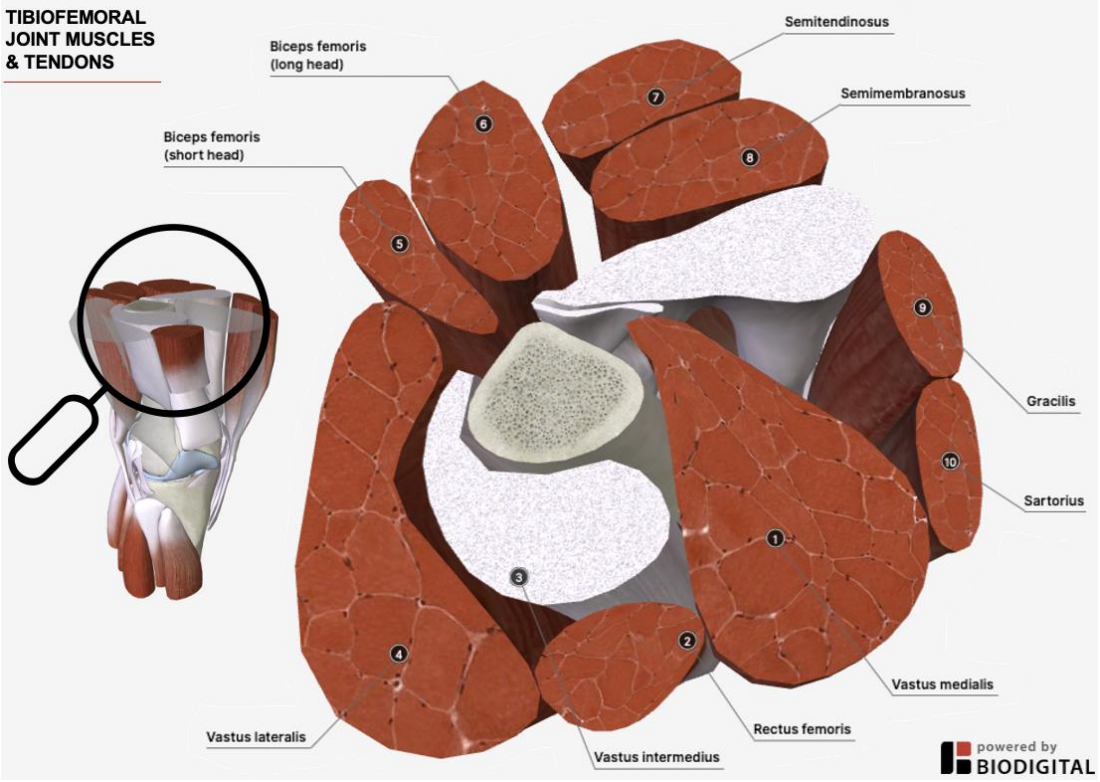

Figure 2.8 *– Cross-sectional area of the right knee, depicting the main muscle groups, including quadriceps (rectus femoris, vastus lateralis, vastus medialis, vastus intermedius), hamstrings (biceps femoris, semitendinosus, semimembranosus), and other surrounding muscles of the tibiofemoral joint (anatomical model powered by BioDigital, image crafted by the author).*

Active Function

Active flexion of the knee is characterized in comparison with passive flexion, by the further interaction of tendons and muscles, causing two main differences: (1) during the previously described third step (section 2.1.2 - Passive Motion), when almost at extension, muscular action helps the ACL further, bringing the medial condyle backwards and medial, and the meniscus with it, resulting in an internal rotation; (2) standing erect, the weight of the body falls in front of a line carried across the centres of the knee-joints, and the typical hyperextension, up to -10° for the passive unloaded flexion (Masouros et al., 2010; Victor et al., 2010), is prevented by muscles action in combination with the tension of the ACL, oblique popliteal, and collateral ligaments.

Walking is the most investigated activity, as gait analysis has been used as a clinical tool. This movement is repetitive, and it involves steps and strides. A normal forward step consists of two phases, the stance phase, and the swing phase (Fig. 2.9). Stance occupies 60% of the gait cycle when one leg bears most, or all of, the body weights. The swing phase occupies only 40% of it, the foot is not touching the walking surface and the body weight is carried by the other leg and foot. The stance phase begins with a heel strike, where the knee extends and flexes up to 15° to

20° degrees in midstance, caused by hamstrings. By utilizing the Quadriceps the knee extends again in the terminal stance and increases to about 35° degrees in pre-swing. During the initial swing, the knee begins to flex up to 60° degrees. During mid-swing, the additional contractions of the sartorius muscle begin the return to knee extension. The muscle activation pattern varies within individuals performing different activities and between individuals; with it, tibiofemoral motion, forces, and moments differ in individuals (Myers et al., 2012; Grey et al., 2019).

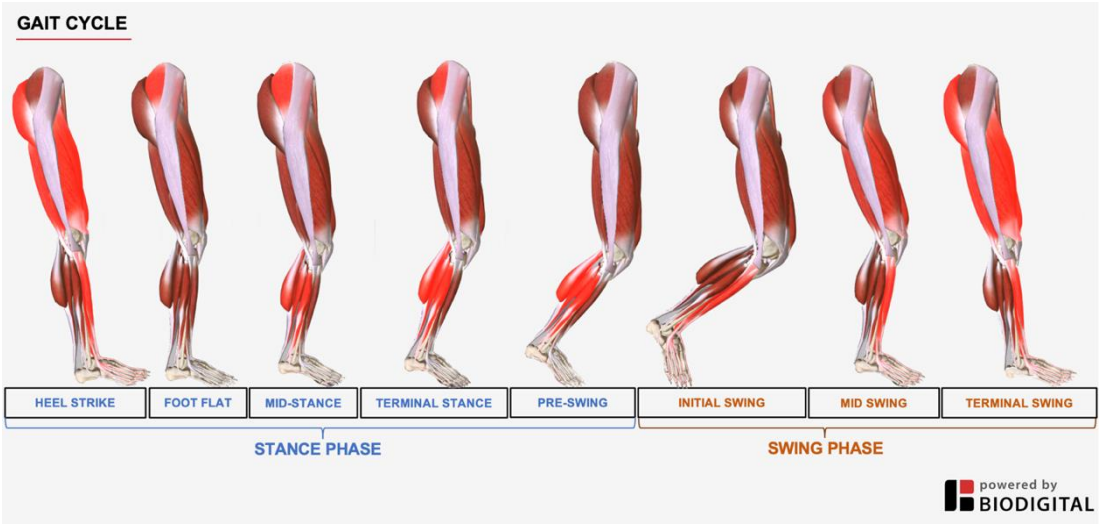

Figure 2.9 *– Gait cycle stride: (1) Stance phase, constituting approximately 60% of the cycle and comprising heel strike, foot flat, midstance, terminal stance, and pre-swing subphases, and (2) Swing phase, representing about 40% and involving initial, mid, and terminal swing (anatomical model powered by BioDigital, image crafted by the author).*

Several studies investigated the six DoF tibiofemoral kinematics during gait (LaFortune et al., 1992; Andriacchi et al., 1998; Gray et al., 2019). Hyperextension reaches up to a maximum of 5.8° degrees standing, while only 3.2° degrees in walking. While flexion can be achieved to up to 160° passively, active flexion can reach up to 130°, constrained by muscles in particular hamstring (Masouros et al., 2010). While ROM values greatly vary between individuals, these FE values are given to an average person. Again, for an average person, the range of IE rotation is about 30° degrees, while AA rotation is between 5° and 10° degrees, across the -10° to 90° degrees FE range (Blankevoort et al., 1988; Moglo and Shirazi-Adl, 2005). While walking, translations reached ranges of AP displacements of about 5 mm (1.3 to 3.6 mm), 3 mm in IS (0.2 to 3.2 mm) and about 4 mm in ML (2.3 to 1.5 mm) (LaFortune et al., 1992). During walking, peak-to-peak displacements of rotation were estimated to be 70.66°, 1.94° and 9.23° degrees, respectively for FE, AA, and IE, while translations were 3.96, 6.42 and 0.97 mm in ML, AP, IS (Gray et al., 2019). The AP translation of the tibiofemoral contact centres in the lateral compartment was revealed to be significantly greater than that in the medial compartment while walking, and their rollback was associated with increasing flexion angles (Gray et al., 2019).

TF articulation bears and transfers compressive and shear loads (Johnal et al., 2005). Forces transmitted inside the healthy TF joint are not measurable in vivo for the healthy knee joint. The maximum knee contact force measured with instrumented implants varied from 1.8 to 3.0 BW

during gait (Fregly et al., 2012). Medial contact forces reached up to 2.74 BW during walking and 3.79 BW during jogging (Kutzner et al., 2017). Furthermore, muscle activation pattern varies within individuals performing different activities and between individuals; with it, tibiofemoral motion, forces, and moments differ in individuals (Myers et al., 2012; Grey et al., 2019).

2.2 Methodological Aspects And Challenges In Capturing The Tibiofemoral Function

There are a variety of methodologies available for tibiofemoral function investigation, including in vivo and ex vivo experimental approaches and in silico modelling.

- By enabling dynamic functional tibiofemoral measurements on alive patients, in vivo experimental studies provide an undeniable contribution toward the investigation of active tibiofemoral joint function (Ramsey et al.,1999). In vivo studies mainly capture knee kinematics during dynamic activities, in both loaded and unloaded conditions, using a variety of techniques, from medical imaging (i.e., CT, MRI, Biplanar fluoroscopy, etc.), to clinical laxity tests, surgical navigation systems, gait analysis, and/or a combination of those. However, their contribution is often hindered by ethical limitations (e.g., invasiveness) and technical constraints, limiting their accuracy and what can be measured predominantly to knee kinematics, joint moments, and muscle activation (Fregly et al., 2012).

- Ex vivo experiments on cadaveric specimens are typically designed to investigate various aspects of tibiofemoral function, including knee joint passive motion, laxity, response to simulated active tasks kinematics/loading, and the dynamic/loaded behaviour of the knee. These experiments provide more accurate measurements compared to in vivo studies (Maletsky et al., 2016). Cadaveric studies correlate well with clinical trials, with joints and tissues having the same intrinsic anatomical and mechanical complexity and individual variability as those in vivo (e.g., sex, age, body mass index, diseased, injured) (Woo et al., 1999). By allowing for more invasive measurements and loading conditions, ex vivo experiments on cadaveric knees allow for further complementary insights into tibiofemoral function than could be gained by performing them on patients. For instance, while requiring compromising the TF joint integrity, they allow for measurements of articular contact/pressure and ligament forces within the TF joint (Maletsky et al., 2016). Besides in vivo techniques, devices, testing rigs and simulators can be employed to replicate laxity tests, as well as to perform passive and/or active tasks, ensuring more accurate, reliable, and controlled loads and/or motion, while also requiring more standardization. Simulating active tasks may also require further in vivo data from different subjects and presents many challenges in reproducing with fidelity complex boundary conditions, such as muscle activation patterns (Maletsky et al., 2016). While robotic testing typically does not constrain the

knee, it applies constraints at the hip and ankle joints. Reference system identification techniques can also influence the motion of the knee as well as results upon correct identification. In addition, these time-consuming and expensive experiments are limited in terms of donor availability and/or missing details, such as tissue preservation conditions and clinical histories, resulting in studies with small sample sizes that do not fully reflect population variability.

- In silico modelling of the knee can provide an estimation of quantities not directly measurable in vivo and ex vivo (Seth et al., 2012; Erdemir et al., 2019) ranging from theoretical/analytical models, to musculoskeletal, finite element and statistical shape-appearance modelling. Besides predicting internal forces and strains without compromising joint integrity, computational models can also study concomitant parameter variations and the effect of singular variables. Models can provide these measurements and allow samples to be tested repeatedly under varying conditions, complementing ex vivo and in vivo research (Erdemir et al., 2019). However, models are only capable of predicting outcomes rather than measuring them, so extensive verification and validation procedures are needed. Their accuracy greatly differs depending on the in vivo/ex vivo data collected and the fidelity of the data collection. In any case, the more detailed the models, the more extensive the experimental dataset required for input, as such more time and computational power are required. Additionally, models rely on significant hypotheses/assumptions to simplify the problem, which can misrepresent complex phenomena and lead to an improper understanding of TF joint function.

Therefore, as experimental in vivo, ex vivo and in silico modelling capture different manifestations of the same phenomenon, there has been a growing tendency to integrate and/or combine multiple approaches in the study of the TF joint. Therefore, this thesis proposes to use ex vivo approaches, to provide accurate quantification of the variability of passive tibiofemoral function, to be integrated with in silico MSK modelling, for the investigation of the effect of individual TF passive motion, and thus of concomitant variations in articular surfaces and laxity, on active tibiofemoral function and their relationship during activities. MSK modelling was selected based on a mapping literature review of TF modelling with a cost-complexity-utility perspective; presented in a separate chapter, this review was motivated by the ongoing debate over invasiveness, accuracy and availability of experimental data required to build and run these models, as well as time-efficiency, costs and benefits, as new technologies emerge (Chapter 5).

2.2.1 Ex vivo Experimental Approaches

TF joints have been studied ex vivo by using a combination of in vivo techniques such as imaging, motion analysis, and laxity tests, and ex vivo mechanical testing to investigate the tibiofemoral passive function. Conventional CT and MRI are static imaging techniques widely used in ex vivo studies. Computer tomography (CT) provides superior spatial resolution, signal-to-noise ratio,

and accuracy relative to bone shape and material properties, as well as to a certain extent relative to muscle and tendon geometry and ligament insertions (Ascani et al., 2015; Gornale et al., 2017) (Fig.2.10-a). In contrast, MRI scans are non-invasive and use magnetic fields to differentiate soft tissue structures and their geometry (Hash et al., 2013). T1 vibe (Fig. 2.10-b) and proton density (Fig. 2.10-c) sequences are employed for their accuracy in assessing 3D ligament shape and integrity, while their segmentation is a time-consuming and costly process, requiring extensive training and exhibiting high inter-rater variability (Burton et al., 2020). MRI is not limited to static imaging; in in vivo research, dynamic MRI offers real-time visualization with lower resolution.

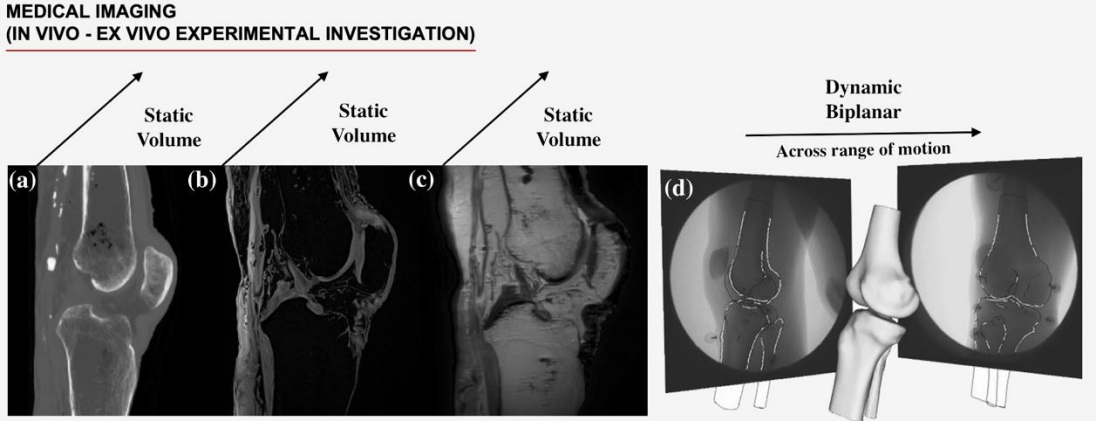

Figure 2.10 *– Medical imaging modalities: (a) CT Scan, (b) MRI T1 Vibe Sequence, (c) MRI Proton Density Sequence, and (d) Biplanar Fluoroscopy. Figure (d) has been reprinted with minor adaptations from The American Journal of Sports Medicine, with permission from SAGE Publications, Inc. (Myers et al., 2012).*

As a non-invasive dynamic imaging technique, biplanar fluoroscopy has become increasingly popular for exploring TF motion ex vivo, but particularly in vivo tracking bones and thus joint kinematics during passive (Lu et al., 2008) and active tasks (Myers et al., 2012; Gray et al., 2019) (Fig. 2.10-d). However, it is less accurate than CT as 3D bone poses is reconstructed from 2D projections, introducing errors, and compromising accuracy (Tersi et al., 2013). Ultrasound has emerged as a modality for dynamically assessing the knee (Niu et al., 2018), providing real-time, non-invasive imaging but with limitations in resolution and depth penetration. The use of imaging in ex vivo studies is more often complimented by other approaches, i.e., rigidly fixed intracortical bone pins (Walker et al., 1988) or again, spatial linkages implanted in cadavers (Rochcongar et al., 2016) to estimate their relative position to the bones and therefore TF motion.

Motion analysis is a widely utilized technique in various research studies for investigating passive motion, both in vivo and ex vivo. Additionally, it finds common application in gait analysis, an in vivo approach used in clinical and research settings to study active motion, particularly during active tasks, and explore TF joint function with a primary focus on motion analysis. While joint forces from ground reaction forces and muscle activation patterns are relevant in vivo studies, motion capture systems are widely adopted ex vivo for measuring knee and TF joint kinematics (Fig. 2.11). The most widely used motion capture system in vivo consists of an 8 to 10-camera stereo-photogrammetric system, capturing either infrared light from passive reflective markers or

sound/electrical waves from active markers (Simon et al., 2004) (Fig. 2.11). While in vivo accuracy of motion captures is limited by soft tissue artefacts, non-avoidable movements of marker position at the skin level (Camomilla et al., 2017; Ramsey et al., 1999), and joint kinematics by assumptions/simplifications of the underlying rigid joint models (Andersen et al., 2010), ex vivo more accurate measurements of the motion can be achieved using bone pin markers, imaging, and appositely designed testing rig. Portable motion capture systems are typically used in ex vivo studies, primarily optical and electromagnetic tracking systems (Maletsky et al., 2015).

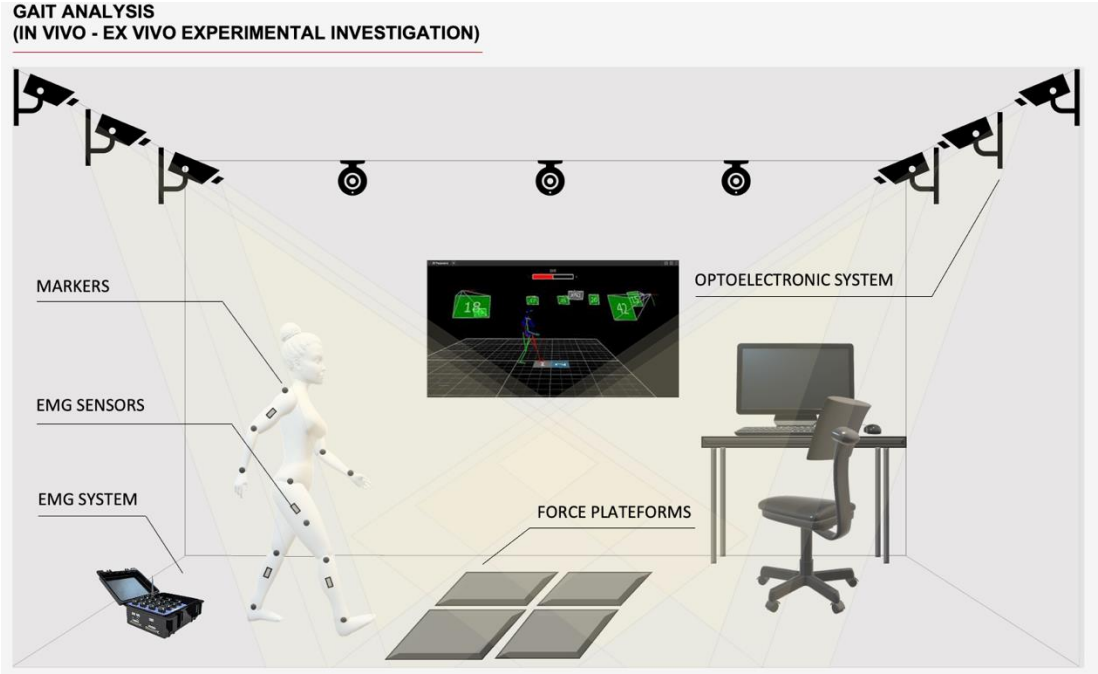

Figure 2.11 *– Biomechanical analysis systems, including stereo photogrammetric motion capture systems with cameras, passive reflective markers, force platforms, and electromyography, commonly used for gait analysis.*

Accuracy in locating individual markers with optical systems was estimated to be approximately 0.25 mm, compared to 0.9 mm with electromagnetic sensors (Glossop et al., 2009); however, it requires direct line of sight from cameras, decreases with camera distance and increases when using multiple markers. Therefore, optical motion capture systems have become increasingly popular for surgical navigation with marker clusters rigidly pinned to intracortical bone, positioned through anatomical landmarks palpation or with imaging (Belvedere et al., 2011; Maderbacher et al., 2016; Gosh et al., 2014); accuracy in TF motion tracking of these systems was estimated to be ±0.5° and ±0.5 mm (Elfring et al., 2009). For instance, Maderbacher et al. (2016) used a surgical navigation system with intracortical bone pinned markers and CT scans to investigate tibiofemoral kinematics ex vivo (Maderbacher et al., 2016). Gosh et al. (2014) used a TKR surgical navigation system to measure knee laxity (Gosh et al., 2014).

Laxity tests assess ligament non-bearing function to measure joint resistance to tibiofemoral displacements/rotations, both in vivo and ex vivo. Knee laxity tests are useful in clinical practice to diagnose ligament injuries, alongside MRIs, as they cause abnormal TF motions due to

increasing knee laxity (Shakoor et al., 2019). There are various manual laxity tests used to diagnose knee ligament injuries, including anterior/posterior drawer tests, Lachman tests, pivot shifts, and varus/valgus tests (Jensen et al.,1990; Lane et al., 2008) which involve displacing/rotating the tibia with the femur fixed, at a specific flexion angle (typically 90 deg). However, manual clinical examinations have been shown to be inconsistent and/or inaccurate in diagnosing knee injuries (Branch et al., 2019). Arthrometers are also available for instrumented laxity quantification purposes with a wide range of reliability and accuracy. Several studies investigated and compared multiple arthrometers in review articles (Anderson et al., 1992; Pugh et al., 2009), and compared devices and manual clinical evaluations (Branch et al., 2019). For instance, evaluation anterior laxity (AP displacements with 89 N applied at 30 degrees flexion) produced different results based on the device used, with 3.55 mm Dyonics Dynamic Cruciate Tester, 4.23 mm Knee Signature System, 7.31 mm KT-1000/2000, 5.94 mm Stryker, and 9.65 mm Genucom (Anderson et al., 1992); these investigations attributed these differences to the variance of the design and the methods and techniques on which they rely. To gain further insight into the function of the TF joints, manual and instrumented laxity tests are complemented by imaging and gait analysis, alongside experimental mechanical testing.

Finally, biomechanical testing of the tibiofemoral joint and knee ligaments covers a wide body of TF research ex vivo. The table below provides a concise summary of ex vivo mechanical testing studies, reported in alphabetic order (Tab. 2.2). Six hundred papers in PubMed were selected considering fifty articles of each combination of the following keywords: 'knee'/'tibiofemoral', 'passive motion'/'laxity', 'ex vivo'/'in-vitro'/'cadaveric'. A total of eighteen studies were selected, after screening in tiles/abstract (1) for adult human studies, (2) intact knees (no pathological/injured) and (3) with data published either in the form of text, tables, or graphics.

Ex vivo experimental testing has been extensively used to investigated tibiofemoral motion and knee laxity, employing various rig designs, and combining them with other devices/techniques, as evidenced by the studies in this shortlist. In this shortlist of studies, tibiofemoral motion and knee laxity have been investigated extensively ex vivo experimental knee testing, through a range of rig knee designs and/or together with other devices/techniques. Cyr and Maletsky (2014) performed manual joint laxity assessment to define knee envelopes, using a triaxial loading cell and two motion tracking arrays, ones rigidly fixed to the femur and one to the tibia (Cyr and Maletsky 2014). In several studies, surgical navigation systems and custom manual testing rigs have been used to measure TF laxity (Ghosh et al., 2014) or kinematics during passive flexion (Belvedere et al., 2011); many of these studies also investigate the knee joint gaps for TKR gap balancing with spacers (Nowakowski et al., 2011; Roth et al., 2016; Shalhoub et al., 2018). Other than knee laxity studies, many of the TK passive motion studies explored more simple passive central flexion paths (Belvedere et al., 2011; Wilson et al., 2000; Wunshel et al., 2012).

Table 2.2 *– A concise review of ex vivo knee cadaveric studies to capturing the tibiofemoral passive function with a combination of approaches - studies in alphabetic order (the author produced this table).*

Study	Specimens (Sex)	Influence of Sex	Data Acquisition Method	Experimental Testing and Rig Design	Coordinate System	Error Analysis	Flexion	Loading (Forces/Moments)	Displacement (Translations /Rotations)	TF Measurement
Ahmed (1992)	22 (13m/9f)	N/A	elettromechanical goniometers (TF kinematics) , buckle transducers (ligament tension)	custom testing device (vertical)	custom	accuracy ±0.5 mm, ±0.5°	40° and 90°	(1) tibial anterior shear up to 167 N, preroted IE rot 10° and 17.5° (2) tibila torque -15 to 20 Nm, compressive 900 N preload, AP pretranslated 4±0.2 mm	(1) tibial anterior translation as a function of anterior shear (2) axial IE rotation as function of torque	TF kinematics loaded/pretransla ted
Belvedere (2011)	22 (14m/8f)	N/A	surgical navigation system - 3 trackers of 5 active markers	custom testing rig with pulley and rope	Grood and Suntay	accuracy ±0.5 mm, ±0.5°	0° - 140° every 10°	central passive flexion path with 100N applied to quadriceps tendon, femur fixed and tibia moving	reported AP, IS and ML translations	TF unloaded passive kinematics central flexion path with muscles
Blankevoort (1990)	4 (1m/3f)	N/A	Roentgen Stereo Photogrammetric system	custom testing device (horizontal)	custom, Euler angles	repeatibility 0.37° and 0.19 mm	5-8 positions between 0° and 95°	combinations of tibial torque ±3 and 6 Nm, axial force 150 and 300 N and AP forces 30 nd 45 N	envelope of passive motion - internal external limit pathways; AA,	envelope of passive motion (laxity)
Boguszewski (2015)	47 (22m/25f)	Y - female increased laxity	3-dimensional digitizer and sensor	robotic testing device	individual anatomic with custom apparatus	N/A	0° - 50° every 10°	±134 N AP force, ±5 Nm IE torque, and ±10 Nm AA moment	laxity - AP transl, IE rot, AA rot, reported as stiffness Nm/deg or N/mm - mean, SD	laxity
Cyr (2014)	28 (27m/1f)	N/A	Optotrak 3020 infrared camera system	manual joint laxity assessments with a 6-DOF triaxial load cell	Grood and Suntay	N/A	0° - 120° every 10°	loads manually applied tibia AA maximum 610 Nm, IE maximum 68 Nm, AP ±5 20 N by 4 N	first three components PCA for each envelope reported in 3D graphs	envelope of passive motion (laxity), interrelationship between DoFs with PCA
Eagar (2001)	7 (5m/2f)	N/A	linear and rotatory variable differential trasformers	computer controlled load system - custom testing device (horizontal)	Grood and Suntay	N/A	0°, 30°, 60°, and 90°	from arbitrary resting position, tibial anterior load of 45 N and posterior of 45 N and anterior again 225 N	limits of motion load-deflection data linear stiffnesses computed (ave, SD, min and max reported)	stiffness
Fleming (2008)	8 (3m/8f)	N/A	Optotrak motion analysis system, thin-film pressure sensor	custom testing device with tensiond device (horizontal)	Grood and Suntay	N/A	quasi-static increments of 0°, 20°, 40°, 60°, 90°, and 110°	combination of laxity (AP -90 and 130 N) and tension base approaches (25, 50 N)	measured AP,IS,ML translations and AA, IE rotations	AP laxity, TF joint compression
Ghosh (2014)	8 (4m/4f)	N/A	surgical navigation system with optical trackers	custom-made rig intramedullary rod	Flexion axes with custom rig by minimizing coupled TF motions	accuracy ±0.5 mm, ±0.5°	0°, 30°, 60°, and 90°	knee subjectively stressed in AA, IE and AP - with 100 N static load on hamstring and quadriceps	laxity - AP transl, IE rot, AA rot, reported as envelopes	envelope of passive motion with muscle
Hsu (2006)	82 (44m/38f)	Y	universal force-moment sensor	robotic arm and custom testing rig system	Custom cartesian axis system	robotic manipulator repeatability 0.2 mm and 0.2°	(1) 0° - 90° every 1° (2-3) at 15° and 30°	(1) passive flexion <0.5 N and 0.2Nm (2) combined rotatory loads 10 N·m in AA and ±5 N·m in IE (3) 134 N AP tibial load	AP, IS, ML translations as well as IE, AA rotations (two curvers 2-3)	stiffness
Lamberto (2016)	1 f	N/A	six-component load cell	industrial robotic arm system position-control device	Anatomical coordinate system	absolute error up to 2.35 mm and 10.36° for 18N	0°, 15°,30°, 45°, 60°, 75° and 90°	moments and forces measured while displacing in each direction up to 100 N forces and 2.5Nm in AA and 1Nm in IE torques	applied AA and IE rotations and ML, AP, and IS displacements	compliance matrices
Lamberto (2019)	2 m	N/A	loads/displacement measured through hexapod system	hexapod robot	hexapod robot coordinate system	N/A	0°, 15°, 30°, 60°, 75°, 90°	moments and forces measured while displacing in each direction up to ±100 N forces and ± 10 Nm torques	applied AA and IE rotations and ML, AP, and IS displacements, to mimick Lackman and Pivot shift testing	compliance matrices

Li (2004)	13 (N/A)	N/A	loads/displacement measurements system	arm robotic manipulator and design rig position-control device	custom cartesian coordinate system	N/A	(2) 0°, 30°, 60°, 90°. 120°, and 150°	(1) passive path of the knee residual forces and moments < 2 N and 0.5 Nm, and (2) with simulated muscle loading a combination of quadriceps 400 N, hamstring 200 N (100 N medial and 100 N lateral)	measured AP translation and IE rotation	TF kinematics unloaded and loaded central flexion with muscles
Maderbacher (2016)	10 (N/A)	N/A	surgical navigation device with intracortical pins optical reference arrays	N/A	Grood and Suntay	N/A	0° to 90° with continuity	manual passive movement	tibial internal rotation and tibiofemoral abduction during flexion	TF kinematics unloaded central flexion
Markolf (2019)	38 (19m/19f)	N/A	3D coordinate measuring machine	custom testing device for flexion testing (horizontal)	N/A	accuracy of 0.02 mm	0° to 90° in 10° increments	a small abduction moment 0.5Nm applied	AP, IS, ML translations and IE, AA rotations	maximum values TF loaded kinematics , effects of axis alignment on coupled tibiofemoral motions
Roth (2015)	10 (6m/4f)	N/A	displacement sensor in each DoF	custom testing device, static (horizontal)	Grood and Suntay	N/A	0° - 120° every 15°	laxity tests with applied forces A-P ± 45 N, and IS ± 100 N, moments AA ± 5Nm and IE ± 3Nm (45N compression - muscles crossing knee)	transaltions and rotations measured function of FE - limits of laxity in AA, IE, AP, IS	limits of passive motion (laxity) and their interelationship
Victor (2009)	6 (3m/3f)	N/A	optical reflective markers and five calibrated infrared cameras	Oxford-style dynamic knee simulator (vertical)	Grood and Suntay	markers accuracy of 0.2 to 0.3 mm	Pass. 0° - 140° and Act. 30° - 120° every 10°	passive unloaded knee flexion task (5 flex-ext) and recorded squatting, including muscles loads configurations (quadriceps, med and lat hamstrings) with 130N vertical load at the ankle	tibial axial rotation and AP translations of femur, and separately of medial and lateral condiles	TF passive kinematics central flexion path with muscle
Wilson (2000)	15 (N/A)	N/A	3-D electromagnetic tracking system Isotrak	custom testing device, static (vertical)	Grood and Suntay/finite elical ax axes	accuracy 0.2°,1.8 mm; repeatibility 0.53°, 0.48 mm	approximatel y 0° - 100°	a central passive flexion path (no forces/moments) manually performed	transaltions and rotations in AA, IE, AP, IS, ML	TF unloaded passive kinematics central flexion path, effect of different set up on TF kinematics
Wunshel (2012)	24 (N/A)	N/A	recorded by robotic system	Oxfrod style dynamic simulator (vertical) vs robotic arm	anatomical, Euler angles	N/A	PP 0° - 90° every 1° AF, 10° - 90° every 5°	unloaded knee passive flexion - minimization forces (PP) and simulated squat (AF) with approximately 100 N on the three quadriceps actuators	transaltions and rotations measured function of FE in AA, IE, AP, IS for passive flexion and simulated active path	TF passive kinematics, unloaded central flexion & loaded with muscles

A wide range of testing rigs are used for assessing passive and active-simulated kinematic tasks, with the joint loaded or unloaded; these rigs typically fall into one of the following categories: static, dynamic, and robotic simulators (Fig. 2.12). Static loading rigs apply loads through bone extremities in different manually reached flexion angles (Fig. 2.12-a); a variety of static custom-built loading rigs have been used in literature to measure knee laxity (Amhed et al., 1992; Blankevoort et al., 1988; Eagar et al., 2001; Fleming et al., 2008; Forlani et al., 2016; Markolf et al., 2019; Roth et al., 2015; Shalhoub and Maletsky, 2014; Torzilli et al., 1994; Wilson et al., 2000). A static loading rig and stereophotogrammetry were used to define the knee passive motion envelope for the first time to describe knee laxity, measuring rotation/displacement associated with the applied moment/force at a variety of flexion angles (Blankevoort et al., 1988). Wilson et al. (2000) investigated a single passive unloaded knee flexion path, capturing the coupling between DoFs with custom manual testing devices and an electromagnetic tracking system; in this study a

minimum of in 0.2°±0.1° and 1.8±0.6 mm accuracy was reported, and 0.53°±0.47° and 0.48±0.3 mm repeatability for rotations and translations respectively (Wilson et al., 2000). Dynamic simulators have been used extensively to reproduce a variety of loading configurations and/or to simulate musculature, replicating dynamic knee physiological conditions, such as Oxford-style rigs or Kansas simulators (Clary et al., 2006; Forlani et al., 2016; Victor et al., 2009; Walker et al., 2015; Wunshel et al., 2012; Zavatsky et al., 1997) (Fig. 2.12-b).

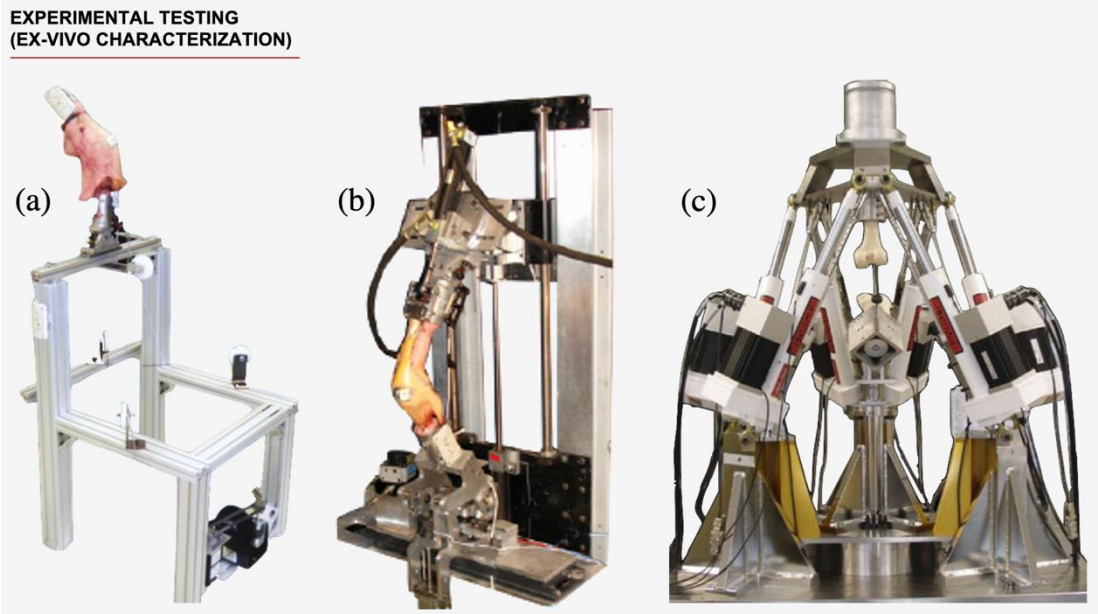

Figure 2.12 *– Ex vivo tests machines for mechanical experimental evaluation of knee cadaver specimens (a) Static Loading Rigs, reprinted with permission from Journal of Biomechanics, Elsevier (Shalhoub and Maletsky, 2014), (b) Dynamic Simulator - Kansas Rig, reprinted with permission from Journal of Knee Surgery, Thieme Medical Publishers (Maletsky et al., 2016), (c) Robotic Testing – Hexapod Robot, reprinted with permission from Medical Engineering & Physics, Elsevier (Lamberto et al., 2019).*

Robotic simulators have also been used to evaluate knee joint performance ex vivo, with one of the most widely used being a robotic arm design (Boguszewski et al., 2015; Fox et al., 1998; Lamberto et al., 2016; Liu et al., 2014; Maletsky et al., 2016); these simulators have been used to test the knee six DoFs, typically maintaining fixed the femur and moving the tibia to desired locations or exerting desired forces onto the joint, with robotic arms or even with sophisticated robotic platforms such as hexapod robots (Lamberto et al., 2019; Lawless et al., 2014) (Fig. 2.12-c). Robotic arm and hexapod robot data were used to derive stiffness/compliance matrices and thus describe experimental displacements as function of the loads, in intact knee and with progressive ligament resection (Lamberto et al., 2016) and from uniaxial tests mimicking laxity tests, Lachman and Pivot-shift (Lamberto et al., 2019).

Moreover, TF studies can provide further insight into length changes of ligaments or their fibre bundles (Blankevoort et al., 1991; Woo et al., 1999); ligament mechanics can be investigated using in situ approaches (studying ligaments within the joint) or ex situ approaches (studying ligaments in isolation). 3D optoelectronic motion capture provides reliable estimates of ligament length ex vivo, upon appropriate insertion site identification and tracking (Neri et al., 2019). Material

properties, fibre recruitment, alignment, and orientation relative to the applied displacements can be estimated through these or more directly measured at the expense of the joint integrity (Jones et al., 1995; Rochcongar et al., 2016; Woo et al., 1999). In dissected knees, ligament stress and strain can also be directly measured by buckle transducers (Ahmed et al., 1992), differential variable reluctance transducers, implantable pressure, and force transducers (Sakane et al., 1994; Cyr et al., 2015), and fibre-optic pressure sensors. Digital image correlation (DIC) has been used to accurately capture the full field of deformation of both cruciate (Readioff et al., 2020) and collateral ligaments (Prusa et al., 2023). However, it is important to note that these studies were conducted on dissected knee joint specimens and cannot be used on intact knees. Ultrasound is also used for dynamic assessments of knee kinematics and collateral ligament function (Slane et al., 2017; Niu et al., 2018). A more direct way to test ligaments and investigate their function is by fastening bone-ligament-bone structures with tensile testing on a variety of testing machines (Woo et al., 1999).

In conclusion, it should be noted that, while Table 2.2 compares the different setup conditions for investigating TF motion ex vivo, comparing results (TF forces/displacements) of different TF studies is a much more difficult task. As shown, methods differ depending on whether rig, standard or customized, or robotic simulators are used, joint loading conditions, rigidly attached joint parts, and whether static or dynamic muscle loadings are included if any. Goldsmith et al. (2014) investigated the passive path spatial repeatability using different robotic simulators, in particular the error induced in passive path repeatability by removing and reinstalling the knee, reporting respectively for translations and rotations 0.23 mm and a minimum of 0.55° intra set-up and of 0.79 mm and 1.2° inter set-up (Goldsmith et al., 2014). Victor et al. (2009) found significant differences in TF kinematics depending on the muscle load conditions applied (Victor et al., 2009). It is also critical to consider coordinate systems and conventions, availability of all data publicly and in the same or similar format (i.e., force-displacement curves, average, standard deviation), data captured with continuity or if interpolated with algorithms, and so forth, when comparing results. This is noticeable especially when the neutral path of the knee passive motion is determined with a robotic arm as the one requiring minimum force (Li et al., 2008), whereas with other testing rigs applying axial load and/or muscle forces, the TF joint can freely choose other paths (Belvedere et al., 2011). This was confirmed by Hacker et al. (2016) that compared tibial rotation obtained with different types of rig designs (i.e., rigs and robotic arms) and/or measurement convention (i.e., Grood and Suntay, finite helical axis) (Hacker et al., 2016). Therefore, the results such as force and/or displacement curves, of a subgroup of these studies and their differences will be analysed in a later section of the thesis dedicated to a broader discussion on passive motion reports.

2.2.2 In silico Musculoskeletal Modelling

An MSK model is a multi-rigid-body dynamic representation of the limbs or body, composed of rigid bones connected by joints defining its movement, actuated by tendons and muscles. MSK modelling combines in vivo gait analysis data, joint models often derived from passive motion studies, and tissue material and mechanical properties from cadaveric tests. Simulations can compute joint angles, joint moments, muscle activation/forces, and joint forces. These models potentially allow for the investigation of the effects of variations in articular surface geometry and ligaments on individual active tibiofemoral joints.

A wide literature is dedicated to the investigation of TF joint using a variety of MSK models. The table below provides a concise summary of models/studies relevant to the understanding of the role of articular geometry and ligamentous constraints on passive and active tibiofemoral kinematics (Tab. 2.3); the studies are reported based on chronological order.

Table 2.3 *– A concise review of MSK models dedicated to knee and tibiofemoral function studies - studies in chronological order (the author produced this table).*

Study	Subjects (Sex)	Knee Model Description	Articular Geometry	Ligaments	Tibiofemoral Kinematics	Body Model Type	Other	Task simulated	Model Output	Focus of the Study
Delph (1990)	5 cadavers	rigid planar mechanism - Yamaguchi (1989)	N/A	N/A	constrained fuction of flexion (0° to 90°)	scaled-generic	no explicit model of patella, Opensim coord. syst.	walking	joint moments	compute joint moments and forces
Shelbourne (2004)	5 m subjects	3D FE model	average-size knee from Garg (1990)	14 elastic elements	6 DoFs tibiofemoral joint from theoretical model Pandy (1998)	scaled-generic Anderson and Pandy (1999, 2001a)	separate PTF model	walking	knee kinematics and ligament forces	pattern of anterior cruciate ligament force in normal walking
Arnold (2010)	21 cadavers	rigid planar mechanism - Walker (1988)	bones from a male subject	N/A	constrained fuction of flexion (0° to 100°)	scaled-generic	no explicit model of patella, Opensim coord. syst.	N/A	joint moments	muscle–tendon lengths and moment arms, compute joint moments and forces
Lenhart (2015)	1 m subject	elastic fundation model (FE model) incorporated, modified subject-specific Walker (1988)	subject-specific data MRI female	14 ligaments bundles of non-linear springs (properties from literature)	secondary DoFs constrained, fuction of flexion (0° to 90°) based on passive simulation	subject-specific	separate 6 DoFs PTF model, Opensim coord. syst.	laxity IE (±5Nm) and AP (±100N) tests, walking	TF kinematics validated with dynamic MRI, TF articular contact pressure	validation of load-dependent behavior TF joint
Valente (2015)	1 m subject	(1) rigid planar - Yamaguchi (1989), (2) modified rigid planar Donnely (2012), (3) spherical anatomical four-bar-linkage - O'Connor (1989)	subject-specific data from MRI	ligaments from MRI and assumed isometric	(1) constrained function of flexion (0° to 90°) (2) 5 DoFs constrained fuction of flexion (0° to 90°) (3) a 1DOF joint with two coupled planar translations	subject-specific Valente (2014)	no esplicit model of patella, Opensim coord. syst.	walking, chair rising, stair ascending	muscle activity, contact forces	compare predictions of three subject specific models with increasing complexity for a variety of active tasks
Xu (2015)	N/A	N/A	based on a lower extremity model with a torso and back joint (Delp et al. 1990; Anderson and Pandy 1999),	10 ligamnt bundles with non linear properties by Blankevoort and Huiskes (1991)	three indipendent rotations and constrained AP, IS translations function of flexion (0° to 120°)	scaled-generic	no esplicit model of patella, Opensim coord. syst.	passive flexion, IE rotation (±30°), A rotation (±15°)	TF kinematics, ligament length	develop an OpenSim gait model with enhanced knee ligament structures
Smith (2016)	1 f subject	elastic fundation model (FE model) incorporated with ligaments	subject-specific data from MRI	14 ligaments nonlinear elastic springs	secondary DoFs constrained, fuction of flexion (0° to 90°) based on passive simulation from Lenhart (2015)	scaled-generic Arnold (2010)	computed muscle control workflow	walking	articualr contact pressure and ligament forces	efficient computation of cartilage contact pressures

Rajagopal (2016)	24 subjects, 21 cadavers	rigid planar mechanism - Walker (1988) modified, joint reference frame was coincident with anatomic approximations of the center of rotation	subject-specific data from MRI of a male	N/A	constrained function of flexion (0° to 120°)	scaled-generic	esplicit model of patella, anatomical coord. syst.	walking	muscle-generated joint moments	high-fidelity lower limb muscles driven simulation of walking
Brito da Luz (2017)	14 (12m/2f) subjects	6 DoFs parallel mechanism (incorporating articulating spheres constrained by isometric rigid ligaments) by Sancisi and Parenti-Castelli (2011)	subject-specific data from MRI for each subjects	4 ligaments segmented (ACL, PCL, MCL, PT)	5 DoFs constrained function of flexion (0° to 90°) based on parallel mechanism	subject-specific	Grood and Suntay coord. syst.	walking	TF DoFs kinematics compared with Sancisi and Parenti-Castelli (2011)	feasibility MRIs for subject-specific parallel mechanism based model
Smale (2018)	11 (7m/4f) subjects	(1) Rajopal (2016), (2) as (1) modified (3) Xu (2015),(4) natural motion obtained by parallel mechanism optimized with patient-specific parameters Conconi (2016, 2018)	subject-specific data from MRI	ligaments were included in all models	(1) constrained function of flexion (0° to 120°), (2) three rotational knee DOFs unprescribed and three translational DOF locked to zero,	subject-specific	N/A	side cut task	TF kinematics, ligament length	effect of MRI-based knee model on kinematics and knee ligament lengths
Hume (2018)	12 (6m/6f) subjects	elastic fundation model (FE model) deformable represenation knee and two FE models of two healthy specimens and ligament deformability	subject-specific data from CT and MRI	7ligament as bundles of point- to-point tension-only non-linear springs calibrated to specimen-specific joint laxity envelopes	(1) passive flexiontask kinematics unconstrained based on FE model (2) kinematically prescribed (3) joint deformable representation, constrained by passive kinematics	subject-specific	PTF model (FE model)	passive knee flexion, maximum isometric knee extension, and maximum isometric knee flexion	knee kinematics and moments, muscle forces, contact pressure	muscle forces alteration of knee kinematics and consequently muscle moment arms and joint torque
Clouthier (2019)	14 subjects	(1) statistical shape knee model (2) elastic fundation model (FE model) incorporated with ligaments generated from (1) and (3) TF kjoint model by Smith (2016)	subject-specific data from MRI	14 ligaments nonlinear elastic springs	tibiofemoral flexion indipendent degree of freedom calculated with IK, secondary degrees of freedom by	37 generated models with PCA from scaled generic	statistical shape model of 14 knees included, patella modelled, concurrent optimization of muscle activations and kinematics (COMAK)	walking	TF rotations, contact forces, anatomical features variation that influence knee function captured from PCA	effect of articular geometry on knee kinematics, cartilage contact, and ligament forces
Martelli (2020)	12 (N/A) subjects	(1) rigid planar Yamaguchi (1989), (2) geometry-based tibiofemoral motion, parallel mechanism Ottoboni (2010)	(1)Dorn (2012)(2) subject-specific data CT male donor	implicit 5, ligaments modelled with paralell mechanism	(1) constrained function of flexion (0° to 90°) (2) secondary 5 DoFs constrained fuction of flexion (0° to 120°) angle based on geometry	(1) bi-axial scaled-generic, (2) scaled geometry-based	no esplicit model of patella, Opensim coord. syst.	standing, walking	TF kinematics compared with biplanar fluoroscpy Gray (2019), contact forces	relationship between tibiofemoral geometry and musculoskeletal function during normal activity

The studies were selected using a combination of the following keywords: 'knee'/'tibiofemoral', 'musculoskeletal model', 'motion'/'kinematics' in PubMed. A total of thirteen studies were selected, after screening in tiles/abstract for (1) healthy knee models (no pathological/injured) and (2) with data on TF kinematics published in text, table or graphic, possibly including ligaments.

These studies can be categorized according to the anatomical or functional complexity of the tibiofemoral joint included, with particular attention to how these models take individual variability into account. The more common and more widely adopted models are average (Arnold et al., 2010) or scaled-generic models towards which a substantial body of research is dedicated (Delph et al., 1990). Although these can predict average trends in kinematics and dynamics, they only provide a crude estimate of the individual function. The six DoF TF joint is often simplified into revolute, slider, universal-planar, or ball-and-socket joints (Seth et al., 2011). The knee is

usually represented as a planar mechanism with secondary rotations and translations coupled with flexion-extension movement (Yamaguchi et al., 1989; Walker et al., 1988).

Besides the aforementioned rigid/average models, three main approaches are utilized for modelling the tibiofemoral function: patient-specific models employing medical imaging and specific mechanisms such as the spatial parallel mechanism (Valente et al., 2015; Smale et al., 2018), probabilistic/statistical approaches (Clouthier et al., 2019), and finite element or elastic foundation models (Hume et al., 2018). Rajagopal et al. (2016) used a subject-specific modified rigid planar knee model (Rajagopal et al., 2016). The use of subject-specific geometry and ligaments from MRIs improved prediction of individual tibiofemoral mechanics and increased simulation time when using elastic foundation, finite element, and deformable knee models (Brito da Luz et al., 2017; Lenhart et al., 2015; Rajagopal et al., 2016; Smith et al., 2016; Valente et al., 2015; Smale et al., 2018; Hume et al., 2018). Researchers have recently investigated the effect of geometry on the musculoskeletal function using a single degree-of-freedom geometry-based motion tibiofemoral model (Martelli et al., 2020). These types of rigid models account for a subject-specific geometry-based motion generated by parallel mechanism description of the knee, which implicitly also include the main ligaments (Brito da Luz et al., 2017; Conconi et al., 2018; Martelli et al., 2020). Tibiofemoral models with deformable components were developed to represent load-dependent elastic nature of the knee (Hume et al., 2018; Lenhart et al., 2015). Musculoskeletal simulations combined with subject-specific finite-element (Hume et al., 2018) or elastic foundation (Lenhart et al., 2015) models of the knee are currently employed to produce more different information including stresses-strains in each individual anatomical structure. Inclusion of anatomical details and ligament representations heavily affects joint predictions, and computational time increases upon fidelity (Kiapour et al., 2014; Lenhart et al., 2015; Smith et al., 2016).

Time and costs increase dramatically with the level of fidelity and detail included. A wide body of research is dedicated to ligament representations, including rigid, linear, and non-linear spring bundles, as well as geometry-based representations because their fidelity heavily impacts joint predictions, leading to inconsistent reports (Erdemir et al., 2019; Kiapour et al., 2014; Lenhart et al., 2015). In a computationally efficient TF contact model with ligament elastic bundles, Navacchia et al. (2019) reported 60 hours spent on 13 cores just to solve a muscle-driven simulation of activity using explicit finite element modelling for the knee (Navacchia et al., 2019). As their clinical adoption to provide subject-specific solutions depend on the time and costs, research is concentrated on finding a compromise between accuracy and efficiency (Killen et al., 2020). Optimization methods reduced the computational effort required by deformable knee simulations time to 76 minutes for a chair rise and 210 for a gait (Navacchia et al., 2018; Lenhart et al., 2015; Smith et al., 2016). While they keep improving over time, the suitability of these models for population studies and clinical applications is limited, indicating the need for further research

and development (Killen et al., 2020). Alternatively, MSK models can embed statistical shape models of the knee (Clouthier et al., 2019). Clouthier et al. (2019) include both a knee statistical shape model generates from MRIs and a MSK statistical model; these models can be used to determine the effect of shape feature variations in population, on knee kinematics, contact mechanics, and ligament loading during gait (Clouthier et al., 2019). A major challenge with these approaches is to maintain sufficient complexity without requiring extensive datasets and expertise, ideally in a computationally efficient and time-effective manner. This will be addressed more in detail in the mapping literature review presented later (Chapter 5).

2.3 Tibiofemoral Research Gaps And Opportunities

2.3.1 Knee Passive Motion Reports

Research on the passive motion of the knee joint has been carried out using a variety of methods and approaches, including in vivo, ex vivo/in-vitro, and in silico studies. The assessment of the passive range of motion is performed routinely in clinical evaluations, referring to the gross limb motion limits in FE rotation. Within TKR surgeries, it indicates the evaluation through manual manipulation of AA and IE rotational range as well. Through the literature, research studies of the range of passive motion include laxity measurements, estimation of the envelope of passive motion, as well as simple coupled guided flexion-extension paths. All these studies are referred to as investigations of the passive range of motion (PROM); as PROM is the direct result of the limits of this passive motion, misinterpretations are likely to occur. As a result, different studies have reported inconsistencies, with an ongoing debate about the appropriate model to describe knee passive kinematics, though passive motion remains an area of consistent study. At a given flexion angle, passive knee laxity is defined by the variation between the maximum possible motion limits of the tibia in one degree of freedom when there is no muscular or internal force present. A single value represents the endpoint measurement at a specific flexion angle; therefore, the angle of flexion plays a crucial role in displacement limits (Daniel et al., 1985). A change in laxity during the AP drawer test, AA, and IE stress test (Khan et al., 2007; Ostrowski et al., 2006) provides an initial indication that connective tissues are compromised; the decreased ability of ligaments to constrain movements results in increased laxity. The results are both primary and secondary motion compromised; however, these tests only analyse one direction and do not evaluate the coupling between different degrees of freedom. In this regard, Blankevoort (Blankevoort et al., 1988) has proposed the concept of an envelope of motion, a set of secondary tibial positional limits throughout the range of flexion, describing within this IE envelope as a region of freedom of movement (Blankevoort et al., 1988). For instance, the pivot shift test is an envelope assessment, evaluating motion limits when the knee is flexed, and the tibia is pushed

towards an internal and valgus position. An abnormal boundary limit suggests a ligament injury and may result in different resistance or manual 'feel' of the knee (Jakob et al., 1987; Jensen et al., 1990); manually investigated envelope boundaries tend to be subjective and difficult to quantify. Blankevoort only described the IE envelope, suggesting the same assessment could have been performed in other secondary motion limits; later studies carried out the investigation of multiple envelopes of passive motion (Cyr and Maletsky 2014; Nielsen et al., 1987; Roth et al., 2015). For instance, Nielsen defined AP, IE, and AA envelopes of motion as a function of flexion (Nielsen et al., 1987), and explained however how the coupling is lost when observing only one secondary motion limit. For four knees, the connection between primary and secondary motion restraint and its effect on secondary motion restraint was examined; motion paths in the extreme internal and external positions were described, but IE and AA coupled motions were not correlated. Conversely, PROM represented as the passive flexion and extension path was able to investigate the coupling controlled mainly by the ligaments and articular geometry. Wilson et al. (2000) found that when the knee is flexed there is a coupled motion between the primary and secondary motions (Wilson et al., 2000). However, many are the paths that within the envelope the tibia can follow leading to undesired variations due to small changes in the experimental set-up (Wilson et al., 2000). It is clear from the literature that ligaments and articular geometries of the knee create secondary coupled motion constraints in the flexion-extension path, as well as an envelope of motion that is typically described in terms of laxity as a function of flexion angle. There is therefore a gap and an opportunity to improve current existing research and, potentially, clinical practices by proposing an approach for PROM assessments that would analyse and connect both the coupling and the envelope of knee passive motion.

As discussed in the section on methodologies to capture tibiofemoral function, there are many methods to assess passive motion, laxity, and envelopes, including manual, instrumented, and robotic manipulation, that differs depending on in vivo or in vitro examinations. While manual manipulation leaves the freedom to assess the entirety of the individual range and is yet the easiest to reproduce in a clinical environment. On the other hand, to quantify displacements and loading, cadaveric studies used instrumented handlebars, loading rigs or robotic simulators, part of the variability can be lost as devices have limitations, for example in the range of displacements for testing (Ahmed et al., 1983; Blankevoort et al., 1988; Bull et al., 2008; Nielsen et al., 1987;). Loading rig measurements may seem like the most effective way to assess joint laxity, but they are not translatable directly into clinical applications. By instrumented laxity tests, it is impossible to accurately determine in vivo initial joint position, motion constraints, applied forces, and measurement systems of load and displacement that the rigs would provide. Additionally, in vivo tests also measure unwanted and unquantifiable muscle activity, which is assumed to be null in rigs. It is important to emphasize that, as with all rigs, there can be unwanted results due to the motion constraint of the system (Blankevoort et al., 1988; Walker et al., 1985); for instance,

displacements imposed at the fixtures might be different from actual displacement at the centre of the joint, similarly for forces applied. For this reason, caution is needed when using displacement to describe the function of a ligament. To identify the guiding function of the ligaments within the envelope, the methodology used should measure the centre path without introducing unwanted external loads. Two are the available options: in the first method, computer-controlled robotic arms identify the position of the knee at flexion steps in which there are negligible resisting forces by a principle of minimization of energy (Li et al., 1999); the second method guides the knee into flexion using an apparatus with negligible friction (Wilson et al., 2000). These two experiments can describe the central path of motion within the envelope. Both methods allow for determining the guiding function of the knee structures and determining the laxity displacement at flexion angles as indicators of structure-function. As part of laxity assessments, envelope measures assess laxity across the entire range of motion and how far the knee can move without being passively restricted. Despite being suggested as an integral part of envelope assessment, the precise identification of the limits of the coupled motion representing the extremes of the envelope have not yet been identified. Differences between Wilson and Blankevoort studies, besides some variability attributable to sampling and sample size, need to be attributed to the methodology and different paths assessed; respectively the first central path within the envelope is also highly susceptible to small set-up differences, and the second along the more reliable boundaries of the envelope. Discrepancies in the results may have been attributed to methodological variations across studies, particularly different set-ups and methodologies employed; these variations encompass factors such as the body that was fixed (tibia or femur), the movement of the fixed body, the choice of measurement device and its estimated accuracy/error, the reference system used (anatomical or mechanical axes), and the convention adopted to describe the movement (helical axis, cardan angles, etc.).

To improve upon methods current ex vivo approaches for quantifying passive knee motion should: (1) assess knee passive motion experimentally capturing both the coupling between DoFs, of tibiofemoral paths, through multiple paths, possibly reliable paths on the boundaries of the unloaded envelope of passive motion, as well as the envelope of passive motion itself should be captured. In particular, a potential protocol involves flexion-extension medial-lateral (varus-valgus) stressed tests surgeon performs intraoperatively to assess gap balancing, by applying a medial and lateral force to the ductal tibia while flexing, defining an unloaded envelope; (2) use/propose accurate and robust methodology; in order to assess the method, assessment of the set-up, accuracy of the tools/devices, analysis of the error and uncertainties, should be performed along with the effect on the results; (3) In addition, standard approaches are needed; currently, different methodologies are employed in these studies, with different conventions, defining the axes of motion using different procedures, or reporting the movement using different frames (i.e., relative movement of the tibia to the femur, etc.), thereby leading to inherently different

measurements. This was the rationale behind the novel ex vivo approach that will be presented in the first study.

2.3.2 Influence Of Sex On Knee Mechanics

There is a well-documented discrepancy in statistics relative to the incidence and severity of knee ligament injuries, laxity, osteoarthritis, total knee replacement success rate, as well as pain level between males and females, in clinics and in a number of different literature studies (Arendt et al., 1999; Asaeda et al., 2017; Srikanth et al., 2005). This motivated the studies of sex-based differences in knee shape and function (Asaeda et al., 2017; Mills et al., 2013), with the aim of producing custom prosthetics or methodologies which would include differences between males and females. However, studies investigating anatomical or functional differences in the knee directly attributable to sex produced conflicting results.

While a few studies suggested there were differences in the knee anatomy and function due to sex, more recent studies have highlighted only a minor role of sexual dysmorphism of knee shape with the size probably influencing the conclusions of the previous studies (Asseln et al., 2018; Guy et al., 2012; Hitt et al., 2003; Mahfouz et al., 2007; Van den Heever et al., 2012; Varadarajan et al., 2009; Voleti et al., 2015). Males display a larger knee size (Conley et al., 2007; Hsu et al., 2021; Li et al., 2014; Van den Heever et al., 2012), larger knee flexor and extensor muscles (Behan et al., 2018; Blackburn et al., 2009) and larger femoral width to depth ratio (Asseln et al., 2018; Gillespie et al., 2011; Hitt et al., 2003; Hsu et al., 2021; Li et al., 2014) than women. Even though studies agree on sex-related differences in knee muscles, bone size and aspect ratio, morphometrical variations between males and females are still debated. Some studies highlighted different femoral trans epicondylar width (Han et al., 2016), contact area in the medial tibiofemoral compartment (Tummala et al., 2018), a less prominent anterior condyle and an increased Q angle in females (Conley et al., 2007; Mahfouz et al., 2007). However, by accounting for the effect of size, reported differences between the shape of the femur and tibia in males and females disappeared or were smaller, hence supporting the notion of modest sexual dysmorphisms of knee shape (Asseln et al., 2018; Dargel et al., 2011; Hsu et al., 2021; Li et al., 2014; Van den Heever et al., 2012; Voleti et al., 2015). Yet, experts have not reached a conclusion.

In vivo, studies during a number of activities showed how women experience higher knee loading than men and different knee kinematics during a variety of exercises (Baldon et al., 2013; Cronström et al., 2016; Graci et al., 2012; Obrebska et al., 2020; Ro et al., 2017; Sigward et al., 2013). While others found no differences (Pletcher et al., 2021; Tanikawa et al., 2013). During normal weight-bearing activity and side-step cutting manoeuvres, women exhibit higher knee abduction than their male counterparts while no differences were found along the remaining axes of motion (Cronström et al., 2016; James et al., 2004; Sigward et al., 2013). Interestingly,

tibiofemoral and ligament geometry in a cohort of elderly women described both the pattern and the variation of all the six axes of tibiofemoral motion while walking, except for a 2.7 – 2.8 mm anterior tibial shift during stance, in a younger mixed cohort (Martelli et al., 2020). Therefore, it appears that the different knee load and kinematics during exercise between males and females are likely attributable to sexual dysmorphisms in anatomical regions other than the knee (Audenaert et al., 2019) and differences in motor coordination (Wilson et al., 2015). As previously discussed, however, accuracy is not the strength of in vivo studies; those differences could be undetectable as smaller than noise/errors, or conversely could be underestimated. Some could be attributed to underlying model simplifications such as scaling, or propagation of errors due to soft tissues artefact for the different mass and fat distribution in men and women, or again misinterpreted with knee models with few degrees of freedom. Moreover, as the individual variability of the knee function is very high, it is hard to distinguish between differences due to individual variability between the groups or how much is attributed to sex, or again whether additional factors such as age and race could be influencing those results. Other differences that can affect knee injury rates and surgery success are the hormones that have been proven to affect the laxity of the joint, to explain further differences.

Ex vivo studies of the function have the potential to shine some light on this issue. As passive motion is directly the product of articular surfaces and ligaments, the investigation of the influence of sex on passive motion could help define differences, if present. However, ex vivo measurements of knee passive motion are most often limited to male cohorts (Cyr and Maletsky, 2014), or restricted to selected axes of motion (Belvedere et al., 2011; Blankevoort et al., 1988a; Eagar et al., 2001; Li et al., 2004; Nowakowski et al., 2012; Roth et al., 2015; Torzilli et al., 1994; Victor et al., 2010; Wilson et al., 2000; Wünschel et al., 2012). Moreover, studies mostly focus on laxity testing with a limited sample size (Blankevoort et al., 1988a; Eagar et al., 2001; Nowakowski et al., 2012; Roth et al., 2015). A recent study on the envelope of passive motion, while being extended to 28 knees, involved males alone (Cyr and Maletsky, 2014). Other studies did not report the sex, age, or conditions of the specimens (Wilson et al., 2000; Wünschel et al., 2012); some others used apparatus to measure the passive motion with different additional muscle loading-constraint conditions (Torzilli et al., 1994; Victor et al., 2010). Belvedere et al. (2011) investigated a passive motion path in a 22-specimen cohort, both males and females; however, it did not investigate sex differences, thereby leaving the envelope of passive motion in both sexes still unclear (Belvedere et al., 2011).

In conclusion, it is evident that sex has a strong influence on knee pathologies and treatments, with women reporting more pain, more injuries and more knee OA, and more successful surgery outcomes. There are contrasting reports in the literature regarding both knee anatomical sex-based differences and active knee function in vivo. Thus, the question regarding males and females is: are there any differences in active knee function between the sexes or are the tools not accurate

enough to detect these small differences? It is fundamental to carry out a more accurate ex vivo assessment of knee passive motion since studies of the envelope of knee passive motion have primarily focused on males only. Additionally, this would shed some light on the presence of anatomical variations at the knee, as passive knee motion is the direct result of the articular surface geometry and ligament constraints. This was the rationale behind the second study in which the novel methodologies will be applied to quantitively investigate knee passive motion population variability as well as differences between males and females.

2.3.3 Ligament Elastic Energy And Joint Response

Different assumptions and approaches are required for modelling the passive or active knee conditions, as they significantly differ, delivering consequently different outcomes. Therefore, passive, and active conditions are often represented by separate models. The tibiofemoral motion of the knee is three-dimensional and highly reproducible during passive flexion-extension (Blankevoort et al., 1990). Motion paths become reproducible and reliable along the envelope boundaries, but their behaviour changes under load outside the envelope. As passive motion is only guided by anatomy and soft tissues, mainly ligaments, and the geometry cannot change, this must be attributed to ligaments. While the body size and condylar geometry of the knee have been shown to be the main variables influencing anterior-posterior tibiofemoral translation (Smoger et al., 2015), ligaments and articular surface geometry accurately model passive knee flexion in three dimensions (Ottoboni et al., 2010). However, numerous unanswered questions persist regarding the role of ligaments and how their function changes when they contribute to both passive and active functions, particularly during the transition between the two. This raises the crucial question of which modelling approach is best suited to capture the intricate dynamics and interactions involved in studying ligament function, especially during the transition phase.

In theory, ligaments contribute to maintaining proper joint kinematics by guiding normal motions, by providing a passive mechanical restraint to prevent abnormal motions and thus elastic response to applied forces and displacement. It appears that tibiofemoral motion during less strenuous activities, like walking, is influenced by tibiofemoral geometry, as evidenced by the close agreement in mean and standard deviation of anterior tibial translation observed during normal walking and non-weight-bearing knee flexion in Myers et al. (2012) (Myers et al., 2012). However, it is important to acknowledge that several factors, including ligaments, muscles, and joint loading, contribute to knee kinematics, and differences may arise between weight-bearing and non-weight-bearing activities (Kefala et al., 2022). Compliant tibiofemoral joint models provide an elastic, load-dependent, representation of tibiofemoral motion and typically require complex model generation and solution processes (Gerus et al., 2013; Navacchia et al., 2019). For example, Navacchia (Navacchia et al., 2019) used knee geometry extracted from both CT and MRI images, and ligament material properties calibrated to in vitro laxity tests to iteratively solve the

tibiofemoral elastic and motion problem in 76–210 minutes for two participants executing a single stride and chair rise cycle. In contrast, rigid tibiofemoral joint models provide a load-independent representation of tibiofemoral motion and are therefore exclusively based on geometry. Rigid models enable computationally efficient analyses for large cohorts, multiple activities, and repeated tasks (Dumas et al., 2012; Ziaeipoor et al., 2019; Martelli et al., 2015; Arnold et al., 2010). Most often, a generic musculoskeletal model is scaled to each participant using measurements of inter-segmental lengths (Delph et al., 2007). On some occasions, tibiofemoral motion is represented by simple revolute, planar, and spherical joint models (Dumas et al., 2012; Martelli et al., 2015). On other occasions, tibiofemoral motion is modelled by more complex articulated joint mechanisms explicitly imposing the consistency between tibiofemoral motion, articular surface, and ligament geometry (Brito Da Luz et al., 2017; Barzan et al., 2019). Martelli compared the tibiofemoral motion in the model against corresponding measurements obtained during normal physical activity (Martelli et al. 2020). Variation of tibiofemoral geometry is a major determinant of tibiofemoral motion in healthy adults during normal activity because the tibiofemoral motion determined exclusively using geometrical information of the tibiofemoral joint described most of the variation in corresponding fluoroscopy measurements during walking. The major differences included the smaller range of knee flexion attributable to the age difference between the different cohorts measured (Favre et al., 2014). Also, the geometry-based tibiofemoral motion did not capture the anterior tibial shift during the early stance of 2.7–2.8 mm and early swing of 5.3 mm in the fluoroscopy measurement, which may be partially attributed to the knee compliance not included in the model. Nevertheless, the geometry-based tibiofemoral motion displayed similar variation to corresponding fluoroscopy measurements for all the six motion components and a similar pattern for five motion components, hence supporting the hypothesis that tibiofemoral geometry determines tibiofemoral motion during normal activity. The problem with such a small discrepancy becomes how much ligaments are contributing, if they do at all, and how to distinguish from other passive and active soft tissue contribute. This becomes particularly complex when different activities are investigated as well as for different individuals and across populations, requiring the use of faster and indirect modelling methodologies to investigate this passive to active soft tissue contributions to match predictions and measurements. The investigation into the passive to active contribution of ligaments to the motion was initially addressed by comparing the passive motion measurements of the unloaded envelope with in vivo tibiofemoral motion during gait in the latter study of the thesis. .

Ligament tissue modelling choices impact the simulation of knee kinematics and mechanics. Sensitivity studies of effect of ligament modelling on knee mechanics have also been investigated (Kiapour et al., 2011). Multiple techniques have been used for modelling the same ligament for this purpose. Kinematics and related outcomes such as have been predicted more accurately through continuum models, while spring elements provide acceptable outcomes with a

computationally faster and less expensive approach (Beidokhti et al., 2017; Naghibi et al., 2019). Regardless of the model used whether it is 1D, 2D, 3D, or from the constitutional model used, a deep inconsistency emerges from this section concerning ligament elasticity. The hypothesis in all these studies was that ligaments provide an elastic contribution, and as such they would dissipate energy to transfer or spread load. Despite the minimal force exerted by gravity in unloaded or passive conditions, the reduced load compared to weight-bearing or active situations means that ligaments remain slack within the knee passive motion envelope, resulting in minimal tension and limited engagement in load transfer. Thus, the unresolved question is how can there be ligament pre-tensioning, stress and strains, or in situ strains, if there is no load that must be transferred in unloaded or passive conditions? All these questions raise an interesting perspective on the ligaments' role during unloaded and passive behaviour, and it suggests the ligaments do not provide much in the way of elasticity, but rather are merely containment networks of normal movement, producing a negligible counterpart in terms of effect on forces and movement, while the real contributions to elasticity are provided by the active components such as tendons and muscles. Most modelling approaches, including even the most basic ones like elastic strings, require detailed ligament representations, extensive data, and complex simulation. However, despite the availability of indirect measurements of ligament structures, such as investigating compliance or stiffness parameters, this also highlights a limitation in modelling approaches.

To conclude, the discrepancy between tibiofemoral motion quantified by biplanar fluoroscopy and the motion generated by geometry-based models has been potentially attributed to the knee joint elasticity, which is influenced by ligaments as well as passive and active soft tissue constraints. Since anatomically detailed elastic foundation knee models are time-consuming, computationally expensive, and require extensive data and expertise to build, no population studies have investigated the individual variability in tibiofemoral joint elasticity. A similar issue prevents their clinical translations as in silico medicine into applications for diagnoses of knee joint pathologies and treatments. Also given the fact that the compliance matrix implicitly encloses this information in a few parameters, this provided the rationale for the third study in which a novel joint elastic MSK model will be presented; in this model, compliance matrices have been used as a means for a more efficient approach to the modelling of the tibiofemoral joint elasticity.

Chapter 3

STUDY 1

Unloaded Knee Passive Motion Envelope: A Novel Ex Vivo Methodology For Determining And Quantifying The Medial And Lateral Extremes

CONTENTS

F. Bucci, M. Taylor, R. Al-Dirini, S. Martelli (2023) – A novel methodology to capture the envelope of knee passive motion. Technical Note. Journal of Orthopaedic Research. *In preparation for submission to peer-reviewed journal.*

Please refer to the appendices for a detailed outline of the author's contribution to this study (Appendix A), for the feasibility study on the use of this methodology in assessing knee passive motion before and after TKR (Appendix B) and for specimen-specific experimental extremes of the knee passive motion (Appendix C).

3.1 Abstract

Experimental measurements of tibiofemoral passive motion provide insights into understanding knee function for improving diagnoses, design, and assessment of surgical procedures for treating knee injuries and diseases. Previous studies have focused on a single central representative path of tibiofemoral passive motion or on knee laxity assessments, with a small sample size, selected motion axis, and/or a limited range of flexion. In studies of knee laxity, the knee passive motion is defined as an envelope, which does not fully explain the widely reported coupling between internal tibial rotation and flexion. A single representative central coupled path, however, cannot capture the envelope and is highly sensitive to small changes in the experimental setup. As of yet, no studies have been conducted on capturing and relating multiple coupling paths and the envelope of the knee passive motion. Therefore, this study aimed to develop a novel ex vivo methodology to quantify the two 6 DoFs tibiofemoral coupled varus and valgus flexion paths, corresponding to medial and lateral extremes of the unloaded knee passive motion envelope, in intact knee specimens. By combining motion capture, custom 3D printed potting, and medical imaging to accurately reconstruct the TF motion, this approach mimics stressed flexion-extension tests to achieve gap balancing performed by surgeons applying lateral and medial forces to the distal tibia. A comprehensive methodological assessment of this methodology was conducted for the analysis of errors, accuracy, and reliability.

The novel methodology was developed on a cohort of six intact knee specimens. Reflective markers were placed on dedicated features of custom 3D printed potting cups created from the tibia and femur from CT scans. Two trials, five repetitions each, of complete flexion-extension were performed by manually applying a medial and a lateral force to the femur. The marker trajectories were recorded using a stereo photogrammetric motion capture system. Six degrees-of-freedom tibiofemoral kinematics were captured and reconstructed, grouped by medial and lateral motion. The effect of the variability of the manual force on the results was investigated, virtual markers reconstruction estimated, and the automated reference system identification process validated using a full lower limb specimen, including the hip and ankle. Reliability of the experimental curves was measured; the medial and lateral extremes were compared with a central representative path and against other passive motion studies in literature.

This protocol can be used to investigate the individual tibiofemoral passive motion. Medial and lateral extremes of the unloaded knee passive motion envelope were reported for the first time. The method underwent evaluation, including error quantification and comparison of the results of the inferred neutral path, which demonstrated consistency with previous investigations. These objective findings strengthen the credibility of this methodology for investigating population variability and the influence of sex in knee joint mechanics.

3.2 Introduction

Diagnostic and surgical tools for treating knee injuries and diseases rely on assessment and reestablishment of knee passive motion to restore the native joint function (Goodfellow et al., 2002; Martelli et al., 2020). During knee arthroplasty, passive motion is assessed intraoperatively, both before and after ligamentous balancing, to minimise potential medial and lateral gap mismatches (Bottros et al., 2006). Stressed flexion-extension tests are performed by the surgeon applying a medial and lateral force to the distal tibia, aiming at an evenly balanced joint gap characterized by a parallel track during flexion-extension in the navigation software (Ishii et al., 2005; Sheth et al., 2017). An extensive ongoing research effort is dedicated specifically to the envelope of passive motion, boundaries defining a slack region within which interventions would not alter the function of ligaments. (Blankevoort et al., 1988). Furthermore, abnormal boundaries of the passive motion envelope indicate a potential ligament injury, manifested often as different stiffness or manual 'feel' during clinical evaluations of knee laxity (Jakob et al., 1987; Jensen et al., 1990; Losee et al., 1994). Accurate measurements of the passive knee motion extent assist in understanding individual tibiofemoral function, thus improving both ligament injury diagnosis and knee surgical treatments (Cyr and Maletsky 2014; Roth et al., 2015). Yet, accurate quantification of the extent of the envelope of passive knee motion and its variability across population are scarce and mainly limited to male populations.

Several approaches have been used to assess passive knee motion with varying levels of accuracy and different results. Clinical assessments of knee laxity (e.g., anterior-drawer or pivot-shift tests), both instrument-guided and manual, resulted in inconsistent measurements between arthrometers, (Anderson et al., 1992; Pugh et al., 2009) intra- and inter-rater variability (Cannon et al., 2002). More accurate quantitative ex vivo investigations included the use of arthrometers (Anderson et al., 1992; Pugh et al., 2009), surgical navigation systems (Martelli et al, 2007; Belvedere et al., 2011; Athwal et al., 2014), and ad-hoc testing rigs and robotic simulators, at times combined with medical imaging and/or motion capture systems (Wilson et al., 2000; Cyr and Maletsky 2014; Roth et al., 2015). These studies investigated either a few degrees of freedom, limited flexion ranges or a single passive motion task performed, often with a limited sample size (Blankevoort et al., 1988; Wilson et al., 2000; Eagar et al., 2001; Victor et al., 2010; Nowakowski et al., 2012; Roth et al., 2015; Cyr and Maletsky 2014). Belvedere et al. (2011) investigated ex vivo a central path of passive flexion through pulleys with a surgical navigation system (Belvedere et al., 2011). Another study investigated the knee laxity envelope through manual manipulations and force sensors (Cyr and Maletsky 2014). Others were performed with the help of motion capture systems (Wilson et al., 2000; Cyr and Maletsky 2014), or again x-ray and bone-pins (Walker et al., 1988), or with a range of static, Oxford-style or horizontal rigs, as well as robotic manipulators (Blankevoort et al., 1988; Wunshel et al., 2012; Liu et al., 2014).

These ex vivo cadaveric studies assessing and measuring knee passive motion generally either investigated knee laxity in order to determine joint resistance at specific flexion angles, investigating each degree of freedom separately (Blankevoort et al., 1988; Cyr and Maletsky 2014; Roth et al., 2015), or measured the secondary degrees-of-freedom coupling of a nominal unloaded central path of flexion within the envelope (Wilson et al., 2000; Belvedere et al., 2011). Combined studies of passive motion coupling envelope, and related laxity, can provide further insight into the tibiofemoral joint and knee ligament function, and potentially mimic flexion-extension medial-lateral (varus-valgus) stressed tests. As of now, no current ex vivo approaches implemented or considered these stressed tests. Furthermore, no ex vivo method has yet been developed to investigate multiple coupled tibiofemoral paths nor to capture both coupling and envelopes of knee passive motion.

The literature on ex vivo passive knee motion is extensive; yet only a few studies have conducted methodological analyses to quantify errors and uncertainties involved with experimentally capturing tibiofemoral joint motion. Studies that employed surgical navigation systems reported manufacturer accuracy, typically ±0.5 mm or ±0.5°; however, they did not account or accurately include analysis of the set-up variability, i.e., distance of markers from tracking device, operator variability in estimation of bony landmarks or experience with the system (Belvedere et al., 2011; Gosh et al., 2014). Similarly, studies of robot systems reported primarily the accuracy declared by the manufacturer; Goldsmith et al., (2014) reported among the other errors the accuracy and repeatability of a robotic system in finding a passive unresisted flexion path, 0.23 mm and 0.55° intra set-up and 0.79 mm and 1.2° after removing and reposing the knee (Goldsmith et al., 2014). In addition to the inherent importance of ensuring that measurements are reliable and accurate, quantifying the effect of set-up variability on these measurements is crucial for analyses such as population variability. Wilson et al. (2000) observed that small changes in experimental set-up caused undesired variability in kinematics when measuring a single representative passive flexion path, as occurs in the slack area within the envelope, therefore reiterating the need of investigating the envelope full extent (Wilson et al., 2000); moreover, despite relatively low rotational error (0.2 degrees), translational error was not-negligible (1.8 mm and 0.6 mm) (Wilson et al., 1996). Comparing the passive motion results from different studies, with different rigs and measurement techniques, adds another level of complexity. Hacker et al. (2016) compared tibial rotation results obtained from different simulators (i.e., Oxford-style, horizontal rigs, and robotic manipulator) using various measurement conventions (i.e., Euler, Grood and Suntay, etc.); the conclusion was that thorough reporting of these experiments is critical, comparability is limited, and results should not be used clinically with average curves potentially useful as knee modelling boundaries (Hacker et al., 2016). Therefore, though few ex vivo studies of knee passive motion report extensive analysis and quantification of errors and uncertainties, their investigation is crucial.

The aim of this work was to develop a novel ex vivo protocol to improve upon methods knee passive motion measurements. Two tibiofemoral coupled varus and valgus flexion paths were capture by applying a medial and lateral force on the free tibiofemoral extreme; these paths respectively correspond also to medial and lateral extremes of the unloaded knee passive motion envelope. This approach was inspired by the tests conducted by surgeons to achieve gap balancing and included the investigation of both multiple coupled paths as well as unloaded envelopes of knee passive motion. For the first time, the TF motion was reconstructed using motion capture analysis combined with medical imaging and custom 3D printed potting cups, designed according to the anatomy of the knee articular surfaces. A comprehensive methodological assessment of this methodology was conducted. Therefore, this study aimed at (1) accurately quantifying medial and lateral extremes of the knee unloaded passive motion envelope in 6 degrees of freedom in cadaveric intact knee specimens and (2) conducting analysis of errors-uncertainties, investigating accuracy, and reliability. Although initially designed for investigating the function of the native knee in intact conditions, this technique has the potential to assess the extremes of the knee passive motion in injured, pathological, and surgically treated knees (e.g., knee arthroplasty). A preliminary feasibility study was conducted before and after knee replacement, and its findings are reported in Appendix B. Furthermore, since the only knee-specific step involved defining the joint coordinate system, this methodology can potentially be applied to various joints with six degrees of freedom.

3.3 Material And Methods

Figure 3.1, included in the "Materials and Methods" section of this study, provides a comprehensive visual representation of the developed protocol and its methodological assessment. By presenting an overview of the protocol development process and its evaluation, Figure 3.1 enhances the clarity and understanding for readers. It serves as a valuable reference to grasp the sequential progression of the protocol and its evaluation effectiveness.

The methodology comprises several essential steps, each contributing to the accurate measurement of passive knee motion. The first step involves imaging and preparation of the knee specimens using custom 3D printed holders (Step 1). Subsequently, the experimental set-up, protocol, and data collection are conducted (Step 2). The next phase involves the virtual reconstruction of the specimen's kinematics (Step 3). Finally, kinematic processing is performed to evaluate the accuracy and confidence of the passive motion measurements (Step 4).

The methodological assessments encompass various aspects critical to the reliability and validity of the proposed approach. These assessments include the identification and understanding of potential sources of error and uncertainties, such as evaluating the impact of variability in manually

applied force. The analysis of errors in marker reconstruction and the accuracy of the anatomical reference system are also explored. Furthermore, the reliability of experimental kinematics is assessed, and comparisons are made with existing literature to validate the findings. Additionally, the inferred central neutral kinematics are compared with experimental measurements to determine the accuracy and consistency of the approach. Each assessment contributes valuable insights into the accuracy, limitations, and potential improvements of the methodology, ultimately strengthening the validity of the findings of this study.

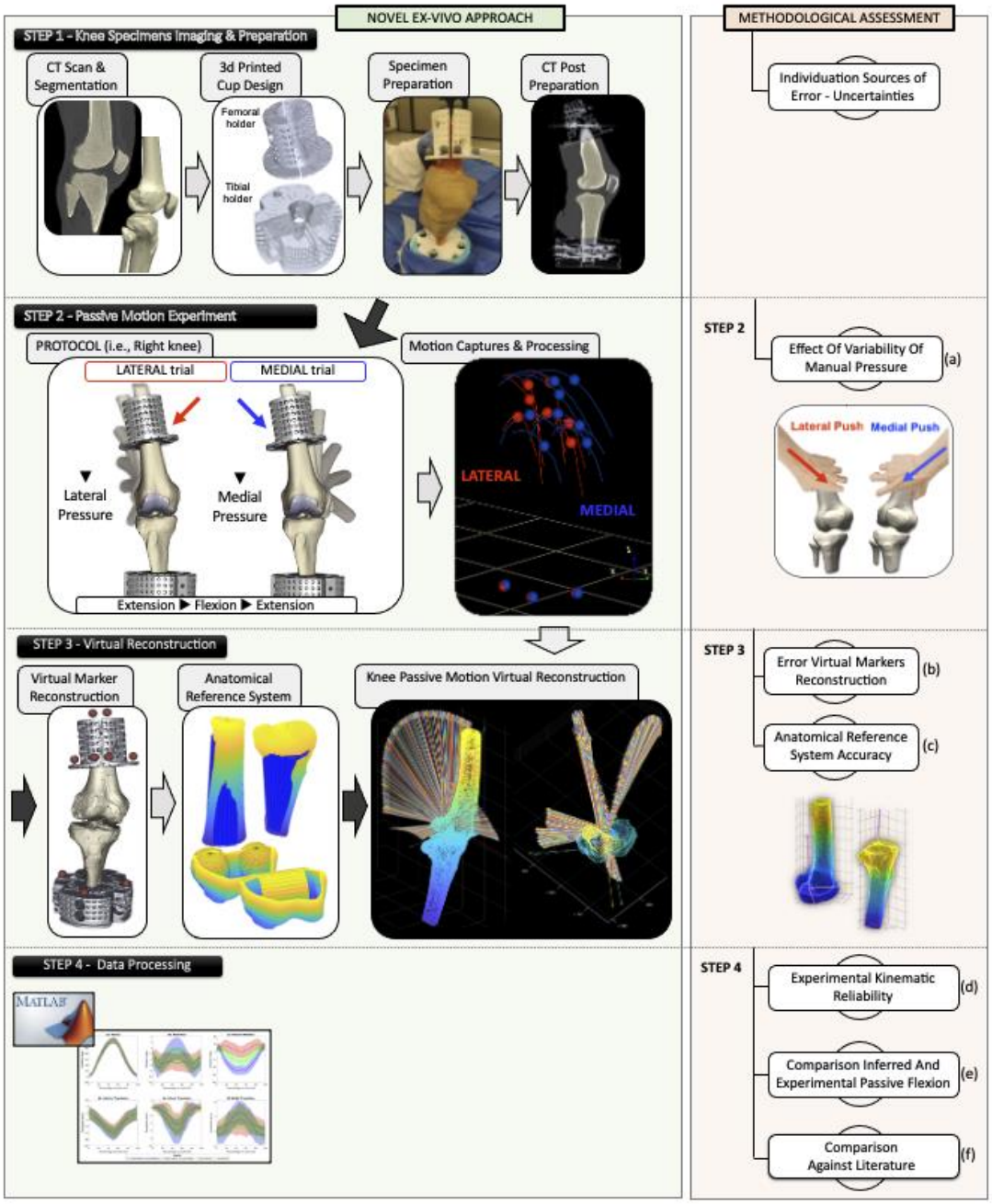

Figure 3.1 *– Novel ex vivo approach and methodological assessment: Step 1 - Specimen imaging and preparation with custom 3D printed holders, Step 2 - Experimental set-up, protocol, and data collection with subpart (a) assessing the variability of manual force applied, Step 3 - Virtual reconstruction and assessment of errors, including (b) marker position and (c) anatomical reference system, and Step 4 - Kinematic processing and confidence in passive motion measurements, incorporating (d) reliability, (e) validation of the neutral trial, and (f) comparison against literature.*

3.3.1 Knee Specimens, Imaging And Preparation

Six fresh frozen intact cadaveric knee specimens, (3 males - 3 females, age = 62 ± 15 years, BMI = 28.2 ± 6) were used. Mid-thigh to mid-shank knee specimens were obtained from a body donation program (Science Care, Phoenix, USA). Ethics approval was obtained from the Social and Behavioural Research Ethics Committee (SBREC) at Flinders University (project number 6832). The exclusion criteria primarily focused on individuals with a history of knee surgery, osteoarthritis, or musculoskeletal conditions affecting normal ambulation for at least one year before death. Furthermore, a BMI criterion above 30 kg/m^2 was applied to prioritize the selection of individuals with better mobility and a lower risk of osteoarthritis. It is worth noting that only one specimen with a higher BMI (BMI = 39.22) was included in the study, while the remaining specimens fell within the intended BMI range. This approach guarantees a more consistent and physically fit study cohort for studying knee joint mechanics in healthy individuals.

Knee specimens were scanned using clinical CT scanners (SOMATOM Force, Siemens Healthcare Sector, Forchheim, Germany; tube voltage 70 - 150 kV; tube current 220 mA) providing an in-plane isotropic pixel size equal to 0.33 mm and 0.3 mm slice thickness (Fig. 3.2-a). CT images of each knee were taken before the specimen preparation and included almost two third of distal femoral and proximal tibial shafts. Bones geometries and cartilage was segmented using Scan IP software (Simpleware ScanIP, Synopsis, Mountain View, California, USA).

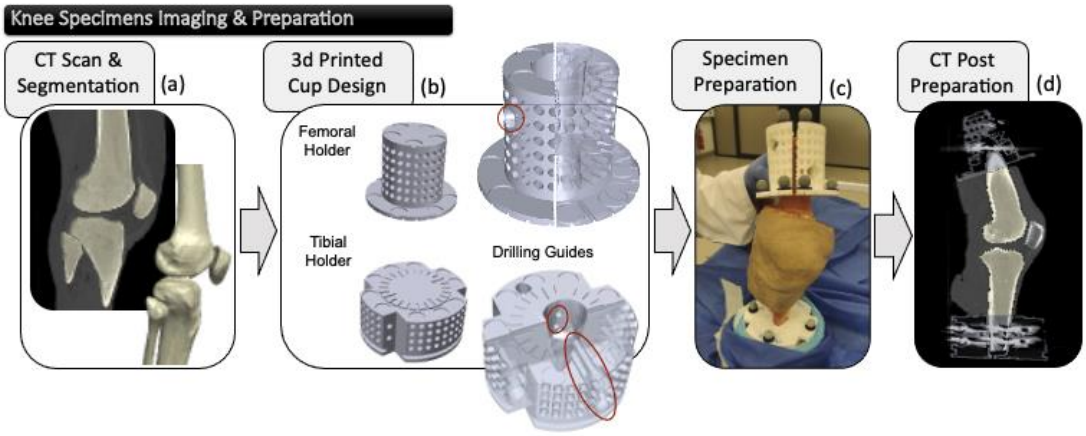

Figure 3.2 *– Imaging and preparation workflow of intact cadaveric knee specimens: (a) CT imaging and segmentation, (b) design of femoral and tibial holders, (c) fixation and preparation using 3D printed holders, and (d) CT scan post-preparation.*

Custom tibial and femoral holder were modelled using Ansys Space Claim software for each specimen (ANSYS, Canonsburg, Pennsylvania, USA) (Fig. 3.2-b). The interfaces between holders and bones were defined by performing a Boolean subtraction of the femoral and tibial individual geometries from the femoral and tibial holder designs. As part of the design, the tibial and femoral holders (in full extension) were designed to align with the joint coordinate system; this is important to know the tibial plateau alignment. Circular 2 mm deep features were created on both the femur and tibia holders for hosting the reflective markers in the motion analysis experiment. A two-part

design was used for holders; drilling guides were included into the design of the holders in predetermined positions (Fig. 3.2-b, highlighted in red circles). The distance from the joint centre to the most proximal point on the femur holder and to the most distal point on the tibia holder were set to 180 mm and 170 mm, respectively. The tibial and femoral holders were 3D printed with Ultimaker 2+ (PLA filament, nozzle 0.4 mm, layer height 0.4 mm, wall thickness 1.5 mm, top/bottom thickness 1mm, infill density 30%, infill pattern grid, brim plate adhesion).

Specimens were thawed for 24 - 36 hours at room temperature. Soft tissues were removed from the distal tibial and proximal femoral ends, with a transversal cut, leaving the knee joint intact. The specimen holders were mounted to the distal femur and proximal tibia bones by aligning the anatomical features of bone with corresponding negative features in the 3D printed specimen holder. The fibula was cut distally below the 3D printed support. Two holes were drilled in the predetermined locations of femur and tibia through the drilling guides. Stainless steel screws were used to lock the specimen holders in position and tighten together the two parts of each holder together with the bones. (Fig. 3.1-c).

The specimen-holders assembly were CT scanned at 40 keV (Fig. 3.2-d) for providing the best contrast between PLA and cortical bone for the purpose of segmenting the bones and the specimen holder. A Metal Artefacts Reduction algorithm (MAR, Siemens, Siemens Healthcare Sector, Forchheim, Germany) was applied to the images for minimizing the screws metal artefacts. Femur, tibia, and holders were segmented (ScanIP, Synopsis, Mountain View, California, USA).

3.3.2 Passive Motion Experiment

The passive motion experiment was conducted in a motion analysis laboratory equipped with a 10-camera motion capture system (VICON, Oxford Metrics Group, Oxford, UK) (Fig. 3.3). A specialized Vicon calibrating device was used to accurately calibrate space and to set the origin of the laboratory space on the floor at the centre of the laboratory space. A table was placed at the origin of the laboratory reference system. The tibia was fixed to the table; the tibial holder was secured with screws to a cup clamped to the table surface. Reflective markers were placed on the circular features on the femoral and tibial holders. A minimum of ten reflective markers were fitted per specimen, three on the tibial cup and seven (or more) on the femoral holder, distributed over their markers' features. The same operator performed all manipulations for consistency and to not introduce intra-operator error. A metronome was used to ensure consistency capturing two passive motion trials. With the tibia fixed to the table and the femur unconstrained and free to move, two passive motion trials were performed by manually manipulating the femoral holder, after preconditioning, according to the protocol described below. The trajectories of the reflective markers were recorded with a 10-camera motion capture system (VICON, Oxford Metrics Group, Oxford, UK) (Fig. 3.3). Markers were manually labelled, and marker trajectories were

processed using Nexus software (VICON, Oxford Metrics Group, Oxford, UK), low pass filtered (fourth-order Butterworth filter, 10 Hz cut-off frequency) and resampled to one hundred frames per cycle using MATLAB (MathWorks, Natick, USA) (Fig. 3.3).

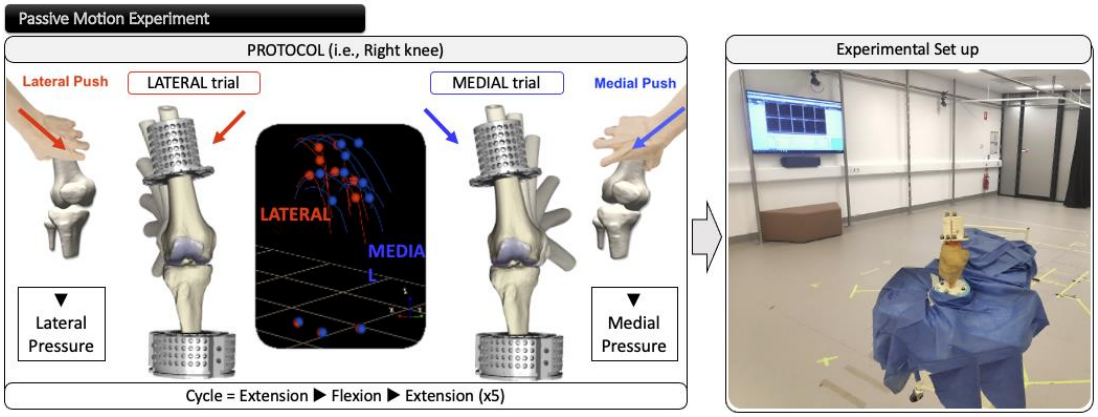

Figure 3.3 *– Visual representation outlining the experimental passive motion protocol, trajectories illustrating the two extremes in passive motion, along with a photograph documenting the experimental set-up in the laboratory.*

Passive Motion Protocol

The passive motion protocol consisted of two trials, as depicted in Figure (Fig. 3.3). The experimental manipulation involved moving the femur within the flexion-extension range while applying medial and lateral force and experiencing resistance to varus and valgus movements.

- In the medial trial, the femur was initially positioned in full extension with medial force applied. It was then moved throughout the flexion range, reaching full flexion before returning to extension, while maintaining a consistent taut feel. Throughout this trial, consistent medial tension was maintained, representing a varus passive flexion path that corresponds to the medial extreme of the unloaded envelope of knee passive motion.

- Similarly, in the lateral trial, the femur was positioned in full extension with lateral force applied. It was then moved throughout the flexion range, reaching full flexion before returning to extension, while maintaining a consistent taut feel. Throughout this trial, consistent lateral tension was maintained, representing a valgus passive flexion path that corresponds to the lateral extreme of the unloaded envelope of knee passive motion.

During the trials, the hand did not encircle or grip the holder. Instead, it solely supported the bottom portion of the holder to control the pace of flexion, while also applying the aforementioned medial and lateral force to minimize rotational constraints and avoid unnecessary restrictions.

These cycles of extension-flexion-extension were then repeated and captured five times for each trial and for each knee. The preconditioning process consisted of five cycles before each trial was captured. The maximum flexions and extensions were subjectively identified based on the

resistance offered by the knee to the manipulation performed during these trials. Therefore, as a potential set-up variable, the effect of the variability of this force applied and its impact on the knee kinematics was assessed.

Effect Of Variability Of The Manual Force On The Results

During the medial and lateral trials, a force was manually applied by hand to the femoral holder, as described previously in the experimental protocol. As the force was manually applied to the femoral holder, the effect of the variability of this force and its impact on the kinematic results was evaluated. Medial and lateral data were collected by pressing against the femoral holder, in the medial and lateral direction, using increasing force.

The manual force applied was measured through a uniaxial load sensor (max capacity 50N, accuracy 0.00981N). Two levels of force were evaluated: a nominal medial push, measured while maintaining femur extension, and a higher force trial achieved by pressing further and applying more force until the feeling of resistance was encountered in the extreme medial position. The same experienced operator performed all manipulations.

The effect of this variability on the tibiofemoral kinematics was quantified as marker trajectories mean and standard deviation error. Statistical differences due to the manual force variability were investigated using a two-tail t-test with statistical parametric mapping (alpha = 0.01, SPM, MATLAB toolbox).

3.3.3 Virtual Reconstruction Of Knee Kinematics

A custom pipeline was used to reconstruct the medial and lateral knee kinematic for each specimen (Fig. 3.4).

The first step required for the reconstruction of the passive motion is the virtual markers in the segmented holders from CT post-preparation (MATLAB, MathWorks, Natick, USA) (Fig. 3.4-a). As the virtual reconstruction procedure of the marker position on segmented 3D printed cups have the potential to generate an error, this procedure and estimation of the error were described and discussed in the subsection below.

Once the virtual markers were recreated in the reference system of the CT image, a registration procedure was used to collocate the femoral and tibial bones and holders into the laboratory environment. NMS Builder was used to register the virtual markers onto the experimentally captured markers in full extension (NMS Builder 2.1v, IOR, Bologna, Italy). As part of this registration, the articular surfaces and holders were moved with the markers to their initial positions (Fig. 3.4-b).

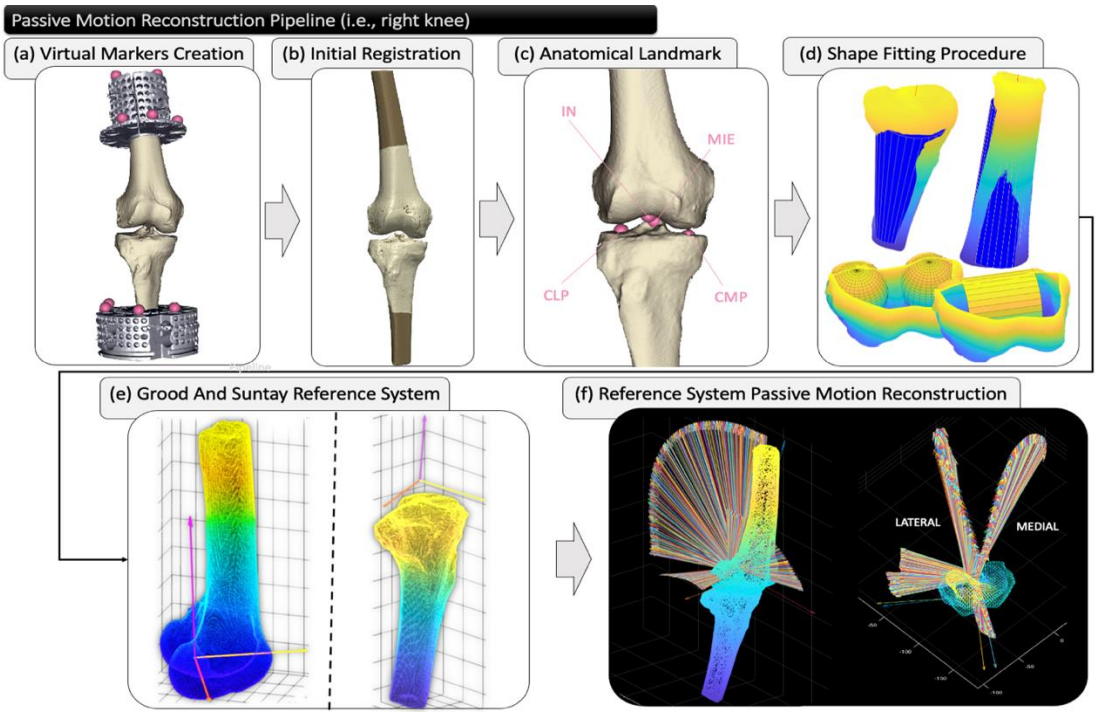

Figure 3.4 *– Flowchart depicting the sequential process for the virtual reconstruction of knee passive motion: (a) creation of virtual markers, (b) initial registration within the laboratory space, (c) virtual palpation of anatomical landmarks, (d) automatic shape fitting, (e) identification of the reference system based on Grood and Suntay (1983) denoted by the red x-axis, the magenta y-axis, and the yellow z-axis, and (f) reconstruction of the reference system across the medial trial.*

Custom MATLAB code was developed to automate the identification of the tibiofemoral passive motion. Grood and Suntay anatomical reference system (Grood and Suntay, 1983) was identified following an earlier procedure to account for the absence of the distal tibia and the proximal femur (Gray et al., 2019). The virtual palpation of four bony landmarks including the Intercondylar notch (IN), mid intercondylar eminence (MIE), medial and lateral centre of the tibial plateau (CMP – CLP) was performed (NMS Builder 2.1v, IOR, Bologna, Italy) five times by the same operator and the results averaged. (Fig. 3.4-c). Automatic shape fitting in MATLAB (MathWorks, Natick, USA) was used to fit truncated cones to the femoral and tibial shaft, spheres to the femoral condyles, and a cylinder was fitted to the two spheres of the femoral condyles (Fig. 3.4-d). The femoral x-axis was identified as the main axis of the cylinder. The femoral origin was located at the foot of the perpendicular between IN and the femoral x-axis. The femoral y-axis was the perpendicular between femoral shaft axis and x-axis. Finally, the femoral z-axis was the orthogonal to the femoral x- and y-axis. The tibial z-axis was parallel tibial shaft axis passing through MIE. Tibial origin was the foot of the perpendicular between femoral origin and tibial z-axis in full extension. The tibial x-axis was orthogonal to tibial z-axis and to the line passing through CLP and CMP. Tibial y-axis was orthogonal to tibial x and z-axis. The figure depicts a visual representation of the tibial and femoral reference systems, wherein the respective axes for the femur and tibia are identified by the red x-axis, magenta y-axis, and yellow z-axis (Fig. 3.4-e). The position of femoral and tibial reference system and articular surfaces was reconstructed, for each frame and cycle of both medial and lateral trials, by registering the virtual markers with experimental marker trajectories, in

MATLAB (The MathWorks, Natick, USA), through an ICP (Iterative Closest Point) algorithm (Fig. 3.4-f).

Reconstruction And Errors Associated With Virtual Markers

The pipeline for the virtual marker reconstruction consisted of three steps. Bones and holders were segmented from the CT images (Simpleware ScanIP, Synopsis, Mountain View, California, USA) (Fig 3.5 - step 1 pipeline). Markers position was determined in the segmented cups through sphere fitting of the circular features (MATLAB, MathWorks, Natick, USA) (Fig. 3.5 - step 2 pipeline). The centre of the reflective markers was determined by offsetting the sphere centres along the plane where circular features lie, by the marker height and minus the diameter of the marker (NMS Builder 2.1v, IOR, Bologna, Italy). The diameter and height of 10 markers were measured using a vernier calliper and averaged over three repeated measurements; the markers' offset was calculated as the sum of plate offset measurements and of the markers' radius. The calliper measurements were reported as means and standard deviations. Three reference systems were created, one for the tibial and two for femoral holders, to individuate the direction perpendiculars to the surface of the markers features (Fig. 3.5 - step 3 pipeline).

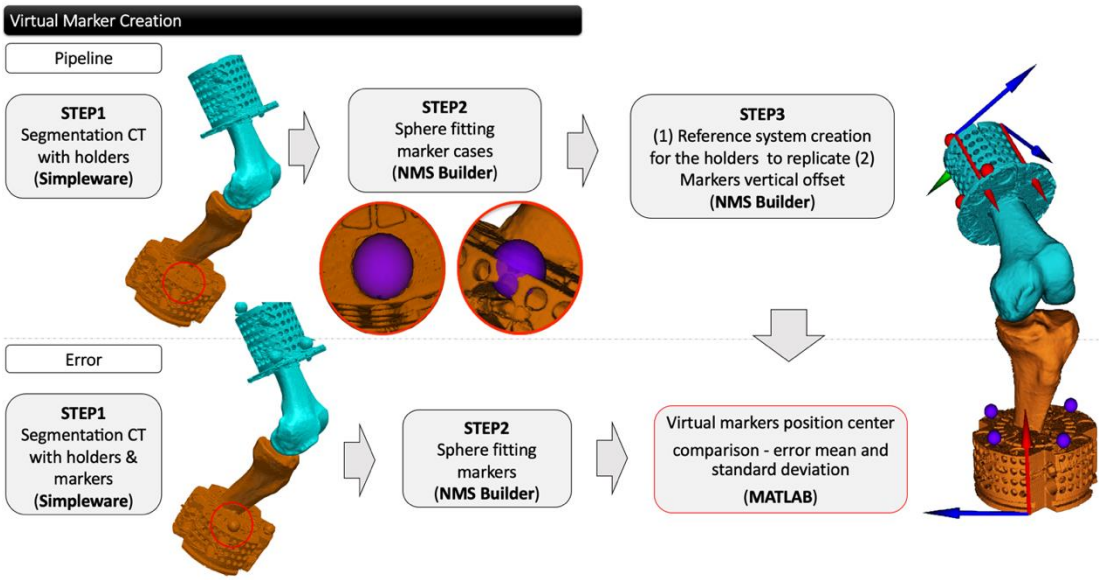

Figure 3.5 *– Diagram illustrating the process of recreating virtual marker positions (top) through image segmentation, shape fitting, reference systems, and detailed marker measurements, and estimating the introduced error (bottom) by comparing against markers captured and segmented in position during CT scanning.*

The necessity of creating two reference systems for the femoral holder comes from a misfit of the two parts of holder fixed to the femur (Fig. 3.6 - right); the misfit was evident in a few specimens, while most reported a visually good fit between custom 3D printed holders and bones (Fig. 3.6 - left). This uneven fit was caused by mineralized periosteum along the Linea Aspera, along with 3D printed imperfections and difficulties in the drilling-mounting procedures and did not concern tibial holders, therefore potentially affecting all specimens to varying degrees. The cases reported

in figure were the best- and worst-case scenarios; in the latter, a radial separation was present between the two halves of the femoral holder, in addition to a small step-off (Fig. 3.6).

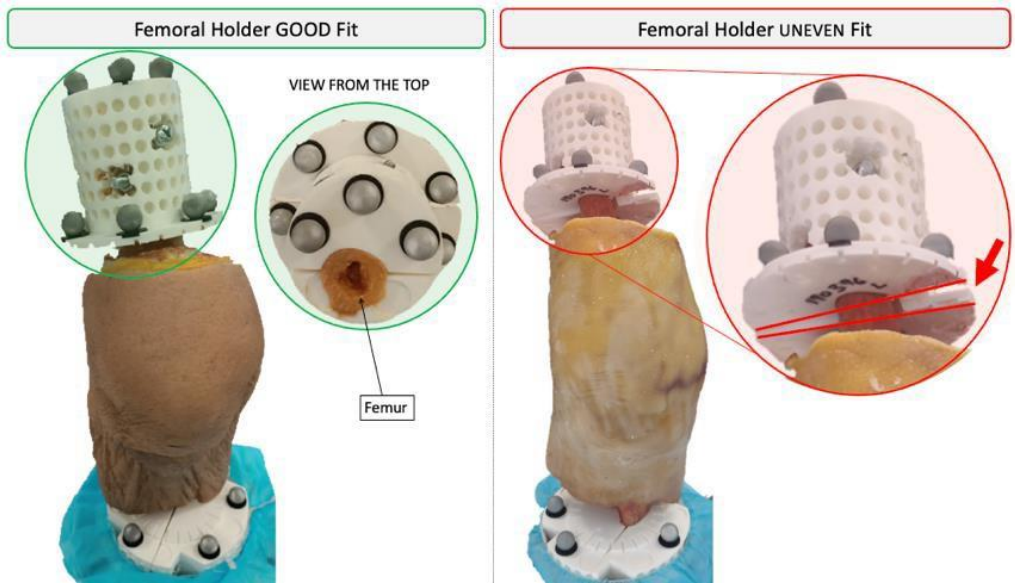

Figure 3.6 *– Post-specimen preparation view of cadaveric knees: a well-fitted femoral holder on the right side in green, and an uneven fit with radial displacement between two holder halves on the left side in red.*

The potential error generated by the virtual markers' reconstruction was estimated as the distance between the markers virtually reconstructed and from the CT scan directly segmented. For one of the specimens, the assembly with the experimental passive reflective markers was CT scanned (40 keV - MAR, Siemens, Siemens Healthcare Sector, Forchheim, Germany) and the markers segmented (Simpleware ScanIP, Synopsis, Mountain View, California, USA) (Fig. 3.5 - step 1 error). The centre of sphere fitting each of the marker segmented was individuated (NMS Builder 2.1v, IOR, Bologna, Italy) (Fig. 3.5 - step 2 error). The estimate of the overall error was obtained by calculating the average of the distances between the centres of the virtual markers and the centres of the CT-scanned passive-reflective marker (Fig. 3.5 - step 3 error).

The Effect Of Missing Distal Tibia And Proximal Femur On The Anatomical Reference System

A full fresh frozen lower limb (male, right, age = 80, BMI = 26.6) was obtained from a body donation program (Science Care, Phoenix, USA). For this specimen, the individuation of the reference system was performed using both the procedure directly reported by Grood and Suntay (GS) (Grood and Suntay, 1983) and that by Gray and co-workers (Gray et al., 2019).

The full lower limb specimen was scanned with a specific medical preoperative MRI knee protocol (Signature-PSI Knee MRI Protocol for Siemens Scanners – Zimmer Biomet, Warsaw, Indiana, USA). This protocol provides low-resolution scan of the hip, knee, and ankle (MAGNETOM Skyra 3T, Siemens Healthcare Sector, Forchheim, Germany) (Fig. 3.7-a). Bones were segmented

in the MRI images using Scan IP software (Simpleware ScanIP, Synopsis, Mountain View, California, USA).

Specimen were thawed for almost 48 hours at room temperature. Hip and foot were resected with a transversal cut around mid-thigh and mid-shank; after resection, the specimen included almost two third of distal femoral shaft and of the proximal tibial shaft. At this point, the protocol preparation reported at the section 3.3.1 was repeated step by step. The knee specimen was CT scanned (SOMATOM Force, Siemens Healthcare Sector, Forchheim, Germany) and bones segmented (Simpleware ScanIP, Synopsis, Mountain View, California, USA) (Fig. 3.7-b). Custom tibial and femoral holder were designed (ANSYS, Canonsburg, Pennsylvania, USA), 3D printed and mounted. The specimen and holder assembly after preparation was CT scanned (40 keV-MAR, Siemens, Siemens Healthcare Sector, Forchheim, Germany) (Fig. 3.7-c). Femur, tibia, and respective holders were segmented using Scan IP software (Simpleware ScanIP, Synopsis, Mountain View, California, USA).

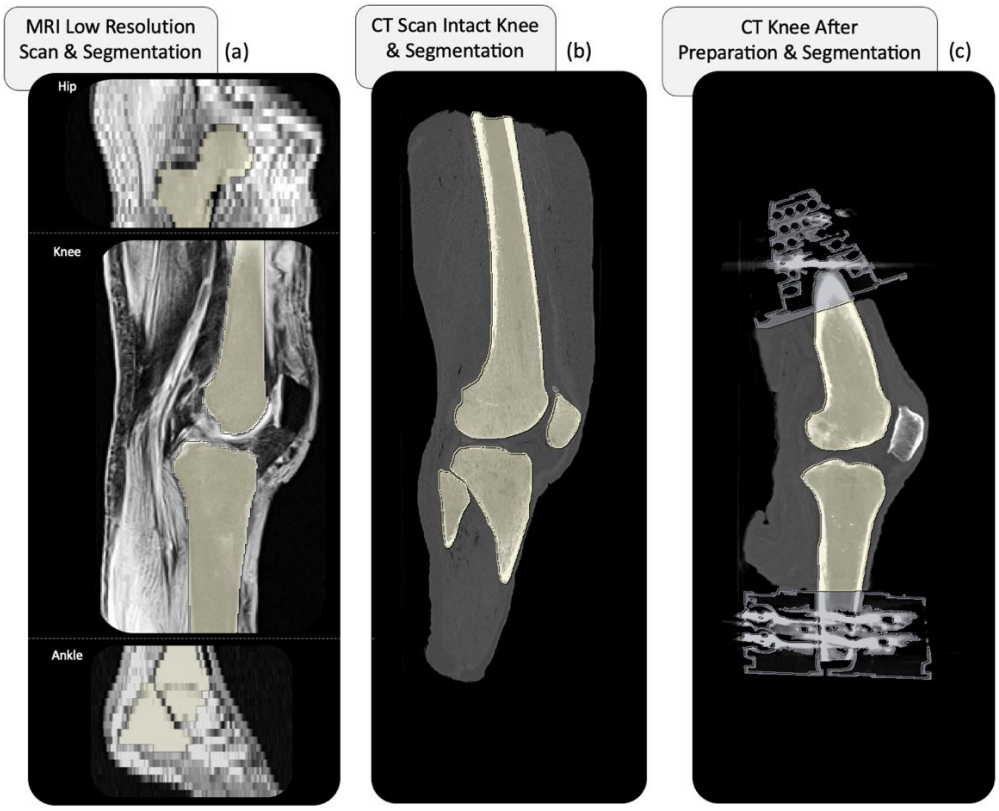

Figure 3.7 *– Comprehensive imaging of the entire lower limb aimed at establishing the anatomical reference system: (a) MRI capturing detailed views of the hip, knee, and ankle, (b) CT scan of the intact knee, and (c) CT scan post-specimen preparation.*

The anatomical reference systems were identified based on GS procedure and with the Gray procedure (Grood and Suntay, 1983; Gray et al., 2019). For GS anatomical reference system, the centre of the head of the femur was identified through sphere fitting, and medial and lateral malleoli virtually palpated from MRI of hip and ankle, in NMS Builder (NMS Builder 2.1v, IOR, Bologna, Italy). Each bony landmark was virtually palpated five times by a single experienced

operator. The GS femoral and tibial reference system was built in NMS Builder (NMS Builder 2.1v, IOR, Bologna, Italy). Gray anatomical reference system of femur and tibia was identified with the automated procedure in MATLAB (MATLAB, MathWorks, Natick, USA), using the custom MATLAB code previously described. Medial and lateral kinematics were calculated with both reference systems (refer to section 3.3.4) and compared with a two-tail t-test (alpha = 0.01, SPM, MATLAB toolbox).

3.3.4 Data Processing

Joint kinematic angles were calculated from relative pose matrices of the local tibial and medial refence systems and calculated for each frame and trial. Translations and rotations were expressed relative to the tibial refence system. Tibiofemoral rotations and translations were calculated using the cardanic sequence z-x-y of KINEMAT motion solver (https://isbweb.org). To compare the kinematic outcomes of this methodology with passive motion studies in literature, a neutral flexion path was inferred from the experimentally measured medial and lateral passive motion to represent a nominal central trial of passive flexion within the envelope. This neutral flexion pattern was calculated for every specimen by averaging the medial and the lateral extremes at each frame and cycle in all DoF. The five-cycle knee kinematics were averaged between cycles for each degree of freedom for medial, lateral, and neutral-inferred trials and the range of motion calculated. The knee passive motion extremes were reported using the following convention: Flexion (+) Extension (-), Abduction (+) Adduction (-), Internal (+) External (-) rotation and Anterior (+) Posterior (-), Superior (+) Inferior (-) and Medial (+) Lateral (-) translations. Rotations and translations were referred to the femur moving relative to the fixed tibia. The described kinematic process was repeated for the six knee specimens. The significance of the normality of the data was assessed with the D'Agostino-Pearson K-squared test. The mean and standard deviation of the six degrees of freedom kinematic measurements were calculated for each cycle, trial, and knee specimen, and as function of flexion-extension. Preliminary results were presented as mean and standard deviation of the medial and lateral extremes of the unloaded knee passive motion envelope, and neutral inferred motion across the six specimens in all six DoFs.

Reliability of the medial and lateral passive motion extremes was estimated as standard deviation of the knee kinematics across five cycles for each specimen. The reliability across the six specimens was calculated as the maximum distance from the average pattern of all specimens and reported for each degree of freedom as a percentage of the average range of motion.

The average pattern or inferred neutral motion path was obtained by averaging the medial and lateral paths. To obtain direct measurements of this central path, the femur was held to control the flexion pace, while minimizing any directional force on the femoral holder. Five trials, each consisting of five extension-flexion-extension cycles, were collected to ensure capturing variations due to the manual force and to

minimize directional force. Comparisons of the inferred central path were made with the direct measurements of the selected motion pattern, and with existing literature. The central paths captured were compared for each degree of freedom with the inferred neutral motion visually and using statistical parametric mapping (alpha = 0.01, SPM, MATLAB toolbox). This information could be used to evaluate the degree of susceptibility to changes in experimental set-up (e.g., different trials of manual flexion) producing a measure of accuracy of such measurement.

Finally, the mean, and standard deviation of the neutral inferred passive flexion of the six specimens was compared against representative nominal central passive motion data existing in literature in all DoFs, where data were available (Walker et al., 1988; Wunshel et al., 2011; Wilson et al., 2000; Belvedere, et al., 2010).

3.4 Results

The first result of this study was the finalized protocol developed presented in the "materials and methods" section (Fig. 3.1). Table 3.1 presents the results of the methodological assessment conducted to evaluate the performance and validity of the protocol. Each step of the methodology is accompanied by its corresponding assessment, providing valuable insights into the protocol's performance and help establish its validity and limitations (Tab. 3.1).

Table 3.1 *– Methodological assessment of the methodology for quantifying the medial and lateral extremes of the unloaded passive motion envelope.*

	Methodological Assessments	Key Findings/Results
Step 1: Imaging and Preparation with Custom 3D Printed Holders	- Identification of potential sources of error and uncertainties	- Successful imaging and preparation of knee specimens using custom 3D printed holders
	- Evaluation of the femoral cup fit	- Inadequate fit of the femoral container, challenge addressed by conducting a CT scan after specimen preparation
Step 2: Experimental Set-up, Protocol, and Data Collection	Assessment of the effect of manual force variability	- Manual force variability was found to have minimal impact on the kinematic results
Step 3: Virtual Reconstruction of Specimen's Kinematics	- Analysis of errors in marker reconstruction	- Accurate virtual reconstruction of marker positions on segmented 3D printed holders
	- Evaluation of the accuracy of the anatomical reference system	- Precise and reliable identification of the anatomical reference system using virtual palpation and automated shape fitting
Step 4: Kinematic Processing for Accuracy and Confidence	- Assessment of the reliability of experimental kinematics	- High reliability of experimental kinematics demonstrated by low standard deviations across multiple trials and specimens
	- Comparison of inferred central neutral kinematics with experimental measurements	- Consistent and accurate measurement of central neutral kinematics in comparison to experimental measurements
	- Validation and comparison with existing literature	- Agreement with existing literature on passive knee motion, validating the accuracy of the protocol and its findings

The following paragraphs will present a detailed analysis of these results.

The manual force of a nominal push towards the medial extreme was estimated to be 6 N as the average of five repeated measures, while pressing more firmly reached 18 N, with a force variation of 12 N. Figure 3.8 illustrates two sets of medial trajectories: the standard trial in light blue and the trajectory of the trial with an increased force applied to the femoral holders for one of the specimens in dark blue; the figure allows for a clear visual comparison, showcasing the negligible effects of the increased force on the medial trajectories. The resultant trajectories of the lateral trial were also analysed qualitatively, and similar results were observed. The effect of manual force (Tab. 3.1), reported as the mean and standard deviation error of the trajectories collected during a standard trial superimposed on trajectories obtained with an increased magnitude of the force on the femoral holders, for the six specimens was 1.24 ± 1.7 [mm] (mean ± SD) across the medial trial.

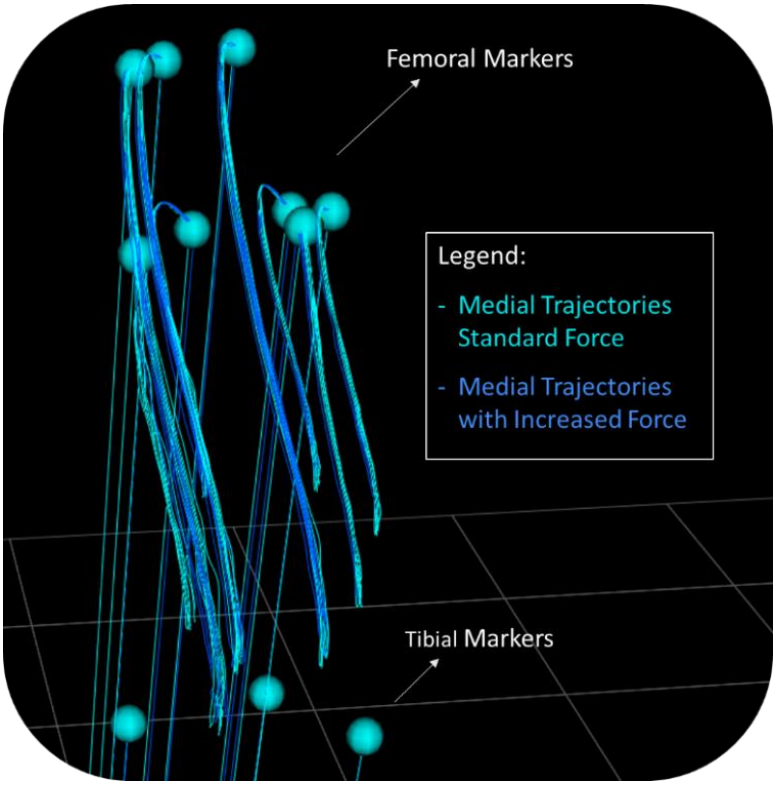

Figure 3.8 *– Comparison of medial trajectories representing in light blue the standard trial, and in dark blue trajectories depicting a trial with an increased force applied to the femoral holders for one of the specimens.*

No statistically significant changes were observed in knee kinematics using these trajectories with different manual forces ($p<0.01$), suggesting that manual force does not affect knee kinematics.

The virtual markers (Tab. 3.1) were created through sphere fitting of the marker cases designed on the femoral and tibial holders with an 8.5mm radius sphere. The average and standard deviation of the height of the markers were 15.46 ± 0.15 [mm] (mean ± SD), and of the markers' diameter 13.43 ± 0.13 [mm] (mean ± SD). The vertical offsets of the spheres from the marker case surfaces were 8.748 ± 0.08 [mm] (mean ± SD).

The difference between the virtual markers positions and their corresponding position measured via stereophotogrammetry was 0.92 ± 0.33 mm (mean ± SD).

Anatomical reference systems obtained using the procedure by Gray presented moderate differences, ~0.3 deg and ~0.2 mm (for the femoral reference system = 0.24 mm, 0.29 deg; for the tibial reference system = 0.17 mm and 0.22 deg), with respect to Grood and Suntay (Grood And Suntay 1983; Gray et al., 2019) (Tab. 3.1, Fig. 3.9). No statistically significant differences were found in the kinematic results obtained using the two anatomical reference systems ($p<0.01$).

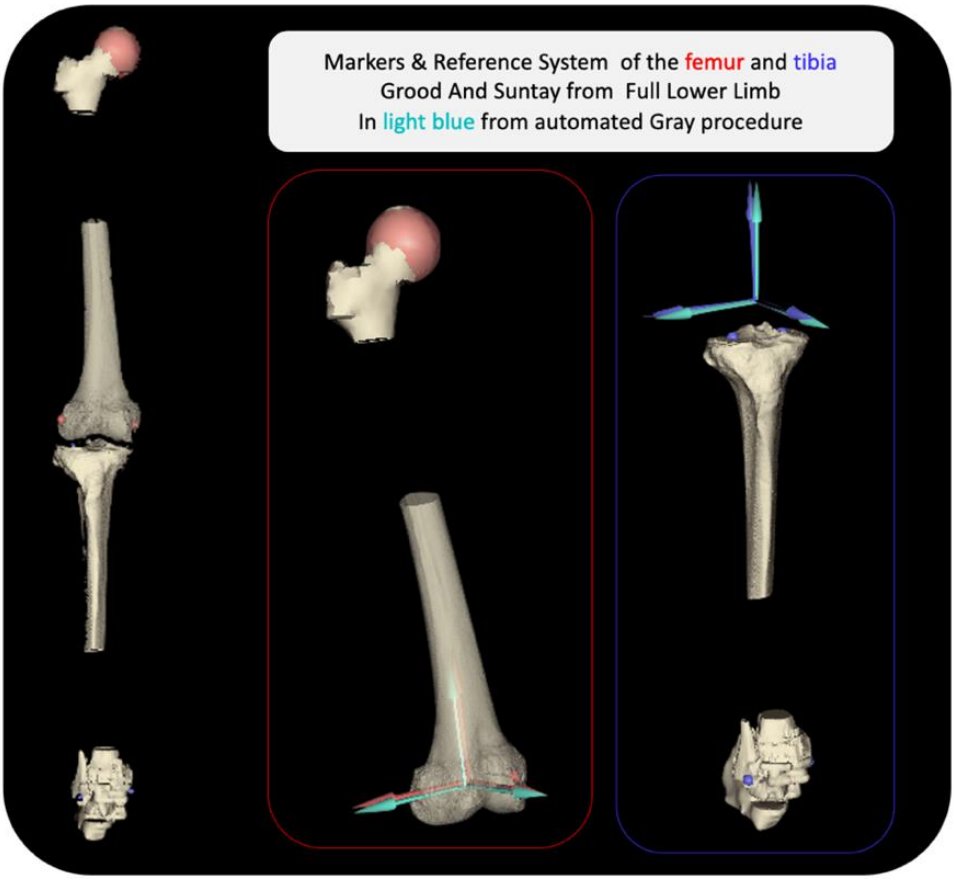

Figure 3.9 *– Grood and Suntay anatomical reference system identification on a full lower limb using bony landmarks and on the same knee after specimen preparation employing the semiautomatic procedure previously described - removing proximal femur and distal tibia, comparison for hip/femur in red and ankle/tibia in blue.*

The reliability assessed across five cycles was below 5% of the range of motion for all the degrees of freedom; variations were 1.54° (1.1%), 0.21° (1.8%), and 0.61° (1.4%), respectively for flexion, abduction, and external rotation, and 0.45 mm (1.9%), 0.66 mm (4.7%), 0.74 mm (3.7%) for anterior, inferior, and medial translations (Tab. 3.1).

Bony articular surfaces position across FE reconstructed from the experimental central passive motion were visually represented falling inside the medial and lateral extremes (Tab. 3.1, Fig. 3.10).

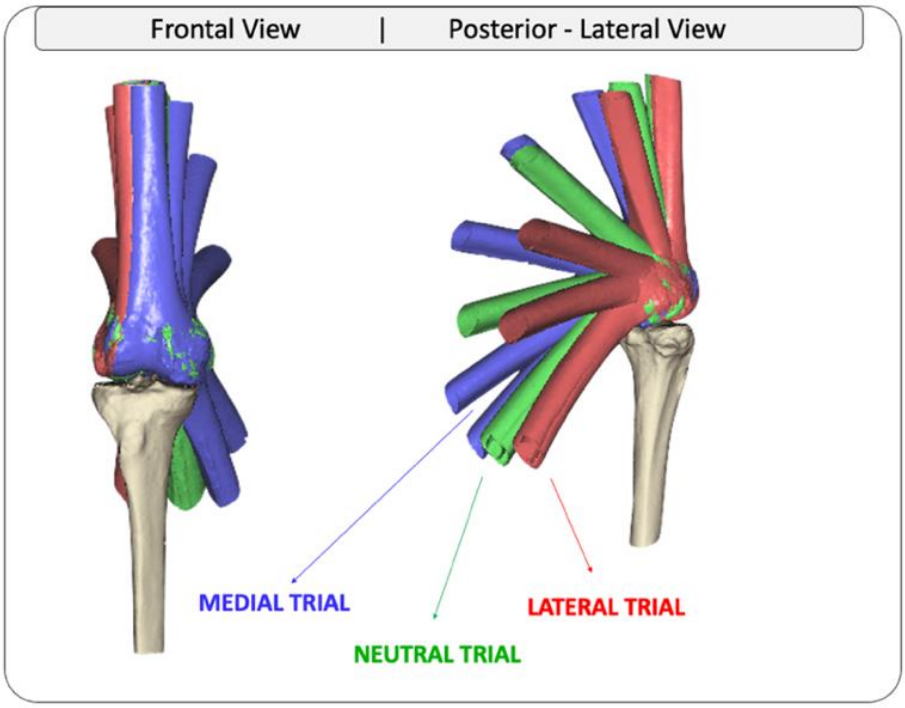

Figure 3.10 *– Frontal and lateral view of the tibiofemoral articular surfaces experimentally captured and virtually reconstructed in blue during the medial kinematic extreme, in red during the lateral kinematic extreme, and in green during a central neutral pattern.*

The neutral-inferred kinematics patterns estimated and experimentally collected and processed were compared in all degrees of freedom (Fig. 3.11). The averaged path closely aligned with the true central path for several degrees of freedom, such as FE, AA rotations, and ML translations. However, at peak flexion, the inferred pattern showed smaller IE rotation and AP translation, and smaller IS translations throughout the entire cycle. Statistically significant moderate differences were detected at 50% of the cycle, at the flexion peak, in AP translation and the first and last 20% in IS translation ($p<0.01$)(Fig. 3.11).

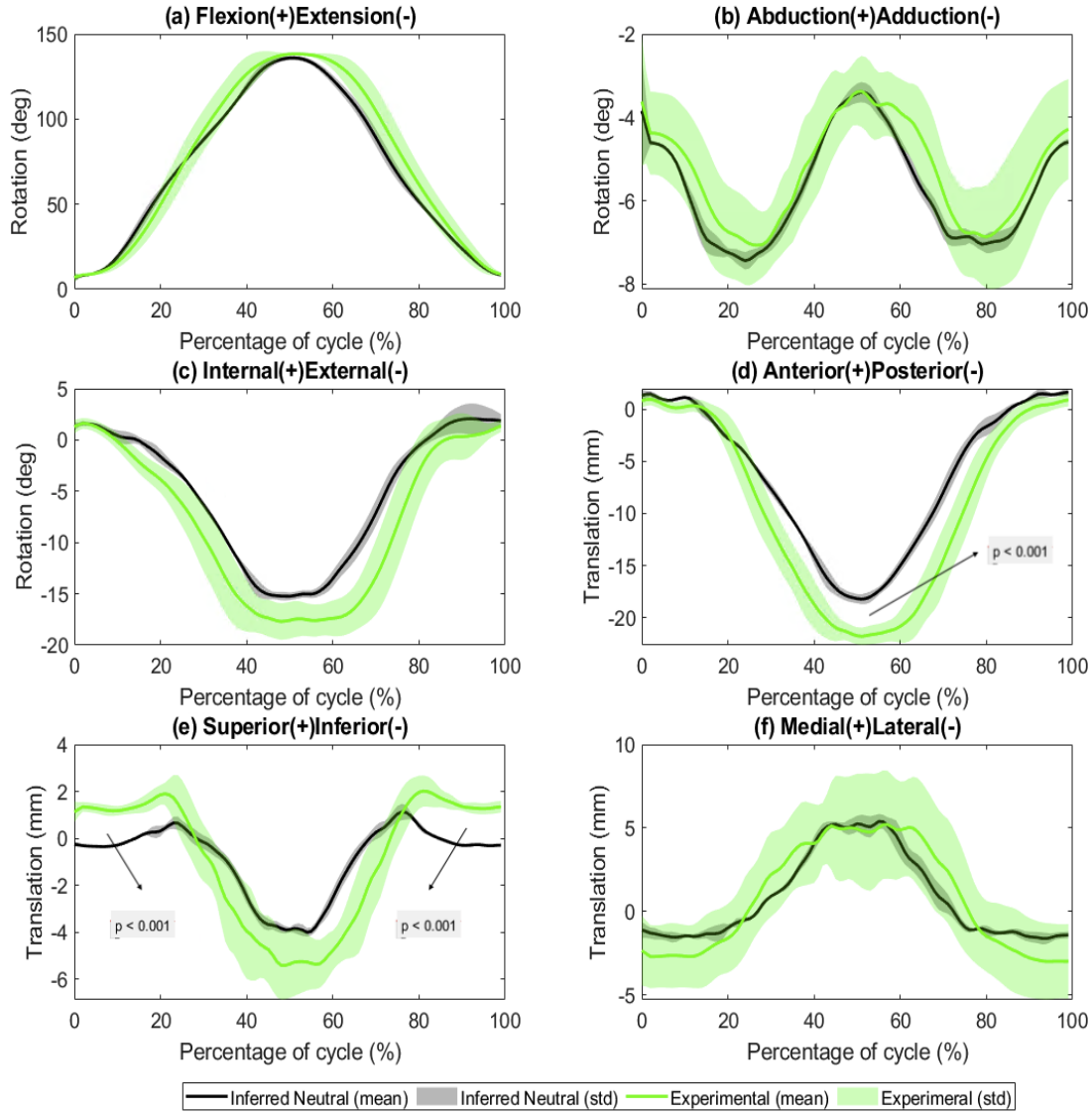

Figure 3.11 *– Mean and standard deviation of the neutral central pattern of passive motion inferred from the mean of medial and lateral extremes in Black, alongside experimentally captured central flexion patterns in Green, for each of the six tibiofemoral degrees of freedom (a) FE, (b) AA, (c) IE rotation, (d) AP, (e) SI, and (f) ML translation.*

Finally, in the figure below, the neutral passive motion inferred from the medial and lateral trials for six specimens with data available in literature on studies of the knee passive motion is presented (Tab. 3.1, Fig. 3.12). Preliminary observation of the trend of the unconstrained knee during a neutral-central passive flexion path showed that secondary rotations and translations are coupled to flexion; at increasing flexion angles with respect to the tibia, the femur translates posteriorly (Fig. 3.12-c), inferiorly (Fig. 3.12-d), and medially (Fig. 3.12-e), while transitioning from internal to external rotation (Fig. 3.12-b), and with initial slight adduction followed by abduction (Fig. 3.12-a). Moreover, extension to flexion and flexion to extension path overlap in all DoFs.

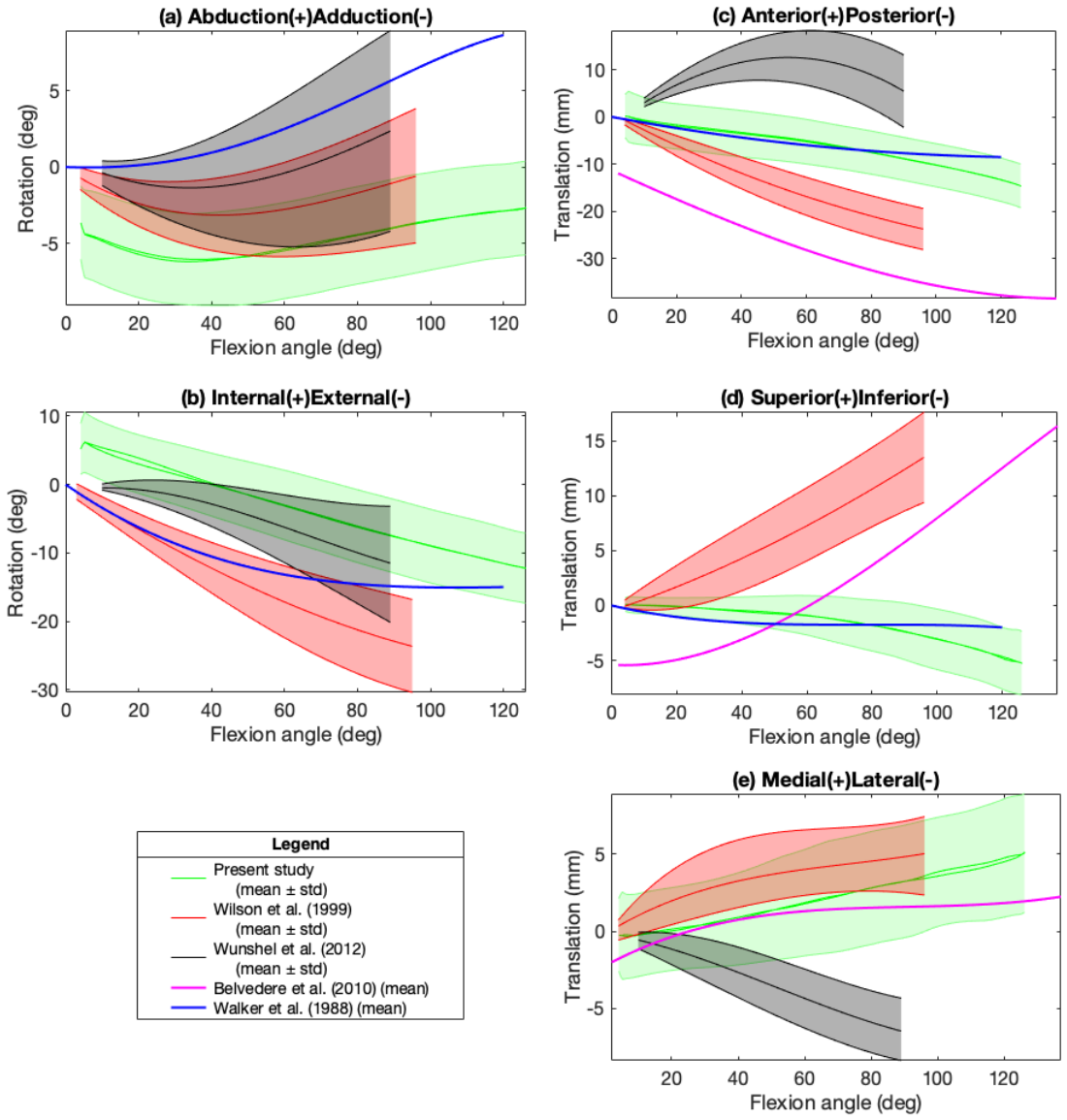

Figure 3.12 *– Experimental tibiofemoral kinematics for a nominal central flexion pattern for 6 specimens compared with data from literature. Mean and standard deviation were presented for (a) AA, (b) IE, (c) AP, (d) IS, (e) ML against flexion angle, in green = the present study, in grey = Wunshel et al. (2012) and in red = Wilson et al. (1999), while mean pattern only for in pink= Belvedere et al. (2010). and in blue = Walker et al. (1988).*

The experimental preliminary six degrees of freedom kinematic results for the medial and lateral extremes across the six specimens, were presented in figure as mean and standard deviation, along with the neutral inferred path (Fig. 3.13). During nominal passive flexion, as well as for the medial and lateral extremes of the passive motion AA, IE rotations, AP, IS and ML translations were coupled with flexion (Fig. 3.13). The extent of the unloaded envelope between the medial and lateral extremes was greater in IE rotation (Fig. 3.13-c), followed by AA (Fig. 3.13-b), ML (Fig. 3.13-f) and IS translation (Fig. 3.13-e).

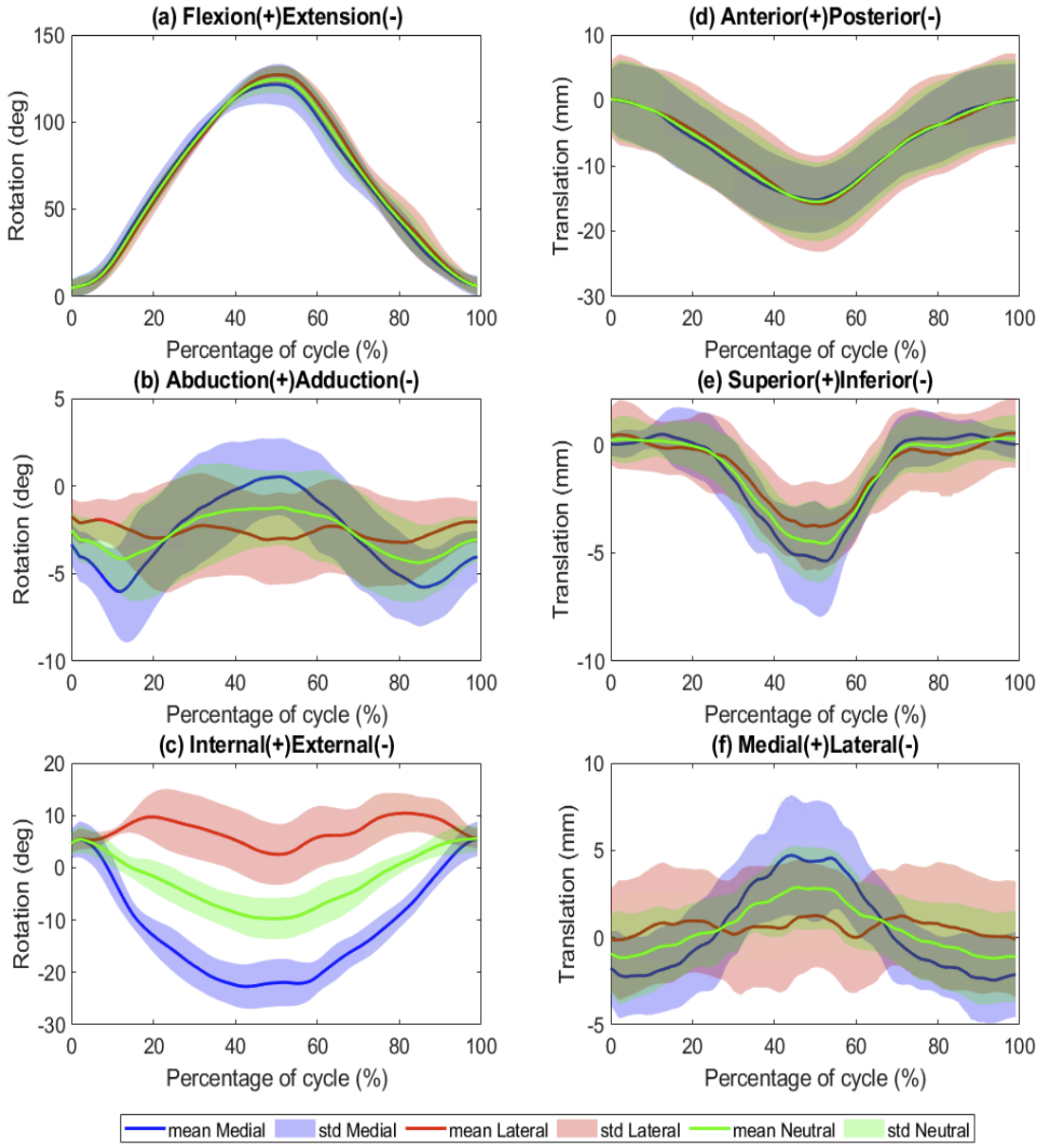

Figure 3.13 *– Preliminary study of six specimens, presenting mean and standard deviation (in blue) for the tibiofemoral medial, (in red) for the lateral extremes of passive motion, and (in green) the inferred neutral central flexion path for (a) FE, (b) AA and (c) IE rotations, (d) AP, (e) SI, and (f) ML translations.*

3.5 Discussion

The objective of the present study was to develop a novel ex vivo protocol and to conduct the analysis of error and uncertainties to assess the feasibility of the use of this protocol for the investigation of the tibiofemoral joint. The study was conducted on six intact specimens from a healthy cohort; the tibiofemoral passive motion achieved through manual manipulation was captured, reconstructed, and quantified through a combination of motion captures and CT imaging techniques with 3D printed custom potting design. The protocol was able to quantify the 6 degrees of freedom tibiofemoral kinematics, associated with the two tibiofemoral coupled varus and valgus flexion paths, respectively medial and lateral extremes of the knee unloaded passive

motion envelope. These measurements presented consistency, low errors, good reliability; the results were comparable to previous investigations in literature. Therefore, results provided confidence on the use of this novel methodology and showed that the outlined protocol may and should be used for the investigation of the knee passive motion and its population variability.

The primary findings of this study focus on the repeatability and consistency of the extremes of passive motion. It was observed that there is no significant variation in medial and lateral passive motion associated with the subjective manual force applied during the trials. The variability in flexion across the five cycles was higher, with variations of approximately 1.5 degrees. In contrast, the variations in the other rotations were less than one degree, and translations were on a submillimeter scale. These variations were nearly comparable to the accuracy of the motion capture system, as supported by previous studies (Chapter 2 - Ex vivo approaches Table 2.2). To address the potential sources of error in the experimental protocol, the potential variability introduced by manual evaluations and manipulation in performing the passive motion was assessed. Although hand manipulation provides valuable qualitative assessments of tibiofemoral function in clinical practice, ex vivo passive motion studies typically employ devices to control knee movements. As manual manipulation was performed to identify the medial and lateral passive motion extremes, the effect of variable manual manipulation was assessed. However, no significant difference was observed in the resultant six degrees of freedom motion. The average trajectory difference of 1.24 mm accounts for overall variations in marker trajectories due to manual force; these differences encompass all three spatial dimensions and are not specific to any degree of freedom. It is important to note that flexion-extension is the DoF more susceptible to variations, being also influenced by factors like compressive properties of the posterior lower limb tissues. Experimental variability, including ligament conditioning, is expected. In conclusion, differences in the captured trajectories, resulting from applying standard and increased magnitudes of force on the femoral holder, can be considered aligned with the millimetre-level accuracy of the Vicon system (Nagymáté et al., 2018) and they are smaller than the variations observed across cycles for both medial and lateral trials. Finally, it is important to note that despite the inherent variability, manual assessments are commonly employed in clinical practice settings, such as knee laxity tests. In fact, these approaches enable a customized assessment of unique range of motion of each specimen or patient. This aspect enhances the relevance and applicability of the findings.

The second significant finding concerns virtual kinematics, anatomical reference system identification, and virtual marker reconstruction. The study conducted a comprehensive assessment of the anatomical reference systems identification, but available intact specimens lacked some anatomical markers recommended by international guidelines for defining joint kinematics (Grood and Suntay, 1983). Existing literature has shown that different reference systems can lead to varying kinematic measurements (Lenz et al., 2008; Martelli et al., 2015). To address this uncertainty, a comparison was made between kinematics obtained using the Gray

procedure and those obtained with the Grood and Suntay reference system (Gray et al., 2019). While the Grood and Suntay reference system is widely used in clinical and research settings, it requires full lower limb anatomy, which was not available in the specimens used (mid-thigh to mid-shank). Consequently, the study adopted the Gray procedure and conducted a validation, using one full lower limb specimen including hip and ankle, which demonstrated promising results, showing similarity with the Grood and Suntay results, with only minor differences observed. However, it is essential to interpret these findings cautiously due to the comparison being limited to a single specimen. Although some slight variations were noted in the initial reference system, no significant differences were found in the resultant kinematics. Additionally, the use of various approaches in identifying the reference system made direct comparisons challenging. One advantage of this approach is the ability to determine the reference system posteriori, after capturing experimental data, allowing for an assessment of its impact on knee passive motion reports. This capability enhances the understanding of the influence of reference system on the final results.

Furthermore, the reconstruction of the kinematic had to rely on an accurate markers position upon which their registration depends. As markers could not be CT scanned with the sample, falling off and moving due to the specimen slightly defrosting and releasing liquid as well as the specimen laying down in the CT, the accuracy of their virtual reconstruction was investigated and confirmed. Potentially being a source of error, virtual reconstructed and CT scanned position were compared with CT scanned markers for one knee and found the error in reproducing them acceptable as accuracy was sub millimetre (comparable to motion capture system accuracy). This was particularly important because the rigid positioning of markers within the custom femoral and tibial potting holders, combined with post-preparation CT scanning, improved the reconstruction of the position of the articular surfaces during tibiofemoral motion. While other rigid body tracking approaches in the literature that often rely on anatomical landmarks for relative positioning, potentially introducing uncertainties and errors, the present methodology, which utilizes custom potting holders and CT scanning post holder fixation, offers improved reliability and accuracy in tracking and reconstructing tibiofemoral articular surfaces during the kinematic trials.

As discussed, the motion reconstruction method employed in this study demonstrates several strengths, including reliability and robustness over manual force variability, the use of custom femoral and tibial potting holders, along with post-preparation CT scanning for accurate marker positioning. Compared to other rigid body tracking approaches relying on anatomical landmarks, our method showcased improved accuracy in capturing knee joint mechanics. However, it is essential to acknowledge the limitation that our motion reconstruction method may be less accurate than robotic manipulations in measuring instantaneous forces. Despite this limitation, the overall assessment and comparisons of this method substantiate its credibility for investigating knee joint mechanics.

The third key findings concerned the experimental comparison of central flexion path measured and derived averaging medial and lateral passive motion extremes. According to literature, the pattern of motion within the envelope is highly sensitive to small variations in experimental setup (Wilson et al., 2000). As such, the hypothesis of consistency in capturing the same central path of flexion-extension can be a source of error. To overcome this issue, the extremes of the unloaded envelope of the passive motion were assessed. These observed extremes patterns of joint motion revealed to be very consistent both intra and inter specimen as previously discussed. Intra specimen kinematics across cycles was very repeatable. The estimation of a neutral central path of passive flexion was required to compare this approach with other studies in literature. The averaged paths inferred from the medial and lateral extremes closely aligned with the experimental central motion path for various degrees of freedom, such as FE, AA rotations, and ML translations. Small differences were observed in IE rotation and AP translation at peak flexion, that can be attributed to the inherent asymmetry between the extremes, while differences in SI translation could be explained by considering the influence of floating axes during the kinematics analysis. Overall, these findings suggested that the averaged paths were representative of the central path and could be used for comparison with other studies. Bony articular surfaces position reconstructed over experimental central passive flexion were falling within an unloaded envelope of which medial and lateral trials are the extremes. Contact was ensured at all times of at least one condyle, with the opening of a small gap in the contact between medial femoral condyle and medial tibial plateau by applying a lateral force, and vice versa.

The fourth key findings concern the credibility of the results, reinforced by comparison with existing literature. Mean and standard deviation of the neutral inferred kinematics across the six specimens used in this preliminary study were plotted against flexion angles and compared with studies from literature (Belvedere et al., 2011; Walker et al., 1988; Wilson et al., 2000; Wünschel et al., 2012). The results were consistent with previous reports, showing a general agreement of the pattern of motion, as well as with the range of variability across individuals, in all six degrees of freedom motion. While rotations appeared to be in strong agreement, with the knee abducting and externally rotating with flexion, translations showed some discrepancies with literature data. The translation of the neutral inferred motion in AP and ML directions agreed with three of four studies, except for Wunshel et al. (2012) (Wunshel et al., 2012). While the femur was reported translating posteriorly and medially with flexion, Wunshel diverged presenting anterior and lateral translations. More variability was shown in the IS translation pattern. In the present study, the femur translated slightly inferiorly with flexion, in agreement with Walker et al. (1988) while Belvedere et al. (2011) and Wilson et al. (2000) measured superior displacements (Walker et al., 1988; Wilson et al., 2000; Belvedere et al., 2011). The differences with the other studies could be explained by changes in the experimental set-up, instrumentation, experimental conditions, etc. i.e., whether the foot and relative weight were present (Belvedere et al., 2011). Other small

incongruencies in the DoF-related offset might be due to absence of muscle involvement and/or task performed and relative absence of engagement of ligamentous constraints, which inevitably changes the pattern of motion as shown by several studies (Torzilli et al., 1994; Victor et al., 2010; Wunshel et al., 2012). Further differences could be explained by the improved methodological accuracy of the motion reconstruction herein presented, in compassion to methods found in literature, i.e., surgical navigation systems (Belvedere et al., 2011), invasive femoral rods with a singular isotrack (Wilson et al., 2000) or standardised robotic procedure (Cyr and Maletsky, 2014; Wünschel et al., 2012). Other differences might be attributed to soft tissues presence in intact specimens that produced a further physiological constraint, when compared with dissected knees, i.e., muscle dissection for robotic weight-bearing testing. Again, potential constraints could be attributed to the fibula, whether it was left hanging or rigidly fixed to the tibia. Despite all the possible sources of errors and uncertainties, there was mostly agreement with literature, thereby reinforcing the credibility and validity of this novel methodology.

The present study has several limitations that should be acknowledged. The limited sample size of six specimens in this study is a potential limitation that may affect the generalizability of the findings. As a result, caution should be exercised when extrapolating the results to a larger population. The mean and standard deviation of the results may vary when the study is expanded to include more participants. It is important to consider that factors such as average knee size and age group distribution may differ in a broader population, potentially influencing the outcomes. Nonetheless, the chosen age group in this study represents most patients who undergo total knee arthroplasty, lending relevance to the findings in a clinical context. To address this limitation and obtain a more comprehensive understanding of the topic, future studies should aim to include larger sample sizes. By doing so, researchers can enhance the generalizability of their results and minimize the potential impact of the limited sample size; this would contribute to a stronger foundation of knowledge in the field (Chapter 4 - Study 2).

The inadequate fit of the femoral container is a methodological limitation, addressed by utilizing CT scanning to precisely reconstruct marker positions in relation to the bone surfaces. This inadequate fit posed challenges in the virtual marker reconstruction, and to minimize error, two reference systems were employed for each part of the holder.

Another potential limitation of the study, previously discussed, concerns some degree of constraint on rotations, particularly internal/external, that may have been present during the medial and lateral trials. However, the performance of five repetitions demonstrated minimal impact on these rotations, with consistent results and comparable standard deviation to the other degrees of freedom, and with a comparison of the neutral inferred central flexion path with other literature studies supporting the conclusion. As previously discussed, a further limitation of this methodological assessment is that the tibiofemoral reference system assessment was conducted on a single specimen. Therefore, caution should be exercised when interpreting these findings.

Finally, the analysis of passive tibiofemoral motion in this study did not include the contribution of tendons and muscles crossing the knee, as they were transacted distally. This omission may have influenced the observed differences compared to previous studies, such as the one conducted by Belvedere et al. (2011), where the effect of the quadriceps tendon under load was noted. It is well-established in the literature that muscle loading significantly affects the kinematics of passive flexion (Belvedere et al., 2011).

This protocol can be more easily reproduced around laboratories, applied to injured and pathological conditions investigations, and findings translated into to clinical practice. According to this study, standardized procedures should be developed for measuring and reporting knee passive motion across laboratories, as there is a significant difference between the unloaded envelope of knee passive motion at the medial and lateral extremes. In the following chapter this methodology was used to investigate inter-subject variability and the influence of sex (Chapter 4). A feasibility study of the use of this methodology to assess restoration of the tibiofemoral function, before and after knee replacement was conducted (supplementary material in Appendix E). Quantification of such an approach could be used to distinguish healthy from pathological knee joint conditions and/or to restore the individual native tibiofemoral function, providing a range of healthy variability across populations, and intraoperative reference measurements. Moreover, this methodology can also be applied to other joints for the investigation of the six degrees of freedom kinematics, as coordinate system individuation is the only knee joint specific action. In conclusion, this approach demonstrated consistent and reliable measurements of the individual extent of the unloaded knee passive motion envelope at its medial and lateral extremes. It offers a valuable method for investigating inter-subject variability in tibiofemoral passive motion and evaluating the influence of sex on the knee envelope.

Chapter 4

STUDY 2

Inter-subject Variability and Influence Of Sex On Knee Passive Motion Envelope Across A Healthy Adult Cohort

CONTENTS

F. Bucci, M. Taylor, R. Al-Dirini, S. Martelli (2023) – Comparison of the envelope of knee passive motion in males and females. Journal of Orthopaedic Research. *Submitted, Manuscript under Review*.

Please refer to the appendices at the end of this thesis for a detailed outline of the author's contribution to this study (Appendix A), for specimen-specimen extremes of knee passive motion (Appendix C), and for the relationship between sex, tibiofemoral anatomy, and experimental passive kinematic extremes (Appendix D).

4.1 Abstract

Women experience higher rates of knee ligament injuries and are more likely to develop knee osteoarthritis than men, motivating the study of sex differences in knee anatomy and motion. Here, we compare the two extremes of the knee passive motion, along all six axes of motion, in males and females using a novel in-vitro protocol.

Thirty healthy human knee specimens were obtained from a body donation program (20 males and 10 females). Reflective markers were placed on dedicated features of custom 3D printed potting cups created for the tibia and femur from CT scans. Two trials, with five repetition per trial, of complete flexion-extension were performed by manually applying medial and lateral forces to the femur. Marker trajectories were recorded using a stereo-photogrammetric motion capture system. Tibiofemoral kinematics, consisting of six degrees-of-freedom, were reconstructed, and grouped by medial and lateral motion, as well as by sex. Statistical parametric mapping (SPM, MATLAB toolbox, $\alpha = 0.05$), was used to compare the data. The largest significant difference between medial and lateral force trials was an 18º mean external rotation. Smaller significant differences were found for adduction (at peak: 4.7º, mean: 1 ± 3º) and medial translation (at peak: 2.9º, mean: 0.3 ± 2.1 mm). Females exhibited statistically significant greater abduction than males when a medial force was applied (at peak: 4.8º, mean difference: 3.5 ± 0.7º, $p<0.05$) whereas no sex-specific differences were found for the remaining axes of motion and lateral trial.

Variation across males and females is consistent and larger than sex-specific differences along all axes of motion. Nevertheless, the results displayed moderately sex-specific passive knee motion observed showing higher abduction in females than males in the medial trial, in agreement with the literature, and no differences along the remaining axes of motion.

4.2 Introduction

Women are more prone than men to knee ligament injury, osteoarthritic degeneration of the articular joint and present higher complication rates following knee arthroplasty (Srikanth et al., 2005) thereby motivating studies of sex-specific differences of knee shape and function (Conley et al., 2007; Varadarajan et al., 2009). Women experience greater knee moments than men and different knee kinematics during a variety of exercises (James et al., 2004; Lephart et al., 2002; Sigward et al., 2013), even though current evidence suggests a minor role of sexual dysmorphism of knee shape (Asseln et al., 2018; Guy et al., 2012; Hitt et al., 2003; Mahfouz et al., 2007; van den Heever et al., 2012; Varadarajan et al., 2009; Voleti et al., 2015), and passive knee motion. However, ex vivo measurements of knee passive motion are most often limited to male cohorts (Cyr and Maletsky, 2014), selected axes of motion (Walker et al., 1988) and a single representative motion within the motion envelope allowed by the articular surfaces and the soft-tissue constraints (Belvedere et al., 2011; Blankevoort et al., 1988; Cyr and Maletsky, 2014; Walker et al., 1988; Wilson et al., 2000; Wünschel et al., 2012).

Previous in vivo studies associated women with higher knee abduction than their male counterparts during a range of exercises including normal weight-bearing activities and more demanding side-step cutting manoeuvres (Cronström et al., 2016; James et al., 2004; Sigward et al., 2013; Tanikawa et al., 2013). The shape of the articular surfaces and the ligaments determine knee motion during walking in both males and females along all six axes of motion, except for about 3 mm anterior tibial translation during early stance (Martelli et al., 2020). Males display a larger knee size (Conley et al., 2007; Hsu et al., 2021; Li et al., 2014; van den Heever et al., 2012), larger knee flexor and extensor muscles (Behan et al., 2018; Blackburn et al., 2009) and larger femoral width to depth ratio (Asseln et al., 2018; Gillespie et al., 2011; Hitt et al., 2003; Hsu et al., 2021; Li et al., 2014) than women. However, others reported no knee shape differences, once the effect of size was accounted for, which supports the notion of a modest sexual dimorphisms of knee shape (Asseln et al., 2018; Dargel et al., 2011; Hsu et al., 2021; Li et al., 2014; van den Heever et al., 2012; Voleti et al., 2015). Therefore, it appears that sex-specific differences of knee motion during exercise are most likely attributable to a sexual dimorphism in anatomical regions other than the knee (Audenaert et al., 2019) and of motor coordination (Wilson et al., 2015). Yet, conclusive experimental evidence of differences between males and females of passive tibiofemoral motion is lacking.

Current in vitro measurements of passive tibiofemoral motion are often limited in sample size (Blankevoort et al.1988; Eagar et al., 2001; Victor et al., 2010 ; Nowakowski et al., 2012; Roth et al., 2015), focus on a single sex (Nowakowski et al., 2012; Cyr and Maletsky, 2014), selected axes (Blankevoort et al.1988; Walker et al., 1988; Hsu et al., 2006; Boguszewski et al., 2015), a restricted

knee flexion range (Torzilli et al., 1994; Blankevoort et al.1988; Eagar et al., 2001; Hsu et al., 2006; Hsu et al., 2006; Boguszewski et al., 2015), or provide a single representative motion pattern within the envelope of passive motion allowed by the articular surface and ligament constraints (Blankevoort et al.1988; Torzilli et al., 1994; Eagar et al., 2001; Hsu et al., 2006; Victor et al., 2010; Nowakowski et al., 2012; Roth et al., 2015; Boguszewski et al., 2015). For example, Blankevoort et al. (1988) reported the envelope of tibiofemoral motion, along 5 axes of motion, using different mild loading conditions (torques ±3/6Nm, 300N axial and 30N AP loading) in 5 to 8 positions over a limited range of knee flexion angles (extension to approximately 95° degrees flexion) in 4 specimens (Blankevoort et al.1988). Other cadaveric laxity studies investigated the anterior posterior translation only (Eagar et al., 2001), flexion ranges between 0° and 90° degrees (Eagar et al., 2001; Nowakowski et al., 2012; Hsu et al., 2006; Boguszewski et al., 2015) and less than 10 specimens (Eagar et al., 2001; Victor et al., 2010; Nowakowski et al., 2012; Roth et al., 2015). Males and females showed different rotational laxity and no differences in anterior-posterior laxity in two larger studies (47, 82), however, they analysed only 15°/30°-degree angles, 0° to 50° flexion range, and differences were inconsistent with laxity being higher for males at 15° degrees and vice versa at 30°, with another using a different age group (29.5 y.o.) (Hsu et al., 2006; Boguszewski et al., 2015). A recent study explored the envelope of passive tibiofemoral motion in 27 male donors (Cyr and Maletsky, 2014). Yet, no study has compared the envelope of passive motion in both males and females.

The aim of the present study is to test the hypothesis that the envelope of passive tibiofemoral motion in males and females are equal. The knee passive motion envelope was measured in male and female donors using an established protocol and compared using statistical parametric mapping.

4.3 Material And Methods

4.3.1 Specimens Cohort Demographic

Thirty fresh frozen human cadaveric knees, mid-thigh to mid-shank, were obtained from a body donation program (Science Care, Phoenix, USA). The demographic composition of the population is shown in Table 4.1, with the specimens used in this analysis including those from the previous study (Chapter 3 - Study 1).

Ethics approval was obtained from the Social and Behavioural Research Ethics Committee (SBREC) at Flinders University (project number 6832). Exclusion criteria included reported history of knee surgery, osteoarthritis, musculoskeletal condition affecting normal ambulation for 1 year, or more, before death and BMI above 30 kg/m2.

Table 4.1 *– Demographic of the adult healthy population of knee specimen donors.*

	Cadaveric Knee Specimens Demographic		
	ALL	**MALES**	**FEMALES**
Population Size			
n	30 knees	20 males	10 females
Age *(years)*			
ave (± std)	66 (± 11)	70(± 10)	60 (± 11)
Height *(cm)*			
ave (± std)	173 (± 10)	173 (± 11)	175 (± 9)
Weight *(kg)*			
ave (± std)	73 (± 19)	74 (± 11)	72 (± 22)
BMI *(kg/m^2)*			
ave (± std)	24.0 (± 5.0)	24.8 (± 5.3)	22.7 (± 4.6)
Leg Side			
right : left	14 : 16	7 : 13	7 : 3

4.3.2 Passive Motion Data Collection

An in-depth description of the methodology used to capture the knee passive motion envelope was covered in the previous chapter (Chapter 3). Specimens were imaged using a clinical CT scanner (SOMATOM Force, Siemens Healthcare Sector, Forchheim, Germany); femur and tibia were segmented using Scan IP software (Simpleware ScanIP, Synopsis, Mountain View, California, U.S.) (Fig. 4.1-a). Specimen-specific tibial and femoral holder (ANSYS, Canonsburg, Pennsylvania, U.S.) were designed to accommodate passive reflective markers and 3d printed (Ultimaker2+) (Fig. 4.1-b). The distance from the joint centre to the most proximal femur holder was 180 mm, and to the most distal tibia holder 170 mm. Specimens were thawed, and soft tissues removed from the tibial distal and femoral proximal ends leaving the knee joint intact, including skin, and the holder fixed through metallic screws (Fig. 4.1-c). The assembly were CT scanned again after preparation (Siemens, Siemens Healthcare Sector, Forchheim, Germany; 40 keV and MAR), bones and holders segmented (ScanIP, Synopsis, Mountain View, California, U.S.) (Fig. 4.1-d). A minimum of ten reflective markers were fitted per specimen. The motion capture protocol included firmly securing the tibia by fixing the tibial holder to a table. Flexion-extension movements of the femur were manually executed, applying medial and lateral force to the holder, as elaborated upon in Chapter 3, and motion capture data were recorded using a 10-camera Vicon system (VICON, Oxford Metrics Group, Oxford, UK). Two trials were collected for each specimen applying a medial and a lateral force while flexing the femur (Fig. 4.1-e). Marker trajectories were recorded for five cycles (cycle = extension-flexion-extension) per specimen and trial, labelled, filtered, and resampled to 100 frames (MATLAB, MathWorks, Natick, USA) (Fig. 4.1-f). The initial relative position of the bony articular surface, the specimen holders and the reflective markers was virtually reconstructed (NMS Builder 2.1v, IOR, Bologna, Italy) (Fig. 4.1-g). The knee anatomical reference system described by Grood and Suntay (Grood and Suntay, 1983) was defined following the procedure described by Gray (Gray et al., 2019) with a custom code (MATLAB, MathWorks, Natick, USA).

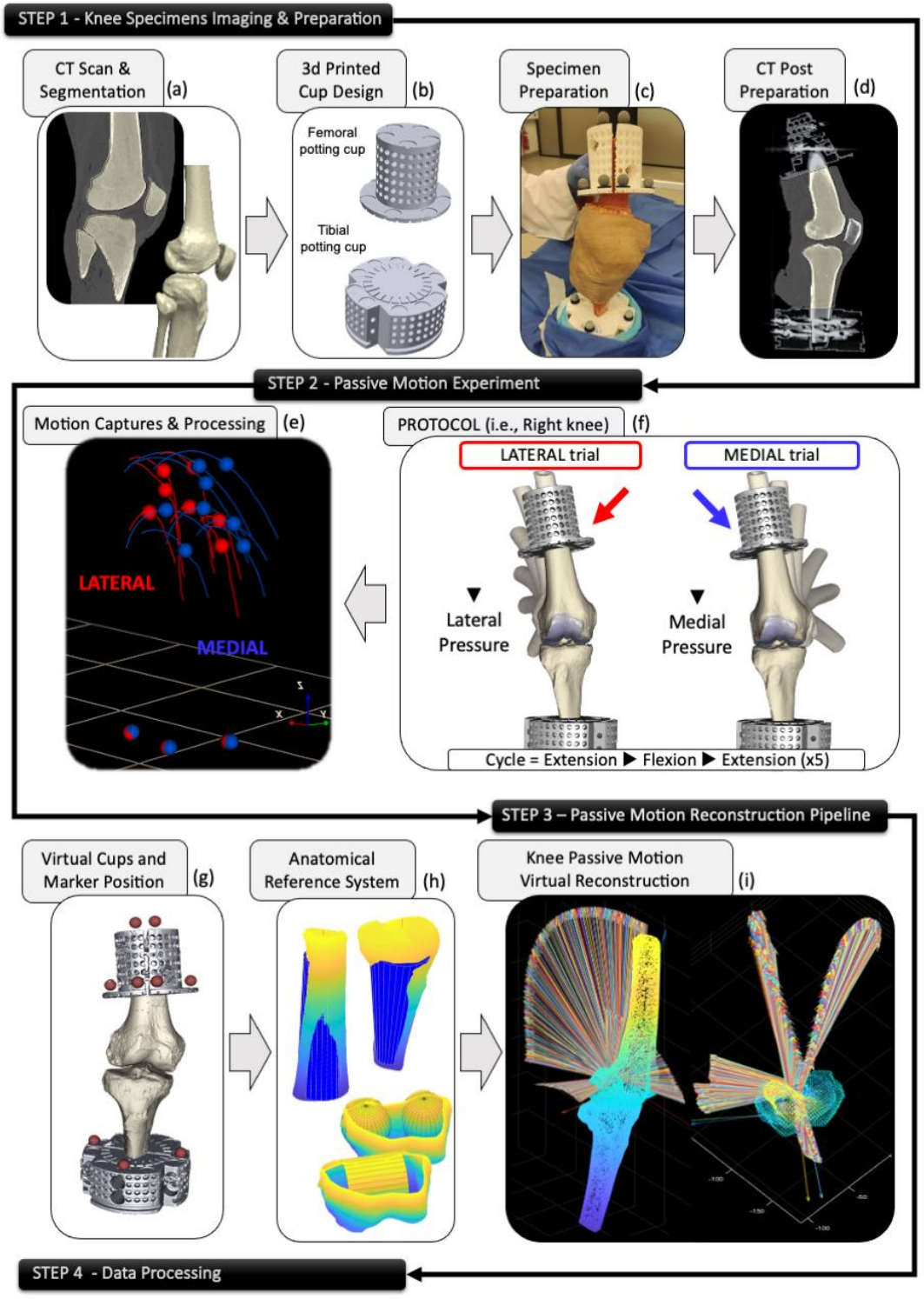

Figure 4.1 *– Novel ex vivo assessment: (step 1, a-d) specimen imaging and preparation with custom 3D printed holders, (step 2, e-f) experimental set-up, protocol, and data collection of the two passive motion medial and lateral trials, (step 3, g-i) their virtual reconstruction, and (step 4) subsequent data processing.*

The same code allowed the reconstruction of the knee reference system and articular surfaces position with continuity, for each frame and cycle of both medial and lateral trials, by registering the virtual markers with their experimental trajectories, in MATLAB, through an ICP (Iterative Closest Point) registration algorithm. Tibiofemoral Flexion (+) Extension (-) – FE, Adduction (+) Abduction (-) – AA, Internal (+) External (-) – IE rotation, Anterior (+) Posterior (-) – AP,

Inferior (+) Superior (-) – IS, Medial (+) Lateral (-) – ML translations were calculated using tibiofemoral motion solver (sequence z-x-y) KINEMAT (https://isbweb.org) for all thirty specimens. Finally, for each specimen a nominal neutral central flexion pattern was inferred by averaging medial and lateral extremes.

4.3.3 Statistical Analysis

The passive knee motion was analysed using descriptive statistics. The normality of the data was assessed with the D'Agostino-Pearson K2 test (alpha = 0.05, SPM, MATLAB toolbox) (Friston et al., 2003) in MATLAB (The MathWorks, Natick, USA). The envelope was defined as the difference between the knee passive motion measured at the medial and lateral extremes. Each extreme was determined for 30 knees and represented with 100 frames, averaged over five cycles, in each of the six degrees of freedom. The average and standard deviation of the range of motion (ROM) was the difference between minimum and maximum values during each motion cycle. The variability across the population was described by mean and standard deviation, for both medial and lateral extremes of motion. The relationship between each degree of freedom of the passive motion, including medial and lateral extremes and the neutral inferred central path, were quantified with a correlation matrix consisting of pair-wise correlations for the entire adult population. The passive tibiofemoral kinematics was analysed using descriptive statistics and statistical parametric mapping. The effect of the direction of the flexion was investigated using a two-tail t-test with statistical parametric mapping (alpha = 0.01, SPM, MATLAB toolbox). The range of motion was compared with sex-specific boxplots. The relationship between each degree of the passive tibiofemoral motion was calculated separately for males and females and compared between sexes using a two-tails student t-test (MATLAB, MathWorks, Natick, USA). Differences between males and females were compared using a two-tail t-test and statistical parametric mapping (alpha = 0.01, SPM, MATLAB toolbox). A power analysis was conducted using GPower, focusing on the range of motion in adduction and abduction for males and females across the population; a t-test means Wilcoxon-Mann-Whitney test (two groups) a priori was employed (alpha =0.05, power = 0.8, GPower3.1).

4.4 Results

4.4.1 Medial And Lateral Extremes Of The Unloaded Knee Passive Motion Envelope

The medial and lateral extremes of the tibiofemoral passive motion were reported in the following table and figure (Tab.4.2, Fig. 4.2). Average patterns of passive motion, for each DoF both medial and lateral extremes, were consistent across the population (Fig. 4.2, Tab.4.2). The individual

average flexion pattern across a cycle covered slight hypertension (negative flexion – between -6 and 10º) to almost 150º flexion (Tab.4.2, Fig. 4.2-a). The medial extremes found the tibiofemoral adducting up to about 10º flexion, while moving towards slight abduction, changing course, to approach an average of 0.28º adduction at peak flexion (Tab.4.2); conversely, along the lateral extreme the knee was in a steadier and more consistent adduction, around -5º (Tab.4.2, Fig. 4.2-b). Internal-external rotation patterns were different for the medial and lateral extremes; the medial extremes showed increasing external rotation with flexion (maximum of -36º at peak flexion), while the lateral presented slight internal rotation (under 10º mean internal rotation) up to 10º flexion, followed by a trend towards external rotation, approaching the 0º at peak flexion (Tab.4.2, Fig. 4.2-c).

Table 4.2 *– Minimum, maximum, mean, and standard deviation of the passive range of motion (pROM) of the tibiofemoral kinematics medial and lateral extremes along the six axes of motion.*

p ROM		**Medial Extremes** (n=30)	**Lateral Extremes** (n=30)
Flexion (+) Extension (-)	[deg]		
mean ± std (% ROM)		125.50 ± 11.84 (9.4%)	125.76 ± 10.49 (8.3%)
min | max (across population)		-10.28 | 150.14	-4.26 | 145.54
Abduction (+) Adduction (-)	[deg]		
mean ± std (% ROM)		8.79 ± 2.79 (31.8%)	6.42 ± 2.44 (38.1%)
min | max (across population)		-13.58 | 9.71	-13.19 | 4.95
at peak flexion (50% cycle)		-0.28º	-5.02º
Internal (+) External (-)	[deg]		
mean ± std (% ROM)		32.21 ± 7.50 (23.2%)	14.05 ± 5.86 (41.7%)
min | max (across population)		-36.11 | 14.52	-20.30 | 29.88
at peak flexion (50% cycle)		-24.29º	-0.20º
Anterior (+) Posterior (-)	[mm]		
mean ± std (% ROM)		16.81 ± 4.57 (27.2%)	16.23 ± 7.62 (46.9%)
min | max (across population)		-31.87 | 5.49	-32.30 | 25.04
at peak flexion (50% cycle)		-15.22º	-14.04º
Superior (+) Inferior (-)	[mm]		
mean ± std (% ROM)		7.86 ± 3.06 (38.9%)	6.20 ± 3.15 (50.8%)
min | max (across population)		-13.39 | 2.96	-13.68 | 7.20
at peak flexion (50% cycle)		-6.66º	-3.92º
Medial (+) Lateral (-)	[mm]		
mean ± std (% ROM)		10.19 ± 3.47 (34.1%)	7.31 ± 3.95 (50.0%)
min | max (across population)		-8.02 | 17.87	-6.64 | 21.24
at peak flexion (50% cycle)		6.45º	3.78º

Medial and lateral extremes of tibiofemoral translations were more consistent than rotations showing knees translating posteriorly, inferiorly, and medially with increasing flexion. The femur consistently translated posteriorly from extension to flexion by an average of -15 mm as knee flexed from 4º to 128º (Tab.4.2, Fig.4.2-d), moved superiorly by 4.2 mm for the medial and 6.14 mm for the lateral trials respectively (Tab.4.2, Fig.4.2-e). Finally, medial translation occurred while the knee flexed, to an average of 4.12 mm for the lateral trial and to a higher average of 6.39 mm for the medial one (Tab.4.2, Fig.4.2-f).

The figure below shows the unloaded knee passive motion envelope as the difference between medial and lateral extremes (Fig. 4.2). The envelope demonstrated a greater extent of motion in

internal-external rotation, and envelopes were also observed in abduction-adduction, medial-lateral, and inferior-superior translations. The 6 DoFs of the movement paths, both medial and lateral, were not affected by the direction of the flexion, whether it was extension to flexion (0% - 50% cycle percentage) or flexion to extension (50% - 100% cycle percentage).

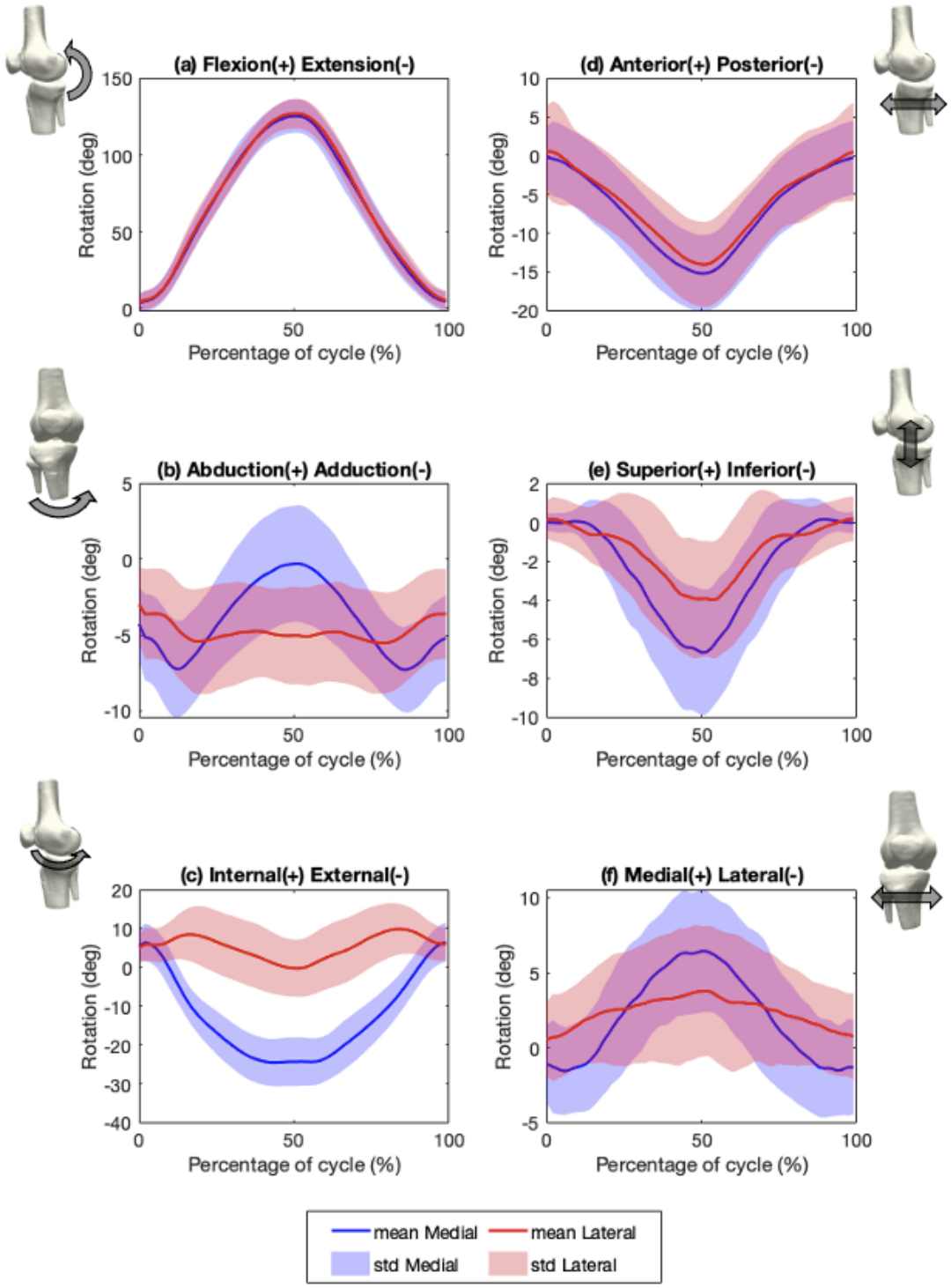

Figure 4.2 *– Mean and standard deviation in blue of the tibiofemoral Medial and in red of Lateral extremes of passive motion for each of the six degrees of freedom, including (a) FE, (b) AA, and (c) IE rotations, (d) AP, (e) SI, and (f) ML translations, as a function of the flexion cycle - 0 to 50% extension to flexion and 50 to 100% flexion to extension.*

The inter specimen variability, expressed as standard deviation across the population, was between 20% to 50% percent ROM for all DoFs and both medial and lateral extremes, except for flexion-extension, which was 9% percent. The variability between individuals was higher than intra specimen variability (<5% of ROM, <2deg rotation and <1mm in translation – Chapter3). The standard deviation of both rotations, abduction-adduction, and internal-external rotations, was approximately 10° degrees (Fig.2 a-c). As for translations, the standard deviations for anterior-posterior translation ranged from 5 to 7 mm, while for medial-lateral and superior-inferior translations, were around 3-4 mm (Table 4.2, Fig. 4.2 d-f).

Statistically significant differences between medial and lateral extremes were found in adduction-abduction, external-internal rotations, and medial-lateral translation (Fig. 4.3-5). The greatest differences were found in the rotations (Fig.4.3-4), while the smaller differences were present in translation (Fig.5). The largest difference between medial and lateral trials was 18° mean internal-external rotation (peak: 29°), with significantly different patterns ($p = 0.001$) between 10 to 90 percent of the cycle. Significant differences were found for abduction-adduction rotation (mean: 2°), between 30 and 70 percent of the cycle ($p=0.001$). Significant difference was found around 90 percent of the cycle in medial-lateral translation (mean: 2 mm) ($p=0.004$); however, it was negligible since it happened within one out a hundred frames in the cycle.

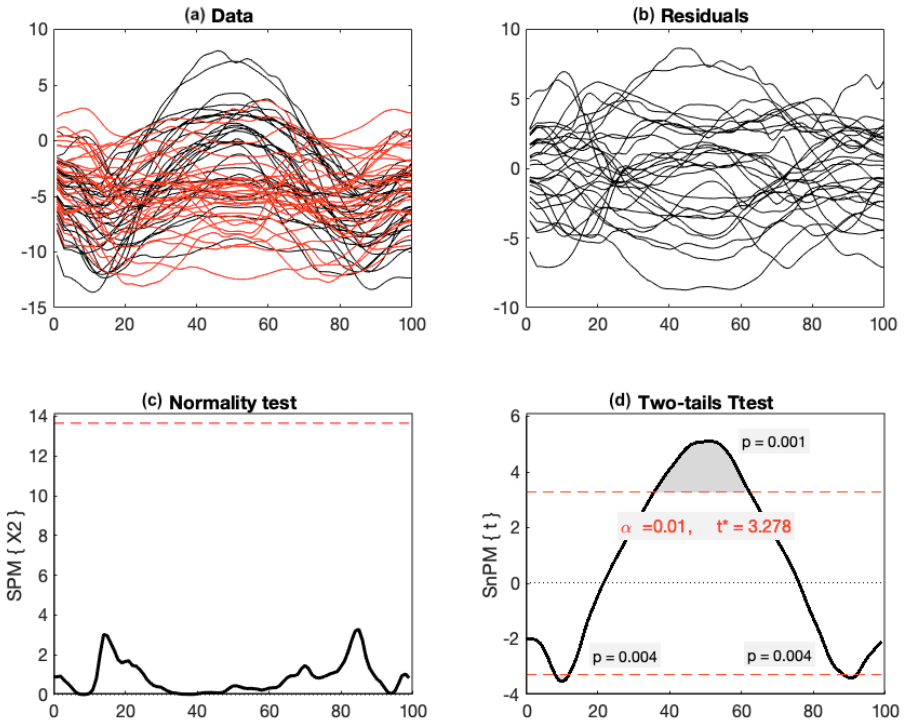

Figure 4.3 *– Exploration of medial and lateral abduction-adduction with statistical parametric mapping, featuring (a) experimental data for the medial (in black) and lateral (in red) trials, (b) their residuals, (c) the result of the normality test, and (d) p-values from the two-tailed t-test.*

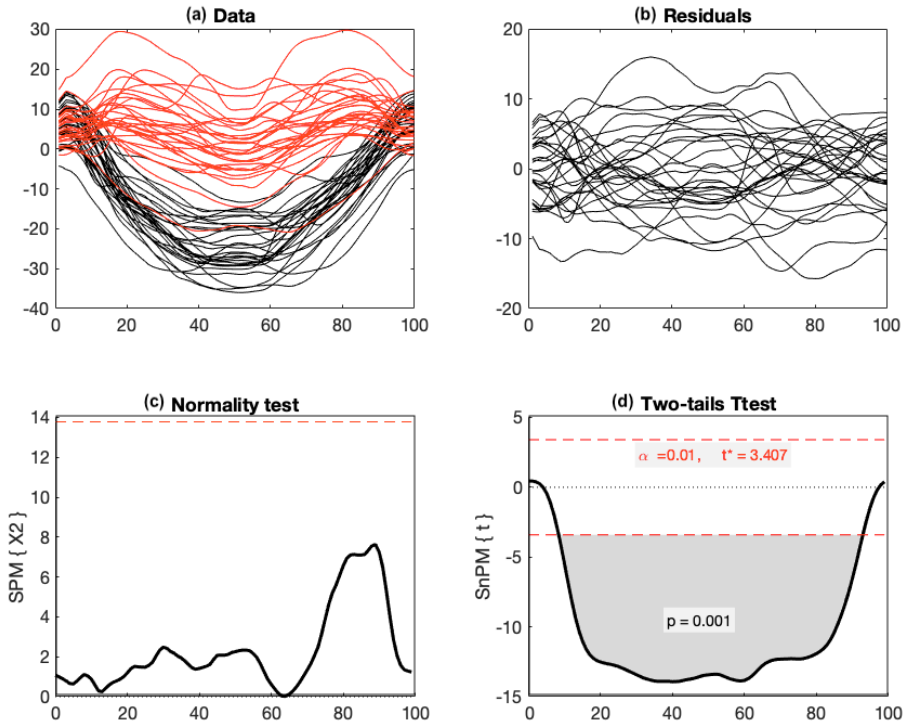

Figure 4.4 – *Exploration of medial and lateral internal-external rotations with statistical parametric mapping, featuring (a) experimental data for the medial (in black) and lateral (in red) trials, (b) their residuals, (c) the result of the normality test, and (d) p-values from the two-tailed t-test.*

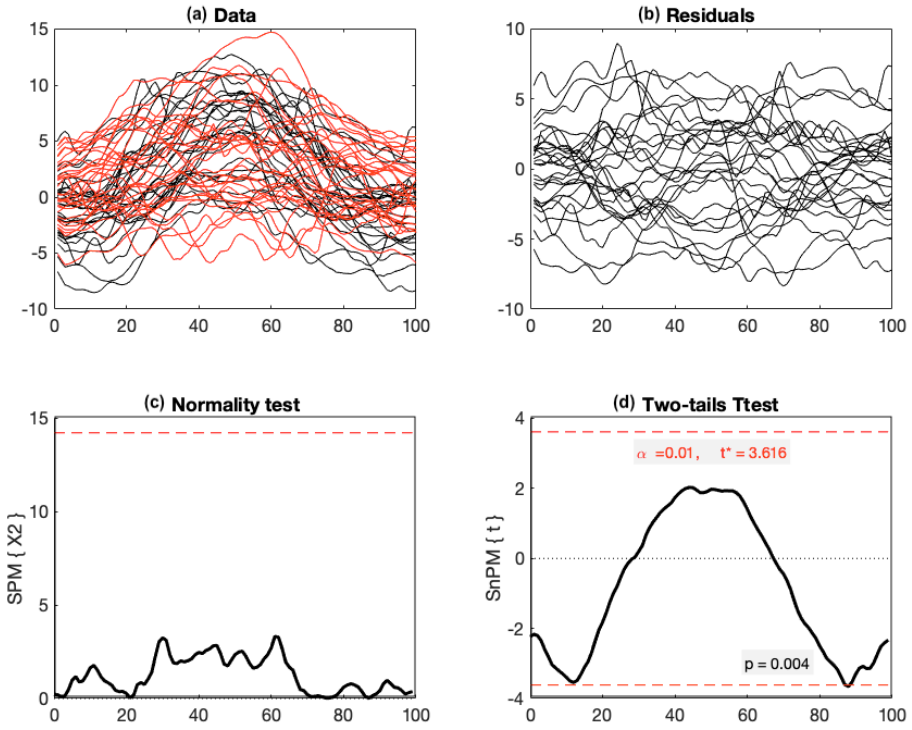

Figure 4.5 – *Exploration of medial and lateral medial-lateral translations with statistical parametric mapping, featuring (a) experimental data for the medial (in black) and lateral (in red) trials, (b) their residuals, (c) the result of the normality test, and (d) p-values from the two-tailed t-test.*

The cross-correlation matrix between degrees of freedom was reported for the medial and lateral extremes of tibiofemoral motion (Tab. 4.3). Moderate ($0.5<r^2<0.7$) or high ($r^2>0.9$) correlations were present in 18 out of 30 pair-wise correlations (Tab. 4.3). The tibiofemoral internal-external

rotation, abduction-adduction, and translations were coupled to the flexion angle (Tab. 4.3). Weak correlation was shown between flexion and abduction ($r^2<0.5$), moderate with internal-external rotations, while translations were highly correlated. Interestingly, medial-lateral translations were strongly negatively correlated to the other two translations and flexion and internal rotations ($r^2>0.8$) (Tab. 4.3). Abduction-adduction presented the weakest correlations with the other 4 DoF (Tab. 4.3). High correlations were also found between internal-external rotations with superior-inferior and medial-lateral translations (Tab. 4.3 – IE, 3rd row and column).

Table 4.3 *– Matrices of cross-correlation between degrees of freedom for the passive range of motion (pROM), in its medial, lateral extremes and neutral path for the adult population.*

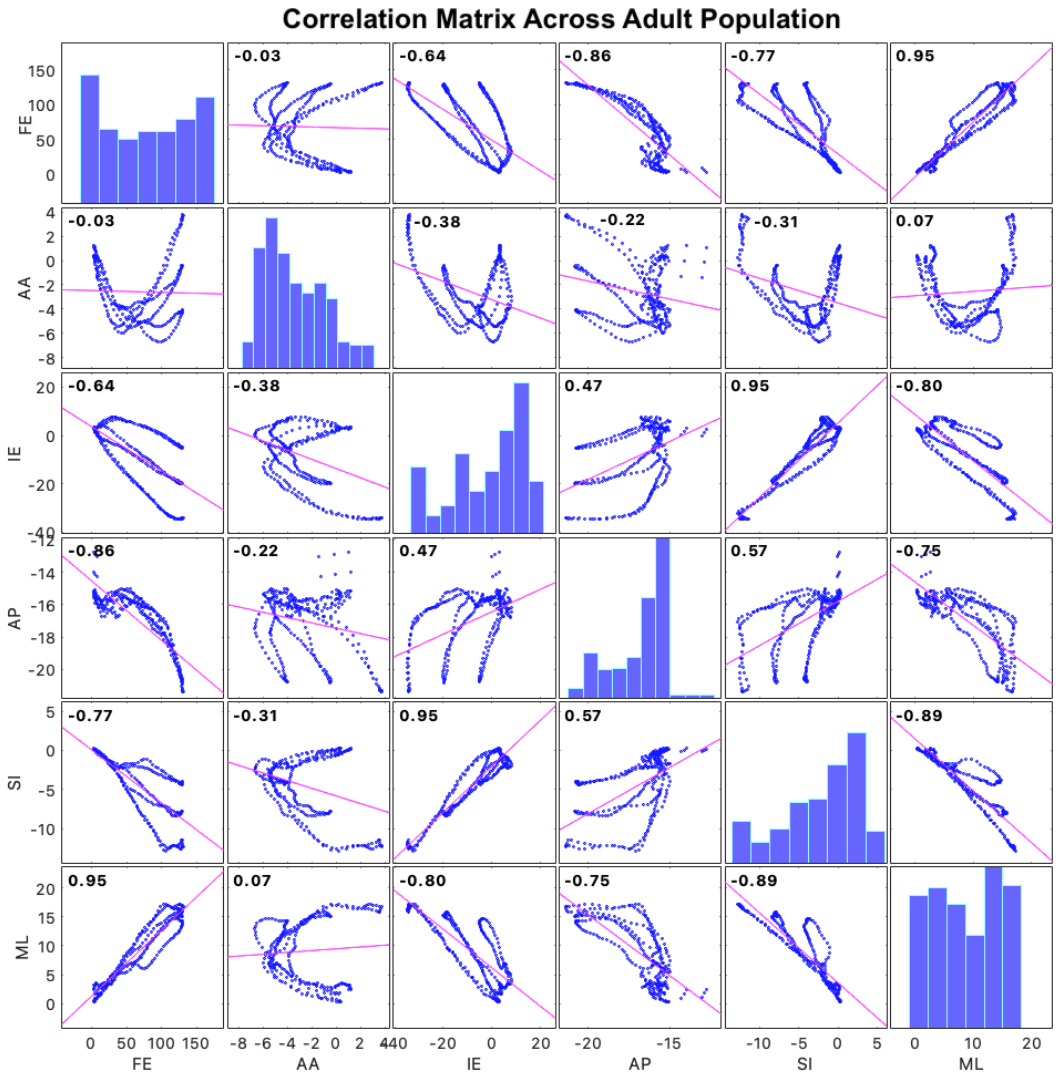

4.4.2 Comparison Between Males And Females

The same medial and lateral extremes of the tibiofemoral passive motion in all degrees of freedom previously reported were shown separately for the male (Fig. 4.6) and female population (Fig. 4.7). Mean patterns were mostly consistent in all DoFs and extremes for both sexes (Fig. 4.6-7), except for medial and lateral translation, abduction-adduction, and lateral internal-external rotation.

Interestingly, the variation of anterior-posterior translation in females, particularly in the lateral extremes, was higher than in males, despite the lower sample size of females (10 females vs 20 males) (Fig. 4.6-d, Fig.4.7-d). High differences between males and females were present for the abduction-abduction of the medial push (Fig. 4.6-b).

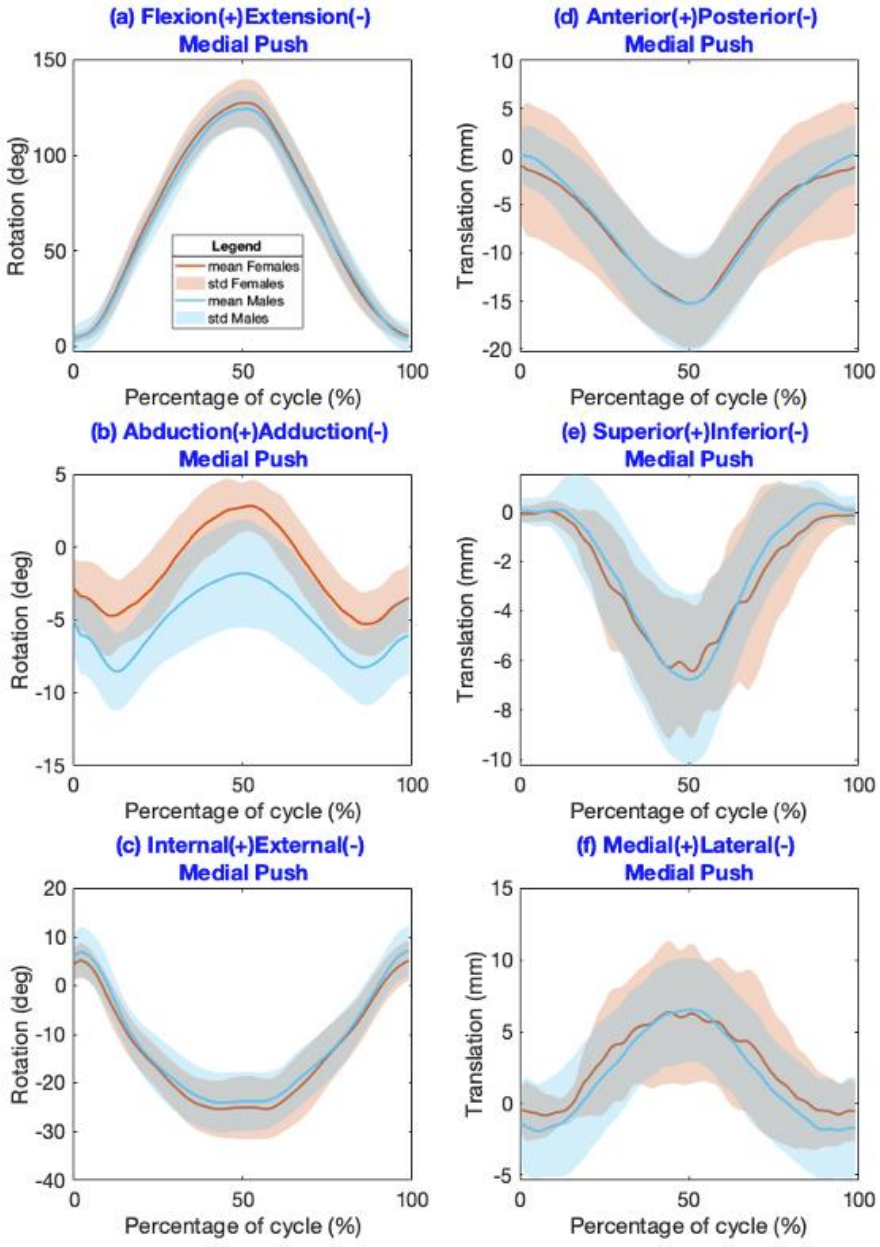

Figure 4.6 *– Mean and standard deviation of the tibiofemoral Medial extremes of passive motion, in blue of Males and in pink of Females, for each of the six degrees of freedom, including (a) FE, (b) AA, and (c) IE rotations, (d) AP, (e) SI, and (f) ML translations, as a function of the flexion cycle - 0 to 50% extension to flexion and 50 to 100% flexion to extension.*

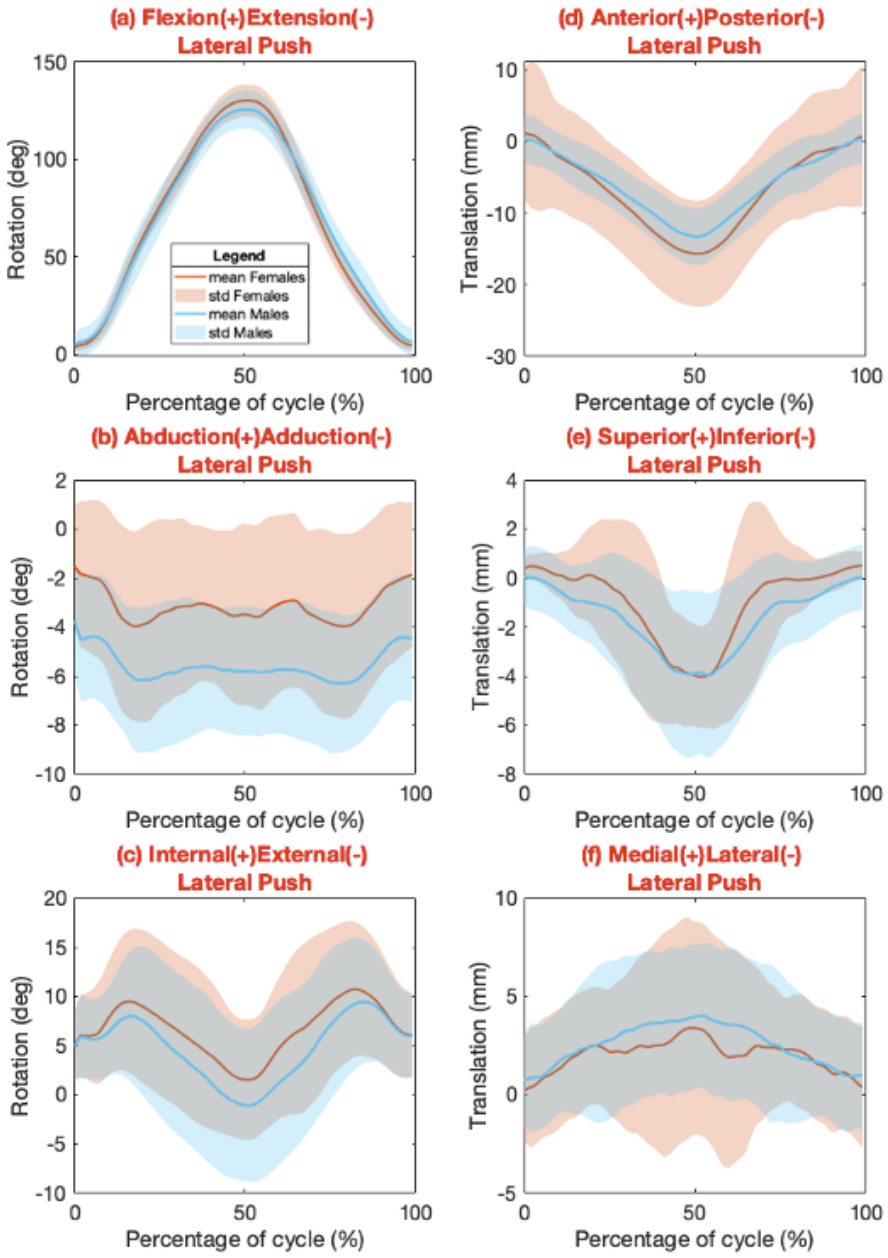

Figure 4.7 *– Mean and standard deviation of the tibiofemoral Lateral extremes of passive motion, in blue of Males and in pink of Females, for each of the six degrees of freedom, including (a) FE, (b) AA, and (c) IE rotations, (d) AP, (e) SI, and (f) ML translations, as a function of the flexion cycle - 0 to 50% extension to flexion and 50 to 100% flexion to extension.*

Statistical parametric mapping two-tails t-test reported statistically significance of these differences between males and females in medial adduction-abduction ($p<0.05$) (Fig. 4.8).

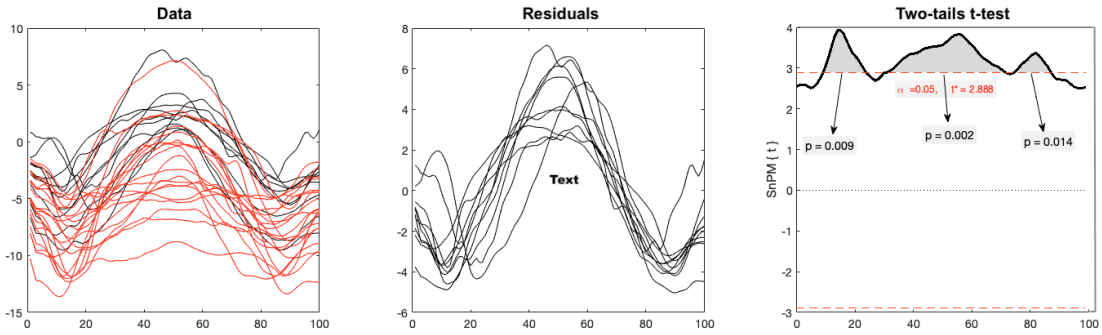

Figure 4.8 *– Statistical parametric mapping highlights significant sex-based differences in the abduction of the medial force trial, showcasing (a) experimental data for the medial (in black) and lateral (in red) trials, (b) their residuals, (c) normality test results, and (d) p-values from the two-tailed t-test.*

Differences between males and females were also present in the ranges of motion. Mean and standard deviation values of the passive range of motion were reported for the medial and lateral population separately (Tab. 4.4).

Table 4.4 *– Passive range of motion (pROM), mean and standard deviation of the tibiofemoral kinematics along six axes of motion for males mean difference and females both medial and lateral trial between 0 degrees and peak flexion.*

p ROM	**Medial Trial Extremes (n=30)**		**Lateral Trial Extremes (n=30)**	
	Males (n=20)	*Females (n=10)*	*Males (n=20)*	*Females (n=10)*
Flexion (+) Extension (-) (mean ± std) [deg]	120.85 ± 13.20	125.26 ± 12.92	120.89 ± 13.1	126.67 ± 8.53
Abduction (+) Adduction (-) (mean ± std) [deg]	7.43 ± 3.66	8.89 ± 1.97	4.22 ± 1.98	5.90 ± 2.53
Internal (+) External (-) (mean ± std) [deg]	31.95 ± 8.29	31.87 ± 6.67	13.58 ± 6.45	11.26 ± 4.49
Anterior (+) Posterior (-) (mean ± std) [mm]	15.68 ± 4.32	15.04 ± 4.07	13.98 ± 3.66	17.41 ± 11.7
Inferior (+) Superior (-) (mean ± std) [mm]	8.04 ± 3.17	7.18 ± 3.00	5.00 ± 2.99	6.04 ± 1.73
Medial (+) Lateral (-) (mean ± std) [mm]	9.45 ± 3.17	9.08 ± 4.54	5.30 ± 1.84	6.49 ± 3.78

Passive range of motion was also compared between males and females, medial and lateral trial, with sex-specific boxplots for each degree of freedom (Fig. 4.9a-f).

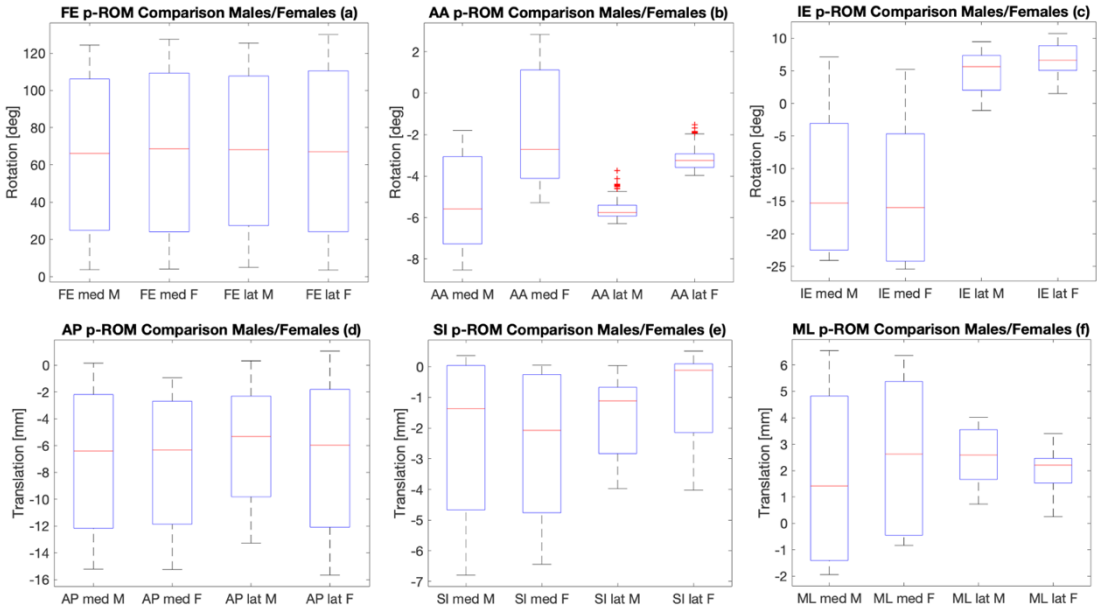

Figure 4.9 *– Comparative analysis of males (M) and females (F) in passive range of motion (p-ROM) for the tibiofemoral medial (med) and lateral (lat) extremes across all six degrees of freedom, arranged on the top from left to right as (a) FE, (b) AA, and (c) IE rotations, and on the bottom, again from left to right, as (d) AP, (e) SI, and (f) ML translations.*

The highest difference observed was in the flexion-extension passive range of motion, larger in females compared with males in both trials (by approximately 5-6 degrees) (Tab. 4.3); similarly, females presented higher abduction-abduction by an average of approximately one degree. However, while both mean and range were consistent in flexion-extension for sex and trial (Fig. 4.9-a), females showed an average of -3 degrees of adduction and males -5 degrees (Fig. 4.9-b) in both medial and lateral trials. Less than one degree/millimetre differences were present for the other DoFs, consistently in both medial and lateral extremes (Fig. 4.9-c, e, f). Once again, females showed higher variability than males in anterior-posterior translations for the lateral trial (Tab. 4.3, Fig. 4.9-d).

Cross-correlation matrix between degrees of freedom was reported for the medial and lateral passive kinematics separately for males (Tab. 4.5) and females (Tab. 4.6). Interestingly, moderate, and high correlations were present in 24 out of 30 pair-wise correlations for males (Tab. 4.5), against the 18 for females (Tab. 4.6) (six DoFs – each with both extremes and central); again, the main differences were in abduction-adduction.

Table 4.5 *– Matrices of cross-correlation between degrees of freedom for the passive range of motion (pROM), in its medial, lateral extremes and neutral path for the male population.*

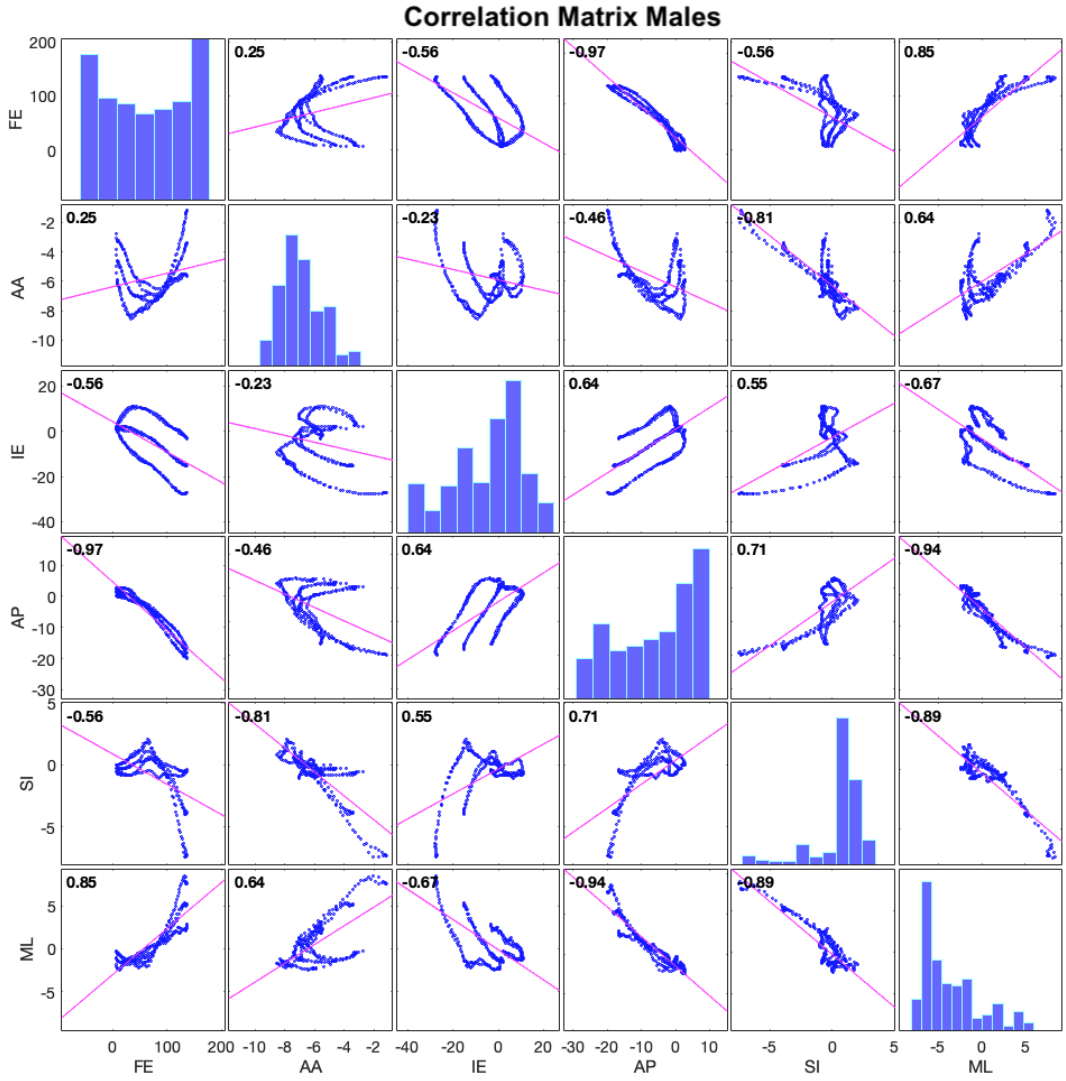

Table 4.6 *– Matrices of cross-correlation between degrees of freedom for the passive range of motion (pROM), in its medial, lateral extremes and neutral path for the male population.*

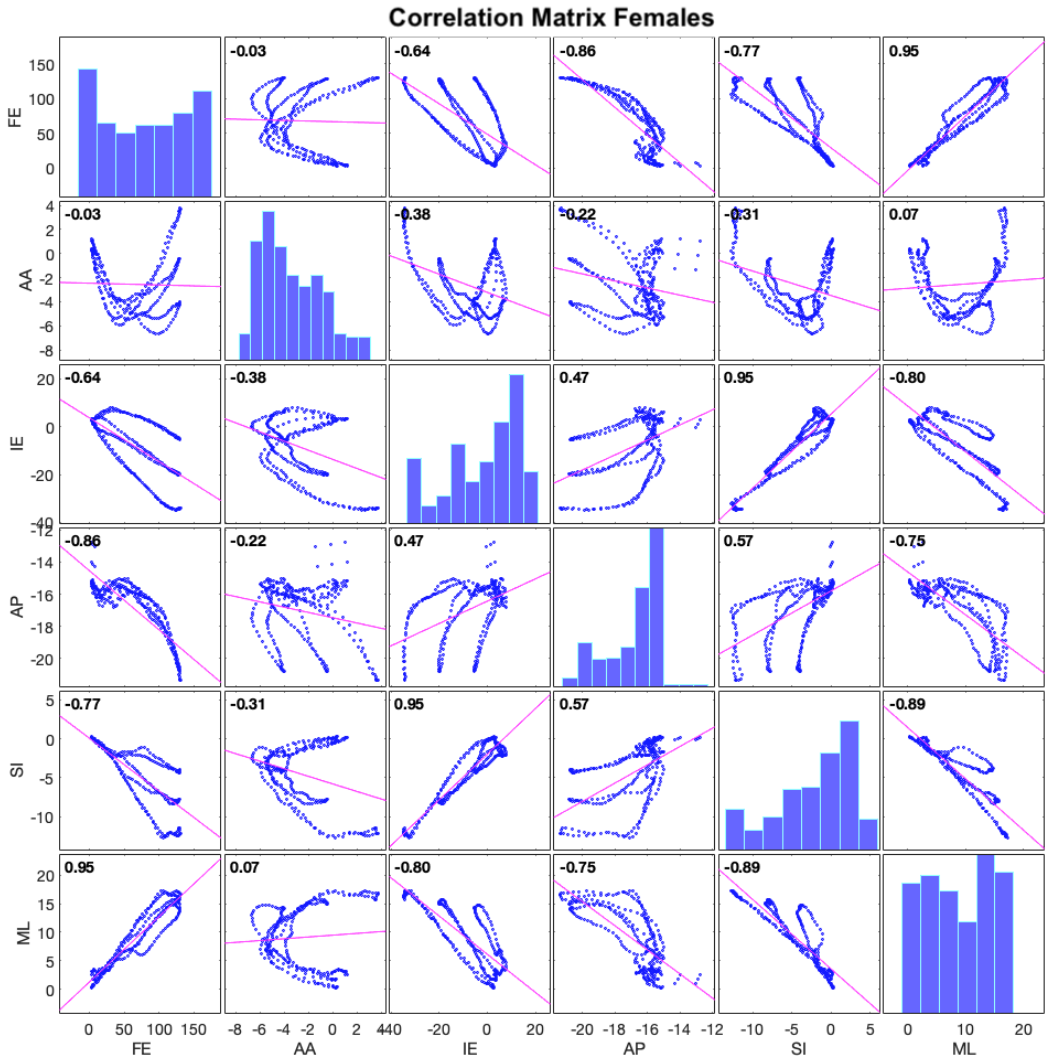

The power analysis was conducted using GPower, focusing on the range of motion in adduction and abduction for males and females across the population revealed an effect size of 0.4476 for the medial trial and of 49.13 for the lateral trial; the t-test means Wilcoxon-Mann-Whitney test (two groups) a priori resulted in a sample size of 132 specimens, 66 for each group – males and females to reach enough power (alpha =0.05, power = 0.8, GPower3.1).

4.5 Discussion

This study compares the envelope of the tibiofemoral passive motion in adult healthy knees from male and female donors. A newly developed experimental protocol (Chapter 3) was used to evaluate inter subject variability of the tibiofemoral unloaded and unresisted passive kinematics; in particular, medial, and lateral extremes of the envelope of passive motion were analysed with

continuity for each specimen, across their individual ranges of flexion-extension. For the first time, kinematics was reported for multiple motion patterns separately for males and females and over an individual flexion-extension arc, exploring medial and lateral extremes of the envelope of passive motion. This procedure improved current methods for determining ex vivo tibiofemoral kinematics by providing information for a relatively large cohort (30) including both sexes, along all the six axes of motion and for two extremes of the envelope of passive motion. Results revealed high individual variability, with consistent variations within sexes, larger than sex-specific differences along all the axes of motion. A minor statistically significant sex-specific difference was found in the abduction of the medial extreme, with females exhibiting higher values, while no significant differences were observed in the remaining degrees of freedom and trials.

The unloaded knee envelopes of motion extremes showed high variability between individuals and across populations. Across the population, the medial extremes of the envelope showed that, while flexing, the femur was rotating externally, approaching abduction from adduction, and translating posteriorly, inferiorly, and medially. The main differences with the lateral extremes were present in abduction-adduction where the extreme showed a steadier adduction trend and approaching external rotation, while mostly rotating internally; the lateral extremes were characterized by the same direction of translation, with lower peaks reached. Another key finding was that there is a high inter subject variability in medial and lateral individual extremes of the envelope. The presence of a passive envelope of motion was reinforced by the differences in all six degrees of freedom presented between the medial and lateral extremes. Furthermore, capturing a singular neutral central pattern of motion can be considered only a partial representation of the individual unresisted tibiofemoral passive motion envelope. The concept of the envelope of passive tibiofemoral joint motion remains relevant and important, since it delineates the motion occurring within the limits of joint laxity. The large differences between the passive motion using a moderate medial and lateral force on the knees supports the development of standardized procedures for measuring and reporting the tibiofemoral passive motion across laboratories. Hence, this could further impact fields from clinic, i.e., total knee arthroplasty pre-planning intra and post-surgery, to knee joint computational and musculoskeletal modelling.

The results from this study define the extremes of the envelope of the tibiofemoral passive motion described as the medial and lateral patterns captured for a healthy adult population. The novel approach herein presented provides insight into the controversial existence of difference between males and females to explain the knee burden bias due to sex and for a healthy knee population. For the first time, multiple motion patterns were reported separately for males and females and over an individual flexion-extension arc, exploring medial and lateral extremes of the envelope of passive motion. This procedure was a clear improvement on current methods as previous reports of ex vivo tibiofemoral kinematics have been inconsistent, due to limited: population sizes; analysing a few instances and/or degree of freedom; a singular nominal motion pattern among all

those possible within the limits of the envelope of unresisted passive motion and questionable measurement practices (Belvedere et al., 2011; Cyr and Maletsky, 2014; Wilson et al., 2000; Wunshel et al., 2012). The findings of this study were reinforced by the sample included in the analysis (n=30), in comparison to the sample size of previous ex vivo studies in literature (i.e., of large literature studies of passive motion in vitro/ex vivo: Belvedere n = 22, Cyr = 28, Wilson n = 15, Wunshel n = 24).

For the first time, the influence of sex on the envelope of the tibiofemoral passive motion was assessed. The null hypothesis stating the presence of differences of the envelope of the tibiofemoral passive motion between males and females was rejected as shown by the results. Results only displayed a moderately sex-specific passive tibiofemoral motion observed for two extremes of the passive motion showing higher adduction abduction in females than males. Some statistically significant differences were found with SPM (statistical parametric mapping) in medial adduction-abduction between males and females at moderate flexion angles, between 40 and 60 degrees of flexion, while no other significant difference was found along the remaining axes of motion and trial. Interestingly, these results find agreement with literature studies in vivo, highlighting higher abduction-adduction moments/motion in females during activities (MacLean et al., 1999; Ford et al., 2003; Peebles et al., 2020), which has been linked to ACL injuries mechanisms (MacLean et al., 2005). The variation within the male and female populations are consistent and larger than sex-specific differences along all the axes of motion. In agreement with anatomical differences between sexes, observed individual kinematic variability between specimens was higher than sex-based differences (Gillespie et al., 2011; Dargel et al., 2011; Asseln et al., 2018). The results of this study suggest that knee interventions should focus on personalized, rather than sex-specific solutions. The wide inter specimens range in both extremes of the passive motion necessitates a patient-specific approach to study the behaviour of the soft tissue restraints in knee computational modelling, to take into account the variability in the population, impacting on surgeon and orthopaedic companies for preoperative planning, on the investigation of the effects of surgical interventions and/or implant designs on the knee/tibiofemoral function which should include a set of models representative of the physiological range of the extremes of passive motion within a population.

There are a few limitations to this study, mostly inherent to the practical limitations of cadaveric testing. As the specimens were mid-thigh to mid-shank, most of the knee muscles were transacted, and hip and ankle muscles were absent, making the reference system identification less accurate. The results are based on a specific age group of adults, slightly skewed towards older, and representative of the population undergoing total knee replacement. Additionally, it is important to note that the study has a relatively small number of female specimens (n=10) compared to males (n=20) within the cohort of thirty specimens. Although this sample size falls within the upper range observed in experimental cadaveric studies of passive knee motion, the power analysis

resulted in the determination of this study being underpower for differences between males and females; therefore, it has limitations in detecting subtle differences between sexes. While it is important to consider statistical power and sample size in the interpretation of the results, it is also crucial to recognize the inherent limitations and constraints of cadaveric studies. Cadaveric studies are often underpowered and face challenges in achieving the test and analysis of large sample sizes due to factors such as costs of these studies, time constraints, limited availability of cadaveric specimens, and practicality such as storage space in freezers in working with these numbers of cadavers. As a result, many cadaveric studies, including this one, while they could be underpowered, are considered investigations that provide valuable data and insights. Furthermore, while it may be preferable to have an equal distribution of male and female subjects, it must be noted that statistical parametric mapping account for the different sample sizes between the two sexes. Nevertheless, the study provides valuable insights into passive knee motion for both male and female subjects. The observed differences in the number of significant correlations between degrees of freedom, between the male and female cohorts may be partly influenced by the difference in sample size, and other factors like individual characteristics and data variance also play a role. Despite the smaller sample size of females, they exhibited higher standard deviation and variability in the data compared to males, potentially due to anatomical variations and tissue properties unique to that group. To further enhance our understanding of potential sex-related differences in knee function, future investigations with a larger sample size would be warranted to increase statistical power and improve the generalizability of the findings. Furthermore, the study is limited to the application of a medial and lateral force to the joint; the same study could potentially be repeated with internal-external moments applied while keeping the other degrees of freedom free.

In conclusion, the the medial and lateral extremes of unloaded knee passive motion differed significantly from one another. This finding suggests that standardized procedures should be adopted for measuring and reporting knee passive motion across laboratories. This kinematics study quantifies the extent of the envelope of the tibiofemoral passive motion by investigating its extremes across a healthy population. A clinically relevant outcome of this thesis is the analysis of tibiofemoral motion variability within a healthy population and the comparison of differences between males and females of the tibiofemoral motion envelope. This study also suggests that knee interventions should be geared towards personalisation, rather than sex-specific solutions, since individual variability was high, but sex influences were only moderate and only had a limited impact on medial abduction-adduction. Future evaluation of in vitro/ex vivo tibiofemoral passive kinematics should include both medial and lateral extremes of the passive motion and should consider individual rather than sex-specific kinematic patterns. As this work considered a specific age group, future research could include a larger age range. Further investigation of the bias of the knee disease burden may evaluate additional kinematic tasks under load and different

combinations of muscle involvement, as the differences in reported injury and pathologies due to sex could be attributable to other factors such as active tibiofemoral motion patterns.

Chapter 5

LITERATURE REVIEW

A Cost - Complexity - Utility Perspective On In silico Knee Joint Modelling: Mapping Literature Review

CONTENTS

F. Bucci, M. Taylor, R. Al-Dirini, S. Martelli (2023) – Mapping review on in silico knee and tibiofemoral joint modelling: a cost - complexity - utility perspective. The knee. Journal Article. *In preparation for submission to peer-reviewed journal.*

Please refer to the appendices at the end of this thesis for a detailed outline of the author's contribution to this study (Appendix A).

5.1 Abstract

The choice of a modelling approach for research is an ongoing debate among researchers. Factors such as time-efficiency, cost-benefit, complexity, invasiveness, accuracy, and availability of experimental data are carefully evaluated. Sample size requirements also play a crucial role, with subject-specific studies employing resource-intensive methodologies and population studies opting for faster but less accurate approaches. To address these challenges and provide guidance, this chapter presents a comprehensive literature review of tibiofemoral joint models. The aim is to identify the most suitable modelling approach for investigating tibiofemoral joint elasticity, considering individual differences and population variability.

The evaluation of cost, complexity, and utility was the primary focus of the literature review, which assessed tibiofemoral joint models. During the data extraction process, model characteristics, computational requirements, validation studies, and reported limitations were systematically recorded. By analysing these factors, valuable insights regarding the strengths and limitations of different models were obtained, enabling researchers to make well-informed decisions based on their specific needs and research questions. The main objective of the review was to comprehensively evaluate these factors and identify the most suitable modelling approach to investigate the passive to active behaviour and the contribution of ligaments in a population, aligned with the final objective of the thesis research. Consequently, the models were further categorized based on their suitability for studying population variability and accounting for individual differences in tibiofemoral joint passive and active behaviour.

The mapping literature review revealed the advantages of musculoskeletal (MSK) models for investigating knee elasticity. MSK models exhibited dynamic analysis capabilities and computational efficiency, providing a comprehensive understanding of the TF joint behaviour, and bridging the gap between passive and active motion. Moreover, the computational efficiency of MSK models facilitated the analysis of large population datasets, enabling broader investigations into the behaviour of the tibiofemoral joint.

The findings from the literature review highlighted the strengths of MSK models in investigating the elastic contribution of soft tissues in the tibiofemoral joint, making them a compelling choice for this research. By adopting an MSK modelling approach, valuable insights can be obtained into the passive to active behaviour of the tibiofemoral joint, as well as the effect of variability in singular anatomical structures and their interaction in the joint function within a population. In conclusion, the mapping literature review in this chapter serves as a critical component, providing guidance in selecting an appropriate modelling approach for investigating the ligament contribution, particularly within a population context.

5.2 Introduction

Knee and tibiofemoral models have been generated using a variety of different modelling approaches, with a range of accuracy, each producing insights depending on the research question. Therefore, determining the optimal modelling approach for every specific application involves balancing between (1) accuracy of the results required, (2) the time and expertise required to generate and solve the model and process the results. This review of TF modelling aims to relate complexity and utility enabling a pragmatic decision-making process in modelling tibiofemoral mechanics.

There are four different main categories of approaches available to investigate the knee and tibiofemoral joint, including theoretical/analytical, finite element, statistical and musculoskeletal modelling (Fig. 5.1). The diversity of these models mainly pertains to the level of abstraction. Depending on the approach selected, they can differ in terms of dimensional scale (representation of structure behaviour changes at different scales), group represented (generic individual, specific subject, or population), and task performed (i.e., passive flexion, gait, squatting, running). Besides modelers subjective choices, the approach is often chosen based on trade-off between research question, availability/possibility (money, time, and expertise) to collect the data required to build them, and outcome in term of variables of interest (kinematics, kinetics, contact or again muscle or ligament forces, etc…). Moreover, in recent years, there has been a tendency to combine multiple approaches, making the panorama and the selection of the most convenient and appropriate approach even more complex.

Through this comprehensive review, valuable insights into the landscape of tibiofemoral modelling are provided, facilitating the selection of the most appropriate and convenient approach for specific investigations.

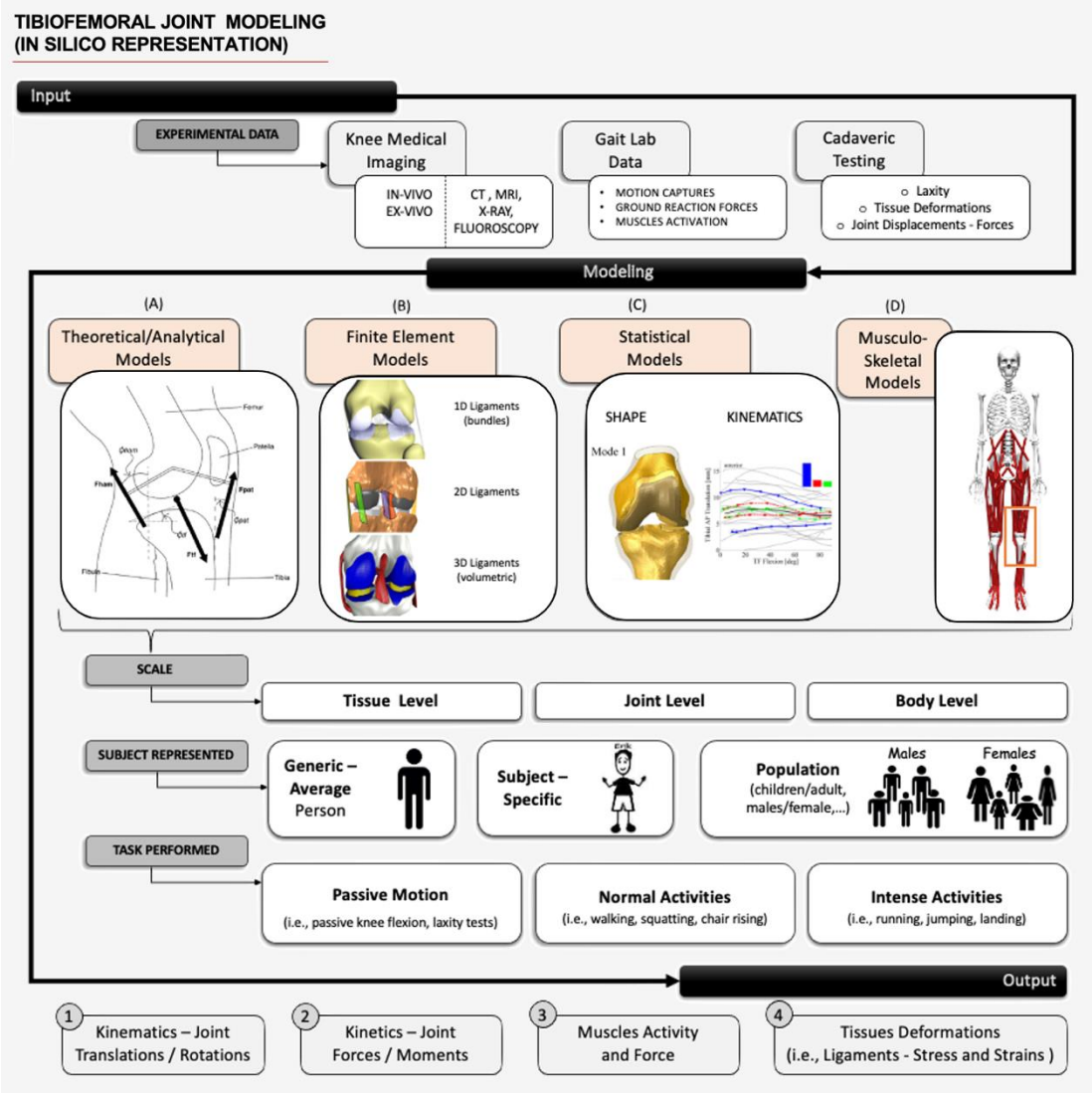

Figure 5.1 *– Knee modelling overview, including (at the top) experimental input data, (at the bottom, 1 to 4) desired output, and (at the centre, A to D) main modelling techniques and approaches, spanning theoretical, finite element, statistical, and musculoskeletal models, or a combination of them, with considerations for abstraction levels, target groups, and tasks, reflecting potential modellers choices influenced by data availability, research focus and resource constraints.*

5.3 Literature Review Of Knee And Tibiofemoral Joint Models

5.3.1 Theoretical/Analytical Models

Mathematical, analytical, and theoretical models are typically the most generic and simplified knee representations and aim at describing a general mechanism. These models can include 2d or 3d representation of the entire body or the knee joint only, with more or less detailed structures necessary to explain the mechanism/function they are investigating. 2D models of the entire body or limb typically investigate muscle and articular forces. 3D knee model studies instead often investigate the articular surfaces contact or other 3d structures. Other models investigate

kinematic or dynamic behaviour through substitutive structures. Theoretical models initially represented the tibiofemoral kinematics as a hinge that flexes and later as screw-home mechanism, with flexion-extension and internal-external rotations as its two degrees of freedom system. The 2D models are only able to describe AP translation during knee flexion. Mathematical 2-dimensional sagittal plane models of the knee joint (Smidt et al.,1973; Yamaguchi and Zajac, 1989; Shelburne and Pandy, 1985; Kernozek and Ragan, 2008) have been used widely used to estimate reaction forces and isometric muscle strength (Fig. 2.15-b). Even 2-dimensional three body segment model of the human knee, including the main ligaments and muscles, under dynamic conditions have been made (Tümer and Engin, 1993). The predictions of these models matched the experimental results qualitatively. Treating the ligaments as lines is just the major of a series of limitations that models, specially 2 dimensional ones, may have. Some studies have presented the TF joint as a ball-and-socket joint (Meng et al., 2017a; Laz and Browne, 2010; Eskinazi and Fregly, 2016; Bendjaballah et al., 1995; Weiss et al., 2005). Others again modelled separately the behaviour along different anatomical planes, as well as the knee passive and active kinematics, as the resistance that the joint offers to different displacements highly differs. Some studies (Eskinazi and Fregly, 2016; Parenti-Castelli et al., 2004b) concluded that the passive knee flexion can be described by a coupled path and predicts that the knee motion is prescribed by ligaments and articular surfaces alone along a single path. These models describe the knee passive motion as a one degree of freedom parallel spatial equivalent mechanism (Ottoboni et al., 2010; Parenti-Castelli et al., 2004a) (Fig. 5.2-a). Tibia, femur, ACL, PCL and MCL modelled as a five rigid link mechanism, with rigid contacts and isometric ligaments constraining the motion along a specific path. Articular surfaces were described as planar firstly to spherical with increasing anatomical accuracy and so leading to models becoming increasingly complex. The same study also shows that there is a limit beyond which the knee model surface approximation accuracy will not improve further. Modelling in 3D has contributed to understanding passive and active motion in relation to articular geometry and ligamentous constraint. In the realm of knee joint passive function, Bradley et al. (1988) proposed a four-bar linkage mechanism that describes the tibiofemoral motion through the intersection of the ACL and PCL ligaments, determining the instant centre of rotation between the femur and tibia (Bradley et al., 1988). This model highlights the importance of the femoral site attachments of the cruciate ligaments and identifies attachment zones where the length of the ligaments can be predicted. Other researchers, such as Blankevoort et al. (1988), have acknowledged that while passive knee motion is highly reliable, it is not unique; instead, there exists an envelope of motion within which the knee offers minimal resistance to motion (Blankevoort et al., 1988). A quasi-static model of the knee which includes the ligaments and capsule, and the three-dimensional geometry of the joint surfaces modelled the articular surfaces as curved by representing them through polynomials (Wismans et al., 1980). The anterior posterior laxity was calculated from the estimations of the relative position of the femur and tibia, ligament forces and elongations, contact points and magnitude and direction of contact forces.

Mommersteeg (Mommersteeg et al., 1996b) developed the same quasi-static model with curved articular surfaces and ligaments represented as multi-bundle structures as proof of concept for varus-valgus and anterior-posterior laxities predictions. An anatomical dynamic mathematical model of the surfaces of femur and tibia in contact represent the 3d motion within several ligamentous constraints modelled as nonlinear elastic springs (Abdel-Rahman and Hefzy, 1998). Ligamentous forces were expressed in terms of these six parameters which described the 6 DoF kinematics. A mathematical model (Blankevoort and Huiskes, 1991) with curved line bony edges, deformable articular contact, and ligament spring elements able to wrap around bones has been developed to describe a quasi-static behaviour of the tibiofemoral joint (Fig. 5.2-c). A 3D mathematical model of the articular surfaces and ligaments, accounting also for these last material properties as non-linear springs, has been developed (Wismans et al., 1980; Andriacchi et al., 1983). However, while the model proves the significant influence of the articular shape in the knee AP laxity, the knee model revealed to be insensitive to changes in the stiffness of the ligament.

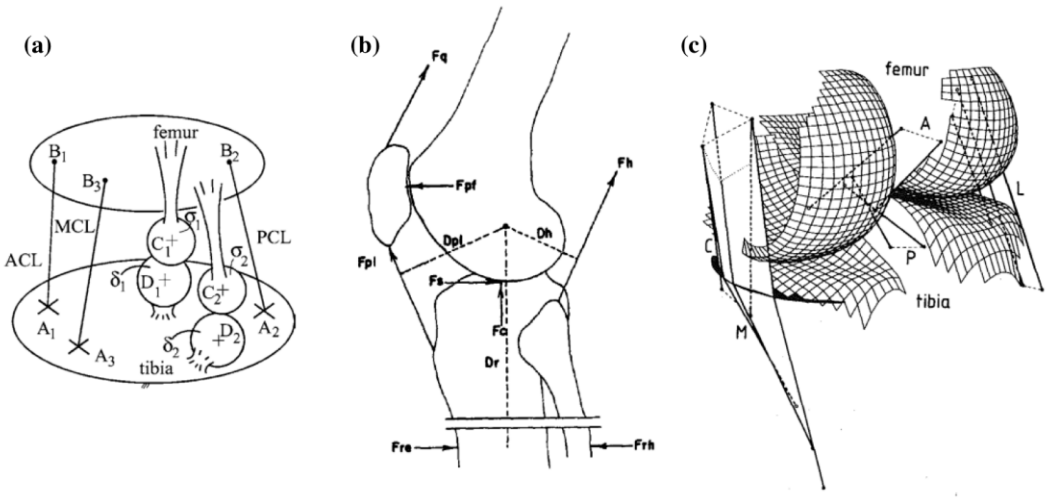

Figure 5.2 *- Theoretical/analytical models of the human knee: (a) one degree of freedom passive kinematic mechanical equivalent, reprinted with permission from the Journal of Engineering in Medicine, SAGE Publications, Inc. (Ottoboni et al., 2010); (b) two-dimensional active function, reprinted with permission from Journal of Biomechanics, Elsevier (Smidt et al., 1973); (c) three-dimensional with ligament inclusion, reprinted with permission from Journal of Biomechanics, Elsevier (Blankevoort and Huiskes, 1996).*

5.3.2 Finite Element Models

Finite element models (FEM) are 3d models that allow subject-specific anatomical and material properties representations, with different levels of anatomical fidelity/accuracy and mechanical representations. The accuracy of the geometry in FEM models of the knee, which is typically derived from CT/MRI images, depends on factors such as the pixel size and contrast in the images (Kazemi et al., 2013). However, these factors may not adequately capture individual differences and irregularities at a smaller scale, such as fine anatomical details or variations. Another important aspect of FEM models is the consideration of specific modelling choices or model features. This includes the identification of the appropriate material behaviour at a tissue level, as FEM models

can adopt various experimentally derived material properties formulations. These models are commonly used for investigating ligament behaviour and/or function, and there is a wide spectrum of models and approaches available, ranging from 1D to 2D parametric models to 3D approaches (Galbusera et al., 2014) (Fig. 5.3).

(1) The most used 1D ligament models are non-linear spring elements. Progressive fiber recruitment during loading is realized through parallel spring bundles (Viceconti et al., 2006a). Across literature, different numbers of bundles have been used to model the same ligaments (Blankevoort et al., 1991; Li et al., 2008). Using fewer than three lines per ligament in the model was found to make it overly sensitive to geometrical changes; seven or more makes the model redundant (Mommersteeg et al., 1996a). While a one-dimensional model is useful to predict knee joint kinematics in a fast way, it possesses many limitations. They do not confer uniformity or provide stresses and strains. Also, the kinematics variability experimentally observed between individuals is not achievable, as even deeply different parameter settings and initial tensions provide almost the same kinematics predictions. Although one-dimensional representations allow a model to describe the joint kinematics and predict ligament forces, it does not provide a unique solution and the reference strains that it predicts are often physiologically unrealistic (Wilson et al., 2003).

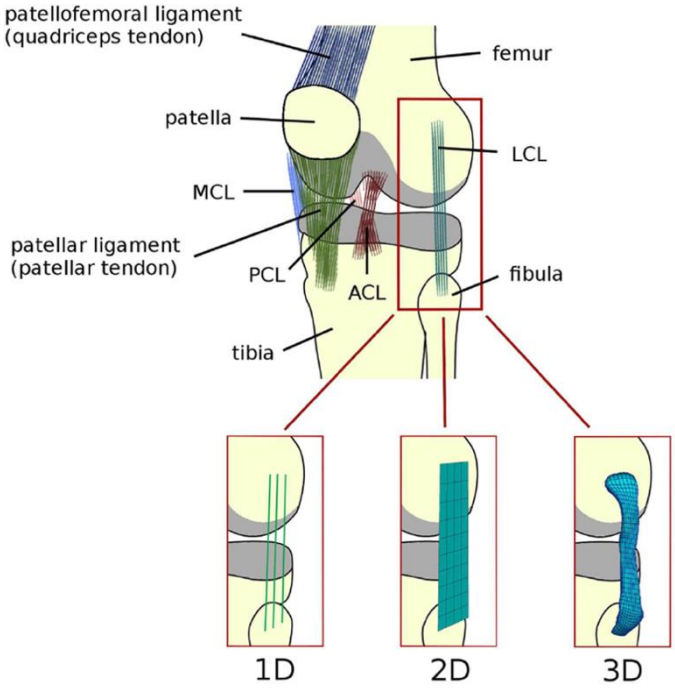

Figure 5.3 *– Schematic knee joint anatomy and ligament representations (ACL, PCL, MCL, LCL) in 1D, 2D, and 3D used in knee computational models, reprinted with permissions from Frontiers in Bioengineering and Biotechnology, Frontiers Media SA (Galbusera et al., 2014).*

(2) Models featuring two-dimensional representations of ligaments can predict quantities such as soft tissue stress, which is not possible with a one-dimensional representation. While being

less complex and computationally heavy than three-dimensional, they are also the least realistic and adaptable approach.

(3) On the other hand, 3D FEM models of ligament can provide stress-strain relationships. These models approximate the subject-specific anatomy in three dimensions and facilitate modelling interactions through wrapping. However, if indications about justified assumptions are present, when soft tissues need to be characterized in a knee model, no univocal guide is present in the literature. Several testing approaches leading to different characterizations are present in literature studies, even for the same soft tissue under the same conditions. This multitude turns to constitutive and tissue models of the knee soft tissues. Literature research, even though systematic and filtered on selected thresholds, result in several ranges of values for different models of the same tissue (Pianigiani et al., 2017). Constitutive models describe material properties assigned to these geometries. Three-dimensional elastic isotropic material models of the ligaments have been used, especially, again, for the ACL (Heegaard et al., 1995) predicting inhomogeneous in situ stresses. Although at a fibres level, this model is inaccurate; material property inhomogeneities in the same ligament are neglected. In addition, simplification in geometry is usually exploited along with neglecting ACL two-bundle behaviour and interactions with PCL. Ligaments have been also widely represented as hyper-elastic materials. In particular, ACL has been attributed to an isotropic feature with nonlinear fibres to reinforce. Inhomogeneous stresses have been found during the flexion, while stress was increasing during anterior tibial displacement. However, initial stress distribution state was arbitrary and generated starting from non-physiological position. Transversely isotropic hyperplastic, have been use for MCL to predict stress and strains (Weiss et al., 1996); initial stretch applied was measured during experimental tests. Constitutive transversely isotropic hyper elastic models have been applied with success to predict strains in the MCL and PCL, as well as with ACL (Ascani et al., 2015; Fitzpatrick et al., 2010). Strain rate has been found to relatively affect ligament behaviour in module (Beillas et al., 2004; Hirschmann and Müller, 2015; E. Peña et al., 2007). In several works (Kazemi et al., 2011; Kazemi et al., 2012), ligament viscoelastic models have been implemented; variants can also be found, concerning the inclusion of internal friction (Donahue et al., 2003) or non-linearity (Hull et al., 2002) and also anisotropic (Yang et al., 2009; Mononen et al., 2012; Shirazi et al., 2008) behaviour. The ligament has been modelled also as isotropic poroelastic elements with non-linear spring elements to represent anisotropy due to collagen fibres (Wilson et al., 2003). Other material approaches modelled soft tissues as a linearly elastic composite (Schmitz and Piovesan, 2016; Amiri et al., 2006). Incompressible composite of undulating collagen fibres embedded in a fluid matrix used a strain energy approach (Fitzpatrick et al., 2010).

The third assumption, probably the most important, involves how different structures interact with each other, passively and/or actively, in loaded and/or unloaded conditions. FEM models are typically used to investigate how each structure behaves in terms of stress and strains, providing the overall motion at given articular forces. Boundary conditions in FEM knee joint modelling, include simplification of the load conditions and contact. In the first case, loading often relies on assumptions, such as dividing dynamic loading into stages of static compressive loads and often neglecting muscles and tendons. Models often do not account for the presence of fluid presence and force inside the joint. Contact is assumed to often be rigid between bones and cartilage, elastic or deformable following several different laws between cartilage and menisci or between femoral and tibial cartilage. However, the complexity of the contact makes convergence challenging, increasing computational time required for numerical convergence (Weiss et al., 2005). Technical difficulties in dynamic contact can also arise by applying free surfaces boundary condition. Besides, contact, computational time grows also with time discretization - function iterations.

Several examples of FE models of the tibiofemoral joint in the literature are presented to showcase the diverse range of modelling approaches, including variations in geometry, material properties, boundary conditions, and computational techniques. Some models represented the TF joint screw-home mechanism through FEM with models including bone and cartilage, beside ligaments (Moglo and Shirazi-Adl, 2005; Peña et al., 2007). Screw-home mechanism resulted being significantly affected by ACL changes in initial strains. To validate the ACL - PCL coupled mechanism and to evaluate the PCL under anterior femoral forces across the flexion, an FEM model of the TF joint (tibia, femur, cartilage, menisci and four main ligaments) has been developed (Moglo and Shirazi-Adl, 2003a); nonlinear elastic, static analyses have been performed. The primary structures found to restrain are the MCL and LCL in extension, while the contribution of the PCL is moderate; in flexion this is progressively inverted. In all these studies, ligaments were modelled as spring elements. More realistic geometry can be implemented; for instance, ligaments have been considered transversely isotropic with hyperplastic properties (Eskinazi and Fregly, 2016) and the roles played in the knee stability and with load transmission were investigated. A non-linear FEM model including anatomy and material properties of bones, menisci, cartilage, and main ligaments (ACL, PCL, LCL, MCL) used ligaments stiffness, initial strains, and attachments, calibrated to match experimental results, as well as their engagement, found in agreement with literature (Bendjaballah et al., 1995). Other studies reproduced computationally knee laxity tests to evaluate knee contact mechanics; some of these conditions performed were drawer, anterior-posterior forces as well as varus-valgus and internal-external rotations (Ahmed et al., 1992; Bendjaballah et al.., 1998; Harris et al., 2016; Maletsky et al., 2016; Yasin et al., 2013). The response was largely influenced by ligament material properties, loading and boundary conditions. ACL material properties sensitivity for a TF FEM model has been

assessed under different loading conditions (Wan et al., 2013); isotropic hyper elasticity model, a transversely isotropic hyper elasticity model with neo-Hookean ground substance description, and a transversely isotropic hyper elastic model with nonlinear ground substance description were found to induce altered joint kinematics, deformations, and strains pattern, while maintaining the same force predictions. Others investigated PCL, MCL and LCL (Bendjaballah et al., 1997; Jilani et al., 1997; Gardiner and Weiss, 2003; Ren et al., 2017). More complex kinetic (forces and moments) and simpler kinetic-kinematic (forces and angles) driven FEM models have been built (Bolcos et al., 2018) to evaluate gait stance phase representation ability. A subject-specific knee model, kinematically driven, has been used to predict the forces in the main ligaments while kneeling at different flexion angles (Yang et al., 2010); geometry and load-elongation curves were feeding a non nonlinear elastic spring ligament's model. Location of the ligament attachment sites on each bone and their reference lengths were determined through an optimization procedure to minimize difference; this was working only at high degree angles suggesting at low flexions the need for different models. Muscles can also be explicitly added into the knee FEM models (Mesfar and Shirazi-Adl, 2005), to simulate activities (flexion angles up to 90°, quadriceps forces up to 411 N); the study showed that muscle forces significantly increased ACL forces, contact forces/areas, joint resistance and tibial translation, while joint flexion substantially reduced them all. Other models such as Guess et al. (2010) developed a subject-specific computational model of the knee with menisci to enhance understanding of knee mechanics and tissue interactions, investigating the role of the menisci with a model included 61 discrete meniscus elements connected via stiffness matrices (Guess et al., 2010).

5.3.3 Statistical Models

The subject and population specific anatomical and functional variability, instead, is the reason why statistical tools have been necessarily introduced in knee joint modelling. FEM models in fact typically only represent a specific-subject or an average. In order to study the variability across population and generalize their conclusions, statistical tools, such as principal component analysis (PCA), were included giving birth to statistical modelling. Statistical shape models are used to represent the variation of shape of the structures across population. For instance, it has been found that females knees are smaller and specific anatomical features differs, such as the tibial slope (Pedoia et al., 2015). Most models represent around 20 subjects, due to the data, time and costs required. Some of the models include only femur and tibia, other includes cartilage, others again the relative position of femur and tibia, and/or ligament geometries. Other type or models present in literature are models combining statistical shape and kinematics models, or statistical kinematics models only. Understanding the potential impact of inter subject variability has been the focus of many researchers. Statistical models have multiple benefits. First, quantifying with data the anatomical variability of the knee naturally present across individuals and populations,

previously discussed (previous section). One of the primary uses of these models concern the representation of anatomical variability of the articular surfaces shape (bones or bones and cartilage). When the only shape is represented, they are so called Statistical Shape Models (SSM). These models have been applied to characterize bone morphology for training sets of subjects representing population variability of femur, tibia, and pelvis. Statistical models have also been extended to include intensity and capture the variability of the relative alignment of the structures, and with the inclusion of material properties. Rao et al. (2013) represented size, shape, and alignment through a statistical shape FEM model of the knee – femur, tibia and patella bones and cartilage, from MRI of 20 adult healthy male specimens in unloaded condition; results were provided in picture (Rao et al., 2013b) (Fig. 5.4). Variability across the population in order of mode of variation was attributable to scaling, tibial AP alignment and shape, IE rotation, AA rotations and medial–lateral width of femoral and tibial cartilage (Rao et al., 2013b).

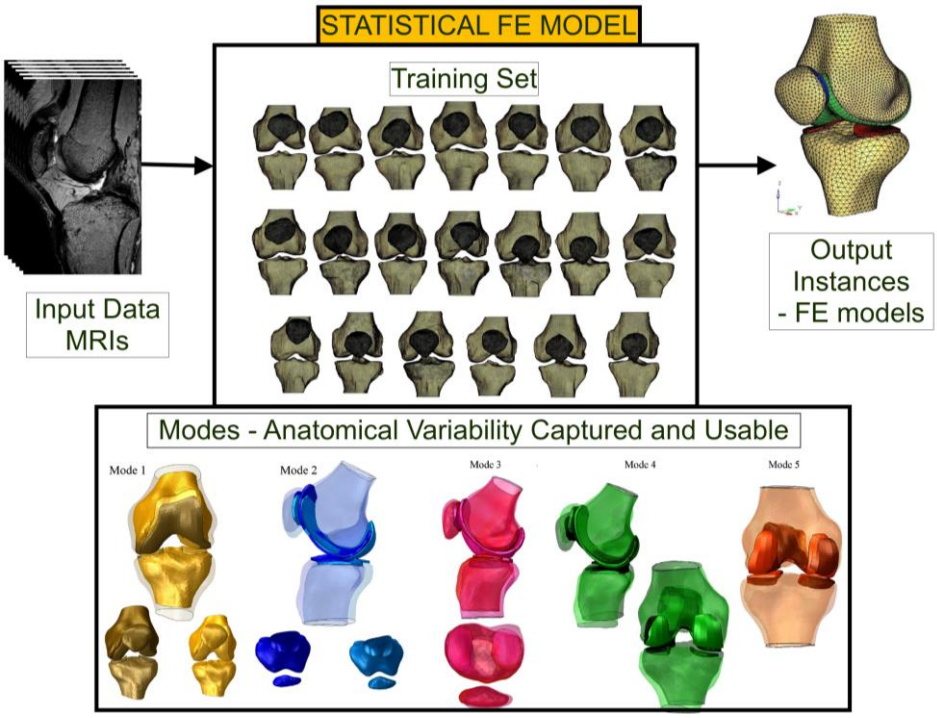

Figure 5.4 *– Statistical finite element model of the human knee, using MRI input data and a training set of FEM derived from population instances, highlighting the exploration of anatomical variability through modes of variation and the generation of FEM models as output instances; reprinted with permission from Medical Engineering & Physics, Elsevier (Rao et al., 2013b).*

Smoger et al. (2015) SSM is based on 20 specimens and includes bone and cartilage data, both imaging and 6 DoF testing of TF and PF kinematics while simulating squats (Smoger et al., 2015). Among the PC modes relative to the relationship between anatomy and kinematics, the first mode captured changes in condylar radius shape and their impact on TF anterior-posterior translation, internal-external rotation, and the lowest point of the femur. Clouthier et al. (2019) integrated MSK and SSM as previously described, investigated the relationship between anatomy, knee kinematics and articular forces while walking (Clouthier et al., 2019). It was found that variations in articular geometry can substantially alter secondary tibiofemoral kinematics, articular cartilage

loading, and ligament loading during gait. In particular, a flatter medial tibial condyle increases external rotation, anterior translation, and ACL force; in a flattened tibial plateau, the articular constraint is reduced, which increases anterior translation and ACL force as the soft tissues become more important to the stability of the joint.

5.3.4 Musculoskeletal Models

Musculoskeletal (MSK) models are a class of multi-rigid-body dynamic representations of the entire body, lower or upper limbs. These models represent the body as a chain of rigid bones connected by joints defining its motion and controlled by actuators that represent tendons and muscles. The main assumptions concern: (1) bones have infinite rigidity, described by mass, the centre of mass, moments of inertia, etc. (2) idealizing/simplifying joints, by using mathematical equations to define kinematical constraints, location, and orientation of joint reference frames, and (3) linearity of muscle-tendon units, where the main bundles are modelled as actuators and linkers connecting the predicted insertion centroids. MSK simulations allow through a workflow called inverse problem the estimation of (1) joint angles/coordinates, (2) joint moments, (3) muscles activation/forces and (4) joint forces from in vivo data (Fig 5.5). Alternatively, the use of computed muscle control (CMC) in solving the forward problem offers improved muscle and tendon predictions; however, it should be noted that CMC simulations tend to overestimate joint reactions as a result of co-contractions (Thelen et al., 2014). However, inverse problems remain the most popular and appealing as they are less computationally expensive, more efficient, and robust when analysing the TF joint. Inverse kinematics (IK) minimizes a sum of weighted squared errors of experimental trajectories of the markers and/or coordinates to reconstruct the joint model pose in each time step (Fig. 5.5-1). Joint moments are calculated through inverse dynamics (ID) by solving Newton-Euler equations of motion recursively to predict muscle moments from joint kinematics and ground reaction forces (Fig. 5.5-2). Solving linear algebraic equations that link net joint moments and muscle forces yields infinite combinations of muscle forces. This problem is solved numerically using static optimization (SO), inverting muscle moment arms matrix Rji and muscle-moment redundancy (i.e., muscles > joint DoFs), however, it does not consider time-dependency and predicts minimal antagonistic muscle contractions (Fig. 5.5-3). The knee joint forces are provided by joint reaction (JR) analysis (Fig. 5.5-4). Assumptions and simplifications in modelling as well as numerical errors in inverse problem estimation can propagate errors and uncertainty and affect results validity (Viceconti et al., 2006b; Hicks et al., 2015), typically assessed by comparison with EMGs (Lloyd and Besier, 2003) or high-resolution experimental data e.g., biplanar fluoroscopy or x-rays with bone pin markers (Hicks et al., 2015). These uncertainties can affect the knee joint kinematics by up to 6.4 degrees, joint moments by 8 Nm, and muscle forces by 130.8 N (Myers et al., 2015).

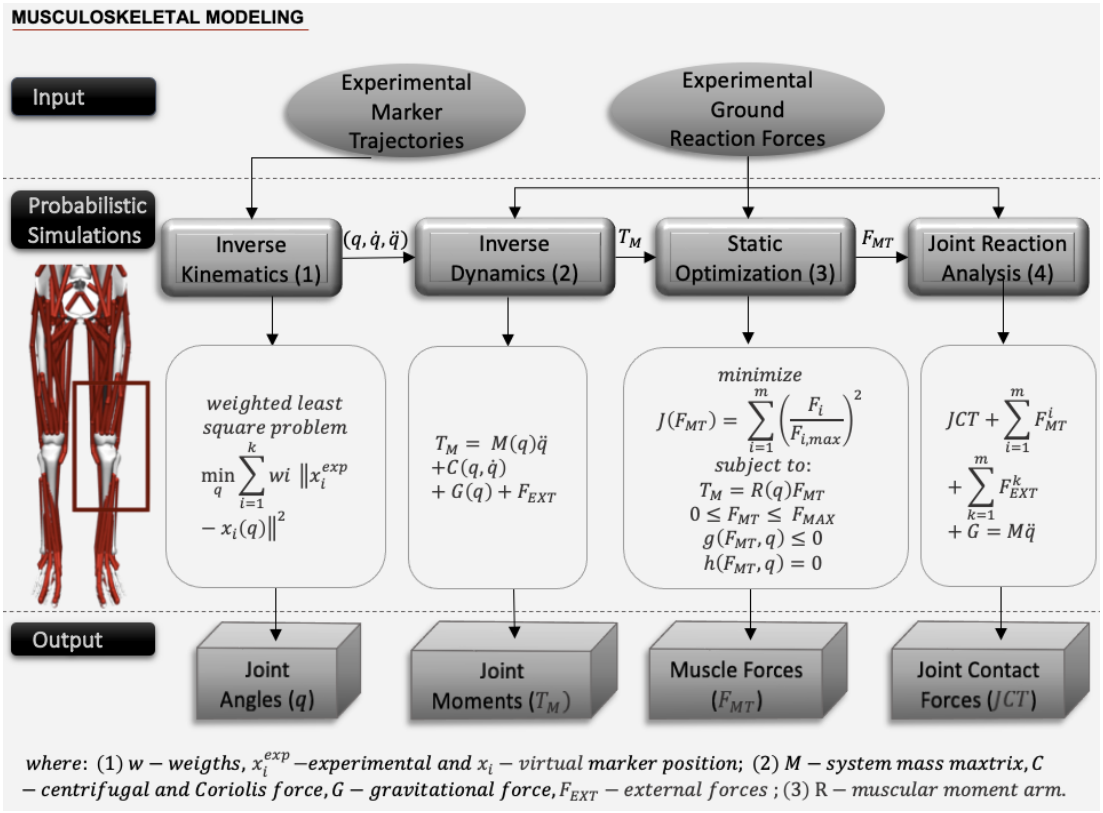

Figure 5.5 *– Conventional MSK modelling workflow input data (experimental motion captures, ground reaction forces) and expected output variables (joint angles, moments, muscle forces, joint contact forces) derived from the underlying equations used for probabilistic simulations (inverse kinematics, dynamics, static optimization, and joint reaction analysis).*

Accuracy of these models is affected by assumptions regarding misrepresented complexity and by the way in which these models account for individual variability. A substantial body of research is dedicated to 'average models' scaled to subject-specific marker poses. A single subject is typically used to develop these models, with values taken from literature or ex vivo testing in cadavers for parameters that cannot be measured in vivo (Anderson and Pandy, 1999; Hoy et al., 1990). The most used OpenSim Lower limb model 2392, for example, is based mostly on one single cadaver (Delph et al., 1990). At present, two approaches are used to personalized models: patient-specific data, i.e., imaging (Scheys et al., 2005) and probabilistic-statistical approach recalling specific instances (Barry et al., 2012). Models can be personalized by using subject-specific data, such as bioimages, motion capture, ground reaction forces, and electromyography obtained in vivo from the patient (Dzialo et al., 2018; Scheys et al., 2005). Combined MSK and FEM models result in more accurate subject-specific knee joint representations (Hume et al., 2018). For instance, a recent study by Xu et al. (2018) showed the importance of integrating MSK and FE models; this study proved how in women, variations in height, tibial morphology, and material properties affect the tibial load bearing capacity (Xu et al., 2018). Customization creates intrinsic limitations since being subject-specific makes it harder to generalize and extend the results to populations. Furthermore, this modelling approach, due to cost of the sources needed to build the model and validate it, expertise and computational power required, uncertainties related to the assumptions are still rarely adopted in clinical applications (Hicks et al., 2015; Killen et al., 2020; Viceconti et

al., 2006b; Valente et al., 2014). The use of statistical approaches has followed naturally; despite the huge amount of data they require for the building phase, they can provide with a few measurements and patient details, provide fast and accurate results. The effective inclusion of detailed anatomical structures and function description is still a challenge. MAP client software (Zhang et al., 2014), recent MSK software, allows users to build models accurate in terms of bone through the use of a statistical bone shape and alignment derived from subject-specific CT-collections; for muscles instead, the geometry needs to be extracted from MRI. This is particularly important considering that MSK models subject-specific are based on stereophotogrammetry due to the soft tissue's artefacts reported variation up to 0.9 BW for the knee reaction forces and 30% in the muscle's strength estimations have been reported (Lamberto et al., 2017). There are also other models that have been developed to improve the accuracy in the predictions. EMG-driven subject-specific models improved tibiofemoral contact forces estimation accuracy of both medial and lateral side respectively by 47% and 7% compared with a generic model (Gerus et al., 2013). Furthermore, EMG-driven force data combined with SO solutions and Bayesian statistic, have been also used for stochastic modelling of muscle recruitment strategies to improve muscle forces estimation (Martelli et al., 2015a). Also, statistical shape models (SSM) are essential to MSK modelling future clinical use/purposes; MSK statistical shape models are faster to generate lower limb model, for specific patients, providing better and more accurate estimation of bone geometry and consequently further prediction capability of muscle and joint reaction forces (Chen et al., 2016).

At the state of the art, an extended body of the literature is dedicated to the study of the joints function using MSK models due to the impossibility of non-invasively measuring muscle strength and joint reactions. In this review, the primary focus is on OpenSim-based models, which are considered the de facto gold standard in musculoskeletal modelling. While OpenSim offers advanced modelling techniques and open-source resources, it is important to acknowledge the existence of other software tools like AnyBody and Adams, which also have their own strengths in developing multibody dynamic knee models. Shelburne et al. (2002) mathematical MSK models provided one of the first example of model focused on knee ligaments mechanics with clinical intent (Shelburne and Pandy, 2002). These models, while being standardized for every patient, were aimed at supporting rehabilitation squatting exercise even after ACL reconstruction for the patient is beneficial. The sagittal plane knee model, accounting for the majority of the ligaments, highlighted through estimating the loading transmission in the joint, how ligaments are safe during this task. These models also account for interaction of bone, muscle, and ligaments of the knee joint model. In a later MSK computational model, with a 6 degrees of freedom knee joint, the same interaction has been investigated (Shelburne et al., 2007); in order to understand the contribution of muscles, ligaments, and ground reaction forces on the tibiofemoral joint loading during daily life activities. Xu et al. (2015) also investigated the knee ligament function through a

multiple degrees of freedom knee joint (Xu et al., 2015). Shelburne et al. (2011) explained the effect of Posterior Tibial Slope (PTS) on the knee and ligament function during standing, walking, and squatting (Shelburne et al., 2011). Shelburne et al. (2005) model has been used to explain the mechanics of the ligament mechanics across the gait cycle (Shelburne et al., 2005). Ali et al. (2017) MSK model with the inclusion of a healthy knee FEM model including soft tissues proves ligament recruitment pattern changes individually due to patient-related variations of ligament attachment locations; this recruitment pattern also differs more at higher flexion-angles during gait (Ali et al., 2017). Other MSK models included detailed FEM model of the knee joint for the prediction and investigation of stress and strains of the tibial cartilage during activities (Halonen et al., 2017); other again to investigate the role of menisci (Hu et al., 2019). In general, all musculoskeletal models, regardless of the specific modelling platform used, are limited in their ability to generalize cadaver findings to represent a wide range of populations. Patient-specific modelling based on MRIs improves the fidelity of the model with respect to joint alignment and articulations, accounting for muscle wrapping, and finally ligament insertions. MRI geometry-based subject-specific MSK models have been found across literature (Smale et al., 2019); however, these models are extremely rare due to the greater effort to build them. Smale et al. (2019) recently published an article on an MSK MRI-based subject-specific model; in particular the model was embedding a four degree of freedom knee model (Smale et al., 2019). Lenhart et al. (2015) also presented a musculoskeletal model built from in vivo MRI data to evaluate the TF and PF mechanics in in vivo dynamic conditions, despite still needing values from cadaveric studies, i.e., knee ligament stiffness. This model is subject-specific representing a female, during a knee laxity test, active flexion and gait (Lenhart et al., 2015). This model integrates a knee elastic foundation model, with subject-specific knee articular bone and cartilage shapes, and many ligaments as non-linear spring bundles. As such, this model can also provide cartilage contact force. Gait results were differing from the models based on cadaveric specimens; this can open a new perspective on the knee function. Other models instead integrate knee detailed FEM models; while providing precious insights on the tibiofemoral function, at the same time, these simulations are computationally expensive. For instance, Lenhart solution requires more than an hour per simulation. On the other hand, Dejtiar et al. (2020), developed MRI-based subject-specific musculoskeletal models with a detailed natural knee joint capable of estimating in vivo ligament, muscle, tibiofemoral joint contact forces and secondary joint kinematics, whose simulations required 6 hours per trial (Dejtiar et al., 2020).

The subject-specific models of Hume et al. (2019) muscle-driven calculate using explicit FEM model of the knee, both tibiofemoral and patellofemoral joint reactions during chair rise and gait is even more expensive (Hume et al., 2019). Navacchia et al. (2019) integrated a PID controller to track gait and chair rise motion of the knee joint with MSK – FEM model of the lower limb to efficiently compute muscle forces prediction (Navacchia et al., 2019). This strategy tries to

represent a trade-off between computational cost of FEM models and model details in MSK simulations. Hume et al. (2018) and (2019) demonstrated also that including deformable knee joint may represent with more fidelity kinematics and torques in relation to muscle forces; in fact, variations of moment arms due to deformable ligament led to flexion torque (Hume et al., 2018, Hume et al., 2019). However, this model is time consuming and computationally expensive. Further complexity is introduced by statistical shape models (SSM) of the knee embedded into the lower limb MSK ones. For instance, Clouthier et al. (2019) developed a statistical model (SSM) of the TF joint with bones, articular cartilage, and ligament geometries of 14 healthy knees from MRI, embedded within MSK model, to investigate the relationship between anatomy, knee kinematics and articular forces while walking (Clouthier et al., 2019). A statistical model for pre-clinical TKR evaluation relative to kinetic waveform data, in particular tibiofemoral joint loads for the gait, from MSK models have been successfully developed (Galloway et al., 2012); notwithstanding, to explain the 95% of variability 17 PC components were needed, revealing the need of more accurate data for further investigations. While the integration of all these tools is powerful, it is also extremely complex to develop and hard to validate; these are the reasons why this type of models is rarely implemented.

Summary - Summing up, tibiofemoral knee joint has been modelled in either 2- or 3-dimensions with the inclusion or accounting for several structures such as bones, with the addition of cartilage or some main ligaments (ACL, PCL, LCL, MCL), to more complete ones, which include more ligaments, tendons, muscles and menisci behaviours and interactions at different levels. As discussed, throughout each approach, FEM models are typically adopted at lower dimensional scale, for the investigation of tissues behaviour and function, while MSK model for a body level investigation. In the same way, while the first are typically used more for subject-specific analysis, MSK are more suitable for investigations of cohorts, while SM are specifically aimed at representing and searching for the variability in wide populations through cohorts. Simplification and assumptions are intrinsic in mathematical and computational modelling and will be necessary no matter how much future advances related to hardware and numerical methods are going to improve.

The anatomical representation is commonly the first assumption to be made. Geometrically, there are a range of alternatives to represent knee joint structures with different accuracy. Depending on the data available, and the focus of the study more or less level of detail is provided. However, at present, high accuracy for all the structures within the same model at both high and low dimensional scales is still hard to achieve, even with image-based models. Especially for FEM models, the resultant geometry accuracy is in fact limited by imaging resolution itself, accuracy of the segmentation techniques, and the smoothing required for meshing that does not preserve individual differences/irregularities (Kazemi et al., 2013). Moreover, realistic surface representation is prevented by obstacles such as numerical and computational efforts required.

Furthermore, the deformable - viscoelastic behaviour of ligaments, cartilageand menisci tissues leave space for uncertainties introduced by possible pre-deformation depending on how and when the joint was scanned. Accuracy is even more limited looking at ligaments which do not have as much shape definition as menisci or cartilage, which are more likely to be anatomically individuated and adjusted through bone geometries. However, despite the growing use of deep and machine learning techniques for segmentation, the complexity and variability of ligament shape, orientation, and attachment locations still present challenges in accurately representing ligaments (Wang et al., 2014). While in MSK modelling geometrical assumptions are necessary (i.e., models often have low anatomical accuracy, exacerbated by scaling and alignment with motion capture data), when representing smaller scales, such as tissue scales, it is crucial to provide further clarifications and engage in discussions to address potential uncertainties that may arise. Numerous sensitivity studies have been conducted to assess the overall uncertainties associated with geometries and their potential impacts on model outputs (Meng et al., 2017b).

The second sequential assumption concerns the identification of the more appropriate material behaviour, at a tissue level. While FEM models have a wide range of material properties used, MSK models typically have a few alternatives, with bones mostly represented as rigid bodies, ligaments through non-linear bundles and muscles and tendons as actuators with an underlying hill type model. On the other hand, FEM models can adopt any of the experimentally derived material properties formulation for bones, cartilage, menisci, ligaments, tendons, and muscles; those differ on specific bone (i.e., cortical thickness femur and tibia in different locations), depending on the ligament (i.e., ACL, PCL, MCL and LCL and the abstraction 1-2-3D models), or again many are the models for the cartilage and menisci, while their combination also changes based on the modeler choices. This difference can be explained as the FEM models rely on tissue level function for the joint to implicitly fulfil its function, while in MSK models this function of the joint is separately defined and as such this information impact the joint description less.

The third assumption, probably the most important, involves how different structures interact with each other, passively and/or actively, in loaded and/or unloaded conditions. This assumption basically defines the mechanical equivalent used as a substitute for the articulation between each structure in creating the joint function. Depending on the approach used, the mechanical equivalent used as a substitute for the articulation between each structure in creating the joint function will be mentioned and discussed in detail in the following sections. FEM models are typically used to investigate how each structure behaves in terms of stresses and strains, providing the overall motion at given articular forces. On the other hand, MSK models aim at representing mainly ligaments, muscles and joints, forces, given ground reaction forces and overall body kinematics through marker trajectories, while typically specific joint kinematic functions, such as knee joint models, are embedded. In both cases, passive and active conditions impact both kinematic and kinetic models/analysis. As such, this assumption has two slightly different

connotations depending on the approach: while it concerns the so-called boundary conditions in FEM modelling; MSK modelling explicitly define with mathematical functions these interactions.

- Boundary conditions in FEM knee joint modelling include simplification of the load conditions and contact. In the first case, loading is typically recurring to assumptions such as dynamic loading and divided in stages of static compressive loads, often neglecting muscles and tendons. Models often do not account for the fluid presence and force inside the joint. Contact is assumed to often be rigid between bones and cartilage, elastic or deformable following several different laws between cartilage and menisci or between femoral and tibial cartilage. However, the complexity of the contact makes convergence challenging, increasing computational time required for numerical convergence (Weiss et al., 2005). Technical difficulties in dynamic contact can also arise by applying free surface boundary conditions. Besides, contact, computational time grows also with time discretization - function iterations.

- MSK models instead have articulations between rigid bodies explicitly defined, to represent joints, while muscle actuators accelerate them. These joint models are typically representation derived from ex vivo data and experiments. Initially described by the only flexion-extension as screw-home mechanism, the TF joint has been modelled as a two degrees of freedom DoF system, flexion-extension, and internal-external rotations, four secondary dependent DoFs by flexion-extension. More recently models included all six rotations and translations. Hence, the tibiofemoral joint has been represented with 1 up to all its six DoFs, with a range of different mechanical equivalents, that will be described in detail in the following section.

5.4 A Cost Complexity Utility Perspective

5.4.1 Introduction

Based on the purpose of the model and the output required, there are four main categories of models used to investigate the knee joint: theoretical/analytical, statistical models, musculoskeletal models at a body scale, finite element models of the knee and tissue level, and with some overlap due to integration of these. Different types of models require different quality and quantity of input data. Average models are based on a small number of subjects and/or using different sources of data for different parameters; for instance, in these models, some of the parameters can be extracted from ex vivo testing or from literature, used with motion capture of other subjects to predict and improve the understanding of the generic function. Although these models serve their intended purpose in describing generic patterns of motion, they are not suitable for investigating individual variability due to the uncertainties created by these parameters. On the other hand, subject-specific models need a well-constructed dataset, require data coming from the

same patients, and higher resolution data not being averaged with smoothening of noise and errors. These models must be paired with the subjects and the findings are relative to the specific patient, which, having patient peculiarities englobed, can and it is likely not to be representative of a group. Statistical models are the actual solution to the problems and limitations presented by the other two types; their limitation is on the sample/patients and complexity. They in fact require high number of subjects to be built in order to have good fidelity with the population they represent, in addition to the intrinsic complexity to deal with statistical tools and analyses. As expected, incorporating multiple sources produces less accurate results with many variables remaining uncontrolled, but it is also less expensive. On the other hand, fully representing a specific subject is extremely expensive, and the findings are intrinsically depending on the individual peculiarities, providing better accuracy but non-generalizable findings. Since there is no optimal solution, the real solution is to stipulate a trade-off based on the research question. The trade for introducing assumptions is simply cataloguing the errors committed and how they propagate from the measurement error to the outputs. In addition, the ease of use or convenience issue is also an important consideration in making this choice because it is an actual issue in many applications. Thus, it is necessary to determine whether the modelling cost is justified based on the complexity and accuracy of the information it provides, which also depends on its utility or intended application. From the previous discussion it emerges how different models reply to different questions, models which differ for input and development as well as for output provided. In turn, different research questions require different modelling approaches and choices, which are dictated also by the modeler ability and appropriateness of the use of the instruments available, and by the sources available to build the model and possibly validate it. The choices of the model must also consider the computational cost of the simulation. As previously discussed, FEM modelling choices are often a necessary compromise between precision and effort, which change and improve as time and technologies go on (Viceconti et al., 2006a). These concepts can be extended to every type of model, from FEM to statistical and MSK models. The difficulty in selecting the right parameters increases with the complexity of the chosen type of model and purpose. Based on all the decisions, different models have been built and these resultant models have a wide range of complexity, cost, and utility. Models can be more or less expensive, based on the sources and the effort to build them.

5.4.2 Materials and Methods

In this section, the methodology employed for the mapping literature review will be outlined. The process began by selecting appropriate literature review keywords and establishing inclusion and exclusion criteria. Additionally, a scoring system was implemented to evaluate the selected studies. For this mapping literature review research, a combined qualitative and quantitative analysis approach by integrating elements of both quantitative and qualitative methods to collect and

analyze data. By employing this approach, a comprehensive understanding of the research topic was sought by considering both numerical data and qualitative observations or interpretations. This methodology proves particularly valuable when investigating complex phenomena, as traditional quantitative methods alone may fail to capture the intricacies of the research subject. To identify relevant studies on tibiofemoral joint modelling, a thorough literature review was conducted. The search strategy involved utilizing specific keywords and applying inclusion/exclusion criteria to identify papers suitable for evaluation. The primary objective was to identify studies that provided detailed descriptions of modelling approaches, as well as insights into their complexity-cost characteristics.

Keywords – To ensure a comprehensive search, a combination of various keywords was used to select relevant studies. These keywords included terms such as 'Tibiofemoral joint', 'Modelling', 'Musculoskeletal model', 'Finite Element model', 'Statistical shape model', 'Analytical model', 'Complexity', 'Cost', 'Validation', 'Computational cost', 'Data sources', 'Integration', 'Multiple models', 'Mechanism', 'Scaling', 'Ligaments', 'Menisci', 'Cartilage', and 'Bones'. By using these keywords in different combinations, the aim was to capture a wide range of studies related to the topic of interest.

Inclusion Criteria – The following criteria were used to include papers in the review:

1. Focused on the modelling of the tibiofemoral joint: The papers had to primarily discuss the modelling of the tibiofemoral joint, which is the joint between the tibia and femur in the knee.

2. Provided a detailed description of the modelling approach: The papers needed to offer a thorough explanation of the methodology used for the modelling process.

3. Described the complexity and cost factors associated with the model: The papers had to discuss the complexity and cost considerations related to the model, providing insights into the resources required for its implementation.

4. Included information on data sources, validation, and computational cost: The papers had to provide information about the data sources used, the validation process employed, and the computational cost associated with the model.

5. Addressed the complexity of the joint mechanism, ligaments, menisci, cartilage, and bones: The papers had to explore the intricacies of the joint mechanism, including the ligaments, menisci, cartilage, and bones involved in the tibiofemoral joint.

6. Accessible in paper or PDF format: The papers needed to be easily accessible in either physical or digital format.

7. Written in English: The papers had to be written in the English language for ease of understanding and evaluation.

Scoring System – To evaluate and compare the complexity-cost characteristics of the identified models, a scoring system was developed. Offset values were used to categorize the different models based on their cost-utility (X) and complexity (Y) characteristics.

- Analytical and theoretical models (Offset X = -1, Offset Y = -1): These models are generally considered to have lower complexity and cost compared to other types of models. The negative offsets indicate that they have fewer anatomical inclusions and require less data sources, resulting in lower computational cost.

- SS models (Offset X = 0, Offset Y = 1): These models capture individual variations, through statistics, making them more complex and potentially requiring more data sources for accurate representation. However, they can provide higher accuracy in specific scenarios, justifying the positive offset for complexity.

- FEM models (Offset X = 1, Offset Y = 0): Finite Element models involve detailed tissue modelling and complex simulations, leading to higher computational cost. The positive offset for cost-utility reflects the significantly higher costs of FE models.

- MSK models (Offset X = 0, Offset Y = -1): Musculoskeletal models represent a balance between simplicity and accuracy, as they capture the overall behavior of the joint without the need for detailed tissue modelling. The negative offset for cost indicates that MSK models are generally computationally more efficient.

It is important to note that while the chosen offsets may result in slight variations in the scores, these variations are intentionally minimal to avoid drastic effects on the overall ranking and comparison of the models. The step size of 1 in the scoring system, employing a binary approach, allows for a clear distinction between different model characteristics, while the small offsets help ensure that each model is appropriately assessed based on its unique features.

The scoring system assigned scores ranging from 0 to 1 for each category, allowing for a more objective assessment of anatomical inclusions, integration, complexity of the joint mechanism, other complexity factors, data sources, validation, and computational cost. The resulting scores were used to generate a Complexity-Cost Diagram, providing a visual representation of the complexity and cost positions of the models. The diagram facilitates the comparison and classification of different tibiofemoral joint models based on their complexity and cost characteristics, aiding in identification of the most suitable models for specific applications. The following sections present the evaluation criteria and the corresponding scoring system for each category, followed by a detailed analysis and discussion of the findings.

Table 5.1 *– Scoring System for Tibiofemoral Joint Models.*

Category	Description	Details
1. Anatomical Inclusions	Evaluates the inclusion of anatomical structures in the models.	
1.1 Bones	Inclusion of bone models representing the femur, tibia, and fibula.	0 = Incomplete, 1 = Complete
1.2 Cartilage	Consideration of cartilage structures and their mechanical properties.	0 = Incomplete, 1 = Complete
1.3 Menisci	Inclusion of meniscus models, considering geometry and interaction with other structures.	0 = Incomplete, 1 = Complete
1.4 Ligaments	Incorporation of ligament models, including cruciate and collateral ligaments (ACL, PCL, MCL, and LCL).	0 = Incomplete, 1 = Complete
1.5 Other Ligaments and Structures	Consideration of additional ligaments or structures, such as transverse ligament or patella.	0 = Incomplete, 1 = Complete
2. Complexity Factors	Assesses the complexity of the modelling approach and joint mechanism representation.	
2.1 Integration of Multiple Models	Integration of different types of models (e.g., MSK, FEM) to represent the joint mechanism comprehensively.	0 = Not Integrated, 1 = Integrated
2.2 Complexity of the Joint Mechanism	Inclusion of joint kinematics, muscle activations, and other relevant factors for a realistic joint function.	0 = Low Complexity, 1 = High Complexity
3. Cost Factors	Evaluates the cost-related aspects of the models.	
3.1 Data Sources	Availability and cost of data sources used in building the models.	0 = Limited/Expensive, 1 = Accessible/Cost-effective
3.2 Validation	Rigor and extent of model validation, comparing predictions with experimental or clinical data.	0 = Limited, 1 = Extensive
3.3 Computational Cost of the Model	Computational efficiency and scalability of the models, considering time and resource requirements.	0 = High Cost, 1 = Low Cost
4. Additional Considerations	Additional factors to consider in the evaluation of tibiofemoral joint models.	
4.1 Adjustments	Adjustments made to the overall complexity and integration of the models.	0 = Limited, 1 = Extensive
4.2 Eventual Accuracy	Ability of the models to provide reliable and precise predictions of joint biomechanics and functional outcomes.	0 = Limited, 1 = High Accuracy

Binary Scoring System: 0 = Incomplete/Limited/Low Complexity/High Cost; 1 = Complete/Integrated/High Complexity/Low Cost/Extensive/High Accuracy

The scoring system presented in Table 5.1 provides a binary approach to evaluate and compare tibiofemoral joint models based on various categories. Each category is assessed as either

incomplete or complete, integrated or not integrated, low complexity or high complexity, high cost or low cost, limited or extensive, and limited or high accuracy. This binary system simplifies the evaluation process and allows for clearer distinctions between different model characteristics.

The category of anatomical inclusions evaluates the completeness of the models in representing key anatomical structures such as bones, cartilage, menisci, ligaments, and other ligaments and structures. Models that include all these structures are considered complete (score = 1), while incomplete models receive a score of 0.

The complexity factors category assesses whether models integrate multiple modelling approaches and capture the complexity of the joint mechanism. Models that integrate different types of models and incorporate various factors related to joint function receive a score of 1 for integration and high complexity, respectively. Models lacking integration or demonstrating low complexity receive a score of 0.

The cost factors category considers the availability, cost, and computational efficiency of the models. Models that use accessible and cost-effective data sources, demonstrate low computational cost, and are scalable receive a score of 1 for data sources, computational cost, and validation. Models with limited data sources, high computational cost, and limited validation receive a score of 0.

Additional considerations include adjustments made to the models' complexity and their eventual accuracy. Models that require extensive adjustments to achieve a balance between complexity and practicality receive a score of 1 for adjustments. Models that provide high accuracy in predicting joint biomechanics and functional outcomes receive a score of 1 for eventual accuracy.

The binary scoring system facilitates a more straightforward evaluation of tibiofemoral joint models, allowing the completeness, integration, complexity, cost-effectiveness, validation, and accuracy of the models to quickly be assessed. This system aids in the selection of appropriate models for specific research or clinical applications by providing clear distinctions between different model characteristics.

The methodology employed for obtaining percentages for each model involved a scoring system with binary criteria for anatomical inclusions, complexity factors, cost factors, and additional considerations. For each model, the total score was calculated by summing up the scores for each category. The maximum possible score was determined as the score a model would achieve if it met all criteria. To calculate the percentage score for each model, the total score was divided by the maximum possible score and multiplied by 100. This approach provided a relative comparison of the complexity-cost characteristics of each model, with a higher percentage indicating a more comprehensive and suitable model for the specific research or clinical application.

5.4.3 Results

The following figure represents the result of the analysis of complexity / cost – utility perspective on knee joint modelling (Fig. 5.6).

Knee models across literature were positioned on the graph based on a score produced for cost utility and complexity as declared in the methodology section:

$$(X_{COST-UTILITY}|Y_{COMPLEXITY})$$

assigned to each model based on the following parameters:

$X_{COST-UTILITY}$ → Cost and utility are placed on the same axis (X-axis) in the graph to represent the trade-off relationship between these two factors. Cost refers to the resources, efforts, and data required for model development and simulation, while utility represents the usefulness and value derived from the output of the model. The placement of cost and utility on the same axis allows for the evaluation of trade-offs. Models positioned towards the lower end of the axis are generally more cost-effective, requiring fewer resources and efforts, but may have limitations in terms of their applicability and insights. Models positioned towards the upper end of the axis offer greater utility, providing more valuable and comprehensive outputs but at a higher cost in terms of data requirements and computational time. By visualizing the trade-off between cost and utility, the graph assists in assessing the balance between investment (cost) and value (utility) when selecting a modelling approach. It provides insights into the relationship between the resources invested and the value derived from the model's output, aiding in informed decision-making based on available resources, research goals, and application requirements.

$Y_{COMPLEXITY}$ → The Y-axis represents the complexity of knee joint models. Complexity refers to the level of intricacy and sophistication involved in developing and utilizing these models. It encompasses various aspects that contribute to the overall complexity of the modelling approach. Complexity can be influenced by factors such as the level of detail in representing anatomical structures, the inclusion of advanced biomechanical mechanisms, the incorporation of subject-specific characteristics, and the utilization of sophisticated computational algorithms. Models positioned higher on the Y-axis are characterized by greater complexity.

These models may incorporate detailed anatomical structures, such as bones, cartilage, and ligaments, along with their intricate interactions. They may also utilize advanced tissue models, accounting for complex material properties and interactions between different tissues. In addition, complex models often involve the integration of multiple modelling approaches, such as combining MSK and FEM techniques. This integration allows for a more comprehensive representation of the knee joint's behaviour and functionality, further increasing the complexity of the model. The complexity of a model also considers the number of input data sources required,

the level of model validation, and the complexity of the output information generated by the model. By understanding the complexity of knee joint models, researchers and practitioners can evaluate the trade-offs between model intricacy and the resources required. Informed decisions can be made about selecting models that align with specific research goals, available data, computational resources, and the desired level of detail and accuracy. The Y-axis provides a relative measure of the complexity of knee joint models, assisting in comparing different modelling approaches and identifying the level of intricacy associated with each.

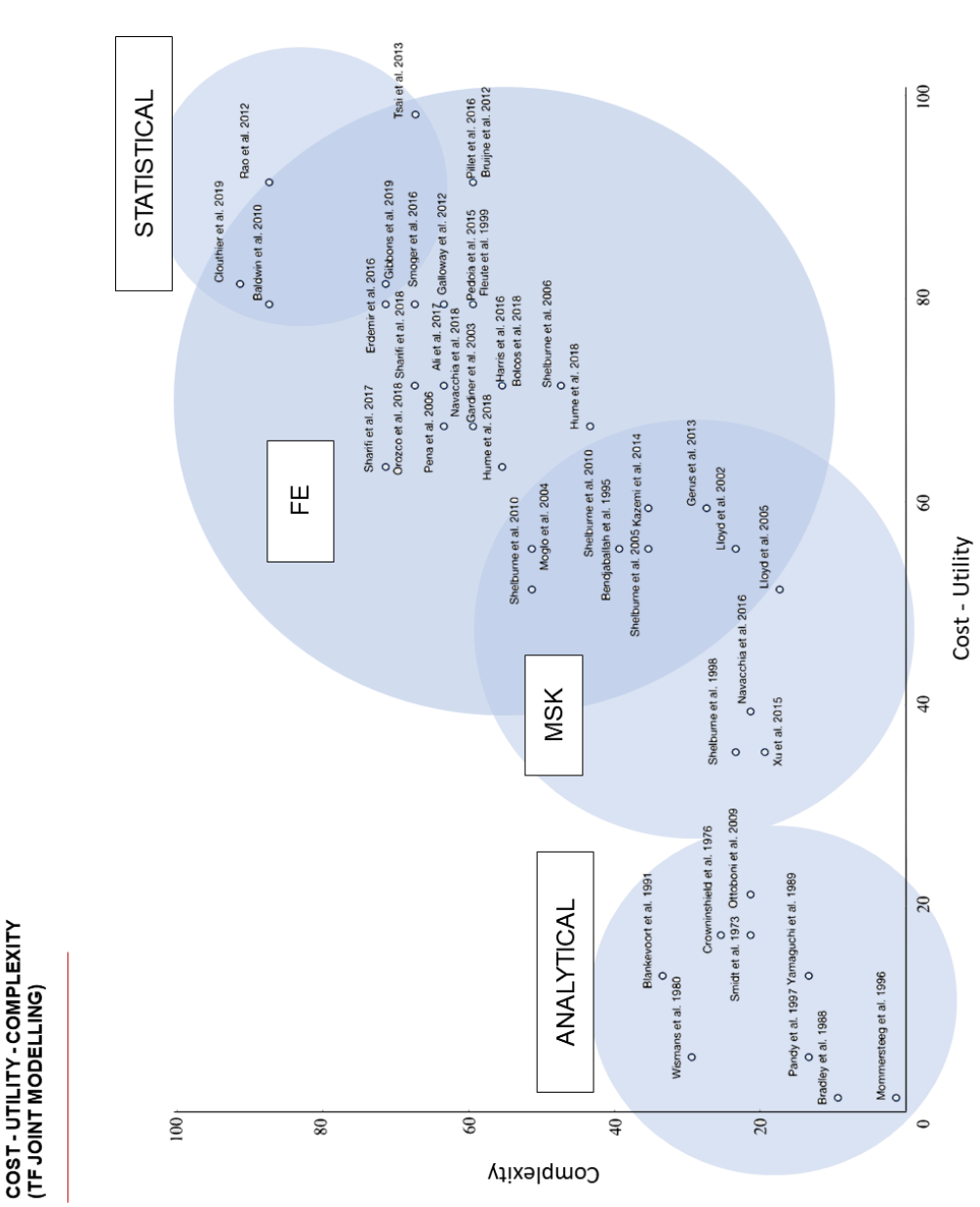

Figure 5.6 *– Cost - Utility - Complexity perspective on knee joint modelling depicting the cost-utility trade-off on the X-axis and model complexity on the Y-axis, offering insights into the balance between resources invested and the value derived from model outputs.*

Overall, the graph and scoring system provide a comprehensive analysis of knee joint modelling approaches, allowing informed decisions on the most appropriate modelling approach based on their specific needs and constraints to be made in both research and clinical contexts.

5.4.4 Discussion

The cost-utility complexity map provides valuable insights into the characteristics of knee joint models, allowing for a comprehensive understanding of their strengths and limitations. By evaluating different model categories based on their complexity and cost-utility positions, more informed decisions can be made in the decision-making process to identify the most suitable models for specific applications. In this analysis, we will explore each model category in detail, considering the provided table entries and additional discussions on their map positions.

Analytical and theoretical models are inherently the least expensive and least complex models, and hold a unique position on the cost-utility complexity map, making them attractive options for various research endeavours. Their inherent simplicity and generic nature result in lower costs and minimal resource requirements, rendering them highly cost-effective. Despite their straightforward design, these models provide valuable output, making them well-suited for initial assessments and preliminary investigations of knee joint behavior. Researchers often turn to analytical and theoretical models to gain quick insights into the underlying mechanisms and generic functional features of the knee joint.

FEM models occupy a distinct position on the cost-utility complexity map, showcasing both their advantages and limitations. While they are associated with higher costs compared to MSK models, these increased expenses are mainly attributed to two key factors: data pre-processing and longer computational times. FEM models require extensive data preparation, such as segmenting detailed anatomical structures from medical imaging data and creating finite element meshes. This process can be time-consuming and labour-intensive, contributing to higher upfront costs. Furthermore, FEM simulations are computationally demanding, as they involve solving complex partial differential equations to predict the mechanical behavior of tissues and structures within the knee joint. The computational complexity can lead to longer simulation times, which also adds to the overall cost of using FEM models. However, the investments in cost for FEM models yield significant benefits, making them a valuable tool in knee joint biomechanics research. FEM models excel in their ability to account for a greater number of anatomical structures within the knee joint. They provide detailed representations of ligaments, menisci, cartilage, and bone geometries, capturing the complex interplay of these structures during joint movement. This high level of anatomical specificity enables FEM models to offer subject-specific simulations, making them more accurate and personalized representations of individual knee joint behavior. Moreover, FEM models incorporate sophisticated material properties for the various tissues, enabling researchers to study how different mechanical characteristics influence knee joint mechanics. This capability allows for in-depth investigations into the effects of tissue properties on joint stability, load distribution, and other biomechanical parameters.

At the lower end of the complexity spectrum, low complexity MSK models represent generic anatomies and focus on simple tasks, providing averaged knee joint behavior. These models are often based on parametrized geometries, which simplify the representation of knee joint structures, and typically account only for bone anatomy. The advantage of such models lies in their computational efficiency and ease of implementation. They are well-suited for preliminary analyses, basic understanding of joint mechanics, and initial assessments of knee joint function. Moving towards the higher end of complexity, high complexity MSK models involve more detailed representations of knee joint structures. They go beyond bones and incorporate soft tissues, such as ligaments, menisci, and cartilage, into the simulation. These soft tissues are essential for capturing the complex interactions and load-bearing mechanisms within the knee joint. The inclusion of soft tissues enhances the accuracy and realism of the model, providing a more comprehensive understanding of knee joint mechanics. Integration of multiple models is another hallmark of high complexity MSK models. Researchers often combine MSK models with finite element models (FEM) to simulate more intricate behaviours and interactions within the knee joint. This integration allows for a more holistic approach, where the mechanical responses of both soft tissues and bones can be studied simultaneously. For instance, FEM models can be used to analyze stress and strain distribution in ligaments and cartilage under various loading conditions, providing insights into tissue health and potential injury risk. In high complexity MSK models, constitutive models for tissues become more sophisticated. These models define the mechanical properties of soft tissues, such as their stiffness and elasticity, under different loading conditions. The use of advanced constitutive models enables researchers to gain a deeper understanding of tissue behavior and its influence on overall knee joint mechanics. Furthermore, high complexity MSK models can account for active loading patterns during motor tasks. These models consider muscle forces and activation patterns that contribute to knee joint movements. The interaction between muscles, ligaments, and bones is intricately simulated, providing valuable insights into the coordination and control of knee joint motion during various activities, such as walking, running, jumping, and pivoting. However, it is important to note that the increased complexity of MSK models comes with certain challenges and limitations. The computational demands of high complexity models are higher, resulting in longer simulation times and increased processing power requirements. Additionally, data acquisition and model development for soft tissues may be more labour-intensive and time-consuming compared to models that only account for bones. Despite these challenges, high complexity MSK models offer a powerful platform for investigating knee joint biomechanics under diverse conditions and provide a detailed understanding of joint behavior. These models have significant applications in studying knee joint injuries, orthopedic surgeries, implant design, and personalized treatment planning. They have the potential to advance clinical practice by guiding interventions and optimizing rehabilitation strategies for individuals with knee joint pathologies. Low-cost or utility models require minimal input data and are relatively fast to build and process solutions. They often involve a small number

of subjects and lack extensive validations. On the other hand, higher costs are attributed to longer computational time, greater monetary investment, a wide range of data sources and subjects, and more rigorous validation processes.

Statistical models offer a cost-effective approach in knee joint biomechanics research, making them valuable tools for studying population-level trends and subject-specific behavior. These models rely on a limited number of parameters and employ complex mathematical and statistical methods to analyze data and make predictions. They are particularly well-suited for studying large cohorts and assessing the prevalence of specific knee joint characteristics within a population. One key advantage of statistical models is their ability to process and analyze data features from multiple subjects simultaneously. By accounting for data from a large number of individuals, these models can identify common trends and variations in knee joint behavior across the population. This capability allows researchers to gain valuable insights into the overall biomechanics of the knee joint in different groups, such as healthy individuals, athletes, or patients with specific knee conditions. Furthermore, statistical models can provide subject-specific predictions based on data patterns observed within the population. While they may not capture the intricacies of individual knee joint behavior with the same level of detail as subject-specific models like FEM or MSK, statistical models offer valuable predictions that can inform clinical decision-making and treatment planning. Despite their cost-effectiveness, statistical models do have some limitations. The increased cost associated with statistical models primarily arises from the need for extensive datasets to accurately represent the target population. Collecting and analysing such datasets can be resource-intensive and time-consuming, especially if the study aims to include a diverse and representative sample of individuals. Additionally, statistical models may have inherent constraints in capturing the fine-grained intricacies of individual knee joint behavior. As they focus on population-level trends, these models may overlook individual variations and personalized responses to different stimuli or loading conditions. This limitation is particularly relevant in clinical applications where the focus may be on individualized treatment planning and patient-specific predictions. Moreover, statistical models are reliant on the quality and quantity of the data available. Incomplete or biased datasets can lead to less accurate predictions and potentially limit the generalizability of the model's findings. Despite these limitations, statistical models play a crucial role in knee joint biomechanics research and have a wide range of applications. They are particularly valuable in scenarios where large-scale data is available, and the focus is on understanding population-level trends, prevalence of knee joint conditions, and risk factors. Statistical models are also useful in epidemiological studies, where the goal is to analyze data from a large number of individuals to gain insights into the distribution and frequency of knee joint characteristics within a specific population.

The overall trend indicates that complexity grows faster than cost, almost following a parabolic curve. However, advancements in technology and techniques aim to reduce costs while

maintaining the desired complexity, making models more appealing for clinical applications. Analysing the timeline for development of new models, it is evident that the trend is to achieve increasingly complex representations with minimal costs, as opposed to the initial intention of simplifying the models. By considering the cost-utility and complexity of knee joint models, informed decisions can be made about selecting the models that better align with specific research objectives and available resources.

5.5 Model Selection and Development Justification

In the previous sections, the mapping literature review and the comprehensive cost-utility and complexity analysis of knee and tibiofemoral joint models provided valuable insights for informed decision-making based on research objectives, available resources, and the need for efficiency. To summarize, the available model types were as follows:

- Analytical or theoretical models: These cost-effective options are suitable for studying passive knee motion or basic biomechanical behaviour, offering valuable insights without extensive data or computational demands.
- MSK models: Striking a balance between cost and complexity, they excel in investigating active knee motion during motor tasks, providing dynamic analysis capabilities and computational efficiency, while offering detailed and accurate representations of the individual knee biomechanics, especially when combined with FE models.
- FE models: Offering highly detailed and patient-specific representations, these models excel in capturing complex tissue properties and anatomical fidelity but may not be ideal for population analyses.
- Statistical models: Efficient for population studies, these models predict trends and subject-specific instances, requiring extensive datasets for comprehensive analysis.

These insights have guided the decision-making process in selecting the most appropriate model for the last study of this thesis. The research objectives of this third study revolve around investigating knee joint elasticity within a population context, while considering individual differences in tibiofemoral joint behaviour. To achieve this, the aim was to bridge the gap between passive and active motion, with modeling simulations, providing a comprehensive understanding of knee biomechanics during motor task. In order to meet the research objectives, the chosen model had to satisfy specific requirements, including:

- incorporating passive rigid motion based on subject-specific geometry.
- simulating active tasks such as gait to study knee joint behaviour under dynamic conditions,
- accounting for individual ligament and soft tissue elasticity.
- demonstrating computational efficiency for large-scale population studies.

Remarkably, no existing model fully met all these criteria, as each modeling approach had its own strengths and limitations. Therefore, the third study was dedicated to the development of a novel musculoskeletal model that could efficiently capture knee joint behaviour across the entire spectrum of passive to active motion within a population context, effectively bridging the gap between the limitations of individual approaches. By addressing these specific needs and requirements, the third study sought to pave the way for a more comprehensive and efficient investigation of knee joint mechanics and behaviour, contributing to advancements in musculoskeletal research and offering potential insights for clinical applications.

In the remaining part of this section, a description of the decision-making process that culminated in the development of this innovative model will be provided, emphasizing the significant contributions of this chapter to its realization.

Overcoming Computational Challenges in Musculoskeletal Modelling

In this thesis, the decision to adopt musculoskeletal modelling as the foundational approach for investigating knee joint behaviour is driven by the insights gained from a comprehensive mapping literature review. The review illuminates the advantages of MSK models, showcasing their potential to bridge the gap between passive and active knee motion analyses through dynamic analysis capabilities and computational efficiency. By combining MSK models with FEM models, researchers can achieve detailed and accurate representations of knee biomechanics during motor tasks and complex loading patterns, rendering them well-suited for the research objectives cantered around investigating knee joint elasticity within a population context while considering individual differences in tibiofemoral joint behaviour.

As a highly efficient and effective modelling approach, MSK models provide a promising foundation for exploring knee joint behaviour across the spectrum of passive to active motion. The incorporation of subject-specific variations allows for a comprehensive understanding of the elastic behaviour of knee joint structures, facilitating large-scale population studies. The subsequent sections of this thesis will delve into the details of this novel approach, providing a step-by-step development and implementation process, as well as presenting the benefits and implications of this innovative model for efficiently investigating knee joint behaviour and advancing the field of musculoskeletal research.

However, it is important to note a significant challenge associated with combining MSK models with FE models: the potential increase in computational time and costs. This poses a significant concern when representing individuals within a population context, as it may lead to prohibitive expenses. The practical implementation of musculoskeletal models in clinical settings can be hindered by lengthy computational times, leading to delayed decision-making, integration issues, increased resource requirements, higher costs, scalability limitations, and the need for specialized

expertise. While recognizing these challenges, it is important to emphasize that the focus of this Ph.D. research is not specifically on the clinical adoption of musculoskeletal models. Instead, the aim has been to address the broader need for faster, less complex, and cost-effective musculoskeletal models.

Therefore, this research not only highlights the advantages of MSK modelling for investigating knee joint behaviour but also emphasizes the critical issue of computational time and cost when combining these models with FE approaches. The subsequent chapters delve into the strategies and solutions that could overcome these challenges, providing novel insights that seek to balance efficiency and accuracy while enabling an effective study of knee joint mechanics within diverse populations. Through this exploration, the goal is to develop a model that efficiently captures the elastic behaviour of knee joint structures, ensuring practical feasibility for large-scale population studies, and advancing our understanding of knee joint biomechanics in various scenarios and activities. As the model is yet to be developed, the current discussion will present a hypothetical but plausible pathway for achieving these objectives.

In the section discussing the available MSK models, a comprehensive summary of the different approaches to implement tibiofemoral TF kinematics was provided, drawing insights from the literature review. Notably, one intriguing possibility emerges for the potential integration of the kinematics obtained in Chapter 4 within these models. By incorporating the kinematic data from Chapter 4, the research could explore the continuum from passive to active motion, providing valuable insights into knee joint behaviour across the population and across different loading scenarios and motor tasks. This integration holds significant promise for enhancing the accuracy and applicability of the model, enabling a more comprehensive understanding of knee joint mechanics and its variability within diverse populations.

A Viable Approach For Efficient Population Studies and Inter-Subject Variability

As declared, the primary research objective of the third study is to develop a computationally efficient musculoskeletal model capable of facilitating efficient population studies, enhancing the feasibility of studying inter-subject variability, and reducing the time and resource requirements for data analysis. Within the current landscape of musculoskeletal modelling, researchers often adopt FEM to achieve highly accurate representations of knee joint behaviour. These FEM models are typically derived from medical imaging data, such as MRI and CT scans, enabling the creation of subject-specific models with detailed anatomical fidelity. However, this level of anatomical accuracy comes at a cost in terms of computational complexity and resource requirements. FEM models used for knee joint simulations often incorporate elastic foundation models to represent the interactions between the knee joint structures and the surrounding tissues, as extensively discussed in the review. Additionally, the behaviour of ligaments, which play a crucial role in knee joint stability, can be modelled in various ways, such as spring elements,

discrete bundles, or more advanced constitutive models. Another critical aspect is the representation of contact between joint surfaces, which involves simulating the interactions between the femur and tibia during motion. Developing and implementing such FEM models requires extensive experimental data and validation efforts to ensure their accuracy and reliability. The process involves collecting data from cadaveric tests, in vivo experiments, and biomechanical studies. Moreover, these FE models necessitate detailed modelling and simulations, often utilizing complex numerical techniques and algorithms to account for the intricate biomechanics of the knee joint.

Despite the valuable insights gained from FEM models, the research community recognizes the challenges associated with their integration into musculoskeletal modelling. The computational time and costs required for subject-specific FEM modelling and simulations limit their applicability for large-scale population studies. Furthermore, as each FE model is tailored to an individual, the potential for comprehensive exploration of knee joint behaviour across diverse populations becomes impractical. To address these limitations and achieve a balance between efficiency and individual variability, the present research proposes an innovative approach that leverages MSK models scaled with rigid tibiofemoral motion derived from individual anatomical geometry. This generic overarching idea presents a promising foundation for a more efficient study of knee joint behaviour within diverse populations. The base of this approach is a scaled MSK model providing the basis for capturing knee joint motion without the computational burden of detailed FEM representations. The key theoretical innovation lies in the use of compliance matrices to account for individual passive motion and laxity variations, relating them to the active tibiofemoral function. By incorporating tibiofemoral compliance matrices, the model aims to simulate passive soft tissue elasticity and account for individual variations in joint behaviour. These compliance matrices are informed by ex vivo experiments and have shown promise in characterizing the tibiofemoral load-displacement relationship. The assumption of linear stiffness/compliance in the model was intentionally made to simplify the analysis and implementation, allowing for a computationally efficient approach. By assuming linearity, the model becomes relatively easy to input individual elastic parameters or coefficients of compliance, which can be derived from in vivo measurements. For the purposes of this study, the linear approximation was considered sufficient to demonstrate the feasibility of the methodology and its potential applications, particularly in relation to investigating elastic linear contributions in joint function. While acknowledging the limitation of linearity, further research and analysis could explore the use of nonlinear fits for more detailed investigations, but it would come with added computational costs and complexity, which may not align with the primary goals of this study. This approach not only streamlines the computational process but also allows for the efficient study of knee joint behaviour across a broader population context. By integrating compliance matrices with scaled MSK models, the research aims to achieve a more comprehensive

understanding of knee joint mechanics while considering individual differences in soft tissue elasticity. The subsequent sections of this thesis will delve into the details of this novel approach, outlining the step-by-step development and implementation process, and presenting the benefits and implications of this innovative model for efficiently investigating knee joint behaviour and advancing the field of musculoskeletal research.

Towards An Efficient Elastic Knee Joint Behaviour Investigation

As mentioned earlier, the purpose of this chapter was to select the most appropriate modelling approach. The primary objective of the upcoming research is to develop an innovative musculoskeletal model that captures the elastic behaviour of the knee and tibiofemoral joint within diverse populations, including various activities. Presently, such a model does not exist, making its development highly promising for advancing our understanding of knee joint mechanics, inter-subject variability, and the broader musculoskeletal research field. Once established, this model can be employed in diverse contexts, such as population studies and investigations of different scenarios and activities. However, it is crucial to acknowledge that developing this model may present challenges and limitations, particularly in striking a balance between accuracy and efficiency. The following chapters will meticulously explore the step-by-step process of constructing this model, highlighting its advantages and potential limitations. Through the development of this model, the research has the potential to greatly facilitate a comprehensive investigation of elastic knee joint behaviour, thereby contributing valuable insights to the field of musculoskeletal research. It holds the promise of enabling in-depth explorations of population variability, pathologies, injuries, and potential clinical applications. Moreover, the model's versatility extends beyond the knee joint, making it applicable to other joints as well. This multifaceted approach opens new possibilities for studying various musculoskeletal structures and their behaviours, ultimately advancing our understanding of human biomechanics, and offering potential benefits for clinical practice.

Chapter 6

STUDY 3

Elastic-Joint Multibody-Rigid Musculoskeletal Model As Efficient Representation Of The Tibiofemoral Joint Laxity

CONTENTS

F. Bucci, M. Taylor, R. Al-Dirini, S. Martelli (2023) – Elastic musculoskeletal joint model as efficient representation of the knee joint laxity. Journal of Biomechanics. *In preparation for submission to peer-reviewed journal.*

Please refer to the appendices at the end of this thesis for a detailed outline of the author's contribution to this study (Appendix A).

6.1 Abstract

Personalized musculoskeletal models enable studying individual features of healthy and pathological tibiofemoral motion. As such, understanding the separate effect of tibiofemoral geometry and elasticity on tibiofemoral motion during normal activity is relevant to both research and clinics. However, complex geometry-based musculoskeletal models embedding tibiofemoral contact surfaces, geometrical and elastic properties of each relevant knee structure are computationally expensive and difficult to completely identify in vivo. One possibility is to model the effect of tibiofemoral geometry on knee motion using fast rigid-body models, and the tibiofemoral elastic response using a lumped-parameters compliance matrix accounting for the effect of all separate elastic structures. The aim of this work is to demonstrate the use of a lumped-parameters compliance matrix to simulate tibiofemoral motion elasticity during normal activity.

The novel in silico approach was demonstrated using anatomically detailed tibiofemoral elastic foundation models available in literature. The active and passive tibiofemoral kinematics, inverse dynamics, muscle activation and force, and finally tibiofemoral contact forces were calculated using the OpenSim Joint and Articular Mechanics framework. The active and passive tibiofemoral motion were calculated by simulating the same gait trial with and without forces. The external forces were calculated from cartilage contact with the elastic foundation knee model. The compliance matrices (CMs) were defined as 6x6 matrices: $[\mathrm{CM}] \cdot \{\Delta F_a - \Delta F_p\} = \{\Delta X_a - \Delta X_p\}$; where (a) and (p) are active and passive relative variation (Δ) of tibiofemoral linear and rotational displacements (X) forces and moments (F) in the knee joint. The CMs were calculated for each frame of the gait cycle and analysed along with the stiffness of each individual motion axis, passive and active kinematics used to calculate the elastic contribution. A sensitivity analysis was conducted on the number of matrices required to predict tibiofemoral motion and joint forces.

The 3D CMs were produced for all rotations and translations along each axis of motion. A comparison between passive motion and active motion was performed to provide credibility to this research and to investigate ligament contribution. A sensitivity analysis was conducted on the number of matrices required to predict tibiofemoral motion and joint forces. This study's method offers a fast and viable alternative to characterize tibiofemoral elasticity and load-dependent behaviour of the knee during physical activity. Future work will provide better understanding of knee elasticity and inclusion of compliance matrices in musculoskeletal models.

6.2 Introduction

Joint anatomy, joint elasticity determined by ligaments and muscles, and the motion task all contribute, at varying degrees, to a variable musculoskeletal function and the success of musculoskeletal clinical treatments (Fitzpatrick et al., 2012). The application of musculoskeletal modelling provides a valuable means to enhance our understanding of musculoskeletal function by facilitating the investigation and quantification of the influence of specific anatomical structures, offering potential applications in various scenarios. Musculoskeletal modelling encompasses various approaches for modelling human joints, each with specific trade-offs in terms of accuracy and computational efficiency, depending on the intended application (Delp et al., 2007). For instance, rigid joint models (Arnold et al., 2010; Delp et al., 1990) are designed to provide a computationally efficient representation primarily based on the average joint motion, based often solely on geometry. These models prioritize functional representation and adaptability for modelling multiple individuals and activities, rather than aiming for high accuracy in reproducing specific individual joint anatomy or function, ultimately allowing for the prediction of more generalized findings. On the other hand, deformable joint models (Hume et al., 2018; Lenhart et al., 2015) prioritize the comprehensive and faithful representation of joint motion by accounting for anatomy, the elastic behaviour of soft tissues, and thus more accurately reproducing individual joint function. While providing more detailed and accurate joint representations, these models require additional input data, computational resources, and implementation time, allowing for the examination of specific influences of anatomical structures on individual joint function, although their findings may be less generalizable compared to rigid joint models.

A variety of approaches are available to model knee joint behaviour, differing in complexity, computational time, and data-associated costs. Simpler and faster multibody dynamics models of the lower limb have simplified the knee to just tibiofemoral rigid joint, with planar motion (Delp et al., 1990; Yamaguchi et al., 1989). Similarly, musculoskeletal models embedding simplified knee motion, based on Walker (1988) can predict average trends in kinematics and dynamics (Walker et al., 1988), but only offer a crude estimation of individual function (Arnold et al., 2010); these models typically provide generic or average geometries, with material properties from the literature (Arnold et al., 2010; Delp et al., 1990; Xu et al., 2015).

Including subject-specific geometry and ligaments, integrating elastic foundation, finite element, or deformable knee models, enhances the prediction of individual tibiofemoral mechanics but increases simulation time (Brito da Luz et al., 2017; Hume et al., 2018; Lenhart et al., 2015; Smith et al., 2016; Smale et al., 2018; Valente et al., 2015). New modelling techniques are enabling the development of increasingly complex tibiofemoral mechanisms that efficiently incorporate subject-specific anatomical variations, such as integrating these mechanisms into generic-scaled

musculoskeletal models (Brito da Luz 2017; Conconi et al., 2018; Martelli et al., 2020). A single degree-of-freedom tibiofemoral model with floating axis based on subject-specific geometry has been recently used to investigate the effect of the geometry into the musculoskeletal function (Martelli et al., 2020). These rigid models account for a subject-specific geometry-based motion generated by parallel mechanism description of the knee (Conconi et al., 2018; Martelli et al., 2020); tibiofemoral statistical shape-kinematic models could also generate geometry-based motion (Appendix D - O'Rourke et al., 2023), or again statical shape models (Clouthier et al., 2019). Although clinicians and researchers are highly interested in tibiofemoral elasticity during normal activity, these models tend to focus primarily on geometry, with secondary tibiofemoral motion constrained and load-dependent knee movements not considered. This overview highlights a gap in terms of providing a modelling method to efficiently investigate the elastic contribution of soft tissues during activities. The presented approach in the study does not aim to produce an anatomically accurate replica of the knee joint or its movement. Instead, the focus is on providing a method to efficiently investigate the elastic contribution of soft tissues during activities, which could be potentially easily adapted to investigate a broader population.

A major focus in current musculoskeletal modelling research is finding an optimal balance between accuracy and efficiency, crucial to ensure their clinical adoption by providing high-fidelity subject-specific representations of the tibiofemoral joint at decreased computational costs (Killen et al., 2020). Deformable knee models have been introduced to represent the elastic and load-dependent nature of the knee (Lenhart et al., 2015; Hume et al., 2018). Inclusion of anatomical details and ligament representations, from rigid to linear and non-linear spring bundles, heavily affects joint predictions, and computational time increases upon fidelity (Kiapour et al., 2014; Lenhart et al., 2015; Smith et al., 2016). Musculoskeletal simulations combined with subject-specific finite-element (Hume et al., 2018) or elastic foundation (Lenhart et al., 2015) models of the knee are currently employed to produce more different information including stresses-strains in each individual anatomical structure. Optimization methods reduced the computational effort required by deformable knee simulation time to 76 minutes for a chair rise and 210 for a gait (Lenhart et al., 2015; Navacchia et al., 2018; Smith et al., 2016). Despite significant improvements over time, musculoskeletal models still face challenges in achieving both computational efficiency and subject-specificity simultaneously, limiting their suitability for certain population studies and clinical applications (Killen et al., 2020). A major challenge with these approaches is to maintain sufficient complexity without requiring extensive datasets and expertise, ideally in a computationally efficient and time-effective manner. One possibility is to model the effect of tibiofemoral geometry on knee motion using fast rigid-body models (Martelli et al., 2020), and the tibiofemoral elastic response using 6x6 lumped-parameters compliance matrices accounting for the effect of all separate elastic structure (Lamberto et al., 2019). These matrices were successfully embedded into musculoskeletal spine models to predict intervertebral motion (Meng et al., 2015).

In Lamberto (2016), ex vivo experimentally derived compliance matrices were used to describe joint displacement as a function of load, as well as knee laxity tests, thereby implicitly representing passive elastic knee structures, i.e., ligaments (Lamberto et al., 2016). However, these matrices were calculated only for a few angles (0° to 90°, every 15° degrees), do not represent the constraint of muscular tissue such as the patellar tendon, and the ex vivo procedure is extremely time-consuming.

This approach aims to bridge the gap between passive and active function, rather than replicating specific anatomical features or movement patterns. In the present study, a novel computationally efficient approach for modelling joint function while accounting for both anatomy and elastic behaviour was presented. The aim of this work was to demonstrate the use of a lumped-parameters compliance matrix to simulate and investigate the tibiofemoral motion during normal activity. Compliance matrices were embedded into musculoskeletal models in order to provide a computationally efficient representation of tibiofemoral elasticity in this study. The concept of compliance matrices derived in vivo (alternatively to ex vivo testing) was introduced to describe passive and active displacements as a function of joint forces. These differences were compared with ex vivo measurements of the passive motion envelope (Chapter 4) and in vivo biplanar fluoroscopy measurements (Martelli et al., 2020) to provide credibility to these matrices and insight into the role of ligaments. This approach was demonstrated with a state-of-the-art anatomically detailed validated musculoskeletal model (Lenhart et al., 2015), and aimed at predicting the same tibiofemoral motion in less time.

6.3 Material And Methods

6.3.1 Lenhart Model And Simulations

A publicly available model by Lenhart (Lenhart et al., 2015) was used for this study. The model is based on MR imaging and gait analysis performed on a 23-year-old female subject (height = 1.65 m, mass = 61 kg) with no history of chronic knee pain, injury, or surgery. The model is a 25-segments, 52-DOFs multibody dynamic system including the tibiofemoral contact surfaces, 14 non-linear spring bundles linking ligament origin footprint to its insertion. The lower extremity model was scaled to the subject based on segment lengths determined in a standing upright posture. Subject-specific tibiofemoral ligament volumes (i.e., MCL, LCL, ACL, and PCL) were included, while ligament cross-sectional areas and stiffness were adapted from other models and cadaveric studies (Blankevoort et al., 1988). Tibiofemoral cartilage contact forces were computed using an elastic foundation model. In this model, the flexion-extension was treated as the primary degree of freedom, while the 5 remaining DoF were secondary. The subject underwent gait analysis during overground walking at a preferred speed; 44 passive reflective marker kinematics

were collected with an eight-camera, passive motion capture system (100 Hz low-pass filtered at 12 Hz)(Motion Analysis, Santa Rosa, CA) and ground reaction forces collected (2000 Hz low-pass filtered at 50 Hz)(faceplate model BP400600, AMTI, Watertown, MA).

The active and passive tibiofemoral kinematics, inverse dynamics, muscle activation and force and tibiofemoral contact forces were calculated using the OpenSim Joint and Articular Mechanics framework (https://simtk.org/projects/opensim-jam); kinematic displacements describe the movement of the tibia relatively to the femur. The active and passive tibiofemoral motion was simulated with Lenhart model during gait. The purpose of simulating the passive tibiofemoral motion was to investigate the relationship between passive and active joint function, by deriving computationally tibiofemoral compliance matrices, for which variations in articular forces and correspondent TF displacements are needed. The parameter changes for simulating passive tibiofemoral motion and their reasoning were as follows:

1. Scaling down external forces to 0.1% – This change was implemented to create a scenario where the external forces, such as ground reaction forces during walking, have a significantly reduced effect on the knee joint, to focus solely on the TF passive behaviour.

2. Setting gravity to zero – By setting gravity to zero, the gravitational forces acting on the lower limb were eliminated, thus isolating the effect of passive forces, and neglecting the contribution of body weight during the simulation.

3. Removing knee-spanning muscles – In passive motion simulation, the focus was on the behaviour of the joint without the active contribution of muscles. By removing knee-spanning muscles, the simulation aimed to isolate and study the passive response. The knee-spanning muscles removed included rectus femoris, tensor fasciae latae, gastrocnemius lateralis, iliacus, psoas, quadriceps femoris, biceps femoris, gracilis, semitendinosus, semimembranosus, vastus medialis, lateralis and intermedius, while gluteus maximus force was reduced by 90%. Due to the absence of specific muscles, replicating the same movement resulted in unrealistic gluteus activation during the simulation, leading to the decision of reducing force to minimize muscle influence.

In passive motion simulation, the forces within the joint should ideally approach zero. However, since mathematical equations may require some forces for solving ID equations, reducing all forces to zero might not be feasible. Therefore, the reduction/minimization of external forces and gravity, as well as the removal of knee-spanning muscles, contributes to creating a scenario closer to passive motion, while still enabling to solve the ID equations.

4. Reducing ligament stiffness by 50% – Reducing the stiffness of ligaments by 50% was an attempt to mimic unloaded passive knee motion conditions, to simulate scenarios where the ligaments are within the envelope, more compliant and not engaged. In this model, the knee

was represented using an elastic foundation model, and the specific movement or kinematics of the knee joint were defined from the MSK simulation. The ligaments were modelled as non-linear spring bundles, with properties that mimic the behaviour of real ligaments. During the simulation of passive motion, it was expected that the knee joint would behave as if there were no external forces acting on it. However, due to the mathematical and physical nature of the simulation, the articular forces within the joint were not exactly zero, even when gravity or external forces were not acting on it. The presence of these internal forces, generated by the mathematical formulation of the model, caused the knee ligaments to be subjected to forces, resulting in them contributing to the response of the joint, contrary to the intended passive scenario. To create a scenario closely resembling passive motion and minimise the forces in the joint, it became necessary to reduce ligament contribution. One way to achieve this was by lowering the ligament stiffness, by progressively reducing it. A 50% reduction in stiffness led to decreased resistance of ligaments to deformation, hence resulting in significantly lower forces during the simulation. This adjustment was critical to mimic the conditions of passive motion where the contribution of ligaments is minimal or negligible.

The articular forces were calculated from cartilage contact with an elastic foundation knee model (Lenhart et al., 2015). Tibiofemoral kinematics and articular contact forces and moments were predicted for a gait cycle. For each of the secondary degrees of freedom, passive to active differences in motion and forces/moments were calculated and expressed respectively in mm, rad, N and Nmm. Differences of passive to active motion and forces/moments were reported across the gait cycle for the active and passive simulation (MATLAB, MathWorks, Natick, USA).

6.3.2 Passive To Active Tibiofemoral Compliance

Compliance matrices (CMs) to provide the passive to active joint displacement as function of the joint load, were defined as 6x6 matrices $[CM] = \{c_{ij}\}$:

$$[CM] \cdot \{F_a - F_p\} = \{X_a - X_p\}$$

$$\{X_a - X_p\} = (\Delta t_{AP} \quad \Delta t_{SI} \quad \Delta t_{ML} \quad \Delta\theta_{AA} \quad \Delta\theta_{IE} \quad \Delta\theta_{FE})$$
$$\{F_a - F_p\} = (\Delta F_{AP} \quad \Delta F_{SI} \quad \Delta F_{ML} \quad \Delta M_{AA} \quad \Delta M_{IE} \quad \Delta M_{FE})$$

where (a) and (p) are active and passive relative variation (Δ) of tibiofemoral linear (t) and angular (θ) displacements, forces (F) and moments (M) in the knee joint coordinate system (with AP antero-posterior, SI superior-inferior, ML medial-lateral, AA adduction-abduction, IE internal-external rotation, FE flexion-extension).

Compliance matrices were computed for each frame of the gait cycle by quantifying the differences between passive and active simulation results (MathWorks, Natick, USA). The compliance matrices were utilized to extrapolate the individual translational and rotational compliances in relation to the gait cycle. The compliance analysis based on the gait cycle involved

resampling the values and calculating a separate compliance matrix for each percentage of the gait cycle. To evaluate compliance based on the flexion angle, the matrices were reorganized based on the flexion angle and subsequently interpolated to generate a dedicated compliance matrix for each specific flexion angle. The relationship of the compliance with the gait cycle percentage and with the flexion angle were qualitatively evaluated through graphical analysis (positive correlation - variables increase together, negative correlation - variables have opposite trends, and no correlation - variables show no relationship).

These matrices were compared with compliance matrices derived experimentally ex vivo (Lamberto et al., 2016) at 0- and 15-degrees flexion (within stance phase). Differences of passive to active motion and forces/moments were reported along with compliance for the stance phase, also plotted against flexion angle (MATLAB, MathWorks, Natick, USA); the swing phase was not reported as no load is transferred through the joint during this phase.

Furthermore, as these matrices were derived from passive to active tibiofemoral motion, to provide credibility to this approach, they were compared with experimentally measured passive (Chapter 4) and active motion during gait measured with biplanar fluoroscopy (Gray et al., 2019) (MATLAB, MathWorks, Natick, USA). The differences obtained between passive and active motion simulated with Lenhart (2015) were compared (Lenhart et al., 2015), with the differences between the active motion pattern across a healthy adult population during gait in the OpenSim reference system publicly available (active biplanar fluoroscopy data – (Martelli et al., 2020)), with the central passive motion pattern measured in the Study 2 for a cadaveric healthy cohort (tibiofemoral passive kinematics - Chapter 4).

6.3.3 Elastic Tibiofemoral Joint Model And Sensitivity Analysis

A generic lower extremity musculoskeletal model was used with a six DOF pelvis, a three DOF ball-in-socket hip, and a one DOF ankle (Arnold et al., 2010), while the 1 DOF knee in FE with AP, ML translations and IE and AA rotations function of the flexion based the equations reported by Walker (Walker et al., 1988) and scaled on Lenhart subject. Experimental data of the same subject were used for the simulations.

A custom MATLAB code (MATLAB, MathWorks, Natick, USA) using OpenSim API (Delph et al., 2007) was written to embed the compliance matrices into a fast rigid-body OpenSim model.

(1) The knee model splines were read from the model, optimized to best fit the knee kinematics from the passive Lenhart model simulation and placed into the knee model. Cubic splines in MSK models are mathematical functions that rigidly define the relationship between secondary degrees of freedom (internal-external rotation, varus-valgus) and the primary degree of freedom (flexion) in the tibiofemoral joint, using only a few coefficients to represent-model its function.

(2) An initial simulation, including Inverse Kinematics (IK), Inverse Dynamics (IK), Static Optimization (SO) and Joint Reaction (JR), was performed with OpenSim APIs in MATLAB.

(3) At this point, the compliance matrix/matrices previously calculated were used as compliance to aim at for each frame, in order to verify the calculations and demonstrate the elasticity. The compliance matrix was defined as follow (Lamberto et al., 2016):

$$CM = \begin{array}{c} \begin{matrix} F_{1X} & F_{2Y} & F_{3Z} & M_{1X} & M_{2Y} & M_{3Z} \end{matrix} \\ \begin{bmatrix} c11 & 0 & 0 & 0 & 0 & 0 \\ 0 & c22 & 0 & 0 & 0 & 0 \\ 0 & 0 & c33 & 0 & 0 & 0 \\ 0 & 0 & 0 & c44 & 0 & 0 \\ 0 & 0 & 0 & 0 & c55 & 0 \\ 0 & 0 & 0 & 0 & 0 & c66 \end{bmatrix} \end{array} \begin{array}{l} \delta T_{1X} - \text{Anterior Posterior} \\ \delta T_{2Y} - \text{Infrior Superior} \\ \delta T_{3Z} - \text{Medial Lateral} \\ \delta R_{1X} - \text{Abduction Adduction} \\ \delta R_{2Y} - \text{Internal External} \\ \delta R_{3Z} - \text{Flexion Extension} \end{array}$$

in this matrix, F represents forces, M represents moments, T represents translations, and R represents rotations, the elements C represent the compliance of each degree of freedom (in direction 1 x, AP translation and AA rotation; direction 2 y, IS translation and IE rotation, finally 3 z, ML translation and FE rotation) – for instance c11 is the compliance relative to x or AP direction, while the symbol δ is a physical symbol representing a variation.

As it was found that the ratio of the forces and torques produced by joint stiffness to the total torque required to balance the model must be the same at all levels for the flexion:

$$\text{ratio} = \text{required torque} * \text{joint compliance}\ ; \text{and} \quad \text{new torque} = \text{ratio}/c_{FE}$$

In order to recalculate the required stiffness, the IK and ID algorithms were executed through APIs, considering the joint compliance. This facilitated the determination of the new flexion based on the new moment, as well as the calculation of other rotations and translations using the remaining compliance/stiffness matrix terms. These new values for translations and rotations were calculated based on these equations:

Independent DoF:

$$(3.1)\ ROT1 - dR_{FLEX/EXT\ new} = (M_{1Z} - \frac{1}{c_{55}} * \delta T_Y - \frac{1}{c_{44}} * \delta T_X)/(1/c_{11})$$

Secondary dependent DoFs:

$$(3.2)\ ROT2 - dR_{INT/EXT\ new} = (M_{2Y} - \frac{1}{c_{66}} * \delta T_Z - c_{44} * \delta T_X)/(1/c_{22})$$

$$(3.3)\ ROT3 - dR_{ADD/ABD\ new} = (M_{3X} - \frac{1}{c_{55}} * \delta T_Y - \frac{1}{c_{66}} * \delta T_Z)/(1/c_{33})$$

$$(3.4)\ TRANSL3 - dT_{MED/LAT\ new} = (F_{3Z} - \frac{1}{c_{22}} * \delta R_{2Y} - \frac{1}{c_{33}} * \delta R_{3X})/(1/c_{66})$$

$$(3.5)\ TRANSL1 - dT_{ANT/POST\ new} = (F_{1X} - \frac{1}{c_{11}} * \delta R_{1Z} - \frac{1}{c_{22}} * \delta R_{2Y})/(1/c_{44})$$

$$(3.6)\ \text{TRANSL2} - \ dT_{INF/SUP\ new} = (\ F_{2Y} - \frac{1}{c_{11}} * \delta R_{1Z} - \frac{1}{c_{33}} * \delta R_{3X})/(1/c_{55})$$

(4) The variations in translations and rotations were recalculated at every step using the appropriate previously calculated compliance matrix (CM), and the process was iterated until the target compliance was met. To recalculate the required compliance, the APIs for IK and ID, specifically the SO and JR functions, were run. This allowed for the necessary calculations and adjustments to be made in order to achieve the desired compliance.

The study presented tibiofemoral motion for all six degrees of freedom as its results. The study conducted an analysis of convergence. This analysis aimed to assess the stability and effectiveness of the iterative process used to recalculate translations and rotations. It evaluated whether the process reached a stable solution and met the target compliance. The results of the convergence analysis were then reported. Predictions were made using four compliance matrices, which accounted for 4% of the total matrices or 100 matrices for the entire gait cycles. The predictions were reported with active and passive kinematics as references. Additionally, the study reported the simulation time as part of its findings.

6.4 Results

In the gait cycle, stance phase covered 0% to 60% and swing phase 60% to 100%, with respectively 15° peak stance phase flexion and peak during the swing phase of 60°flexion. The differences between passive to active tibiofemoral kinematics and forces/moments calculates were reported in the following figures for each DoF across gait cycle (Fig. 6.2, 6.3).

Passive to active compliance matrices were compared with compliance matrices derived experimentally ex vivo in 3D, (Lamberto et al., 2016) at 0°- and 15°-degree flexion, chosen as within stance phase; these matrices presented values of the same magnitude and coherent with the compliance represented.

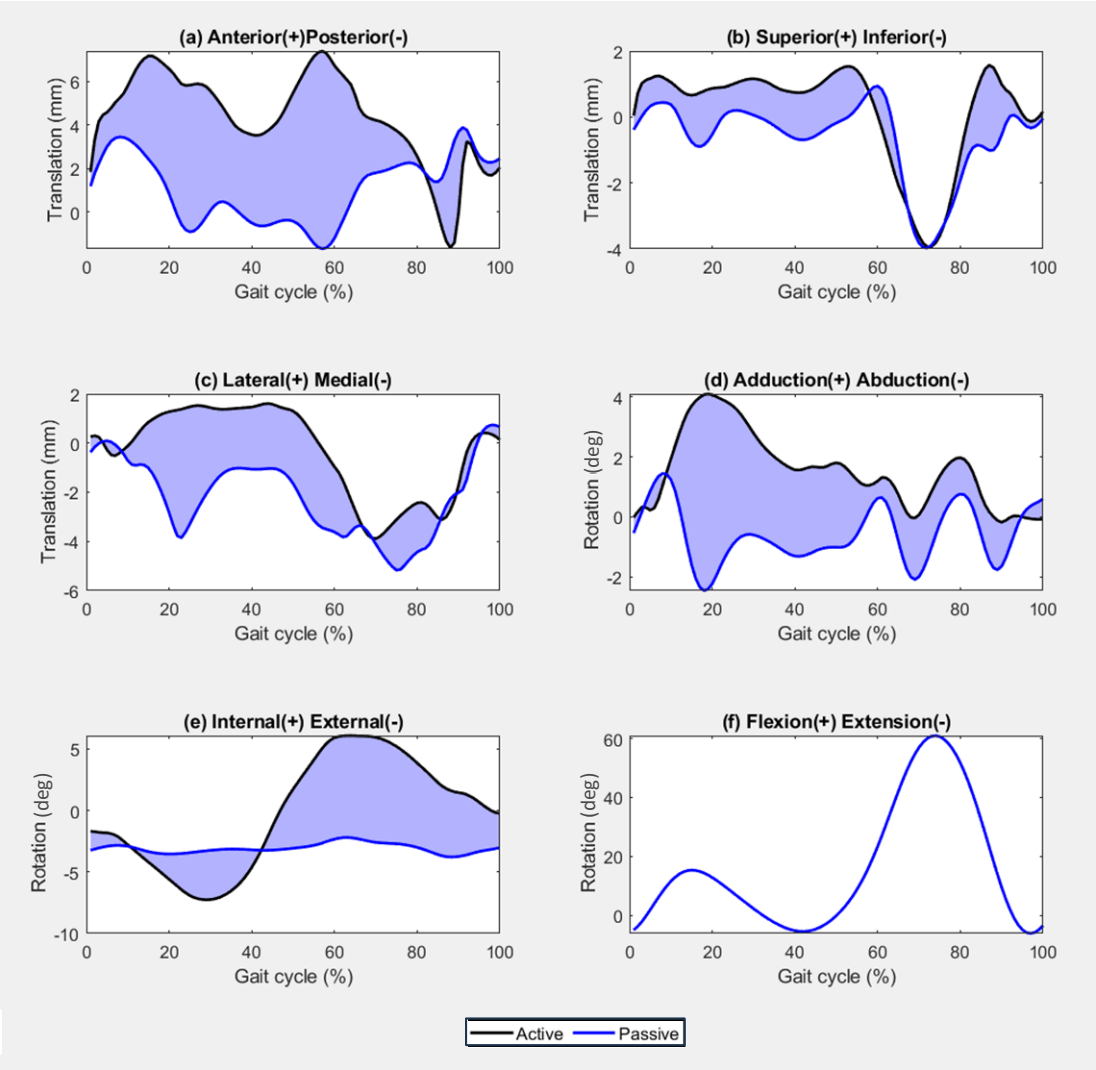

Figure 6.1 *– Six degrees of freedom tibiofemoral kinematic differences between passive and active conditions (in mm and deg) in (a) anterior-posterior translation, (b) superior-inferior translation, (c) medial-lateral translation, (d) abduction-adduction, (e) external-internal rotation, and (f) flexion-extension, during gait simulated with the Lenhart model (Lenhart et al., 2015).*

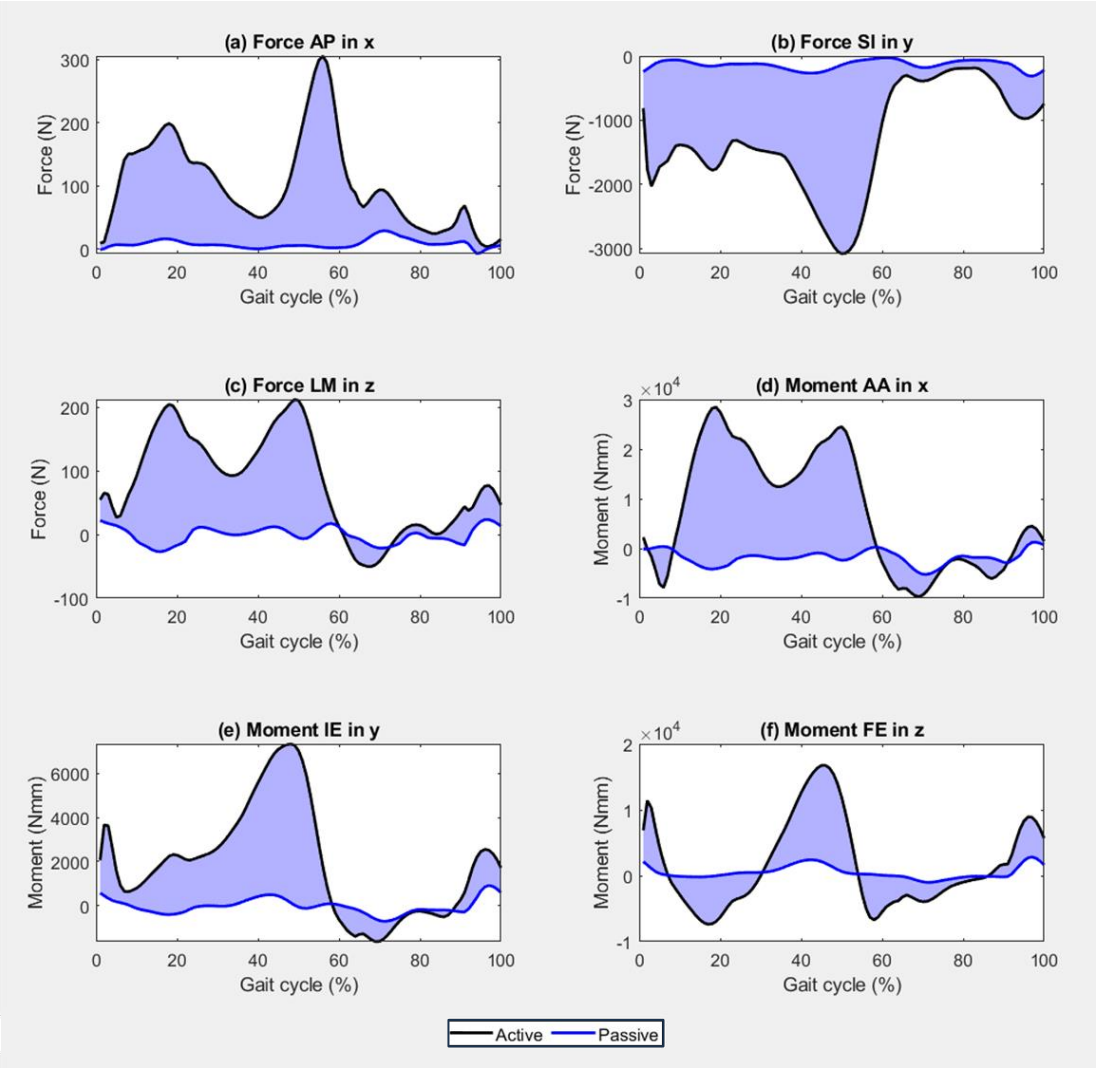

Figure 6.2 *– Six degrees of freedom tibiofemoral kinetic differences between passive and active conditions (in N and Nmm) in (a) anterior-posterior force, (b) superior-inferior force, (c) medial-lateral force, (d) abduction-adduction moment, (e) external-internal moment (f) flexion-extension moment, during gait simulated with the Lenhart model (Lenhart et al., 2015).*

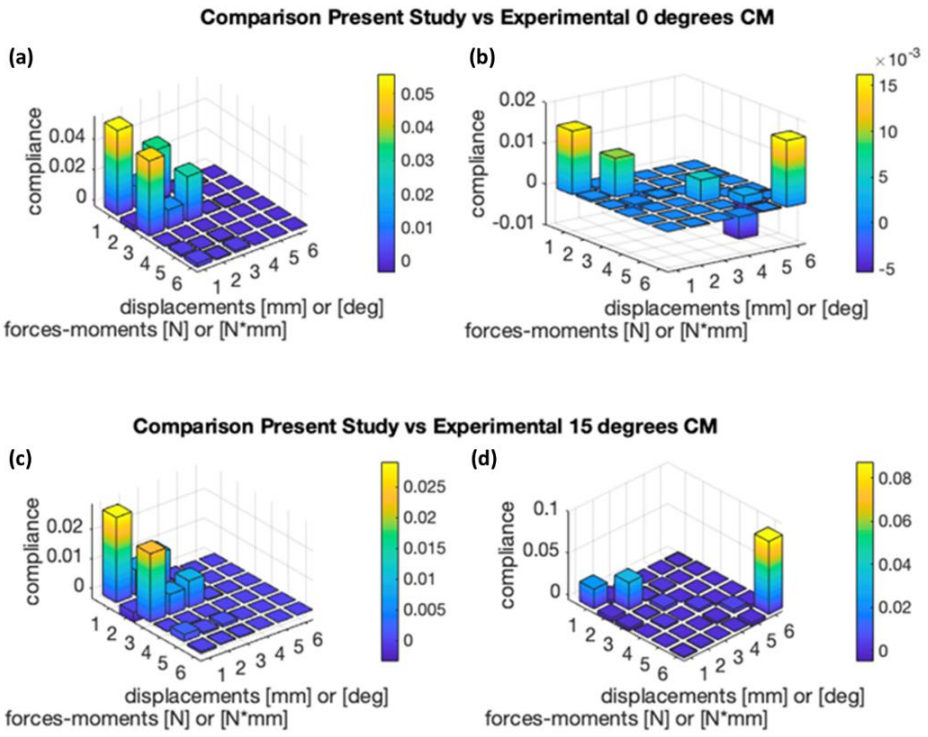

Figure 6.3 *– Comparison of (a, c) simulated passive-to-active tibiofemoral compliance and (b, d) ex vivo experimentally measured compliance at 0-degree flexion in the top row and at 15 degrees in the bottom row in 3D, where 1 to 3 represent translations and forces in x, y, z (mm and N) and 4 to 6 represent rotations and moments in the x, y, and z directions (deg and Nmm)(Lamberto et al., 2016).*

Anterior-posterior translation presented the highest differences in comparison to the medial-lateral and inferior-superior translation (Fig. 6.4-a, Fig. 6.5-a, Fig. 6.6-a). Peak differences of translation and force were both approximately 55-60% of the gait cycle respectively of 9mm and 300 N; a second peak was present at approximately 20-25% of the gait cycle, corresponding to 6.7 mm and 182 N (Fig. 6.4-a, -b). Compliance ranged from -0.128 to 0.08 mm/N. Compliance highest peak was at 40 percent of 0.08 mm/N, after a steady decrease in early stance and increase at the end of it (Fig. 6.4-c); other peaks were present, alternated to the peak differences of motion/forces (at the beginning of the stance)(Fig. 6.4-c). The compliance in AP revealed to be a function of the flexion angle, with a stronger relationship with respect to the gait cycle phases (Fig. 6.4-d). The compliance calculated based on the flexion angle was on average 0.0236 mm/N, highest interval was between -5° and 5° degrees flexion (~0.06 mm/N), and between 45° to 55° degrees flexion (~0.04 mm/N) (Fig. 6.4-d).

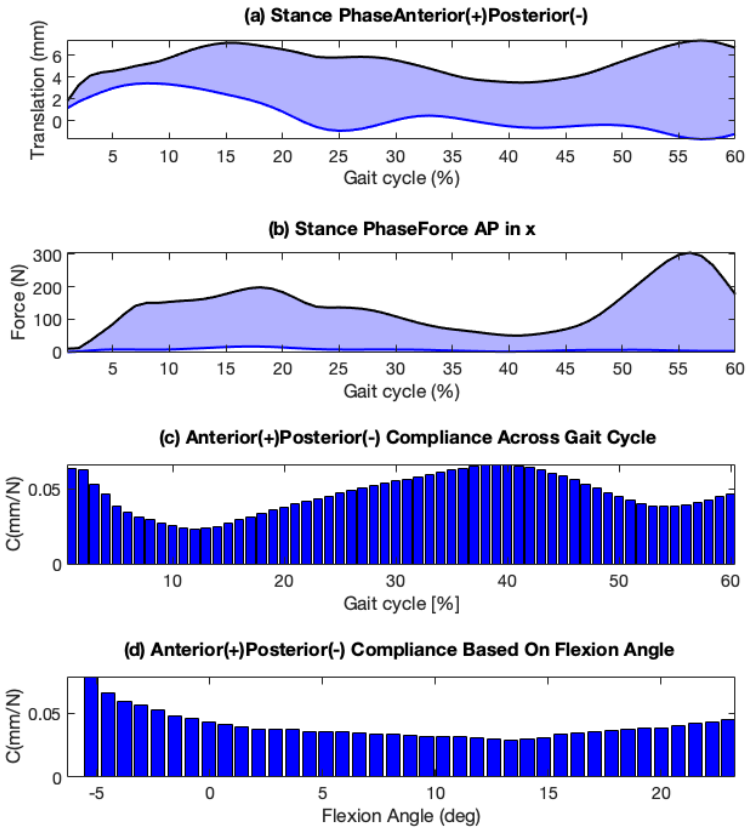

Figure 6.4 *– Tibiofemoral differences between passive and active conditions in anterior-posterior (a) translations, (b) forces, compliance calculated across the stance phase and reported against (c) percentage of gait cycle and against (d) flexion angle.*

Inferior-superior translation presented an almost steady difference (~1mm) between 0 to 60 percent of the gait cycle, with average forces around - 2000 N (Fig. 6.5-a, -b); peak difference of the forces was -3000 N at 50 percent of the gait cycle, while a peak in kinematic difference was present just after 15% of 1.25mm (Fig. 6.5-a, -b). Compliance was small and ranged from -0.0007 to 0.0001 mm/N (Fig. 6.5-c). Compliance decreased at the beginning and increase at the end of the stance, while for the rest it remained steady with an average of -0.0008 mm/N (Fig. 6.5-c). Compliance was steady also for flexion with a negative peak of -0.0005 mm/N up to 17 degrees flexion, to then become positive (Fig. 6.5-d).

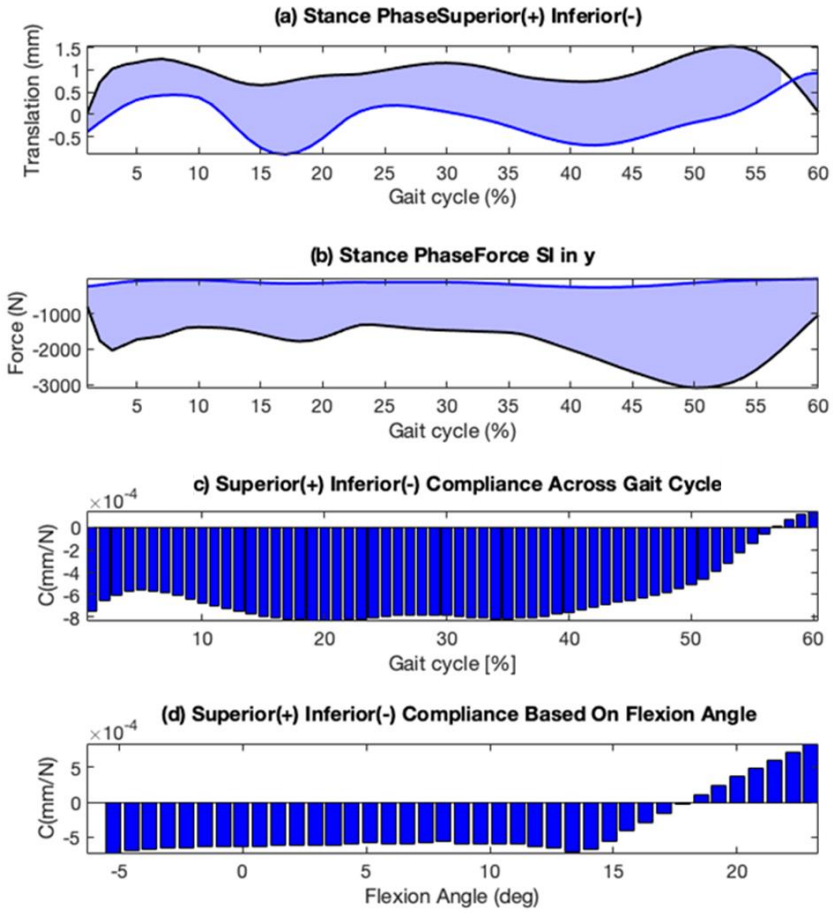

Figure 6.5 *– Tibiofemoral differences between passive and active conditions in inferior-superior (a) translations, (b) forces, compliance calculated across the stance phase and reported against (c) percentage of gait cycle and against (d) flexion angle.*

Medial-lateral translation also presented most of its differences between 0% and 60% percent of the gait cycle, with a translation peak of approximately 5 mm and of 200N force just after 20%, while a second peak of 1mm and 200N around 50% (Fig. 6.6-a, -b). Compliance was relatively small with two peaks at around 25% and just before 60% for the first and second half of the swing phase of ~ 0.07 mm/N (Fig. 6.6-c), both peaks were after 25° degrees knee flexion (Fig. 6.6-d).

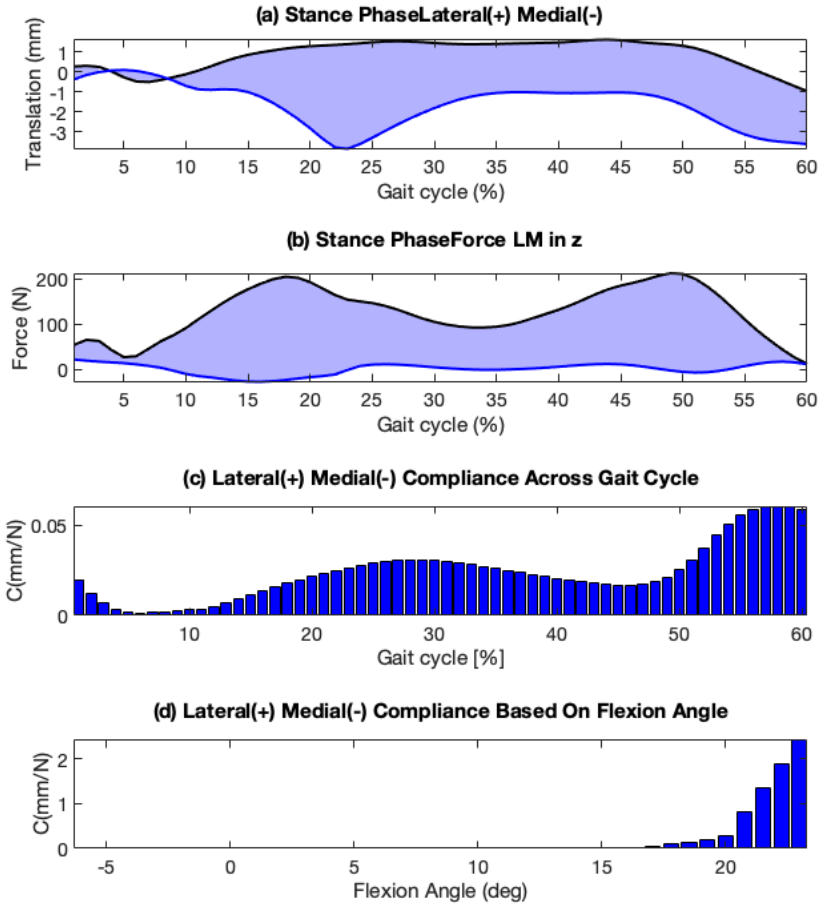

Figure 6.6 *– Tibiofemoral differences between passive and active conditions in medial-lateral (a) translations, (b) forces, compliance calculated across the stance phase and reported against (c) percentage of gait cycle and against (d) flexion angle.*

Differences in abduction-abduction were evenly distributed between 0% and approximately 55% percent of the gait cycle with 6° degrees at approximately 20% (Fig. 6.7-a), and two moment peaks at 20% and 50% percent of approximately 2e4 Nmm (Fig. 6.7-b). Compliance was very low and negligible across the entire gait cycle (Fig. 6.7-c) but showed a clear relationship with flexion steadily decreasing from 40° to 60° degrees flexion, but still with negligible values, from 5e-7 to -3e-5 (Fig. 6.7-d).

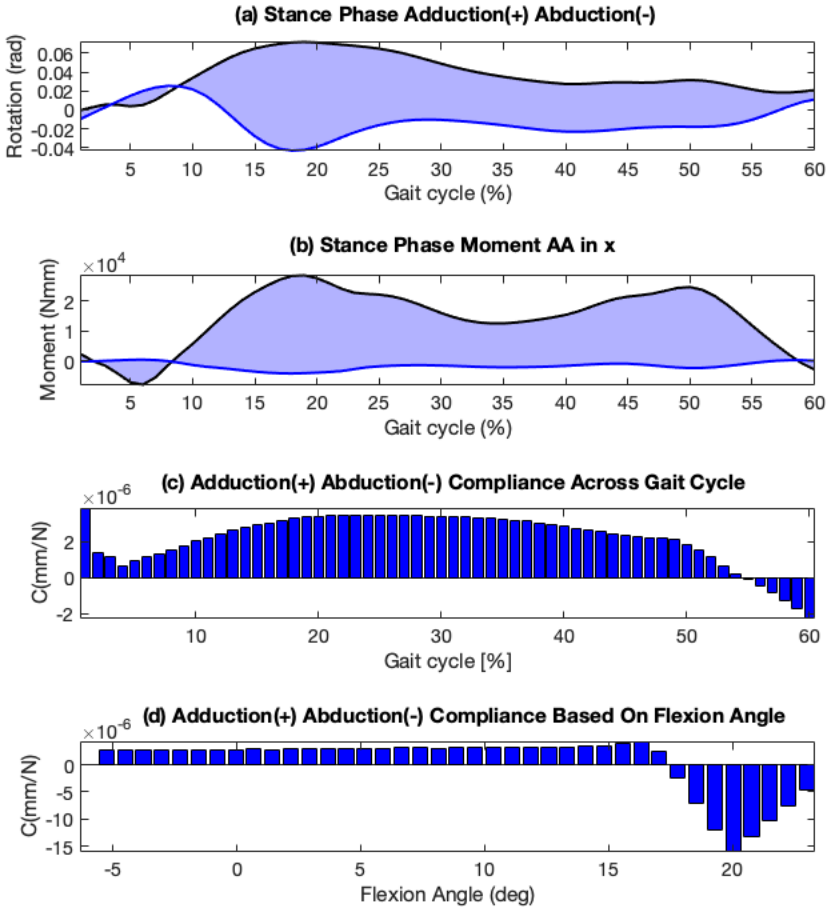

Figure 6.7 *– Tibiofemoral differences between passive and active conditions in abduction-adduction (a) rotations, (b) moments, compliance calculated across the stance phase and reported against (c) percentage of gait cycle and against (d) flexion angle.*

Differences in internal-external rotation were connoted by two peaks: a negative peak for the stance and a positive for the swing, of 4° and 8° degrees (Fig. 6.8-a), and a peak in the moments around 50% of 7e3 Nmm (Fig. 6.8-b). Compliance had the same connotations for abduction-abduction, almost negligible across the entire gait cycle (Fig. 6.8-c) and showing a clear relationship with flexion steadily decreasing from 40° to 60° degrees flexion, but still with negligible values, up to -3e-4 (Fig. 6.8).

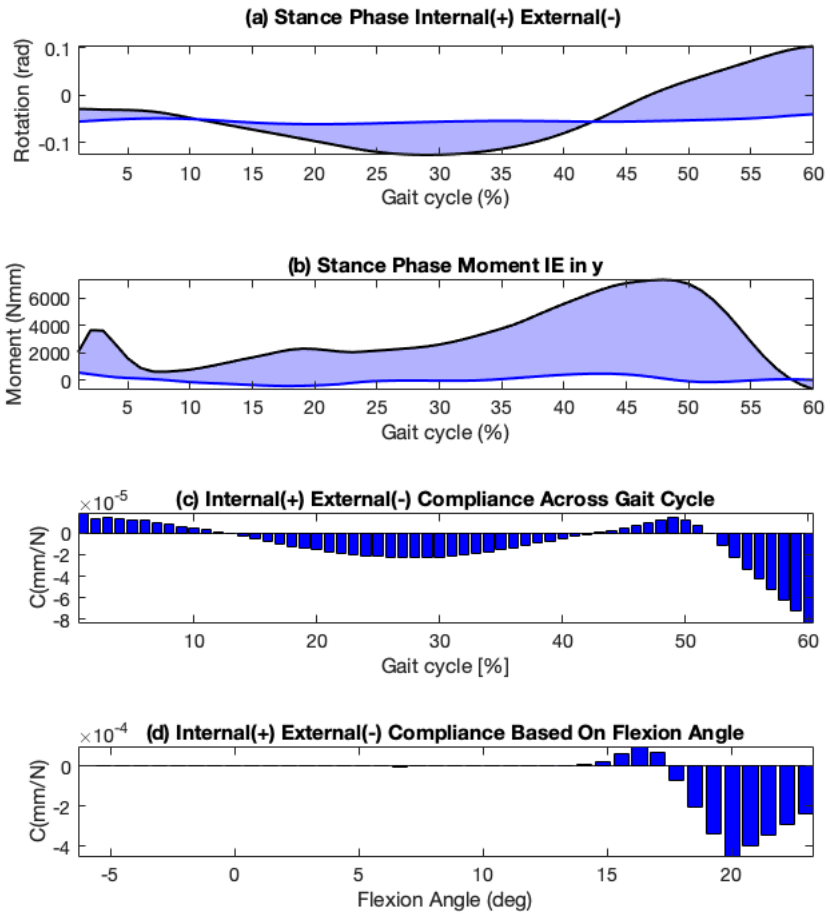

Figure 6.8 – *Tibiofemoral differences between passive and active conditions in internal-external (a) rotations, (b) moments, compliance calculated across the stance phase and reported against (c) percentage of gait cycle and against (d) flexion angle.*

Figure 6.9 depicts a comparison between experimentally observed differences in tibiofemoral (TF) kinematics during active and passive motion and those derived from musculoskeletal (MSK) simulations. The graphs show variations in (a) anterior-posterior translation, (b) inferior-superior translation, (c) medial-lateral translation, (d) adduction-abduction, and (e) internal-external rotation. Experimental differences between active and passive TF kinematics are shown in green, while differences from MSK simulations are represented in blue. Additionally, the figure includes the mean pattern of active motion during gait in healthy adults (Martelli et al., 2020), and the neutral passive motion pattern measured in Chapter 4 for a cadaveric healthy cohort. This comparison has been performed to validate the approach used in calculating compliance matrices and to gain insights into the contribution of ligaments and other soft tissues to tibiofemoral joint function during active and passive motion. The similarities between passive to active motion differences obtained with the MSK model and experimental differences support the credibility of the approach. The comparison of the unloaded envelope differences with the differences between passive to active motion also helps to understand the contribution of ligaments towards active joint function.

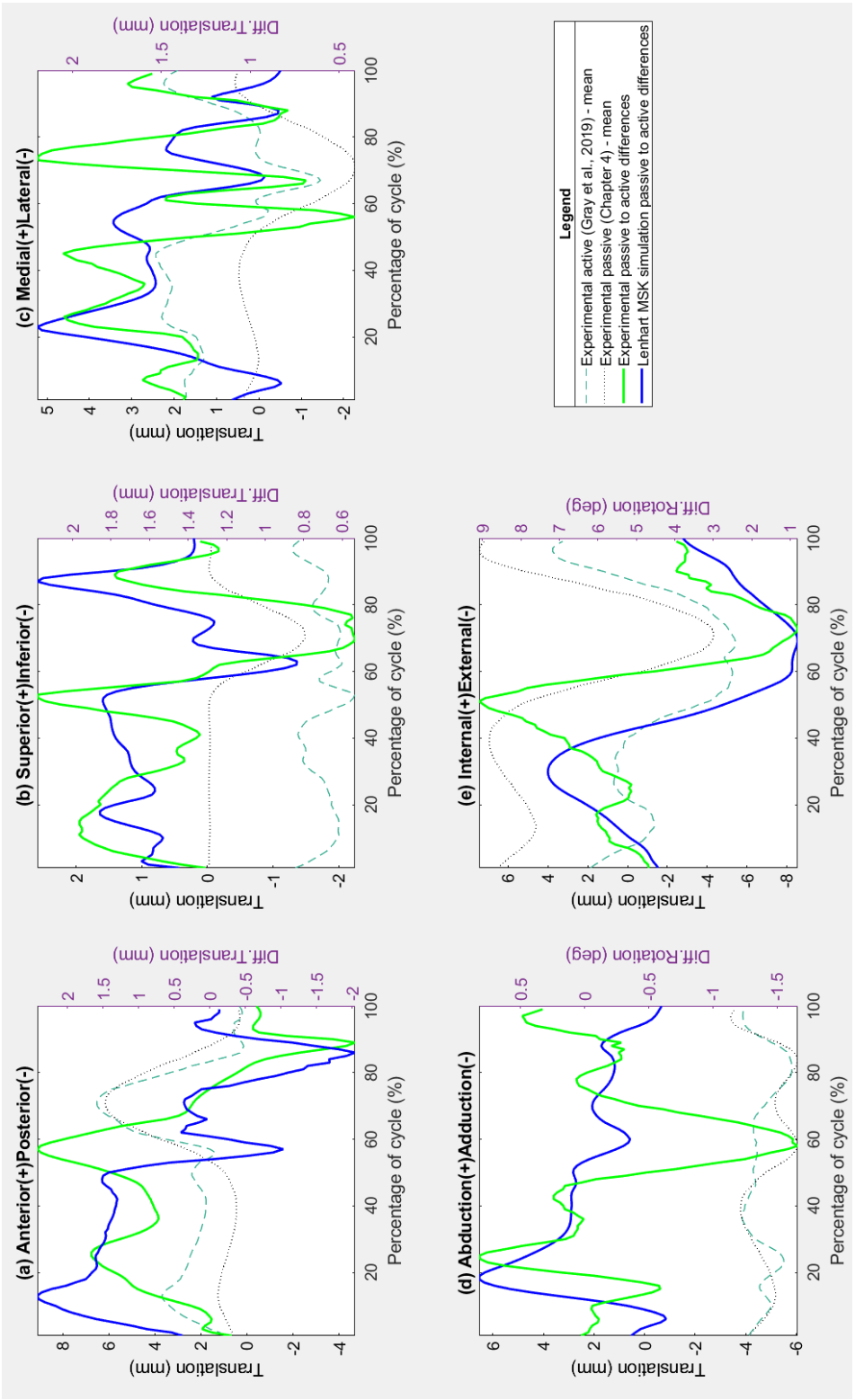

Figure 6.9 *– Comparison of experimentally derived and MSK-simulated differences in passive-to-active tibiofemoral kinematics, showing the mean pattern of active motion in healthy adults during gait (green dashed line, Martelli et al., 2020), the neutral passive motion pattern from a cadaveric healthy cohort (dotted black line, Chapter 4), their experimental differences (solid-line green), and differences between simulated passive and active gait cycle using the Lenhart model (blue, Lenhart et al., 2015), reported for (a) anterior-posterior, (b) inferior-superior, (c) medial-lateral translations, (d) adduction-abduction, and (e) internal-external rotation against percentage of gait cycle.*

The study found that when using all 100% of the matrices, it was possible to obtain negligible differences in the predicted active motion. However, as the number of matrices was reduced, the error increased. Specifically, when using fewer than 4 compliance matrices, the error became more significant. Additionally, the time required to compute the results decreased from a few minutes when using all matrices to a few seconds when using only 4 compliance matrices.

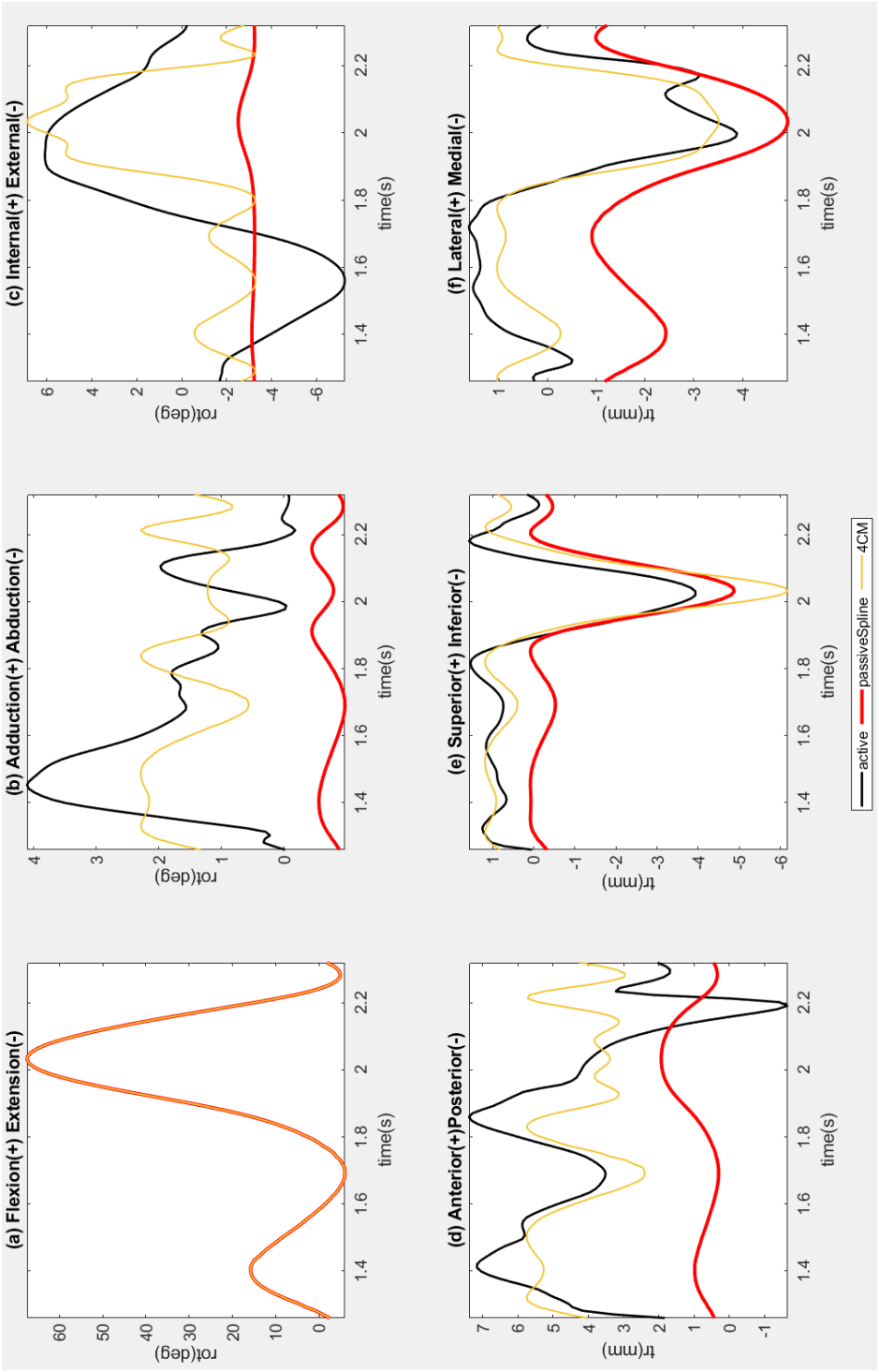

Figure 6.10 *– Results of the elastic tibiofemoral motion simulated using the current methodology adopting 4 compliance matrices (in yellow) across each degree of freedom: (a) flexion-extension, (b) adduction-abduction, (c) internal-external rotations, and (d) anterior-posterior, (e) superior-inferior, (f) lateral-medial translations, compared against the active tibiofemoral motion during gait simulation (target) in black (Lenhart et al., 2015) and the baseline motion representing passive motion based on a rigid knee model in red.*

6.5 Discussion

The use of musculoskeletal modelling can help prevent injury and degenerative disease (Xu et al., 2016), enhance orthopaedic treatments (Niki et al., 2013), and validate computational model predictions (Kim et al., 2009). However, as clinical adoption of personalized MSK models with deformable knee models are limited by their computational and time expenditure, the current focus

is on finding a compromise between accuracy and efficiency (Killen et al., 2020). An analysis of tibiofemoral motion during normal activity using a lumped-parameter compliance matrix was presented as a novel computationally efficient approach for modelling tibiofemoral joint function. Passive to active compliance matrices derived from modelling and representing tibiofemoral elasticity from passive knee structures during walking were analysed based on flexion and gait cycle percentages. These matrices were compared to ex vivo matrices, while passive to active motion differences from the mode were compared with the differences between ex vivo passive motion (Chapter 4) and with biplanar fluoroscopy measurements in vivo (Martelli et al., 2020). This approach demonstrated with a state-of-the-art anatomically detailed validated musculoskeletal model (Lenhart et al., 2015), predicting the same tibiofemoral motion in less time.

First and foremost, a limitation of this study is the fact that during the swing phase of the gait cycle, the joint is not under load, hence compliance should not be considered and/or analysed; therefore, the results were only reported for the stance phase of the gait cycle. The study of the passive to active compliance analysis revealed that the flexion angle has an overall impact on the compliance of the majority of secondary degrees of freedom, except for AP translation, which is more effectively described as a function of the different stages of the gait cycle. Compliance was the highest in AP direction, which is supported by other evidence to reflect the current discrepancies between experimental motion and geometry-based models (Martelli et al., 2020). Rotational compliance of AA and IE were function of the flexion angle, while no trend is observed when the compliance was plotted against gait cycle percentage; conversely, compliance, in particular in AP, while depending on flexion, had a stronger relationship with gait cycle phases.

The magnitude of the values of compliance obtained with the passive to active CMs were comparable with ex vivo CMs (Lamberto et al., 2016). Furthermore, passive to active tibiofemoral motion differences were comparable to difference between experimentally measured passive motion and active tibiofemoral kinematics, providing credibility to this approach and to the use of compliance matrices to represent the elasticity or change in cross contribution of individual articular surfaces and the ligament constraints. As rationale, proof of concept and for future investigation of active tibiofemoral function elasticity and variability in individuals, the unloaded passive knee envelope previously measured from cadavers was compared to measurements of active tibiofemoral motion from literature. As a result of this analysis, we have also gained insight into how ligaments and soft tissues constrain the movement of the joints, including how they make a small but important contribution towards an active function, especially during the stance phase and the early swing. The study findings suggest that the variability of the unloaded envelope outweighs the differences observed between passive and active motion for rotations, indicating that ligament elasticity may not be a major contributing factor to these differences. However, in the case of translation, where the envelope differences are comparable to the differences between passive and active motion, the ligaments may have a minor or negligible contribution to the active

function. While ligament elasticity may contribute to the observed differences, it is important to note that muscle activity also plays a role in overall elasticity. Therefore, the study suggests that ligament elasticity may play a role, likely as a minor determinant rather than being the sole determinant, and the involvement of muscles should be considered. Nevertheless, it is important to acknowledge that there are limitations. One of the main is that the experimental data and simulation data come from different populations; the fluoroscopy data (Martelli et al., 2020) used for comparison were not acquired for the same subjects/population of the experimental passive motion data (cadaveric study – Chapter 4). Furthermore, the simulation data represented a singular subject. Despite these limitations, this comparison provides valuable insights into the performance and limitations of the simulation.

This study presents a fast and viable method to characterize the in vivo tibiofemoral elasticity and load-dependent behaviour of the knee during physical activity. The methodology was demonstrated using a rigid knee model based on Lenhart, including custom splines derived from passive kinematics to achieve active knee behaviour (kinematics, forces/moments at the knee) using all calculated matrices. A sensitivity analysis was performed to determine the required number of compliance matrices for maintaining relatively good accuracy, with at least 4 matrices deemed necessary. As the number of matrices used increased, the error diminished, leading to a more accurate active simulation from a passive rigid model. The computational time for producing active simulations ranged from minutes to seconds, depending on the number of matrices simulated. The results highlight the trade-off between computational efficiency and accuracy, with a higher number of matrices leading to a more precise representation of active knee behaviour.

A number of necessary assumptions were made, and limitations were present in this study. The assumption of linear stiffness/compliance in the model was intentionally made to simplify the analysis and implementation, allowing for a computationally efficient approach. While the results demonstrate a nonlinear pattern, it is essential to consider that the primary objective of this study was to investigate the elastic linear contribution of ligaments and muscles. By assuming linearity, the model becomes relatively easy to input individual elastic parameters or coefficients of compliance, which can be derived from in vivo measurements. Using a nonlinear fit to the data would undoubtedly provide a more accurate representation of the compliance behaviour. However, it would significantly increase the computational complexity and time required for the simulations, making the approach less practical for the specific scope of this study. Therefore, the decision to use linear approximation was driven by the need to balance accuracy with computational efficiency, aligning with the objectives of the research. For the purposes of this study, the linear approximation was considered sufficient to demonstrate the feasibility of the methodology and its potential applications, particularly in relation to investigating elastic linear contributions in joint function. While acknowledging the limitation of linearity, further research and analysis could explore the use of nonlinear fits for more detailed investigations, but it would

come with added computational costs and complexity, which may not align with the primary goals of this study. Another crucial assumption is related to the estimation of compliance matrices. Typically, compliance matrices are derived from ex vivo cadaveric specimens through optimization of loads and displacements in loading rigs. However, it should be noted that this process of estimating compliance matrices ex vivo in cadaveric specimens is distinct from the passive to active musculoskeletal-based compliance matrices utilized in our study. Therefore, additional caution shall be taken when comparing ex vivo matrices with passive to active MSK-based compliance matrices. Furthermore, it was necessary, and generally is necessary, to make these assumptions in order to effectively demonstrate the methodology and evaluate the joint response to various activities. By making these assumptions, we were able to establish a framework for analysing the joint response and gain insights into its behaviour during different activities. However, it is crucial to acknowledge that, as discussed in Chapter 5, the process of modelling inherently introduces uncertainties and errors due to the various assumptions made. While we recognize the limitations and potential errors associated with these assumptions, they are inevitable in the modelling process. In order to effectively demonstrate the methodology and evaluate the joint response in passive conditions the following assumptions were necessary. The parameter changes made to achieve passive behaviour in the simulation of tibiofemoral motion are essential assumptions with certain limitations. Scaling down external forces, setting gravity to zero, and removing knee-spanning muscles were necessary steps to create a scenario where the knee joint behaves passively. However, due to mathematical constraints, some internal forces persisted within the joint. To address this, ligament stiffness was reduced by 50% to minimize their contribution and mimic unloaded passive knee motion. These assumptions, while helping to approximate passive behaviour, may not precisely replicate true passive motion scenarios, and further refinements could be explored in future studies.

Secondarily, gait alone was investigated while other motor tasks involving a greater range of motion and different joint forces, i.e., running or squatting, may present different CM analyses and sensitivities. Moreover, to prove the validity of this prediction, further studies must be conducted. A third limitation is that the results reported here are based on data from one subject representative of a healthy population; therefore, caution must be utilized when comparing these results with data from populations or from subjects suffering from pathologies. Concerning any clinical application caution must be exercised as this proof of concept requires more extensive verification and validation processes. Data from ex vivo studies, in-silico modelling and active tibiofemoral functional measurements were gathered to prove the concept of the elasticity and to provide credibility towards this novel approach to joint modelling. Further research could provide the inclusion of elasticity through individual compliances from ex vivo testing and/or combined with experimental passive motion through the splines to represent individual geometry, for the tibiofemoral function investigation.

While this study successfully demonstrated the methodology and feasibility of using compliance matrices to predict kinematics based on forces in a computationally efficient manner, there are several areas for future research to explore. Different assumptions and approaches are required to model passive and active knee conditions, and the role of ligaments in contributing to these states and the transition between them is not well understood. This raises questions about the best modelling approach for this complexity. The modelling of ligament elasticity and its contribution to load transfer lacks consistency, and the actual role of ligaments in providing elasticity is uncertain. There is a need to investigate the contribution of ligaments compared to other passive and active soft tissues. The discrepancy between fluoroscopy-based measurements and geometry-based models suggests the influence of knee joint elasticity, including ligaments and other soft tissue constraints. However, current modelling approaches are time-consuming, computationally expensive, and lack individual variability and clinical translation. Further research is needed to explore the variability in tibiofemoral joint elasticity in population studies and its application in diagnosing knee joint pathologies and treatments. This study has laid the foundation for a novel approach to investigate tibiofemoral joint function. However, future work should concentrate on incorporating experimental data for force inputs and exploring the inclusion of experimental data to study individual variations and population variability. By addressing these aspects, this methodology can provide valuable insights into the elastic behaviour of the knee joint. Furthermore, this methodology has the potential to be applied in studying the effects of various surgical interventions or pathologies on tibiofemoral joint function. In practical implementations of this approach, it would be advantageous to utilize data from experimental measurements obtained ex vivo or in vivo to acquire forces. For example, data from hexapod robot testing of cadaveric knees (Lamberto et al., 2016; Lambert et al., 2019), or even better, in vivo non-invasive knee joint laxity measurements in living individuals, could be utilized to provide the necessary force inputs for the model (Pedersen et al., 2019). By incorporating such experimental data, it would be possible to predict individual-specific tibiofemoral kinematics and compliance behaviour, enabling a more personalized and patient-specific analysis. This approach holds the potential to expand into clinical analysis. Additionally, by modifying the compliance matrices to reflect changes in ligament or soft tissue properties resulting from surgery or injury, it would be feasible to simulate the impact on joint mechanics and explore potential treatment options. Compliance matrices have shown the ability to capture variations in laxity induced by pathologies or injuries (Lambert et al., 2019). Thus, this approach has the potential to reveal the complicated relationship between knee loading and kinematics in healthy, pathologic, and repaired populations. This approach was applied to the tibiofemoral joint, however, conceptually it could be applied to the investigation and modelling of other joints.

Chapter 7

CONCLUSIONS

Principal Findings, Conclusions And Future Directions

CONTENTS

7.1 Principal Findings

The overall objective of this research was to advance understanding of and develop methods for assessing inter-subject variability of tibiofemoral passive and active joint function. **There is high variability of healthy tibiofemoral function among individuals** that has long been recognized. Quantification and understanding of this variability are challenging due to fragmented information, the many factors at play, and the lack of suitable approaches. In this thesis, the principal findings include new methodologies and population studies combined to achieve the aims of this work. This study also provides the framework for a deeper understanding of tibiofemoral ligaments, the role that they play in both passive and active functions, as well as during the transition from passive-to-active function.

As tibiofemoral joint mechanics depends on three main factors, the geometry of the articular surfaces, passive motion characteristics, and muscle loading (Blankevoort et al., 1988), it is crucial to investigate the inter-subject variability of each of these singular factors and their concomitant variations across populations. This was the aim of the wider Virtual Human Knee project of which this research is part. In particular, the VHK aimed at investigating the effect of concomitant variation of anatomy and laxity on the knee function during normal physical activities in a healthy adult population. The principal findings of this thesis and the wider research associated to it will be therefore reported following this structure.

7.1.1 Tibiofemoral Articular Surfaces And Function

As the anatomy helps to perform the function, many studies have reported high anatomical variability among individuals, primarily utilizing statistical shape models to comprehensively assess both the extent of this variability independently, and the broader impact of anatomical variation on the tibiofemoral joint function (Clouthier et al., 2019; Rao et al., 2013; Smoger et al., 2015). A statistical shape-kinematics model of the tibiofemoral joint was built based on the data generated from this research and it is presented in ***Appendix E.*** In this study, the model is used to investigate the relationship between main anatomical variation of the tibiofemoral joint and the kinematics; the element of novelty in comparison with studies present in literature are (1) the investigation of a passive motion task (2) in males and females and (3) the potential causality of inter-subject anatomical variability in determining the motion and therefore the function with a partial least squares regression model (O'Rourke et al., 2023). The primary drivers of kinematic variations, particularly in the AP direction, were the first three PLS components (PLS1, 2, 3), which captured geometric changes in articular surface congruency. Further variations in femoral condyle width, intercondylar space, tibia plateau size and conformity, and tibia eminences heights contributed to the explanation of internal-external rotation variations (PLS2, 4). Finally, the

overall size of the knee appeared to have the greatest influence on abduction-adduction motion, while also having some impact on internal-external rotation.

Statistical shape models rely on segmentations of extensive data sets of knee medical imaging. Even though imaging techniques have advanced, and geometry extraction processes have become more automated, facilitating, and reducing the effort of developing models from CTs and MRIs, the entire process remains extremely time-consuming (Kaur et al., 2021). ***Appendix E*** of this thesis presents a novel algorithm, texture enhanced statistical region merging, applied to automatic segmentation of knee bone segmentation from CTs (Howes et al., 2021). Performance metrics comparisons with existing literature demonstrated that this methodology competes with the best currently available tools (Wu et al., 2014).

7.1.2 Tibiofemoral Ligaments, Passive Soft Tissues And Function

In the absence of force, articular surfaces, including bones and cartilage topography, guide knee passive motion by acting as purely geometrical constraints. This results in high sensitivity to small forces (i.e., changes in the set-up), that lead to high variability of the tibiofemoral passive motion when investigating a central flexion path, as within the unloaded knee passive motion envelope (Wilson et al., 2000). Tibial and femoral articular bony interfaces may require the input of soft tissue structures to prevent excessive TF motion when load is applied. Among these, ligaments mainly restrain abnormal movements and ensure stability, defined as joint paths offering minimum resistance to motion. The contributions of these structures appear to be limited to controlling excessive motion under non-physiological loads and being involved in normal physical activities solely when the force is not perpendicular. It is clear from literature that ligaments and articular geometries of the knee create secondary coupled motion constraints in the flexion-extension path, as well as an envelope of motion that is typically described in terms of laxity as a function of flexion angle. Ex vivo cadaveric studies are typically more accurate than in vivo approaches and are divided in two categories generally either assessing knee laxity, each degree of freedom separately (Blankevoort et al., 1988; Cyr and Maletsky 2014; Roth et al., 2015), or the secondary degrees-of-freedom coupling of a nominal unloaded central path of flexion within the envelope (Belvedere et al., 2011; Wilson et al., 2000; Wunshel et al., 2012). As of now, no ex vivo approach combined the investigation of multiple passive flexion paths, envelope, and related laxity. Further, as part of TKR to achieve gap balancing, associated with surgical navigation characteristic parallel tracking, stressed flexion-extension tests are performed by applying lateral and medial forces to the distal tibia (Bottros et al., 2006; Sheth et al., 2017); as of now, these tests have not been considered or included in currently available protocols. In addition, in these studies, analysis and quantifications of errors and uncertainties are rare (Goldsmith et al., 2014; Wilson et al., 2000), with the majority presenting solely a qualitative discussion of the limitations of the methodologies, or the manufacturer reported accuracy of the devices used, thereby complicating

the understanding of these discrepancies and the comparison between different passive motion studies (Hacker et al., 2016). Therefore, the aim of the ***first study*** was to accurately quantify multiple couple paths and relate them to the envelope of knee passive motion. The novel methodology quantified and captured, two varus valgus tibiofemoral passive flexion paths, medial and lateral extremes of unloaded envelope in 6 DoFs cadaveric intact knee specimens. From the analysis of errors-uncertainties, it emerges that this protocol could and should be used to investigate the individual tibiofemoral passive motion. Consistency, low errors, good reliability, and results were comparable to previous investigations. **The unloaded knee passive motion envelope is characterized by reliable and consistent medial and lateral extremes, varus and valgus coupled tibiofemoral flexion paths.**

In order to quantify inter-subject variability of the knee passive motion, measurements of these unloaded passive motion envelope extremes in a healthy cohort of thirty specimens, for both males and females, were performed using the ex vivo approach developed. As the influence of sex on the knee function is an ongoing and still open debate, differences between males and females were investigated. Literature studies reveal contrasting results, some confirming (Gillespie et al., 2011) and some disproving (Asseln et al., 2018) the existence of sex-based dimorphisms of knee anatomy. The results of in vivo investigations of sex-based differences in tibiofemoral joint mechanics varied considerably, some showing no differences (Tanikawa et al., 2013) and others showing statistically significant differences varying from study to study (Cronström et al., 2016). The accurate quantification of the extent of the envelope of the knee passive motion and its variability across populations are scarce, and limited to male populations, thereby leaving the influence of sex on knee passive motion open for debate; higher incidence of injuries, pathologies, and worse treatment outcomes among females remains unexplained. In the ***second study***, this novel methodology was therefore used to quantitatively measure the variability across a healthy adult population and to investigate the influence of sex (specimen-specific passive motion is presented in ***Appendix C***). **As a whole, sex has minor influence on the knee passive motion envelope, and its significance is limited to medial abduction; individual variability was higher than any differences between male and female in all DoFs and both extremes.** Therefore, knee interventions should be geared towards personalisation, rather than sex-specific solutions, since individual variability was high, while sex differences negligible or minor.

Moreover, the knee passive motion is guided by the geometry of articular surfaces, and as such, its variability should be determined by concomitant variation of anatomical features. As such further insight into the differences of the tibiofemoral function due to sex could be provided using the statistical shape-kinematic tibiofemoral model presented in the previous section, to investigate anatomical variability, sex-based motion differences and their relationship (**Appendix E**).

Originally designed for healthy knees, the ex vivo approach developed was suitable for knee passive motion assessments of injured and pathological knees; as the problem of understanding and quantifying the individual variability of the tibiofemoral function affects the ability to restore it with surgeries, a feasibility study before and after knee replacement was successfully conducted using the novel ex vivo methodology in **Appendix C**. This method provides a valid tool to accurately assess motion differences pre-op, post-op and between liners. To provide generalizable results, more work will be required. Ideally, the aim would be a potential clinical translation of the presented methodology to predict the individual extremes of unloaded passive motion envelope based on shape through the statistical kinematic shape model, assess the pathological motion, and try to restore the predicted native motion through surgical pre-planning, i.e. cutting guides, choice of the implant and liner, and total knee replacement procedure, to recreate this target motion, with the aim of repristinating the lost individual function and improving outcome of the knee arthroplasty.

At the foundation of the tibiofemoral function, there is the mechanical role of ligaments. The ***hypotheses*** within passive knee motion envelopes: ligaments do not significantly influence tibiofemoral path, when recruited act as constraints defining envelope boundaries, and outside, provide a mild elastic response through their individual stiffness and combined action. These first two hypotheses were verified by the high susceptibility of the tibiofemoral path within the envelope of knee passive motion, and by the presence of reliable and robust medial and lateral extremes of the unloaded knee passive motion envelope, within which all the central flexion paths lie. Through literature, it has been found that there is a small discrepancy between experimental active measurements in vivo, compared to modelling the TF function on individual geometry of the articular surfaces with a rigid passive joint and active structures, and it is attributed to knee elasticity. Therefore, it was hypothesised that (3) ligaments, when recruited outside the envelope, provide a modest but crucial elastic contribution, leaving muscles as major contributors for the overall knee elasticity observed. As part of the evaluation of this hypothesis, the unloaded envelope of passive motion (**Chapter 4**), within which no ligament work should be expected, was compared with in vivo measurements of the active tibiofemoral joint motion (Martelli et al., 2020). The unloaded envelope differences were found larger than differences between passive to active motion for both rotations, where ligaments appear not to contribute towards; however, envelope differences were found comparable to the differences between passive to active motion, with ligaments appearing to provide a minor or negligible contribution towards the active function.

7.1.3 Tibiofemoral Muscles, Active Structures And Function

Currently anatomically detailed tibiofemoral models, which enable the study of active ligament contributions during normal exercise, are computationally expensive and time-consuming; the investigation of the variability of tibiofemoral elastic responses across populations is scarce. A

mapping review was conducted on cost complexity utility perspective, presented in ***Chapter 5,*** and provided the framework for the range of models available in-silico to investigate elasticity in a population. This review highlighted how anatomically detailed MSK models of the individual tibiofemoral joint, capable of predicting individual elastic response and investigating the contribution of ligaments during activities, are complex, computationally expensive, and time-consuming, thus, not allowing for population studies. As a result, the function of the tibiofemoral joint within individuals, its variability across populations, and the role played by ligaments in those, has not been fully understood yet. One possibility is to model the effect of tibiofemoral geometry on knee motion using fast rigid-body models (Martelli et al., 2020), and the tibiofemoral elastic response using 6x6 lumped-parameters compliance matrices accounting for the effect of all separate elastic structure (Lamberto et al., 2019). Therefore, the ***third study*** of this thesis was the development of a computationally efficient elastic knee joint musculoskeletal model. This study presented also for the first-time compliance matrices from passive to active tibiofemoral function, and their analysis based on flexion and gait cycle stage. **Compliance matrices provided an efficient representation of tibiofemoral elasticity, a modelling bridge between passive and active tibiofemoral function in musculoskeletal models, without explicit structure representation.** Future work is required to extend the application of this methodology to a population analysis for the investigation of the inter-subject variability of the tibiofemoral function elasticity. A potential benefit of this method is that compliance values/stiffness from in vivo laxity testing can be included. The present method can be used to examine the effects of concomitant variations in anatomy and laxity on tibiofemoral mechanics, through the use of these matrices. These models could potentially embed subject-specific anatomy (provided by the statistical shape model), specimen-specific tibiofemoral passive motion joint (through a novel ex vivo approach), and embed laxity measurements, already obtained with the hexapod within the VHK project on the same population and investigate their relationship with tibiofemoral function during normal physical activities.

7.2 Conclusions And Future Directions

The knee research community is currently exploring the interactions between ligament structures, articular surfaces, and muscles, both passively and actively, within the tibiofemoral structure, as well as how these interactions differ across populations. The research results of this study have direct implications, both in terms of implant design, ligament reconstruction, rehabilitation, therapy, and prevention of both knee ligament and joint injuries, as well as regarding training and targeted exercise, for implant design, ligament reconstruction, rehabilitation, treatment, and prevention. The generation of novel knowledge and technology could predict categories more at risk, i.e., females, improve future knee ligament reconstruction methods, provide an insight into

osteoarthritis causes, development, and treatment, and improve the outcomes of knee replacement. Finally, a growing interest is being shown in developing in silico musculoskeletal models for clinical applications, towards which this research directly contributes to making their generation easier and providing faster fruition.

The further investigations prompted by this thesis have demonstrated the relevance of this research: (1) a study on the relationship between geometry and function has already been conducted by integrating the experimental data in a statistical shape model of the tibiofemoral joint, and it is reported in the appendices (**Appendix E**); (2) within a separate project investigating total knee replacement, the use of the ex vivo approach developed, has been used to investigate the restoration of the individual function before and after total knee replacement.

As direct continuation of this research, to provide more accurate information on the variability of the tibiofemoral elasticity among individuals, the novel elastic knee joint model could be used for its investigation in a healthy population. To this end, further understanding and insight could be provided by using the adult population investigated for the passive motion study. In particular, the individual passive motion could be inserted into generic lower limb scaled musculoskeletal models, along with their individual compliance matrices from hexapod testing (already carried out), to estimate the tibiofemoral elasticity and its variability in a healthy adult population. Moreover, the differences in elasticity between males and females could be investigated. Further research could be done by extending the use of the novel ex vivo methodology to investigate the joint restoration in a population, or to investigate different implants and inserts.

Further work has already been planned relative to, (1) the experimental individual TF passive motion is currently in use for validation of kinematic models; (2) research is in progress concerning the application of all these models and approaches, in studying the effect of tibial osteotomy.

References

REFERENCES

Abdel-Rahman, E. M., & Hefzy, M. S. (1998). Three-dimensional dynamic behaviour of the human knee joint under impact loading. Medical engineering & physics, 20(4), 276-290.

Adouni, M., Faisal, T. R., & Dhaher, Y. Y. (2020). Computational frame of ligament in situ strain in a full knee model. Computers in Biology and Medicine, 126, 104012.

Ahmed, A. M., Burke, D. L., Duncan, N. A., & Chan, K. H. (1992). Ligament tension pattern in the flexed knee in combined passive anterior translation and axial rotation. Journal of Orthopaedic Research, 10(6), 854-867.

Aljehani, M. S., Christensen, J. C., Snyder-Mackler, L., Crenshaw, J., Brown, A., & Zeni Jr, J. A. (2022). Knee biomechanics and contralateral knee osteoarthritis progression after total knee arthroplasty. Gait & Posture, 91, 266-275.

Amiri, S., Cooke, D., Kim, I. Y., & Wyss, U. (2006). Mechanics of the passive knee joint. Part 1: the role of the tibial articular surfaces in guiding the passive motion. Proceedings of the Institution of Mechanical Engineers, Part H: Journal of Engineering in Medicine, 220(8), 813-822.

Amiri, S., Cooke, D., Kim, I. Y., & Wyss, U. (2007). Mechanics of the passive knee joint. Part 2: interaction between the ligaments and the articular surfaces in guiding the joint motion. Proceedings of the Institution of Mechanical Engineers, Part H: Journal of Engineering in Medicine, 221(8), 821-832.

Amis, A. A., Bull, A. M. J., Farahmand, F., Senavongse, W., & Shih, Y. F. (2004). Patellofemoral joint biomechanics. Patellofemoral disorders: diagnosis and treatment, 37-53.

Andersen, M. S., Benoit, D. L., Damsgaard, M., Ramsey, D. K., & Rasmussen, J. (2010). Do kinematic models reduce the effects of soft tissue artefacts in skin marker-based motion analysis? An in vivo study of knee kinematics. Journal of biomechanics, 43(2), 268-273.

Anderson, F. C., & Pandy, M. G. (1999). A dynamic optimization solution for vertical jumping in three dimensions. Computer methods in biomechanics and biomedical engineering, 2(3), 201-231.

Anderson, A. F., Snyder, R. B., Federspiel, C. F., & Lipscomb, A. B. (1992). Instrumented evaluation of knee laxity: a comparison of five arthrometers. The American journal of sports medicine, 20(2), 135-140.

Anderson, F. C., & Pandy, M. G. (2001). Dynamic optimization of human walking. J. Biomech. Eng., 123(5), 381-390.

Anderson, F. C., & Pandy, M. G. (2001). Static and dynamic optimization solutions for gait are practically equivalent. Journal of biomechanics, 34(2), 153-161.

Andriacchi, T. P., Mikosz, R. P., Hampton, S. J., & Galante, J. O. (1983). Model studies of the stiffness characteristics of the human knee joint. Journal of biomechanics, 16(1), 23-29.

Andriacchi, T. P., Alexander, E. J., Toney, M. K., Dyrby, C., & Sum, J. A. (1998). A point cluster method for in vivo motion analysis: applied to a study of knee kinematics. Journal of biomechanical engineering, 120(6), 743-749.

Arnold, E. M., Ward, S. R., Lieber, R. L., & Delp, S. L. (2010). A model of the lower limb for analysis of human movement. Annals of biomedical engineering, 38(2), 269-279.

Arnoux, P. J., Subit, D., Masson, C., Chabrand, P., & Brunet, C. (2005). Knee ligaments mechanics: From experiments to FE simulations. Revue Européenne des Eléments, 14(4-5), 577-600.

Asaeda, M., Deie, M., Kono, Y., Mikami, Y., Kimura, H., & Adachi, N. (2019). The relationship between knee muscle strength and knee biomechanics during running at 6 and 12 months after anterior cruciate ligament reconstruction. Asia-Pacific journal of sports medicine, arthroscopy, rehabilitation and technology, 16, 14-18.

Ascani, D., Mazzà, C., De Lollis, A., Bernardoni, M., & Viceconti, M. (2015). A procedure to estimate the origins and the insertions of the knee ligaments from computed tomography images. Journal of biomechanics, 48(2), 233-237.

Asseln, M., Hänisch, C., Schick, F., & Radermacher, K. (2018). Gender differences in knee morphology and the prospects for implant design in total knee replacement. The Knee, 25(4), 545-558.

Athwal, K. K., Hunt, N. C., Davies, A. J., Deehan, D. J., & Amis, A. A. (2014). Clinical biomechanics of instability related to total knee arthroplasty. Clinical Biomechanics, 29(2), 119-128.

Audenaert, E. A., Pattyn, C., Steenackers, G., De Roeck, J., Vandermeulen, D., & Claes, P. (2019). Statistical shape modelling of skeletal anatomy for sex discrimination: their training size, sexual dimorphism, and asymmetry. Frontiers in bioengineering and biotechnology, 7, 302.

Australian Institute of Health and Welfare. (2020). Osteoarthritis. Retrieved from https://www.aihw.gov.au/reports/chronic-musculoskeletal-conditions/osteoarthritis

Baldon, R. D. M., Lobato, D. F., Furlan, L., & Serrão, F. (2013). Gender differences in lower limb kinematics during stair descent. Journal of applied biomechanics, 29(4), 413-420.

Baldwin, M. A., Laz, P. J., Stowe, J. Q., & Rullkoetter, P. J. (2009). Efficient probabilistic representation of tibiofemoral soft tissue constraint. Computer methods in biomechanics and biomedical engineering, 12(6), 651-659.

Baldwin, M. A., Clary, C. W., Fitzpatrick, C. K., Deacy, J. S., Maletsky, L. P., & Rullkoetter, P. J. (2012). Dynamic finite element knee simulation for evaluation of knee replacement mechanics. Journal of biomechanics, 45(3), 474-483.

Barink, M., Kampen, A. V., Malefijt, M. D. W., & Verdonschot, N. (2005). A three-dimensional dynamic finite element model of the prosthetic knee joint: simulation of joint laxity and kinematics. Proceedings of the Institution of Mechanical Engineers, Part H: Journal of Engineering in Medicine, 219(6), 415-424.

Barry, M. J., Kwon, T. H., & Dhaher, Y. Y. (2010, December). Probabilistic musculoskeletal modelling of the knee: A preliminary examination of an ACL-reconstruction. In 2010 Annual International Conference of the IEEE Engineering in Medicine and Biology (pp. 5440-5443). IEEE.

Behan, F. P., Maden-Wilkinson, T. M., Pain, M. T., & Folland, J. P. (2018). Sex differences in muscle morphology of the knee flexors and knee extensors. PLoS One, 13(1), e0190903.

Beidokhti, H. N., Janssen, D., van de Groes, S., Hazrati, J., Van den Boogaard, T., & Verdonschot, N. (2017). The influence of ligament modelling strategies on the predictive capability of finite element models of the human knee joint. Journal of biomechanics, 65, 1-11.

Bellemans, J., Carpentier, K., Vandenneucker, H., Vanlauwe, J., & Victor, J. (2010). The John Insall Award: both morphotype and gender influence the shape of the knee in patients undergoing TKA. Clinical Orthopaedics and Related Research®, 468(1), 29-36.

Belvedere, C., Leardini, A., Giannini, S., Ensini, A., Bianchi, L., & Catani, F. (2011). Does medio-lateral motion occur in the normal knee? An in-vitro study in passive motion. Journal of biomechanics, 44(5), 877-884.

Bendjaballah, M. Z., Shirazi-Adl, A., & Zukor, D. J. (1998). Biomechanical response of the passive human knee joint under anterior-posterior forces. Clinical Biomechanics, 13(8), 625-633.Bendjaballah, M., Shirazi-Adl, A., & Zukor, D. J. (1997). Finite element analysis of human knee joint in varus-valgus. Clinical biomechanics, 12(3), 139-148.

Benjaminse, A., Gokeler, A., Fleisig, G. S., Sell, T. C., & Otten, B. (2011). What is the true evidence for gender-related differences during plant and cut maneuvers? A systematic review. Knee Surgery, Sports Traumatology, Arthroscopy, 19(1), 42-54.

Biden, E., O'Connor, J., & Goodfellow, J. (1984, February). Tibial rotation in the cadaver knee. In Transactions of the 30th Meeting of the Orthopaedic Research Society (Vol. 30).

Blackburn, J. T., Bell, D. R., Norcross, M. F., Hudson, J. D., & Kimsey, M. H. (2009). Sex comparison of hamstring structural and material properties. Clinical Biomechanics, 24(1), 65-70.

Blankevoort, L., & Huiskes, R. (1991). Ligament-bone interaction in a three-dimensional model of the knee.

Blankevoort, L., Huiskes, R., & De Lange, A. (1988). The envelope of passive knee joint motion. Journal of biomechanics, 21(9), 705-720.

Boguszewski, D. V., Cheung, E. C., Joshi, N. B., Markolf, K. L., & McAllister, D. R. (2015). Male-female differences in knee laxity and stiffness: a cadaveric study. The American journal of sports medicine, 43(12), 2982-2987.

Bottros, J., Gad, B., Krebs, V., & Barsoum, W. K. (2006). Gap balancing in total knee arthroplasty. *The Journal of arthroplasty*, *21*(4), 11-15.

Bradley, J., FitzPatrick, D., Daniel, D., Shercliff, T., & O'Connor, J. (1988). Orientation of the cruciate ligament in the sagittal plane. A method of predicting its length-change with flexion. The Journal of Bone & Joint Surgery British Volume, 70(1), 94-99.

Branch, T. P., Stinton, S. K., Siebold, R., Freedberg, H. I., Jacobs, C. A., & Hutton, W. C. (2017). Assessment of knee laxity using a robotic testing device: a comparison to the manual clinical knee examination. Knee Surgery, Sports Traumatology, Arthroscopy, 25(8), 2460-2467.

Bredbenner, T. L., Eliason, T. D., Potter, R. S., Mason, R. L., Havill, L. M., & Nicolella, D. P. (2010). Statistical shape modelling describes variation in tibia and femur surface geometry between Control and Incidence groups from the osteoarthritis initiative database. Journal of biomechanics, 43(9), 1780-1786.

Bull, A. M., Kessler, O., Alam, M., & Amis, A. A. (2008). Changes in knee kinematics reflect the articular geometry after arthroplasty. Clinical orthopaedics and related research, 466, 2491-2499.

Burton II, W., Myers, C., & Rullkoetter, P. (2020). Semi-supervised learning for automatic segmentation of the knee from MRI with convolutional neural networks. Computer Methods and Programs in Biomedicine, 189, 105328.

Camomilla, V., Dumas, R., & Cappozzo, A. (2017). Human movement analysis: The soft tissue artefact issue. Journal of biomechanics, 62, pp-1.

Cannon, W. D. (2002). Use of arthrometers to assess knee laxity and outcomes. Sports Medicine and Arthroscopy Review, 10(3), 191-200.

Chandrashekar, N., Mansouri, H., Slauterbeck, J., & Hashemi, J. (2006). Sex-based differences in the tensile properties of the human anterior cruciate ligament. Journal of biomechanics, 39(16), 2943-2950.

Chen, Z., Zhang, Z., Wang, L., Li, D., Zhang, Y., & Jin, Z. (2016). Evaluation of a subject-specific musculoskeletal modelling framework for load prediction in total knee arthroplasty. Medical engineering & physics, 38(8), 708-716.

Clary, C. W. (2006). Design and validation of a knee-loading rig to perform clinical injury assessments in vitro (Doctoral dissertation, University of Kansas).

Clouthier AL, Smith CR, Vignos MF, et al. (2019). The effect of articular geometry features identified using statistical shape modelling on knee biomechanics. Medical Engineering & Physics 66:47-55.

Conconi, M., Pompili, A., Sancisi, N., & Parenti-Castelli, V. (2021). Quantification of the errors associated with marker occlusion in stereophotogrammetric systems and implications on gait analysis. Journal of Biomechanics, 114, 110162.

Conconi, M., Sancisi, N., & Parenti-Castelli, V. (2018). Subject-specific model of knee natural motion: A non-invasive approach. In Advances in Robot Kinematics 2016 (pp. 255-264). Springer, Cham.

Conconi, M., Sancisi, N., & Parenti-Castelli, V. (2020). Prediction of Individual Knee Kinematics from an MRI Representation of the Articular Surfaces. IEEE Transactions on Biomedical Engineering, 68(3), 1084-1092.

Conley, S., Rosenberg, A., & Crowninshield, R. (2007). The female knee: anatomic variations. JAAOS-Journal of the American Academy of Orthopaedic Surgeons, 15, S31-S36.

Cooper, R. J., Wilcox, R. K., & Jones, A. C. (2019). Finite element models of the tibiofemoral joint: A review of validation approaches and modelling challenges. Medical engineering & physics, 74, 1-12.

Cristiani, R., Engström, B., Edman, G., Forssblad, M., & Stålman, A. (2019). Revision anterior cruciate ligament reconstruction restores knee laxity but shows inferior functional knee outcome compared with primary reconstruction. Knee Surgery, Sports Traumatology, Arthroscopy, 27, 137-145.

Cronström, A., Creaby, M. W., Nae, J., & Ageberg, E. (2016). Gender differences in knee abduction during weight-bearing activities: A systematic review and meta-analysis. Gait & posture, 49, 315-328.

Curreli, C., Di Puccio, F., Davico, G., Modenese, L., & Viceconti, M. (2021). Using Musculoskeletal Models to Estimate in vivo Total Knee Replacement Kinematics and Loads: Effect of Differences

Cyr, A. J., & Maletsky, L. P. (2014). Unified quantification of variation in passive knee joint constraint. Proceedings of the Institution of Mechanical Engineers, Part H: Journal of Engineering in Medicine, 228(5), 494-500.

Cyr, A. J., Shalhoub, S. S., Fitzwater, F. G., Ferris, L. A., & Maletsky, L. P. (2015). Mapping of contributions from collateral ligaments to overall knee joint constraint: an experimental cadaveric study. Journal of Biomechanical Engineering, 137(6).

Daniel, D. M. (1991). Assessing the limits of knee motion. The American Journal of Sports Medicine, 19(2), 139-147.

Daniel, D. M., Malcom, L. L., Losse, G., Stone, M. L., Sachs, R., & Burks, R. (1985). Instrumented measurement of anterior laxity of the knee. JBJS, 67(5), 720-726.

Dargel, J., Michael, J. W., Feiser, J., Ivo, R., & Koebke, J. (2011). Human knee joint anatomy revisited: morphometry in the light of sex-specific total knee arthroplasty. The Journal of arthroplasty, 26(3), 346-353.

Delp, S. L. (1990). Surgery simulation: a computer graphics system to analyze and design musculoskeletal reconstructions of the lower limb. Stanford University.

Delp, S. L., Anderson, F. C., Arnold, A. S., Loan, P., Habib, A., John, C. T., ... & Thelen, D. G. (2007). OpenSim: open-source software to create and analyze dynamic simulations of movement. IEEE transactions on biomedical engineering, 54(11), 1940-1950.

DeVita, P., Aaboe, J., Bartholdy, C., Leonardis, J. M., Bliddal, H., & Henriksen, M. (2018). Quadriceps-strengthening exercise and quadriceps and knee biomechanics during walking in knee osteoarthritis: a two-centre randomized controlled trial. Clinical Biomechanics, 59, 199-206.

Dejtiar, D. L., Dzialo, C. M., Pedersen, P. H., Jensen, K. K., Fleron, M. K., & Andersen, M. S. (2020). Development and evaluation of a subject-specific lower limb model with an eleven-degrees-of-freedom natural knee model using magnetic resonance and biplanar X-ray imaging during a quasi-static lunge. Journal of biomechanical engineering, 142(6), 061001

Duda, G. N., Brand, D., Freitag, S., Lierse, W., & Schneider, E. (1996). Variability of femoral muscle attachments. Journal of biomechanics, 29(9), 1185-1190.

Dyrby, C. O., & Andriacchi, T. P. (2004). Secondary motions of the knee during weight bearing and non-weight bearing activities. Journal of Orthopaedic Research, 22(4), 794-800.

Dzialo, C. M. (2018). Personalized musculoskeletal modelling: Bone morphing, knee joint modelling, and applications.

Eagar, P., Hull, M. L., & Howell, S. M. (2001). A method for quantifying the anterior load–displacement behaviour of the human knee in both the low and high stiffness regions. Journal of Biomechanics, 34(12), 1655-1660.

Erdemir, A., Guess, T. M., Halloran, J., Tadepalli, S. C., & Morrison, T. M. (2012). Considerations for reporting finite element analysis studies in biomechanics. Journal of biomechanics, 45(4), 625-633.

Erdemir, A. (2016). Open knee: open-source modelling and simulation in knee biomechanics. The journal of knee surgery, 29(02), 107-116.

Erdemir, A., Besier, T. F., Halloran, J. P., Imhauser, C. W., Laz, P. J., Morrison, T. M., & Shelburne, K. B. (2019). Deciphering the "art" in modelling and simulation of the knee joint: overall strategy. Journal of biomechanical engineering, 141(7).

Eskinazi, I., & Fregly, B. J. (2015). An open-source toolbox for surrogate modelling of joint contact mechanics. IEEE Transactions on Biomedical Engineering, 63(2), 269-277.

Fitzpatrick, C. K., Baldwin, M. A., Laz, P. J., FitzPatrick, D. P., Lerner, A. L., & Rullkoetter, P. J. (2011). Development of a statistical shape model of the patellofemoral joint for investigating relationships between shape and function. Journal of biomechanics, 44(13), 2446-2452.

Fitzpatrick, C. K., Clary, C. W., Laz, P. J., & Rullkoetter, P. J. (2012). Relative contributions of design, alignment, and loading variability in knee replacement mechanics. Journal of Orthopaedic Research, 30(12), 2015-2024.

Flandry, F., & Hommel, G. (2011). Normal anatomy and biomechanics of the knee. Sports medicine and arthroscopy review, 19(2), 82-92.

Fleming, B. C., Carey, J. L., Spindler, K. P., & Murray, M. M. (2008). Can suture repair of ACL transection restore normal anteroposterior laxity of the knee? An ex vivo study. Journal of Orthopaedic Research, 26(11), 1500-1505.

Fleming, B. C., Hulstyn, M. J., Oksendahl, H. L., & Fadale, P. D. (2005). Ligament injury, reconstruction, and osteoarthritis. Current opinion in orthopaedics, 16(5), 354.

Ford, K. R., Myer, G. D., & Hewett, T. E. (2003). Valgus knee motion during landing in high school female and male basketball players. Medicine & Science in Sports & Exercise, 35(10), 1745-1750.

Forlani, M., Sancisi, N., Conconi, M., & Parenti-Castelli, V. (2016). A new test rig for static and dynamic evaluation of knee motion based on a cable-driven parallel manipulator loading system. Meccanica, 51(7), 1571-1581.

Fox, A. J., Bedi, A., & Rodeo, S. A. (2012). The basic science of human knee menisci: structure, composition, and function. Sports health, 4(4), 340-351.

Fregly, B. J., Besier, T. F., Lloyd, D. G., Delp, S. L., Banks, S. A., Pandy, M. G., & D'lima, D. D. (2012). Grand challenge competition to predict in vivo knee loads. Journal of orthopaedic research, 30(4), 503-513.

Freutel, M., Schmidt, H., Dürselen, L., Ignatius, A., & Galbusera, F. (2014). Finite element modelling of soft tissues: material models, tissue interaction and challenges. Clinical Biomechanics, 29(4), 363-372.

Friston, K. J. (2003). Statistical parametric mapping. In Neuroscience databases (pp. 237-250). Springer, Boston, MA.

Gardiner, J. C., & Weiss, J. A. (2003). Subject-specific finite element analysis of the human medial collateral ligament during valgus knee loading. Journal of orthopaedic research, 21(6), 1098-1106.

Gerus, P., Sartori, M., Besier, T. F., Fregly, B. J., Delp, S. L., Banks, S. A., ... & Lloyd, D. G. (2013). Subject-specific knee joint geometry improves predictions of medial tibiofemoral contact forces. Journal of biomechanics, 46(16), 2778-2786.

Ghosh, K. M., Blain, A. P., Longstaff, L., Rushton, S., Amis, A. A., & Deehan, D. J. (2014). Can we define envelope of laxity during navigated knee arthroplasty?. Knee Surgery, Sports Traumatology, Arthroscopy, 22(8), 1736-1743.

Gibbons, K. D., Clary, C. W., Rullkoetter, P. J., & Fitzpatrick, C. K. (2019). Development of a statistical shape-function model of the implanted knee for real-time prediction of joint mechanics. Journal of Biomechanics, 88, 55-63.

Giori, N. J., Beaupre, G. S., & Carter, D. R. (1993). Cellular shape and pressure may mediate mechanical control of tissue composition in tendons. Journal of Orthopaedic Research, 11(4), 581-591.

Goldsmith, M. T., Smith, S. D., Jansson, K. S., LaPrade, R. F., & Wijdicks, C. A. (2014). Characterization of robotic system passive path repeatability during specimen removal and reinstallation for in vitro knee joint testing. Medical Engineering & Physics, 36(10), 1331-1337.

Goodfellow, J. W., & O'Connor, J. (2002). The mechanics of the knee and prosthesis design. In LCS® Mobile Bearing Knee Arthroplasty (pp. 3-15). Springer, Berlin, Heidelberg.

Gornale, S. S., & Patravali, P. U. (2017). Medical imaging in clinical applications: algorithmic and computer based approaches. Basic Chapter,"Engineering and Technology: Latest Progress", 65-104.

Graci, V., Van Dillen, L. R., & Salsich, G. B. (2012). Gender differences in trunk, pelvis and lower limb kinematics during a single leg squat. Gait & posture, 36(3), 461-466.

Gray, H. (1878). Anatomy of the human body (Vol. 8). Lea & Febiger. - book.

Gray, H. A., Guan, S., Thomeer, L. T., Schache, A. G., de Steiger, R., & Pandy, M. G. (2019). Three-dimensional motion of the knee-joint complex during normal walking revealed by mobile biplane x-ray imaging. Journal of Orthopaedic Research®, 37(3), 615-630.

Grood, E. S., & Suntay, W. J. (1983). A joint coordinate system for the clinical description of three-dimensional motions: application to the knee. Journal of biomechanical engineering, 105(2), 136-144.

Guess, T. M., Thiagarajan, G., Kia, M., & Mishra, M. (2010). A subject specific multibody model of the knee with menisci. Medical engineering & physics, 32(5), 505-515.

Guy, S. P., Farndon, M. A., Sidhom, S., Al-Lami, M., Bennett, C., & London, N. J. (2012). Gender differences in distal femoral morphology and the role of gender specific implants in total knee replacement: a prospective clinical study. The Knee, 19(1), 28-31.

Hacker, S. P., Ignatius, A., & Dürselen, L. (2016). The influence of the test setup on knee joint kinematics–a meta-analysis of tibial rotation. Journal of Biomechanics, 49(13), 2982-2988.

Halonen, K. S., Dzialo, C. M., Mannisi, M., Venäläinen, M. S., de Zee, M., & Andersen, M. S. (2017). Workflow assessing the effect of gait alterations on stresses in the medial tibial cartilage-combined musculoskeletal modelling and finite element analysis. Scientific reports, 7(1), 17396.

Harris, M. D., Cyr, A. J., Ali, A. A., Fitzpatrick, C. K., Rullkoetter, P. J., Maletsky, L. P., & Shelburne, K. B. (2016). A combined experimental and computational approach to subject-specific analysis of knee joint laxity. Journal of biomechanical engineering, 138(8).

Hash, T. W. (2013). Magnetic resonance imaging of the knee. Sports Health, 5(1), 78-107.

Hicks, J. L., Uchida, T. K., Seth, A., Rajagopal, A., & Delp, S. L. (2015). Is my model good enough? Best practices for verification and validation of musculoskeletal models and simulations of movement. Journal of biomechanical engineering, 137(2).

Hitt, K., Shurman, J. R., Greene, K., McCarthy, J., Moskal, J., Hoeman, T., & Mont, M. A. (2003). Anthropometric measurements of the human knee: correlation to the sizing of current knee arthroplasty systems. JBJS, 85(suppl_4), 115-122.

Howes, M., Bajger, M., Lee, G., Bucci, F., & Martelli, S. (2021, November). Texture enhanced Statistical Region Merging with application to automatic knee bones segmentation from CT. In 2021 Digital Image Computing: Techniques and Applications (DICTA) (pp. 01-08). IEEE.

Hoy, M. G., Zajac, F. E., & Gordon, M. E. (1990). A musculoskeletal model of the human lower extremity: the effect of muscle, tendon, and moment arm on the moment-angle relationship of musculotendon actuators at the hip, knee, and ankle. Journal of biomechanics, 23(2), 157-169.

Hsu, C. P., Lee, P. Y., Wei, H. W., Lin, S. C., Lu, Y. C., Lin, J. C., & Huang, C. H. (2021). Gender differences in femoral trochlea morphology. Knee Surgery, Sports Traumatology, Arthroscopy, 29(2), 563-572.

Hu, J., Xin, H., Chen, Z., Zhang, Q., Peng, Y., & Jin, Z. (2019). The role of menisci in knee contact mechanics and secondary kinematics during human walking. Clinical Biomechanics, 61, 58-63.

Hume, D. R., Navacchia, A., Ali, A. A., & Shelburne, K. B. (2018). The interaction of muscle moment arm, knee laxity, and torque in a multi-scale musculoskeletal model of the lower limb. Journal of biomechanics, 76, 173-180.

Ithurburn, M. P., Longfellow, M. A., Thomas, S., Paterno, M. V., & Schmitt, L. C. (2019). Knee function, strength, and resumption of preinjury sports participation in young athletes following anterior cruciate ligament reconstruction. journal of orthopaedic & sports physical therapy, 49(3), 145-153.

Iwaki, H., Pinskerova, V., & Freeman, M. A. R. (2000). Tibiofemoral movement 1: the shapes and relative movements of the femur and tibia in the unloaded cadaver knee. The Journal of bone and joint surgery. British volume, 82(8), 1189-1195.

Jakob, R. P., Staubli, H. U., & Deland, J. T. (1987). Grading the pivot shift. Objective tests with implications for treatment. The Journal of Bone & Joint Surgery British Volume, 69(2), 294-299.

James, C. R., Sizer, P. S., Starch, D. W., Lockhart, T. E., & Slauterbeck, J. (2004). Gender differences among sagittal plane knee kinematic and ground reaction force characteristics during a rapid sprint and cut maneuver. Research quarterly for exercise and sport, 75(1), 31-38.

Jensen, K. (1990). Literature Review: Manual Laxity Tests for Anterior Cruciate Ligament Injuries. Journal of Orthopaedic & Sports Physical Therapy, 11(10), 474-481.

Jilani, A., Shirazi-Adl, A., & Bendjaballah, M. Z. (1997). Biomechanics of human tibio-femoral joint in axial rotation. The Knee, 4(4), 203-213.

Johal, P., Williams, A., Wragg, P., Hunt, D., & Gedroyc, W. (2005). Tibiofemoral movement in the living knee. A study of weight bearing and non-weight bearing knee kinematics using 'interventional'MRI. Journal of biomechanics, 38(2), 269-276.

Johnston, M. V., Keith, R. A., & Hinderer, S. R. (1992). Measurement standards for interdisciplinary medical rehabilitation. Archives of Physical Medicine and Rehabilitation, 73(12-S), S3-23.

Kainz, H., Killen, B. A., Wesseling, M., Perez-Boerema, F., Pitto, L., Garcia Aznar, J. M., ... & Jonkers, I. (2020). A multi-scale modelling framework combining musculoskeletal rigid-body simulations with adaptive finite element analyses, to evaluate the impact of femoral geometry on hip joint contact forces and femoral bone growth. PLoS One, 15(7), e0235966.

Kaur, M., Sofat, S., & Chouhan, D. K. (2021). Review of automated segmentation approaches for knee images. IET Image Processing, 15(2), 302-324.

Kazemi, M., & Li, L. P. (2014). A viscoelastic poromechanical model of the knee joint in large compression. Medical engineering & physics, 36(8), 998-1006.

Kernozek, T. W., & Ragan, R. J. (2008). Estimation of anterior cruciate ligament tension from inverse dynamics data and electromyography in females during drop landing. Clinical biomechanics, 23(10), 1279-1286.

Khan, W. S., Nokes, L., Jones, R. K., & Johnson, D. S. (2007). The relationship of the angle of immobilisation of the knee to the force applied to the extensor mechanism when partially weight-bearing: a gait-analysis study in normal volunteers. The Journal of Bone & Joint Surgery British Volume, 89(7), 911-914.

Kiapour, A. M., & Murray, M. M. (2014). Basic science of anterior cruciate ligament injury and repair. Bone & joint research, 3(2), 20-31.

Kiapour, A. M., Wordeman, S. C., Paterno, M. V., Quatman, C. E., Levine, J. W., Goel, V. K., ... & Hewett, T. E. (2014). Diagnostic value of knee arthrometry in the prediction of anterior cruciate ligament strain during landing. The American journal of sports medicine, 42(2), 312-319.

Killen, B. A., Brito da Luz, S., Lloyd, D. G., Carleton, A. D., Zhang, J., Besier, T. F., & Saxby, D. J. (2021). Automated creation and tuning of personalised muscle paths for OpenSim musculoskeletal models of the knee joint. Biomechanics and Modelling in Mechanobiology, 20(2), 521-533.

Killen, B. A., Falisse, A., De Groote, F., & Jonkers, I. (2020). In Silico-Enhanced Treatment and Rehabilitation Planning for Patients with Musculoskeletal Disorders: Can Musculoskeletal Modelling and Dynamic Simulations Really Impact Current Clinical Practice?. Applied Sciences, 10(20), 7255.

Kim, T. K., Phillips, M., Bhandari, M., Watson, J., & Malhotra, R. (2017). What differences in morphologic features of the knee exist among patients of various races? A systematic review. Clinical Orthopaedics and Related Research®, 475(1), 170-182.

Kopf, S., Pombo, M. W., Szczodry, M., Irrgang, J. J., & Fu, F. H. (2011). Size variability of the human anterior cruciate ligament insertion sites. The American journal of sports medicine, 39(1), 108-113.

Kutzner, I., Bender, A., Dymke, J., Duda, G., Von Roth, P., & Bergmann, G. (2017). Mediolateral force distribution at the knee joint shifts across activities and is driven by tibiofemoral alignment. The bone & joint journal, 99(6), 779-787.

Lafortune, M. A., Cavanagh, P. R., Sommer Iii, H. J., & Kalenak, A. (1992). Three-dimensional kinematics of the human knee during walking. Journal of biomechanics, 25(4), 347-357.

Lamberto, G., Amin, D., Solomon, L. B., Ding, B., Reynolds, K. J., Mazzà, C., & Martelli, S. (2019). Personalised 3D knee compliance from clinically viable knee laxity measurements: A proof of concept ex vivo experiment. Medical Engineering & Physics, 64, 80-85.

Lamberto, G., Martelli, S., Cappozzo, A., & Mazzà, C. (2017). To what extent is joint and muscle mechanics predicted by musculoskeletal models sensitive to soft tissue artefacts?. Journal of biomechanics, 62, 68-76.

Lamberto, G., Richard, V., Dumas, R., Valentini, P. P., Pennestrì, E., Lu, T. W., ... & Cappozzo, A. (2016). Modelling the human tibiofemoral joint using ex vivo determined compliance matrices. Journal of Biomechanical Engineering, 138(6).

Lane, C. G., Warren, R., & Pearle, A. D. (2008). The pivot shift. JAAOS-Journal of the American Academy of Orthopaedic Surgeons, 16(12), 679-688.

Lansdown, D., & Ma, C. B. (2018). The influence of tibial and femoral bone morphology on knee kinematics in the anterior cruciate ligament injured knee. Clinics in sports medicine, 37(1), 127-136.

LaPrade, R. F., Engebretsen, A. H., Ly, T. V., Johansen, S., Wentorf, F. A., & Engebretsen, L. (2007). The anatomy of the medial part of the knee. JBJS, 89(9), 2000-2010.

Lawless, I. M., Ding, B., Cazzolato, B. S., & Costi, J. J. (2014). Adaptive velocity-based six degree of freedom load control for real-time unconstrained biomechanical testing. Journal of biomechanics, 47(12), 3241-3247.

Laz, P. J., & Browne, M. (2010). A review of probabilistic analysis in orthopaedic biomechanics. Proceedings of the institution of mechanical engineers, Part H: Journal of Engineering in Medicine, 224(8), 927-943.

Leathers, M. P., Merz, A., Wong, J., Scott, T., Wang, J. C., & Hame, S. L. (2015). Trends and demographics in anterior cruciate ligament reconstruction in the United States. The journal of knee surgery, 390-394.

Lenhart, R. L., Kaiser, J., Smith, C. R., & Thelen, D. G. (2015). Prediction and validation of load-dependent behaviour of the tibiofemoral and patellofemoral joints during movement. Annals of biomedical engineering, 43(11), 2675-2685.

Lenz, N. M., Mane, A., Maletsky, L. P., & Morton, N. A. (2008). The effects of femoral fixed body coordinate system definition on knee kinematic description.

Lephart, S. M., Ferris, C. M., Riemann, B. L., Myers, J. B., & Fu, F. H. (2002). Gender differences in strength and lower extremity kinematics during landing. Clinical Orthopaedics and Related Research®, 401, 162-169.

Li, G., Lopez, O., & Rubash, H. (2001). Variability of a three-dimensional finite element model constructed using magnetic resonance images of a knee for joint contact stress analysis. J. Biomech. Eng., 123(4), 341-346.

Li, P., Tsai, T. Y., Li, J. S., Wang, S., Zhang, Y., Kwon, Y. M., ... & Li, G. (2014). Gender analysis of the anterior femoral condyle geometry of the knee. The Knee, 21(2), 529-533.

Livesay, G. A., Rudy, T. W., Woo, S. L. Y., Runco, T. J., Sakane, M., Li, G., & Fu, F. H. (1997). Evaluation of the effect of joint constraints on the in situ force distribution in the anterior cruciate ligament. Journal of Orthopaedic Research, 15(2), 278-284.

Lloyd, D. G., & Besier, T. F. (2003). An EMG-driven musculoskeletal model to estimate muscle forces and knee joint moments in vivo. Journal of biomechanics, 36(6), 765-776.

Lonner, J. H., Jasko, J. G., & Thomas, B. S. (2008). Anthropomorphic differences between the distal femora of men and women. Clinical orthopaedics and related research, 466(11), 2724-2729.

Maderbacher, G., Keshmiri, A., Krieg, B., Greimel, F., Grifka, J., & Baier, C. (2019). Kinematic component alignment in total knee arthroplasty leads to better restoration of natural tibiofemoral kinematics compared to mechanic alignment. Knee Surgery, Sports Traumatology, Arthroscopy, 27(5), 1427-1433.

Mahfouz, M. R., Merkl, B. C., Abdel Fatah, E. E., Booth Jr, R., & Argenson, J. N. (2007). Automatic methods for characterization of sexual dimorphism of adult femora: distal femur. Computer methods in biomechanics and biomedical engineering, 10(6), 447-456.

Maletsky, L., Shalhoub, S., Fitzwater, F., Eboch, W., Dickinson, M., Akhbari, B., & Louie, E. (2016). In vitro experimental testing of the human knee: a concise review. The journal of knee surgery, 29(02), 138-148.

Maletsky, L. P., Sun, J., & Morton, N. A. (2007). Accuracy of an optical active-marker system to track the relative motion of rigid bodies. Journal of biomechanics, 40(3), 682-685.

Markolf, K. L., Graff-Radford, A., & Amstutz, H. C. (1978). In vivo knee stability. A quantitative assessment using an instrumented clinical testing apparatus. The Journal of bone and joint surgery. American volume, 60(5), 664-674.

Markolf, K. L., Mensch, J. S., & Amstutz, H. C. (1976). Stiffness and laxity of the knee--the contributions of the supporting structures. A quantitative in vitro study. JBJS, 58(5), 583-594.

Martelli, S., & Pinskerova, V. (2002). The shapes of the tibial and femoral articular surfaces in relation to tibiofemoral movement. The Journal of bone and joint surgery. British volume, 84(4), 607-613.

Martelli, S., Calvetti, D., Somersalo, E., & Viceconti, M. (2015). Stochastic modelling of muscle recruitment during activity. Interface focus, 5(2), 20140094.

Martelli, S., Sancisi, N., Conconi, M., Pandy, M. G., Kersh, M. E., Parenti-Castelli, V., & Reynolds, K. J. (2020). The relationship between tibiofemoral geometry and musculoskeletal function during normal activity. Gait & Posture, 80, 374-382.

Martelli, S., Zaffagnini, S., Bignozzi, S., Lopomo, N., & Marcacci, M. (2007). Description and validation of a navigation system for intra-operative evaluation of knee laxity. Computer Aided Surgery, 12(3), 181-188.

Masouros, Bull, A. M. J., & Amis, A. A. (2010). (i) Biomechanics of the knee joint. Orthopaedics and Trauma, 24(2), 84-91.

Matsuda, Y., Ishii, Y., Noguchi, H., & Ishii, R. (2005). Varus-valgus balance and range of movement after total knee arthroplasty. The Journal of Bone and Joint Surgery. British volume, 87(6), 804-808.

McGibbon, C. A., Brandon, S., Bishop, E. L., Cowper-Smith, C., & Biden, E. N. (2021). Biomechanical study of a tricompartmental unloader brace for patellofemoral or multicompartment knee osteoarthritis. Frontiers in bioengineering and biotechnology, 8, 1528.

McGinley, J. L., Baker, R., Wolfe, R., & Morris, M. E. (2009). The reliability of three-dimensional kinematic gait measurements: a systematic review. Gait & posture, 29(3), 360-369.

McLean, S. G., Huang, X., & Van Den Bogert, A. J. (2005). Association between lower extremity posture at contact and peak knee valgus moment during sidestepping: implications for ACL injury. Clinical biomechanics, 20(8), 863-870.

McLEAN, S. G., Neal, R. J., Myers, P. T., & Walters, M. R. (1999). Knee joint kinematics during the sidestep cutting maneuver: potential for injury in women. Medicine and science in sports and exercise, 31(7), 959-968.

Meng, Q., Fisher, J., & Wilcox, R. (2017). The effects of geometric uncertainties on computational modelling of knee biomechanics. Royal Society Open Science, 4(8), 170670.

Meng, X., Bruno, A. G., Cheng, B., Wang, W., Bouxsein, M. L., & Anderson, D. E. (2015). Incorporating six degree-of-freedom intervertebral joint stiffness in a lumbar spine musculoskeletal model—method and performance in flexed postures. Journal of biomechanical engineering, 137(10).

Meyer, H. (1853). Knee joint mechanics. Arch Anat Physiol Wiss Med, 497-547.

Mills, K., Hunt, M. A., & Ferber, R. (2013). Biomechanical deviations during level walking associated with knee osteoarthritis: a systematic review and meta-analysis. Arthritis care & research, 65(10), 1643-1665.

Moglo, K. E., & Shirazi-Adl, A. (2003). Biomechanics of passive knee joint in drawer: load transmission in intact and ACL-deficient joints. The Knee, 10(3), 265-276.

Moglo, K. E., & Shirazi-Adl, A. (2005). Cruciate coupling and screw-home mechanism in passive knee joint during extension–flexion. Journal of biomechanics, 38(5), 1075-1083.

Moglo, K. E., & Shirazi-Adl, A. (2003). On the coupling between anterior and posterior cruciate ligaments, and knee joint response under anterior femoral drawer in flexion: a finite element study. Clinical Biomechanics, 18(8), 751-759.

Momersteeg, T. J. A., Blankevoort, L., Huiskes, R., Kooloos, J. G. M., Kauer, J. M. G., & Hendriks, J. C. M. (1995). The effect of variable relative insertion orientation of human knee bone-ligament-bone complexes on the tensile stiffness. Journal of biomechanics, 28(6), 745-752.

Mootanah, R., Imhauser, C. W., Reisse, F., Carpanen, D., Walker, R. W., Koff, M. F., ... & Hillstrom, H. J. (2014). Development and validation of a computational model of the knee joint for the evaluation of surgical treatments for osteoarthritis. Computer methods in biomechanics and biomedical engineering, 17(13), 1502-1517.

Morton, N. A., Maletsky, L. P., Pal, S., & Laz, P. J. (2007). Effect of variability in anatomical landmark location on knee kinematic description. Journal of Orthopaedic Research, 25(9), 1221-1230.

Mukherjee, S., Nazemi, M., Jonkers, I., & Geris, L. (2020). Use of computational modelling to study joint degeneration: a review. Frontiers in bioengineering and biotechnology, 8, 93.

Myers, C. A. (2015). Probabilistic musculoskeletal simulation methods to address intersegmental dependencies of the knee, hip, and spine (Doctoral dissertation, University of Denver).

Myers, C. A., Torry, M. R., Shelburne, K. B., Giphart, J. E., LaPrade, R. F., Woo, S. L., & Steadman, J. R. (2012). In vivo tibiofemoral kinematics during 4 functional tasks of increasing demand using biplane fluoroscopy. The American journal of sports medicine, 40(1), 170-178.

Naghibi, H., Mazzoli, V., Gijsbertse, K., Hannink, G., Sprengers, A., Janssen, D., ... & Verdonschot, N. (2019). A non-invasive MRI based approach to estimate the mechanical properties of human knee ligaments. Journal of the mechanical behavior of biomedical materials, 93, 43-51.

Navacchia, A., Hume, D. R., Rullkoetter, P. J., & Shelburne, K. B. (2019). A computationally efficient strategy to estimate muscle forces in a finite element musculoskeletal model of the lower limb. Journal of biomechanics, 84, 94-102.

Navacchia, A., Myers, C. A., Rullkoetter, P. J., & Shelburne, K. B. (2016). Prediction of in vivo knee joint loads using a global probabilistic analysis. Journal of biomechanical engineering, 138(3).

Neri, T., Testa, R., Laurendon, L., Dehon, M., Putnis, S., Grasso, S., ... & Philippot, R. (2019). Determining the change in length of the anterolateral ligament during knee motion: a three-dimensional optoelectronic analysis. Clinical Biomechanics, 62, 86-92.

Nielsen, S. (1987). Kinesiology of the knee joint. An experimental investigation of the ligamentous and capsular restraints preventing knee instability. Danish Medical Bulletin, 34(6), 297-309.

Niu, K., Sluiter, V., Homminga, J., Sprengers, A., & Verdonschot, N. (2018). A novel ultrasound-based lower extremity motion tracking system. Intelligent Orthopaedics: Artificial Intelligence and Smart Image-guided Technology for Orthopaedics, 131-142.

Noble, P. C., Gordon, M. J., Weiss, J. M., Reddix, R. N., Conditt, M. A., & Mathis, K. B. (2005). Does total knee replacement restore normal knee function?. Clinical Orthopaedics and Related Research®, 431, 157-165.

Novo, C. D., Alharbi, S., Biden, E. N., & Tingley, M. (2011). Spatial characterization of the accuracies in "Vicon" Motion Analysis Laboratory. Fredericton: University of New Brunswick. Retrieved, 19(2), 2021.

Nowakowski, A. M., Majewski, M., Müller-Gerbl, M., & Valderrabano, V. (2012). Measurement of knee joint gaps without bone resection:"physiologic" extension and flexion gaps in total knee arthroplasty are asymmetric and unequal and anterior and posterior cruciate ligament resections produce different gap changes. Journal of Orthopaedic Research, 30(4), 522-527.

O'Rourke, D., Bucci, F., Burton, W. S., Al-Dirini, R., Taylor, M., & Martelli, S. (2023). Determining the relationship between tibiofemoral geometry and passive motion with partial least squares regression. Journal of Orthopaedic Research®.

Obrębska, P., Skubich, J., & Piszczatowski, S. (2020). Gender differences in the knee joint loadings during gait. Gait & Posture, 79, 195-202.

Ostrowski, J. A. (2006). Accuracy of 3 diagnostic tests for anterior cruciate ligament tears. Journal of athletic training, 41(1), 120.

Ottoboni, A., Parenti-Castelli, V., Sancisi, N., Belvedere, C., & Leardini, A. (2010). Articular surface approximation in equivalent spatial parallel mechanism models of the human knee joint: an experiment-based assessment. Proceedings of the Institution of Mechanical Engineers, Part H: Journal of Engineering in Medicine, 224(9), 1121-1132.

Pal, S. (2014). Design of artificial human joints & organs (Vol. 1). Boston, MA: Springer US. – book

Pandy, M. G., & Shelburne, K. B. (1997). Dependence of cruciate ligament loading on muscle forces and external load. Journal of biomechanics, 30(10), 1015-1024.

Papaioannou, G., Demetropoulos, C. K., & King, Y. H. (2010). Predicting the effects of knee focal articular surface injury with a patient-specific finite element model. The Knee, 17(1), 61-68.

Papaioannou, G., Nianios, G., Mitrogiannis, C., Fyhrie, D., Tashman, S., & Yang, K. H. (2008). Patient-specific knee joint finite element model validation with high-accuracy kinematics from biplane dynamic Roentgen stereogrammetric analysis. Journal of Biomechanics, 41(12), 2633-2638.

Parenti-Castelli, V., Leardini, A., Di Gregorio, R., & O'Connor, J. J. (2004). On the modelling of passive motion of the human knee joint by means of equivalent planar and spatial parallel mechanisms. Autonomous Robots, 16(2), 219-232.

Pedersen, D., Vanheule, V., Wirix-Speetjens, R., Taylan, O., Delport, H. P., Scheys, L., & Andersen, M. S. (2019). A novel non-invasive method for measuring knee joint laxity in four dof: In vitro proof-of-concept and validation. Journal of biomechanics, 82, 62-69.

Pedoia, V., Lansdown, D. A., Zaid, M., McCulloch, C. E., Souza, R., Ma, C. B., & Li, X. (2015). Three-dimensional MRI-based statistical shape model and application to a cohort of knees with acute ACL injury. Osteoarthritis and cartilage, 23(10), 1695-1703.

Peebles, A. T., Dickerson, L. C., Renner, K. E., & Queen, R. M. (2020). Sex-based differences in landing mechanics vary between the drop vertical jump and stop jump. Journal of Biomechanics, 105, 109818.

Pena, E., Calvo, B., Martinez, M. A., & Doblare, M. (2006). A three-dimensional finite element analysis of the combined behavior of ligaments and menisci in the healthy human knee joint. Journal of biomechanics, 39(9), 1686-1701.

Pena, E., Martinez, M. A., Calvo, B., Palanca, D., & Doblaré, M. (2005). A finite element simulation of the effect of graft stiffness and graft tensioning in ACL reconstruction. Clinical Biomechanics, 20(6), 636-644.

Pianigiani, S., Croce, D., D'Aiuto, M., Pascale, W., & Innocenti, B. (2017). Sensitivity analysis of the material properties of different soft-tissues: implications for a subject-specific knee arthroplasty. Muscles, Ligaments and Tendons Journal, 7(4), 546.

Pillet, H., Bergamini, E., Rochcongar, G., Camomilla, V., Thoreux, P., Rouch, P., ... & Skalli, W. (2016). Femur, tibia and fibula bone templates to estimate subject-specific knee ligament attachment site locations. Journal of Biomechanics, 49(14), 3523-3528.

Pletcher, E. R., Dekker, T. J., Lephart, S. M., & Sell, T. C. (2021). Sex and age comparisons in neuromuscular and biomechanical characteristics of the knee in young athletes. International Journal of Sports Physical Therapy, 16(2), 438.

Pugh, L., Mascarenhas, R., Arneja, S., Chin, P. Y., & Leith, J. M. (2009). Current concepts in instrumented knee-laxity testing. The American journal of sports medicine, 37(1), 199-210.

Qi, Y., Sun, H., Fan, Y., Li, F., Wang, Y., & Ge, C. (2018). Three dimensional finite element analysis of the influence of posterior tibial slope on the anterior cruciate ligament and knee joint forward stability. Journal of Back and Musculoskeletal Rehabilitation, 31(4), 629-636.

Rajagopal, A., Dembia, C. L., DeMers, M. S., Delp, D. D., Hicks, J. L., & Delp, S. L. (2016). Full-body musculoskeletal model for muscle-driven simulation of human gait. IEEE transactions on biomedical engineering, 63(10), 2068-2079.

Ramsey, D. K., & Wretenberg, P. F. (1999). Biomechanics of the knee: methodological considerations in the in vivo kinematic analysis of the tibiofemoral and patellofemoral joint. Clinical biomechanics, 14(9), 595-611.

Rao C, Fitzpatrick CK, Rullkoetter PJ, et al. (2013). A statistical finite element model of the knee accounting for shape and alignment variability. Medical Engineering and Physics; pp. 1450-1456.

Readioff, R., Geraghty, B., Comerford, E., & Elsheikh, A. (2020). A full-field 3D digital image correlation and modelling technique to characterise anterior cruciate ligament mechanics ex vivo. Acta Biomaterialia, 113, 417-428.

Ren, D., Liu, Y., Zhang, X., Song, Z., Lu, J., & Wang, P. (2017). The evaluation of the role of medial collateral ligament maintaining knee stability by a finite element analysis. Journal of orthopaedic surgery and research, 12(1), 1-10.

Renault, J. B., Aüllo-Rasser, G., Donnez, M., Parratte, S., & Chabrand, P. (2018). Articular-surface-based automatic anatomical coordinate systems for the knee bones. Journal of Biomechanics, 80, 171-178.

Ro, D. H., Lee, D. Y., Moon, G., Lee, S., Seo, S. G., Kim, S. H., ... & Lee, M. C. (2017). Sex differences in knee joint loading: cross-sectional study in geriatric population. Journal of Orthopaedic Research, 35(6), 1283-1289.

Robertsson, O., Dunbar, M., Pehrsson, T., Knutson, K., & Lidgren, L. (2000). Patient satisfaction after knee arthroplasty: a report on 27,372 knees operated on between 1981 and 1995 in Sweden. Acta Orthopaedica Scandinavica, 71(3), 262-267.

Rochcongar, G., Pillet, H., Bergamini, E., Moreau, S., Thoreux, P., Skalli, W., & Rouch, P. (2016). A new method for the evaluation of the end-to-end distance of the knee ligaments and popliteal complex during passive knee flexion. The Knee, 23(3), 420-425.

Roth, J. D., Hull, M. L., & Howell, S. M. (2015). The limits of passive motion are variable between and unrelated within normal tibiofemoral joints. Journal of Orthopaedic Research®, 33(11), 1594-1602.

Rovick, J. S., Reuben, J. D., Schrager, R. J., & Walker, P. S. (1991). Relation between knee motion and ligament length patterns. Clinical Biomechanics, 6(4), 213-220.

Sanchez, A. R., Sugalski, M. T., & LaPrade, R. F. (2006). Anatomy and biomechanics of the lateral side of the knee. Sports medicine and arthroscopy review, 14(1), 2-11.

Scheys, L., Jonkers, I., Schutyser, F., Pans, S., Spaepen, A., & Suetens, P. (2005, May). Image based methods to generate subject-specific musculoskeletal models for gait analysis. In International Congress Series (Vol. 1281, pp. 62-67). Elsevier.

Seth, A., Sherman, M., Reinbolt, J. A., & Delp, S. L. (2011). OpenSim: a musculoskeletal modelling and simulation framework for in silico investigations and exchange. Procedia Iutam, 2, 212-232.

Shah, R. F., Martinez, A. M., Pedoia, V., Majumdar, S., Vail, T. P., & Bini, S. A. (2019). Variation in the thickness of knee cartilage. The use of a novel machine learning algorithm for cartilage segmentation of magnetic resonance images. The Journal of arthroplasty, 34(10), 2210-2215.

Shakoor, D., Guermazi, A., Kijowski, R., Fritz, J., Roemer, F. W., Jalali-Farahani, S., & Demehri, S. (2019). Cruciate ligament injuries of the knee: A meta-analysis of the diagnostic performance of 3D MRI. Journal of Magnetic Resonance Imaging, 50(5), 1545-1560.

Shalhoub, S., Moschetti, W. E., Dabuzhsky, L., Jevsevar, D. S., Keggi, J. M., & Plaskos, C. (2018). Laxity profiles in the native and replaced knee—application to robotic-assisted gap-balancing total knee arthroplasty. The Journal of Arthroplasty, 33(9), 3043-3048.

Sharifi, M., Shirazi-Adl, A., & Marouane, H. (2018). Computation of the role of kinetics, kinematics, posterior tibial slope and muscle cocontraction on the stability of ACL-deficient knee joint at heel strike–Towards identification of copers from non-copers. Journal of Biomechanics, 77, 171-182.

Sharma, L., Lou, C., Felson, D. T., Dunlop, D. D., Kirwan-Mellis, G., Hayes, K. W., ... & Buchanan, T. S. (1999). Laxity in healthy and osteoarthritic knees. Arthritis & Rheumatism: Official Journal of the American College of Rheumatology, 42(5), 861-870.

Shelburne, K. B., & Pandy, M. G. (1997). A musculoskeletal model of the knee for evaluating ligament forces during isometric contractions. Journal of biomechanics, 30(2), 163-176.

Shelburne, K. B., & Pandy, M. G. (2002). A dynamic model of the knee and lower limb for simulating rising movements. Computer Methods in Biomechanics & Biomedical Engineering, 5(2), 149-159.

Shelburne, K. B., Kim, H. J., Sterett, W. I., & Pandy, M. G. (2011). Effect of posterior tibial slope on knee biomechanics during functional activity. Journal of Orthopaedic Research, 29(2), 223-231.

Shepherd, D. E. T., & Seedhom, B. B. (1999). Thickness of human articular cartilage in joints of the lower limb. Annals of the rheumatic diseases, 58(1), 27-34.

Sheth, N. P., Husain, A., & Nelson, C. L. (2017). Surgical techniques for total knee arthroplasty: measured resection, gap balancing, and hybrid. JAAOS-Journal of the American Academy of Orthopaedic Surgeons, 25(7), 499-508.

Shirazi, R., & Shirazi-Adl, A. (2009). Analysis of partial meniscectomy and ACL reconstruction in knee joint biomechanics under a combined loading. Clinical biomechanics, 24(9), 755-761.

Shoemaker, S. C., Adams, D., Daniel, D. M., & Woo, S. L. (1993). Quadriceps/anterior cruciate graft interaction. An in vitro study of joint kinematics and anterior cruciate ligament graft tension. Clinical orthopaedics and related research, (294), 379-390.

Shrive, N. G., O'connor, J. J., & Goodfellow, J. W. (1978). Load-bearing in the knee joint. Clinical orthopaedics and related research, (131), 279-287.

Sigward, S. M., Pollard, C. D., Havens, K. L., & Powers, C. M. (2012). The influence of sex and maturation on knee mechanics during side-step cutting. Medicine and science in sports and exercise, 44(8), 1497.

Simon, S. R. (2004). Quantification of human motion: gait analysis - benefits and limitations to its application to clinical problems. Journal of biomechanics, 37(12), 1869-1880.

Slane, L. C., Slane, J. A., D'hooge, J., & Scheys, L. (2017). The challenges of measuring in vivo knee collateral ligament strains using ultrasound. Journal of biomechanics, 61, 258-262.

Smale, K. B., Conconi, M., Sancisi, N., Krogsgaard, M., Alkjaer, T., Parenti-Castelli, V., & Benoit, D. L. (2019). Effect of implementing magnetic resonance imaging for patient-specific OpenSim models on lower-body kinematics and knee ligament lengths. Journal of biomechanics, 83, 9-15.

Smidt, G. L. (1973). Biomechanical analysis of knee flexion and extension. Journal of biomechanics, 6(1), 79-92.

Smith, C. R., Lenhart, R. L., Kaiser, J., Vignos, M. F., & Thelen, D. G. (2016). Influence of ligament properties on tibiofemoral mechanics in walking. The journal of knee surgery, 29(02), 099-106.

Smoger LM, Fitzpatrick CK, Clary CW, et al. (2015). Statistical modelling to characterize relationships between knee anatomy and kinematics. Journal of Orthopaedic Research; pp. 1620-1630.

Söderman, T., Werner, S., Wretling, M. L., Hänni, M., Mikkelsen, C., Sundin, A., & Shalabi, A. (2021). Knee function 30 years after ACL reconstruction: a case series of 60 patients. Acta Orthopaedica, 92(6), 716-721.

Srikanth, V. K., Fryer, J. L., Zhai, G., Winzenberg, T. M., Hosmer, D., & Jones, G. (2005). A meta-analysis of sex differences prevalence, incidence, and severity of osteoarthritis. Osteoarthritis and cartilage, 13(9), 769-781.

Stagni, R., Fantozzi, S., Cappello, A., & Leardini, A. (2005). Quantification of soft tissue artefact in motion analysis by combining 3D fluoroscopy and stereophotogrammetry: a study on two subjects. Clinical biomechanics, 20(3), 320-329.

Tanikawa, H., Matsumoto, H., Komiyama, I., Kiriyama, Y., Toyama, Y., & Nagura, T. (2013). Comparison of knee mechanics among risky athletic motions for noncontact anterior cruciate ligament injury. Journal of applied biomechanics, 29(6), 749-755.

Taylor, M., Bryan, R., & Galloway, F. (2013). Accounting for patient variability in finite element analysis of the intact and implanted hip and knee: a review. International journal for numerical methods in biomedical engineering, 29(2), 273-292.

Tersi, L., Barré, A., Fantozzi, S., & Stagni, R. (2013). In vitro quantification of the performance of model-based mono-planar and bi-planar fluoroscopy for 3D joint kinematics estimation. Medical & biological engineering & computing, 51(3), 257-265

Thelen, D. G., & Anderson, F. C. (2006). Using computed muscle control to generate forward dynamic simulations of human walking from experimental data. Journal of biomechanics, 39(6), 1107-1115.

Thelen, D. G., Won Choi, K., & Schmitz, A. M. (2014). Co-simulation of neuromuscular dynamics and knee mechanics during human walking. Journal of biomechanical engineering, 136(2), 021033.

Torzilli, P. A., Deng, X., & Warren, R. F. (1994). The effect of joint-compressive load and quadriceps muscle force on knee motion in the intact and anterior cruciate ligament-sectioned knee. The American journal of sports medicine, 22(1), 105-112.

Trent, P. S., Walker, P. S., & Wolf, B. (1976). Ligament length patterns, strength, and rotational axes of the knee joint. Clinical orthopaedics and related research, (117), 263-270.

Tumer, S. T., & Engin, A. E. (1993). Three-body segment dynamic model of the human knee.

Valente, G., Pitto, L., Stagni, R., & Taddei, F. (2015). Effect of lower-limb joint models on subject-specific musculoskeletal models and simulations of daily motor activities. Journal of biomechanics, 48(16), 4198-4205.

Van den Heever, D. J., Scheffer, C., Erasmus, P., & Dillon, E. (2012). Classification of gender and race in the distal femur using self-organising maps. The Knee, 19(4), 488-492.

Van der Kruk, E., & Reijne, M. M. (2018). Accuracy of human motion capture systems for sport applications; state-of-the-art review. European journal of sport science, 18(6), 806-819.

Varadarajan, K. M., Gill, T. J., Freiberg, A. A., Rubash, H. E., & Li, G. (2009). Gender differences in trochlear groove orientation and rotational kinematics of human knees. Journal of Orthopaedic Research, 27(7), 871-878.

Viceconti, M., Testi, D., Taddei, F., Martelli, S., Clapworthy, G. J., & Jan, S. V. S. (2006). Biomechanics modelling of the musculoskeletal apparatus: status and key issues. Proceedings of the IEEE, 94(4), 725-739.

Victor, J., Labey, L., Wong, P., Innocenti, B., & Bellemans, J. (2010). The influence of muscle load on tibiofemoral knee kinematics. Journal of orthopaedic research, 28(4), 419-428.

Voleti, P. B., Stephenson, J. W., Lotke, P. A., & Lee, G. C. (2015). No sex differences exist in posterior condylar offsets of the knee. Clinical Orthopaedics and Related Research®, 473(4), 1425-1431.

Walker, P. S., Rovick, J. S., & Robertson, D. D. (1988). The effects of knee brace hinge design and placement on joint mechanics. Journal of biomechanics, 21(11), 965-974.

Wang, Y., Fan, Y., & Zhang, M. (2014). Comparison of stress on knee cartilage during kneeling and standing using finite element models. Medical engineering & physics, 36(4), 439-447.

Weaver, D. S. (2000). Skeletal tissue mechanics. - book

Webster, K. E. (2021). Return to Sport and Reinjury Rates in Elite Female Athletes After Anterior Cruciate Ligament Rupture. Sports Medicine, 51(4), 653-660.

Weiss, J. A., & Gardiner, J. C. (2001). Computational modelling of ligament mechanics. Critical Reviews™ in Biomedical Engineering, 29(3).

Wilson, D. R., Feikes, J. D., Zavatsky, A. B., & O'connor, J. J. (2000). The components of passive knee movement are coupled to flexion angle. Journal of Biomechanics, 33(4), 465-473.

Wilson, J. L. A., Dunbar, M. J., & Hubley-Kozey, C. L. (2015). Knee joint biomechanics and neuromuscular control during gait before and after total knee arthroplasty are sex-specific. The Journal of arthroplasty, 30(1), 118-125.

Wismans, J. A. C., Veldpaus, F., Janssen, J., Huson, A., & Struben, P. (1980). A three-dimensional mathematical model of the knee joint. Journal of biomechanics, 13(8), 677-685.

Woo, S., Weiss, J. A., & MacKenna, D. A. (1990). Biomechanics and morphology of the medial collateral and anterior cruciate ligaments. In Biomechanics of diarthrodial joints (pp. 63-104). Springer, New York, NY.

Wu, D., Sofka, M., Birkbeck, N., & Zhou, S. K. (2014, September). Segmentation of multiple knee bones from CT for orthopedic knee surgery planning. In International Conference on Medical Image Computing and Computer-Assisted Intervention (pp. 372-380). Springer, Cham.

Wünschel, M., Leichtle, U., Obloh, C., Wülker, N., & Müller, O. (2011). The effect of different quadriceps loading patterns on tibiofemoral joint kinematics and patellofemoral contact pressure during simulated partial weight-bearing knee flexion. Knee Surgery, Sports Traumatology, Arthroscopy, 19(7), 1099-1106

Xie, F., Yang, L., Guo, L., Wang, Z. J., & Dai, G. (2009). A study on construction three-dimensional nonlinear finite element model and stress distribution analysis of anterior cruciate ligament.

Xu, C., Reifman, J., Baggaley, M., Edwards, W. B., & Unnikrishnan, G. (2019). Individual differences in women during walking affect tibial response to load carriage: the importance of individualized musculoskeletal finite-element models. IEEE Transactions on Biomedical Engineering, 67(2), 545-555.

Yamaguchi, G. T., & Zajac, F. E. (1989). A planar model of the knee joint to characterize the knee extensor mechanism. Journal of biomechanics, 22(1), 1-10.

Yang, Z., Wickwire, A. C., & Debski, R. E. (2010). Development of a subject-specific model to predict the forces in the knee ligaments at high flexion angles. Medical & biological engineering & computing, 48, 1077-1085.

Zavatsky, A. B. (1997). A kinematic-freedom analysis of a flexed-knee-stance testing rig. Journal of biomechanics, 30(3), 277-280.

Zavatsky, A. B., Oppold, P. T., & Price, A. J. (2004). Simultaneous in vitro measurement of patellofemoral kinematics and forces. Journal of biomechanical engineering, 126(3), 351-356.

Zbrojkiewicz, D., Vertullo, C., & Grayson, J. E. (2018). Increasing rates of anterior cruciate ligament reconstruction in young Australians, 2000–2015. Medical Journal of Australia, 208(8), 354-358.

Zhang, J., Sorby, H., Clement, J., Thomas, C. D. L., Hunter, P., Nielsen, P., ... & Besier, T. (2014). The MAP client: user-friendly musculoskeletal modelling workflows. In Biomedical Simulation: 6th International Symposium, ISBMS 2014, Strasbourg, France, October 16-17, 2014. Proceedings 6 (pp. 182-192). Springer International Publishing.

Appendix A

CONTRIBUTION

Statement Of Contribution

CONTENTS

Outline Of The Author Contribution To Ch.3 - First Study

In this chapter, F Bucci was the main contributor to the study design, experimental protocol, specimen preparation, CT and MRI imaging collection and segmentation, collection, acquisition, and processing of all the data, analysis and interpretation of the results, graphical representation, manuscript formulation and subsequent manuscript drafting. F Bucci developed the methodology to reconstruct medial and lateral passive motion extremes. F Bucci performed all data analyses and interpretation of results. F Bucci wrote the draft manuscript which was edited with feedback from principal supervisor (S Martelli) and followed by feedback from supervisors (M Taylor, R Al-Dirini).

Outline Of The Author Contribution To Ch.4 - Second Study

In this chapter, F Bucci was the main contributor to specimen preparation, CT imaging collection and segmentation, data collection, data acquisition, analysis and interpretation, graphical representation, manuscript formulation and subsequent manuscript drafting. F Bucci extended the used of the methodology, developed by herself, and presented in Chapter 3, to 30 knee cadaveric specimen, representative of a healthy adult population. F Bucci performed all data analyses and interpretation of results. F Bucci wrote the draft manuscript which was edited with feedback from principal supervisor (S Martelli) and followed by feedback from supervisors (M Taylor, R Al-Dirini).

Outline Of The Author Contribution To Ch.5 - Literature Review

In this appendix, F Bucci was the main contributor to the study concept, design, literature review and graphical representations. F Bucci conducted the mapping review with the objective of evaluating a cost - complexity - utility perspective on in silico tibiofemoral joint modelling. F Bucci wrote the draft manuscript which was edited with feedback from principal supervisor (S Martelli) and followed by feedback from supervisors (M Taylor, R Al-Dirini).

Outline Of The Author Contribution To Ch.6 - Third Study

In this chapter, F Bucci was the main contributor to the study design, computational simulations, data analysis and interpretation, graphical representation, manuscript formulation and subsequent manuscript drafting. F Bucci developed the methodology for compliance matrix integration into a generic MSK model. The compliance matrix was derived from simulation of a publicly available musculoskeletal model, as the methodology was validated against this model by R Lenhart (Lenhart et al., 2015). F Bucci performed all data analyses and interpretation of results. F Bucci wrote the draft manuscript which was edited with feedback from principal supervisor (S Martelli) and followed by feedback from supervisors (M Taylor, R Al-Dirini).

Outline Of The Author Contribution To Ch.7 - Third Study

In this chapter, F Bucci was the main contributor for manuscript formulation and subsequent manuscript drafting. F Bucci wrote the draft manuscript which was edited with feedback from principal supervisor (S Martelli) and followed by feedback from supervisors (M Taylor, R Al-Dirini).

Outline Of The Author Contribution To Appendices

Appendix B

In this chapter, F Bucci was the main contributor to the study design, experimental protocol, specimen preparation, CT and MRI imaging collection and segmentation, collection, acquisition, and processing of all the data, analysis and interpretation of the results, graphical representation, manuscript formulation and subsequent manuscript drafting. F Bucci extended the used of the methodology, developed and presented in Chapter 3, to one of the cadaveric knee specimens after TKR with different inserts. This feasibility study is part of the preliminary work relative to the investigation of knee joint function restoration after TKR. F Bucci performed all data analyses and interpretation of results. F Bucci wrote the draft manuscript which was edited with feedback from principal supervisor (S Martelli) and followed by feedback from supervisors (M Taylor, R Al-Dirini).

Appendix C

In this appendix, F Bucci was the main contributor to graphical representations. F Bucci reported the extremes of the passive motion for all 30 knee cadaveric specimens.

Appendix D

This appendix was adapted from the following journal article: D. O'Rourke, **F. Bucci**, M. Taylor, R. Al-Dirini, S. Martelli (2023) – Determining the relationship between tibiofemoral geometry and passive motion with partial least squares regression. Journal of Orthopaedic Research. *Submitted, Manuscript under Review.*

In this paper, F Bucci was responsible for specimens' preparation, CT and MRI imaging data collection and segmentation, motion data collection/acquisition. Data produced by F Bucci with the methodology in chapter 3 and analysed in chapter 4 were used to extend the analysis of the influence of sex on the relationship between knee geometry and passive motion. F Bucci performed all motion data analyses and contributed to the manuscript draft and revision.

Appendix E

This appendix was adapted from the following journal article: M. Howes, M. Bajger, G. Lee, **F. Bucci**, S. Martelli (2021) – Texture enhanced Statistical Region Merging with application to automatic knee bones segmentation from CT. Conference Paper. International Conference on Digital Image Computing: Techniques and Applications (DICTA). *Manuscript Published.*

In this paper, F Bucci was responsible for CT imaging data collection and ground truth for the segmentation. F Bucci contributed to the data analyses, to the manuscript draft and critical revision.

Appendix B

PRELIMINARY STUDY

The Extremes Of Unloaded Passive Knee Motion Before And After Total Knee Replacement: A Preliminary Study Of Feasibility

CONTENTS

Please refer to the appendices at the end of this thesis for a detailed outline of the author's contribution to this study (Appendix A).

B.1 Abstract

Knee kinematics substantially differs before and after total knee replacement (TKR), affecting pain, function, satisfaction, and revision. Understanding passive preoperative-postoperative kinematic changes may help identify causes of poor clinical outcome. However, ex vivo studies of the knee kinematics pre- and post-TKR generally analyse only one nominal flexion pattern with navigation systems, do not examine the direct influence of TKR on the same individuals, do not include all 6 degrees of freedom (DOFs) and/or the entire range of motion.

The purpose of this study was to determine with a novel assessment the six degrees of freedom kinematics of the medial and lateral extremes of the unloaded knee passive motion envelope, before and after TKR and with different liners.

The feasibility study was successfully conducted to compare passive motions of an intact and implanted knee specimen. The approach revealed small differences in abduction and in anterior-posterior translation between native and replaced knee, while in medial-lateral and inferior-superior showed differences also between liners. This new approach offers a means of studying passive motion in healthy, injured, pathological, and postoperatively treated knees. Future work will extend the study and focus on the potential clinical translation of the presented methodology to assess the restoration of the native individual knee joint function after total knee replacement.

B.2 Introduction

Knee kinematics substantially differs before and after total knee replacement (TKR), affecting pain, function, satisfaction, and revision (Blakeney et al., 2019; Noble et al., 2005). Understanding passive preoperative-postoperative kinematic changes may help identify causes of poor clinical outcome. However, current literature study on passive motion differences before and after total knee replacement are still scares. Ex vivo studies of the knee kinematics pre- and post-TKR generally analyse only one nominal flexion pattern with navigation systems or active motion through knee rigs, did not include all 6 degrees of freedom (DOFs) and restricted ranges of motion (Patil et al., 2005; Steinbruck et al., 2016). For instance, Maderbacher only analysed the rotational components and limited range of motion between 0°- and 90°-degrees flexion in 10 cadaveric knees using a surgical navigation system (Maderbacher et al., 2017). Other studies investigated slightly higher ranges, up to 120° simulating a squat for 8 specimens with a knee rig applying tendon and muscle forces (Steinbruck et al., 2016). Studies have shown that tibiofemoral kinematics play an instrumental role in the management of knee function and pain after TKR (Akbari Shandiz et al., 2016).

A preliminary feasibility study was conducted to compare passive motions in an intact and implanted knee specimens comparing medial and lateral extremes of the unloaded knee passive motion envelope. The purpose of with this study was to determine accurately the individual passive kinematics in the six degrees of freedom; in particular the medial and lateral extremes of the knee passive motion envelope were captured and medial kinematic compared, before and after TKR and with different liners. The focus of this study was on the potential clinical translation of the presented methodology to assess the restoration of the native individual knee joint function after total knee replacement.

B.3 Material And Methods

A knee specimen of an 80-year-old male (BMI = 26.6) with no reported history of knee surgery and osteoarthritis was obtained from a body donation program (UTN, Phoenix, USA).

The specimen preparation and protocol were presented in a previous study (Chapter 3). Specimen was CT scanned (0.33x0.33x0.3, SOMATOM Force, tube voltage 70 - 150 kV; tube current 220 mA). The knee potted with custom 3d-printed holders designed based on CT femur and tibia segmentation (ScanIP, Simpleware, Exeter, UK). The knee envelope of the passive motion was determined from two medial and lateral knee kinematics trials. Two five flexion-extension cycles were manually performed on the knee specimens with a minimal medial and lateral force (6 – 8 N). Trajectories of markers affixed to the holders were recorded using a 10-camera stereo-photogrammetric system (VICON, Oxford, UK). Local anatomic coordinate systems were defined for each bone and the knee kinematics for the six axes of motion were estimated by calculating the relative pose of the local femur co-ordinate system with respect to the tibia throughout the flexion cycle.

TKR was subsequently performed on the knee with an implant from Zimmer and robotic assistance by an experienced surgeon (Zimmer Biomet, Warsaw, Indiana) (Fig. C.1).

Figure B.1 *– Visual representation of a prepared intact and implanted knee specimen, featuring passive reflective markers for motion capture analysis, in accordance with the experimental setup and protocol outlined in Chapter 3 of the study.*

The protocol for capturing the medial and lateral extremes was repeated with three different sample liners; after each motion capture session, the surgeon opened the knee suture and replaced the liners. CT were performed before and after specimen preparation and with the implant to virtually reconstruct the relative position between markers and articular surfaces of the femoral and tibial components (post-op, 40 keV reconstructed CT, filter MAR, SOMATOM Force, tube voltage 70 - 150 kV; tube current 220 mA). The images were segmented. The virtual passive motion reconstruction was performed following the methodology; anatomical reference systems were based on Grood and Suntay (1983) with Gray et al. (2019) procedure (Grood and Suntay, 1983; Gray et al., 2019). The kinematics calculated from relative pose matrices (KINEMAT Toolbox, MATLAB 2020b, The MathWorks Inc., USA).

Preliminary results for the medial and lateral intact trials and the medial only TKR were processed. Mean and standard deviation of the medial extremes of the intact knee passive envelope were compared with kinematic post TKR with the different liners (MATLAB, MathWorks, Natick, USA). The following is a summary of the study (Fig. C.2).

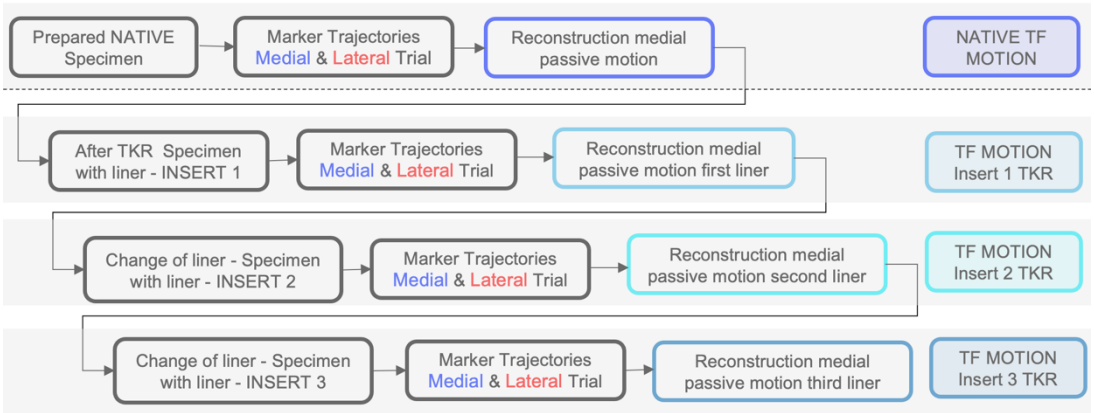

Figure B.2 *– Schematic overview of the feasibility study, presenting the process from the prepared knee native specimen with experimental passive motion and reconstruction, to the knee replacements with the first tibial insert (or liner), and so on conducting the passive motion experiment for three different types of liners.*

B.4 Results And Discussion

The feasibility study was successfully conducted to compare passive motions of an intact and implanted knee specimen. The six degree of freedom medial kinematic pattern were mostly consistent preop and postop (Fig. C.3). The variability across the five cycles shows that reliability of the medial and lateral extremes of the unloaded envelope. The approach revealed small differences in abduction were the native knee allowed for higher rotation. Anterior-posterior translation was also higher between native and replaced knee, with consistency across liners. Both medial-lateral and inferior-superior translations showed differences pre- and post-op, but also across liners.

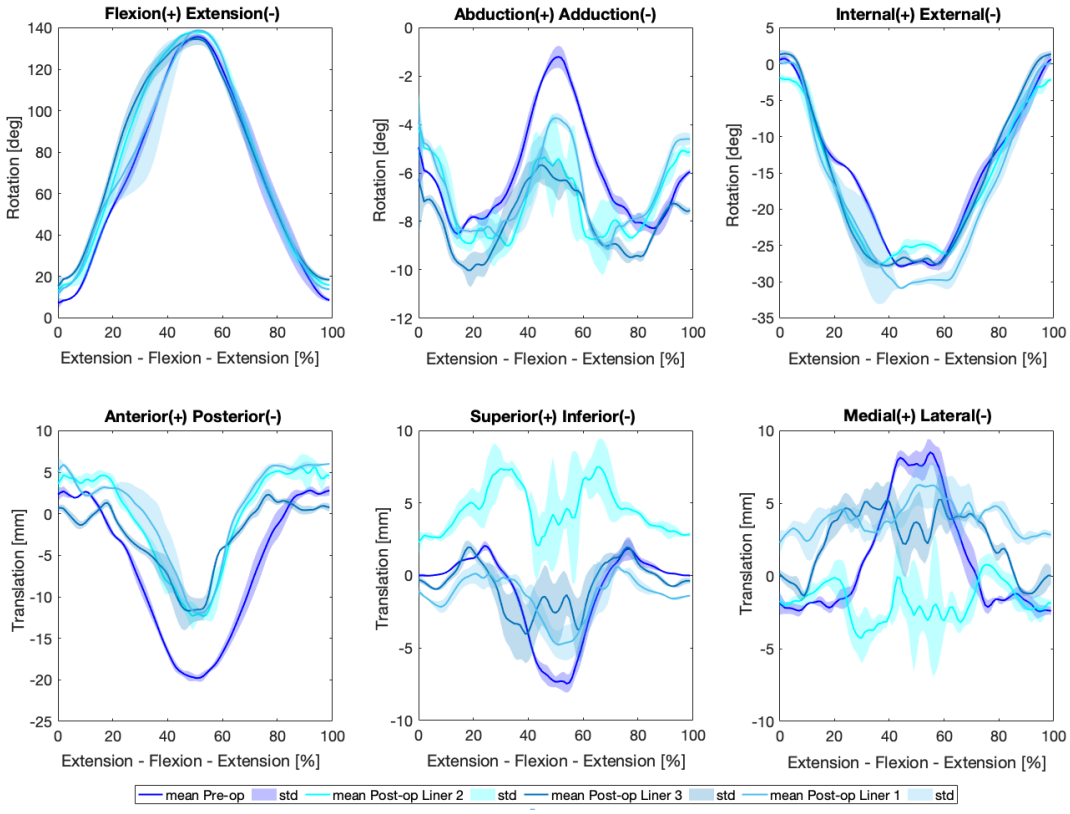

Figure B.3 *– Comparison between intact vs implanted tibiofemoral kinematics of the medial extreme of the unloaded knee passive motion envelope; AP IS and ML translations and AA IE rotations pre- and post-op.*

This study presented the differences in kinematics pre–and post–TKR with different inserts. This method provides a valid tool to accurately assess motion differences pre-op, post-op and between liners. While there is good agreement in the kinematic pattern between intact and post TKR, variations between liners were found mainly in superior and medial translation, with one of the liners not preforming as well as the others. This study showed similarity between kinematics before and after TKR. However, as differences were present, none of the insert seemed restore completely the native medial extreme of the unloaded envelope of knee passive motion. There were a number of limitations in this study. The study included one single knee specimen, and the medial extremes only were analysed. Moreover, the liners were demonstrative (and not the one regularly used for surgeries), providing less fixation as they have a different mechanism to lock them in on the tibial tray.

Future work will require larger sample size to provide more generalizable performance and results. Ideally, the ultimate aim would be potential clinical translation of the presented methodology to predict the individual extremes of unload passive motion envelope based on shape, assess the pathological motion, and try to restore the predicted native motion through surgical pre-planning - choice of the implant and total knee replacement procedure, to meet this target motion, with the aim of repristinate the lost individual function and improve outcome.

B.5 References

Blakeney, W., Clément, J., Desmeules, F., Hagemeister, N., Rivière, C., & Vendittoli, P. A. (2019). Kinematic alignment in total knee arthroplasty better reproduces normal gait than mechanical alignment. Knee Surgery, Sports Traumatology, Arthroscopy, 27(5), 1410-1417.

Patil, S., Colwell Jr, C. W., Ezzet, K. A., & D'Lima, D. D. (2005). Can normal knee kinematics be restored with unicompartmental knee replacement?. JBJS, 87(2), 332-338.

Steinbrück, A., Schröder, C., Woiczinski, M., Müller, T., Müller, P. E., Jansson, V., & Fottner, A. (2016). Influence of tibial rotation in total knee arthroplasty on knee kinematics and retropatellar pressure: an in vitro study. Knee Surgery, Sports Traumatology, Arthroscopy, 24(8), 2395-2400.

Noble, P. C., Gordon, M. J., Weiss, J. M., Reddix, R. N., Conditt, M. A., & Mathis, K. B. (2005). Does total knee replacement restore normal knee function?. Clinical Orthopaedics and Related Research®, 431, 157-165.

Maderbacher, G., Keshmiri, A., Springorum, H. R., Maderbacher, H., Grifka, J., & Baier, C. (2017). Influence of component rotation in total knee arthroplasty on tibiofemoral kinematics—a cadaveric investigation. The Journal of Arthroplasty, 32(9), 2869-2877.

Akbari Shandiz, M., Boulos, P., Saevarsson, S. K., Yoo, S., Miller, S., & Anglin, C. (2016). Changes in knee kinematics following total knee arthroplasty. Proceedings of the Institution of Mechanical Engineers, Part H: Journal of Engineering in Medicine, 230(4), 265-27.

Appendix C

ADDITIONAL MATERIAL

Specimen-Specific Extremes Of The Unloaded Knee Passive Motion Envelope

CONTENTS

Please refer to the appendices at the end of this thesis for a detailed outline of the author's contribution to this study (Appendix A).

C.1 Specimen-Specific Passive Motion

This appendix presents the specimen-specific extremes of the envelope of the knee passive motion. Table 1 provide side, sex, age, weight, and height of the specimens analysed.

Table C.1 – Specimens demographics: leg side, sex, age, height, and weight.

Cadaveric Knee Specimens Demographic						
	SIDE	**SEX**	**AGE** (yo)	**HEIGHT** (cm)	**WEIGHT** (kg)	**BMI** (kg/m^2)
Specimen n° 1	Right	female	72	160	64	24.80
Specimen n° 2	Right	female	68	160	74	28.87
Specimen n° 3	Right	male	71	175	92	29.97
Specimen n° 4	Right	male	73	183	73	21.70
Specimen n° 5	Right	male	76	173	66	22.04
Specimen n° 6	Right	female	72	165	79	29.12
Specimen n° 7	Left	male	82	180	85	26.08
Specimen n° 8	Left	male	74	168	47	16.62
Specimen n° 9	Left	male	74	178	64	20.09
Specimen n° 10	Left	male	60	178	66	20.95
Specimen n° 11	Left	male	77	173	53	17.79
Specimen n° 12	Left	female	74	160	66	25.68
Specimen n° 13	Left	male	78	178	68	21.52
Specimen n° 14	Left	male	77	170	86	29.75
Specimen n° 15	Right	female	43	155	59	24.56
Specimen n° 16	Left	male	77	183	97	28.88
Specimen n° 17	Left	male	76	183	74	22.10
Specimen n° 18	Left	male	50	173	117	39.22
Specimen n° 19	Left	male	70	185	105	30.61
Specimen n° 20	Left	male	56	180	79	24.40
Specimen n° 21	Right	female	59	155	36	15.11
Specimen n° 22	Left	female	54	157	54	21.58
Specimen n° 23	Right	female	53	175	59	19.20
Specimen n° 24	Right	male	58	175	73	23.63
Specimen n° 25	Left	male	57	180	82	25.10
Specimen n° 26	Right	male	57	180	82	25.10
Specimen n° 27	Right	female	54	157	54	21.58
Specimen n° 28	Left	female	53	175	59	19.20
Specimen n° 29	Right	male	58	198	84	21.38
Specimen n° 30	Right	male	80	173	79	26.61

For each specimen, mean and standard deviation across five cycles for the six DoF passive kinematics were plotted against the percentage of cycle. Medial and lateral extremes were also plotted against flexion angles along with an inferred neutral passive flexion path. Cycles represent a complete path of hyperextension/full extension to full flexion (0 to 50%), and back (100%) with respectively medial and lateral force applied at the femur cup.

C.1.1 Specimen 1

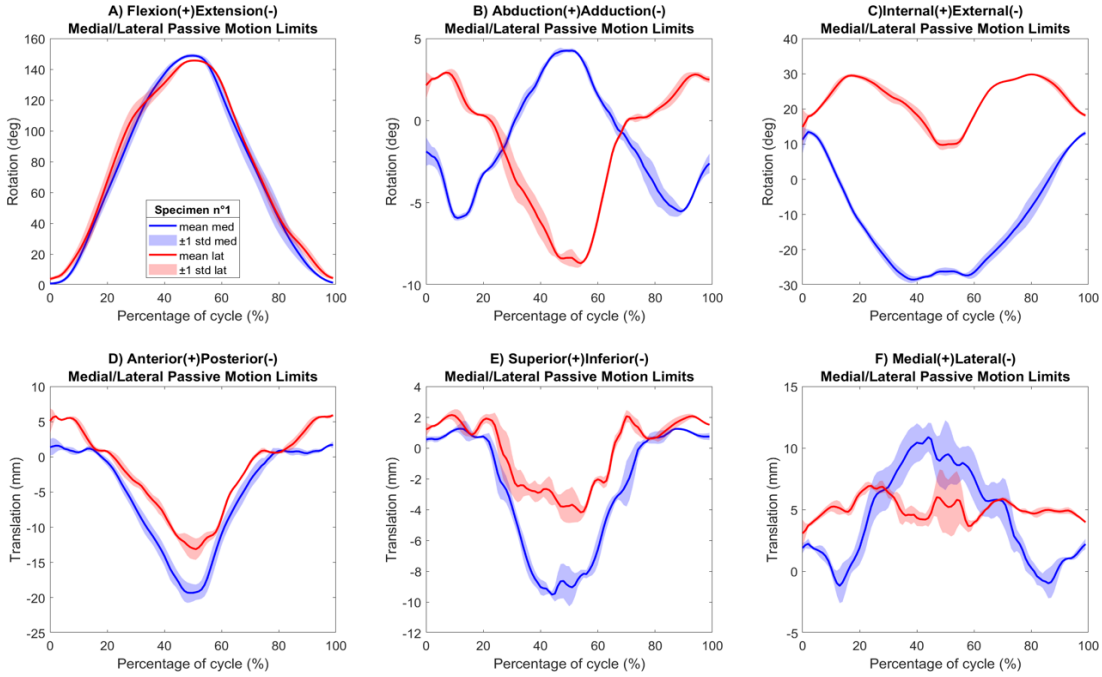

Figure C.1.1.1 *– Specimen1 medial (blue) and lateral (red) experimental TF motion: FE, AA, IE rotations and AP, SI, and ML translations mean and standard deviation.*

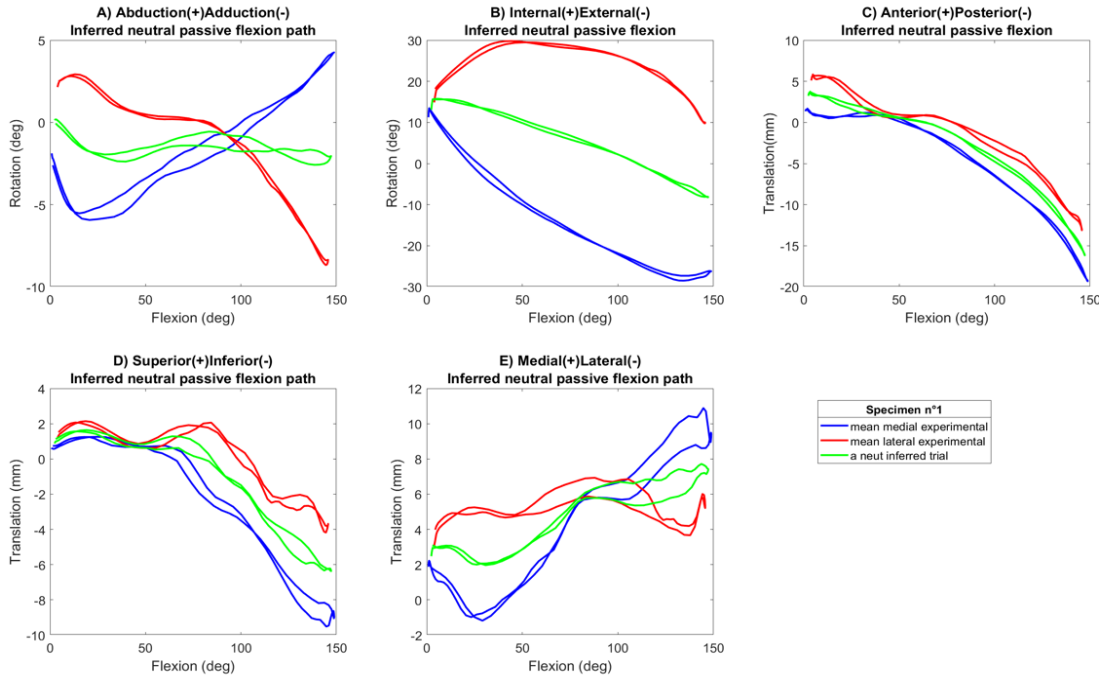

Figure C.1.1.2 *– Specimen1 medial (blue), lateral (red) experimental TF motion and inferred neutral flexion path (green): rotations and translations against FE.*

C.1.2 Specimen 2

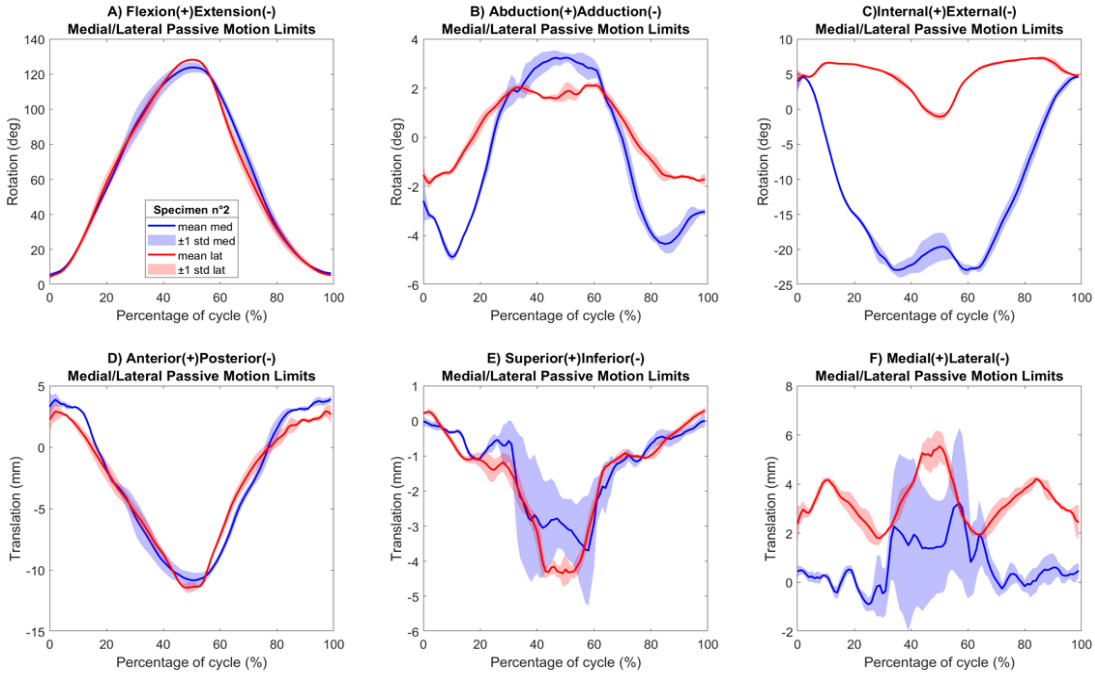

Figure C.1.2.1 *– Specimen2 medial (blue) and lateral (red) experimental TF motion: FE, AA, IE rotations and AP, SI, and ML translations mean and standard deviation.*

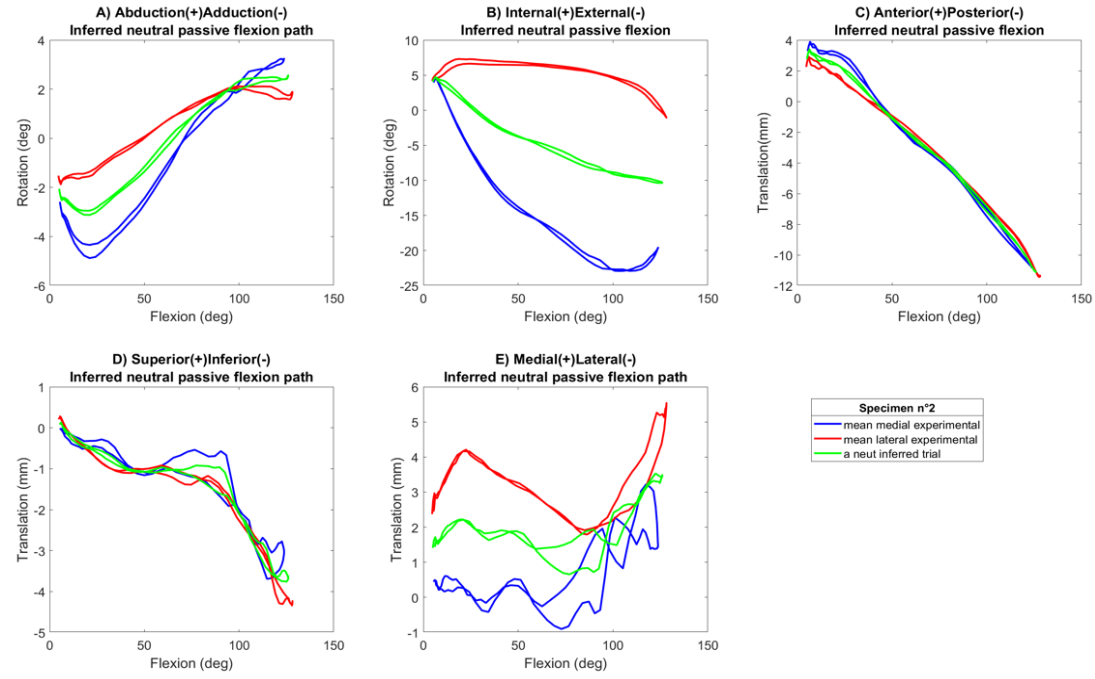

Figure C.1.2.2 *– Specimen2 medial (blue), lateral (red) experimental TF motion and inferred neutral flexion path (green): rotations and translations against FE.*

C.1.3 Specimen 3

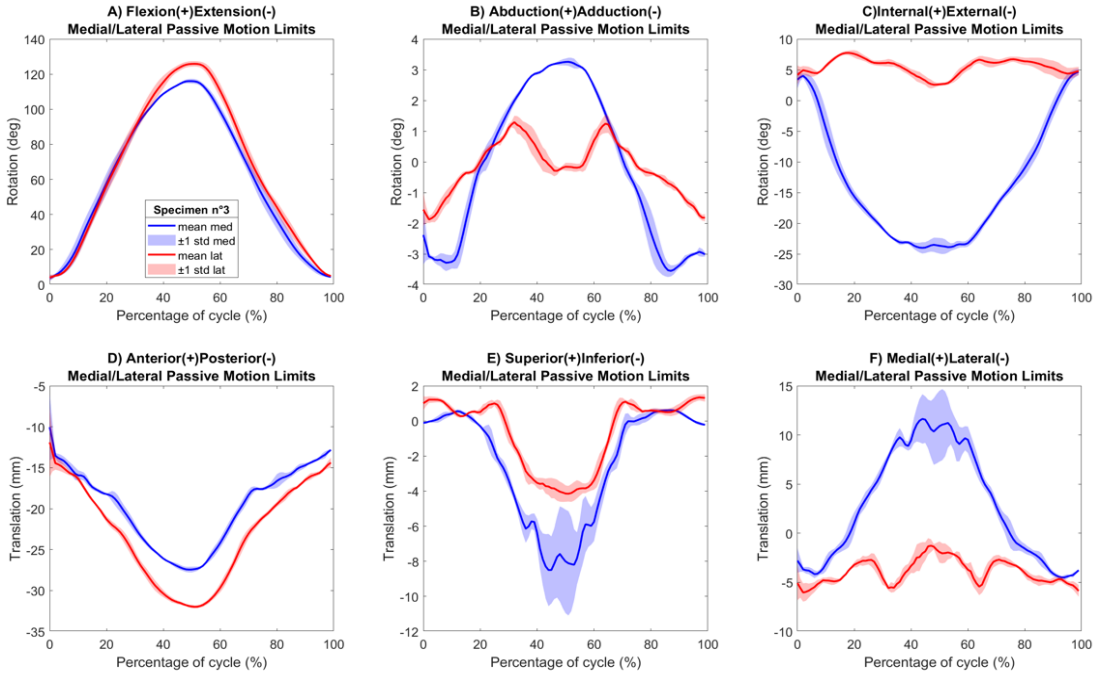

Figure C.1.3.1 *– Specimen3 medial (blue) and lateral (red) experimental TF motion: FE, AA, IE rotations and AP, SI, and ML translations mean and standard deviation.*

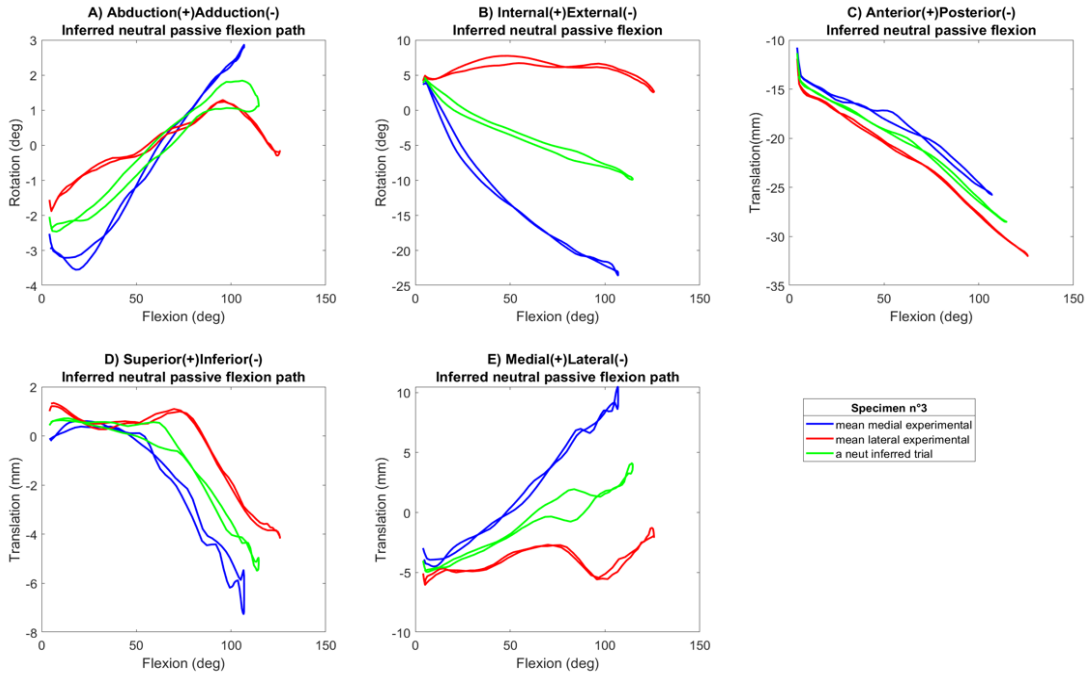

Figure C.1.3.2 *– Specimen3 medial (blue), lateral (red) experimental TF motion and inferred neutral flexion path (green): rotations and translations against FE.*

C.1.4 Specimen 4

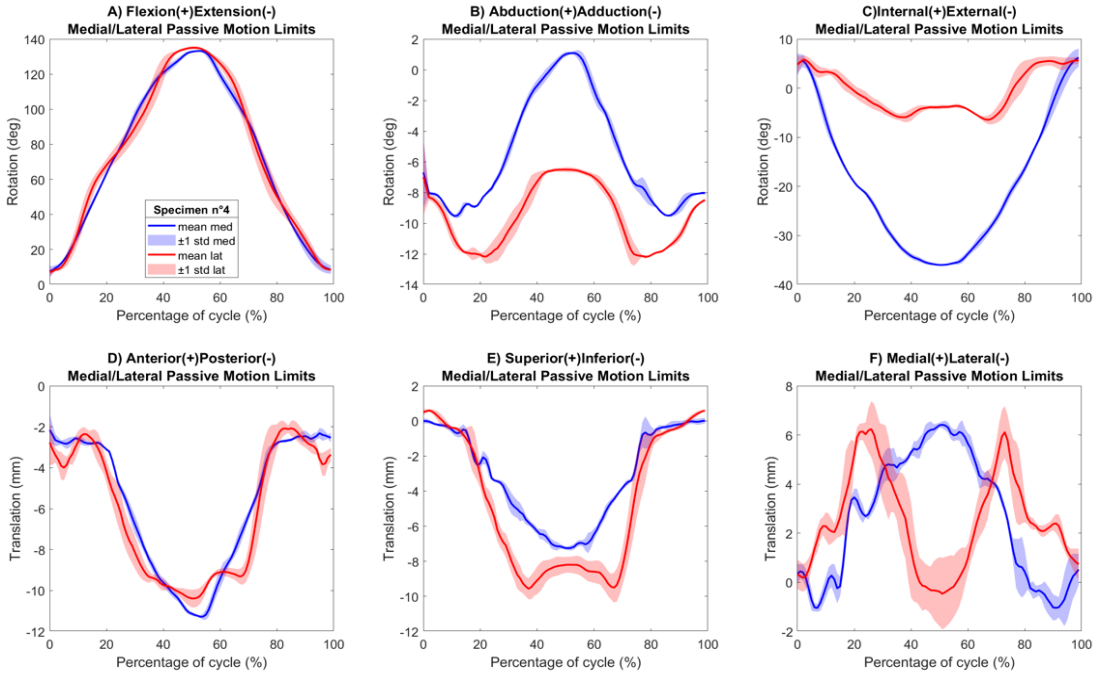

Figure C.1.4.1 *– Specimen4 medial (blue) and lateral (red) experimental TF motion: FE, AA, IE rotations and AP, SI, and ML translations mean and standard deviation.*

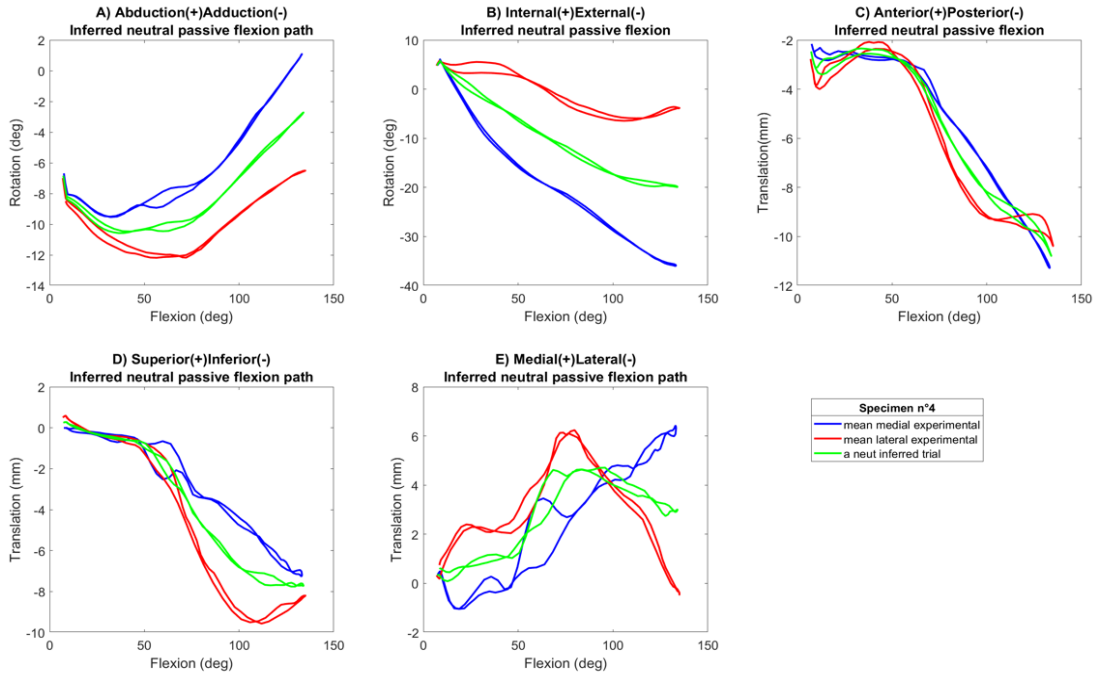

Figure C.1.4.2 *– Specimen4 medial (blue), lateral (red) experimental TF motion and inferred neutral flexion path (green): rotations and translations against FE.*

C.1.5 Specimen 5

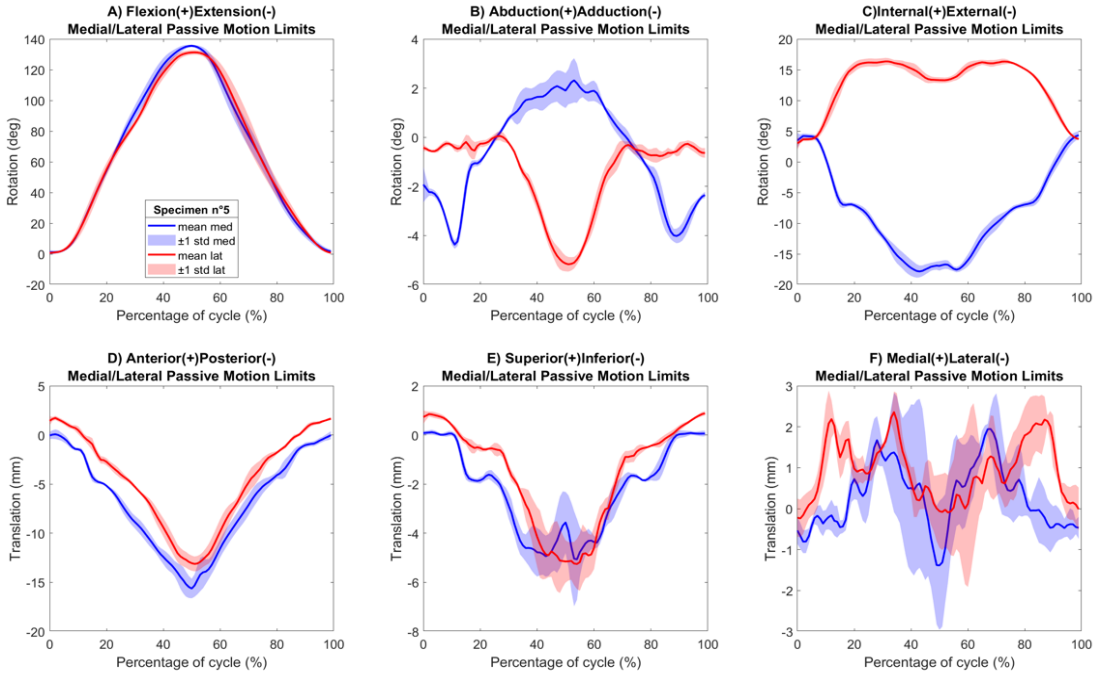

Figure C.1.5.1 *– Specimen5 medial (blue) and lateral (red) experimental TF motion: FE, AA, IE rotations and AP, SI, and ML translations mean and standard deviation.*

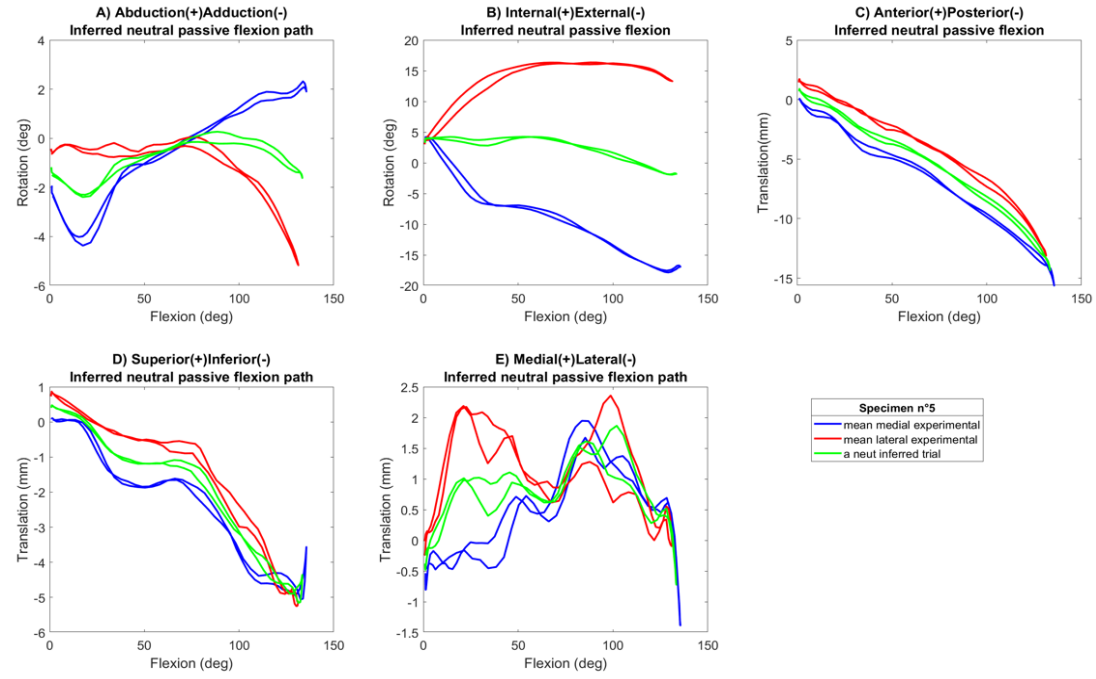

Figure C.1.5.2 *– Specimen5 medial (blue), lateral (red) experimental TF motion and inferred neutral flexion path (green): rotations and translations against FE.*

C.1.6 Specimen 6

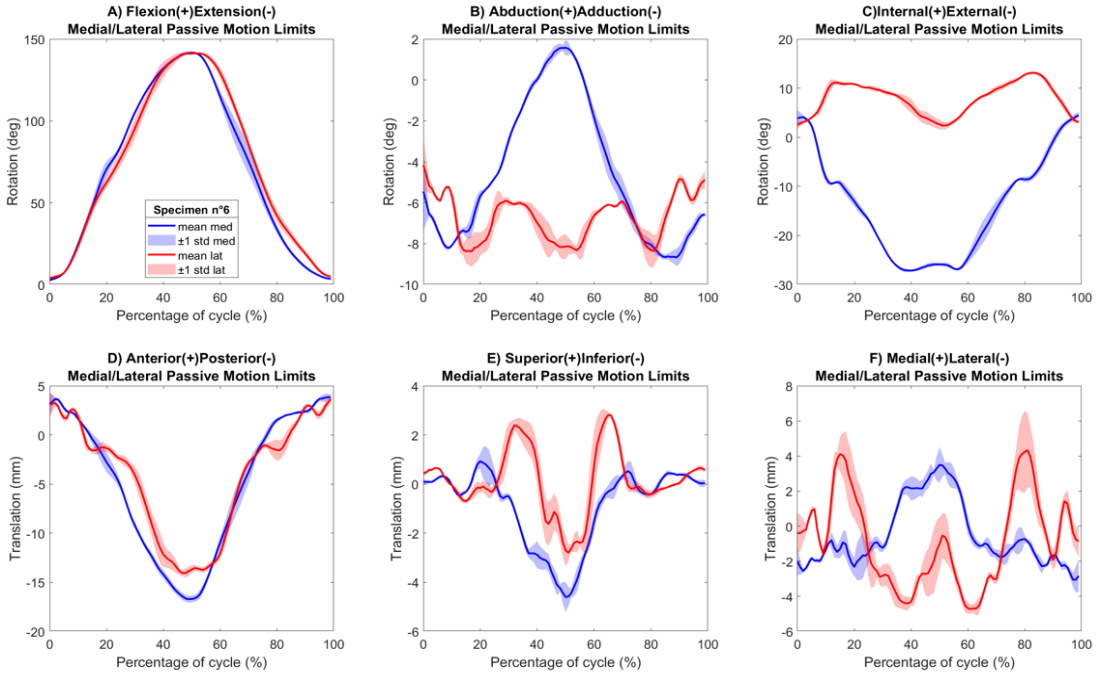

Figure C.1.6.1 *– Specimen6 medial (blue) and lateral (red) experimental TF motion: FE, AA, IE rotations and AP, SI, and ML translations mean and standard deviation.*

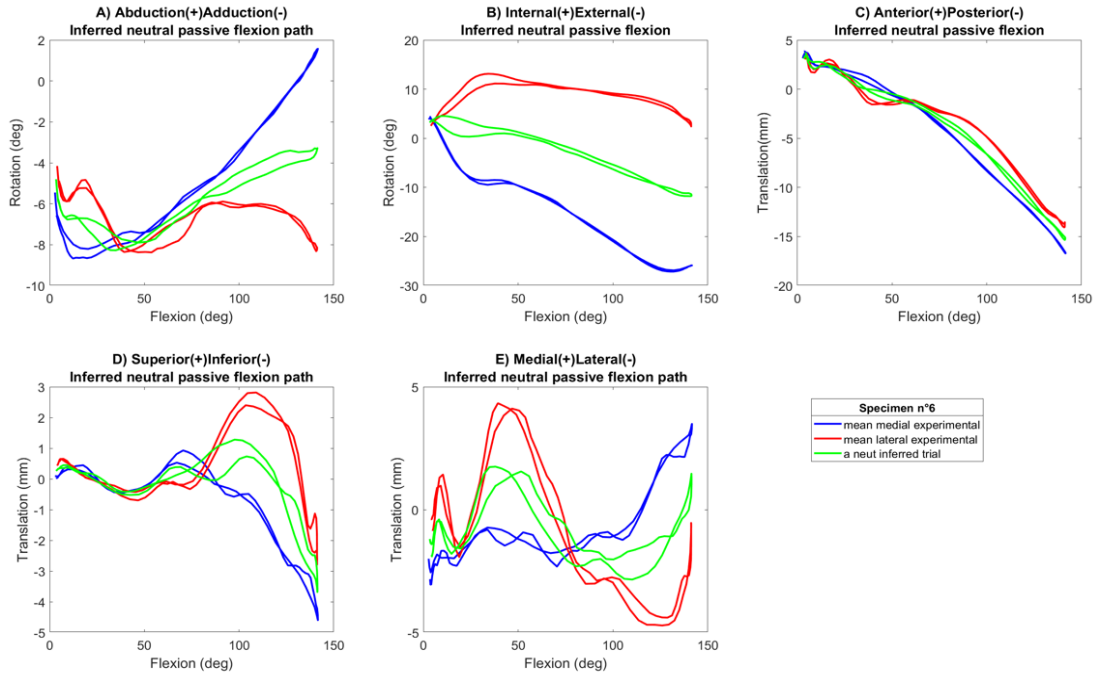

Figure C.1.6.2 *– Specimen6 medial (blue), lateral (red) experimental TF motion and inferred neutral flexion path (green): rotations and translations against FE.*

C.1.7 Specimen 7

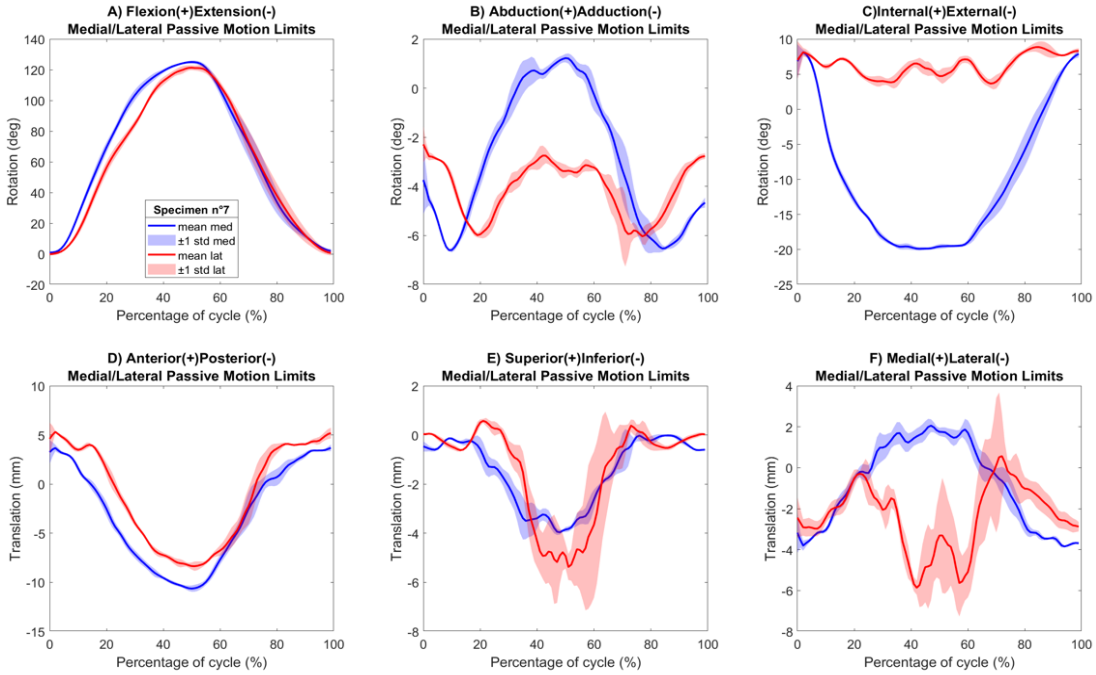

Figure C.1.7.1 *– Specimen7 medial (blue) and lateral (red) experimental TF motion: FE, AA, IE rotations and AP, SI, and ML translations mean and standard deviation.*

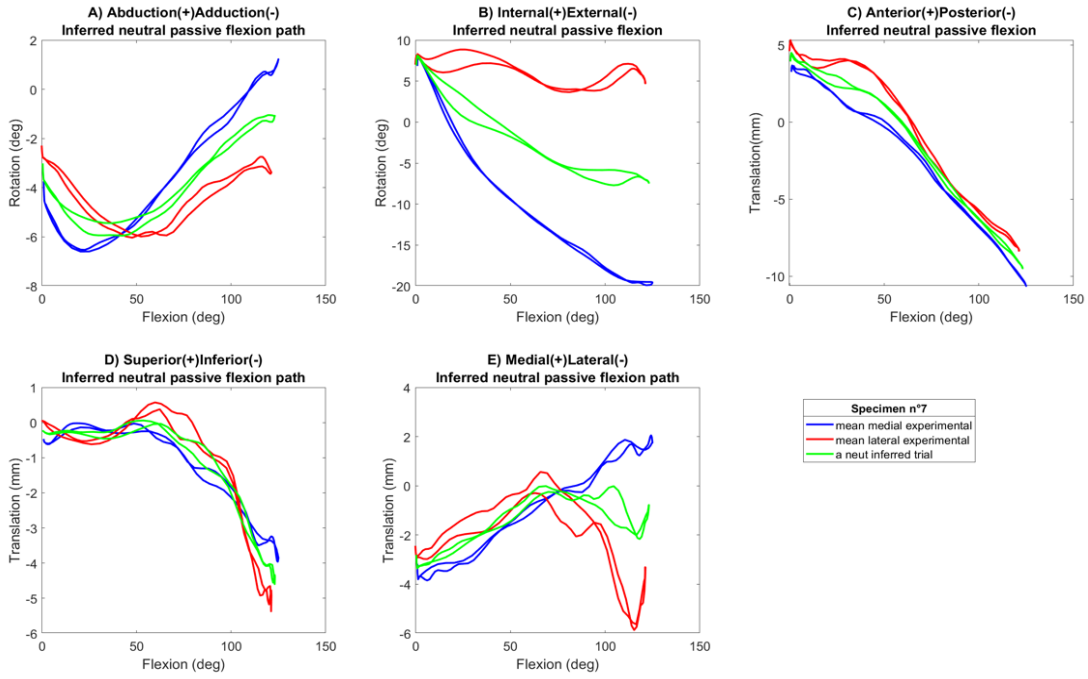

Figure C.1.7.2 *– Specimen7 medial (blue), lateral (red) experimental TF motion and inferred neutral flexion path (green): rotations and translations against FE.*

C.1.8 Specimen 8

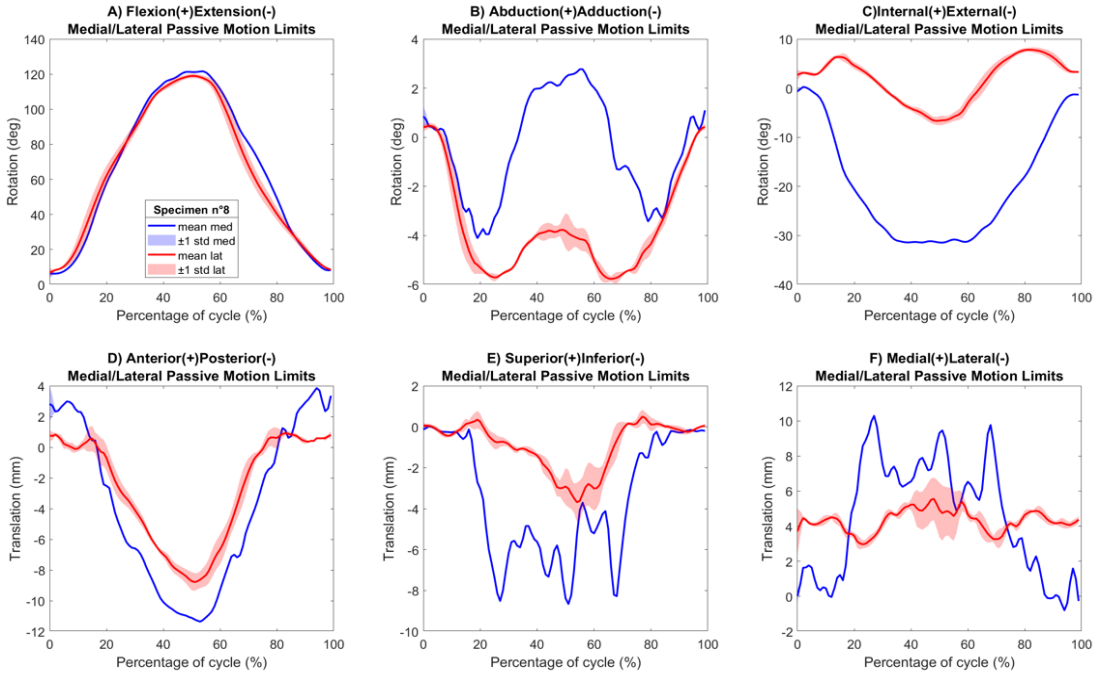

Figure C.1.8.1 *– Specimen8 medial (blue) and lateral (red) experimental TF motion: FE, AA, IE rotations and AP, SI, and ML translations mean and standard deviation.*

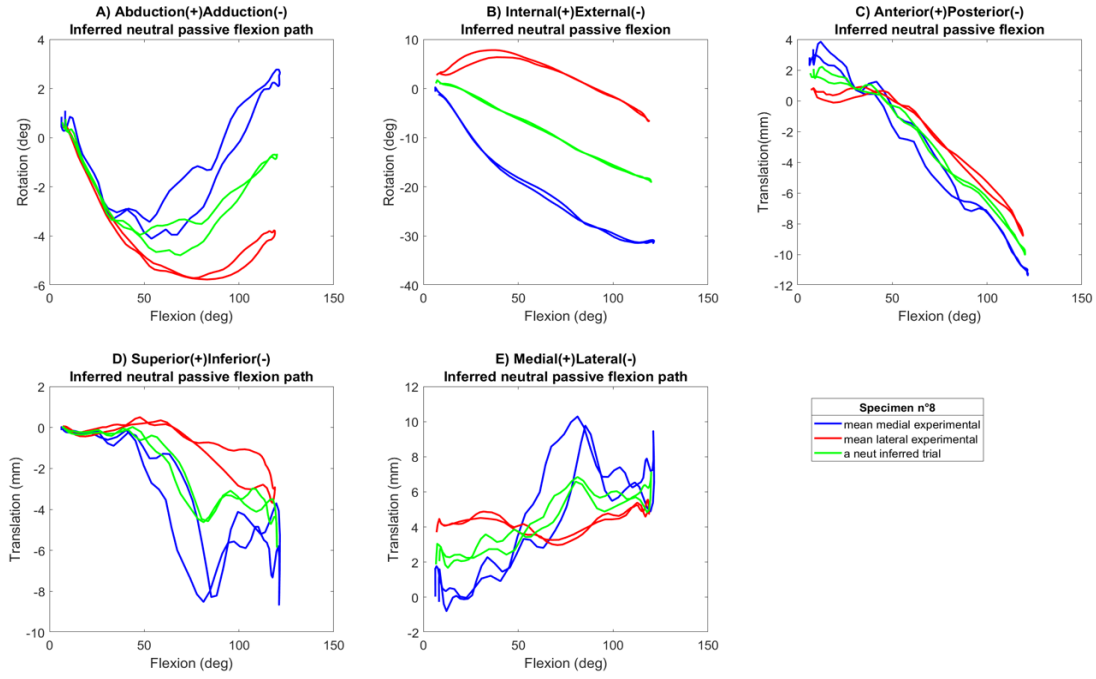

Figure C.1.8.2 *– Specimen8 medial (blue), lateral (red) experimental TF motion and inferred neutral flexion path (green): rotations and translations against FE.*

C.1.9 Specimen 9

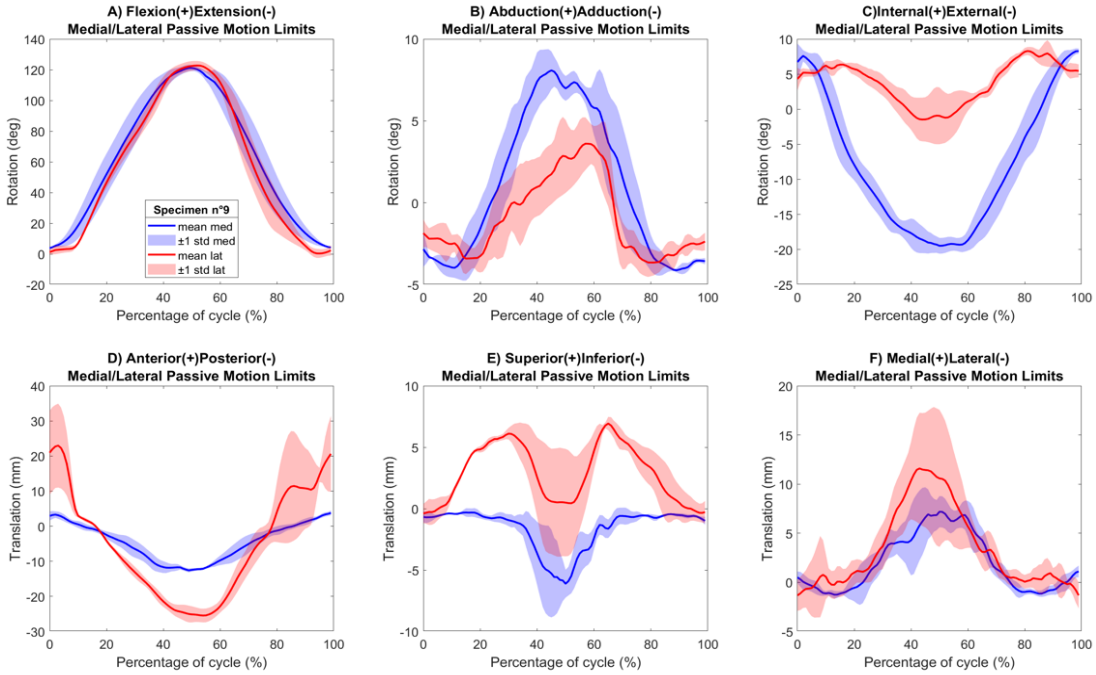

Figure C.1.9.1 *– Specimen9 medial (blue) and lateral (red) experimental TF motion: FE, AA, IE rotations and AP, SI, and ML translations mean and standard deviation.*

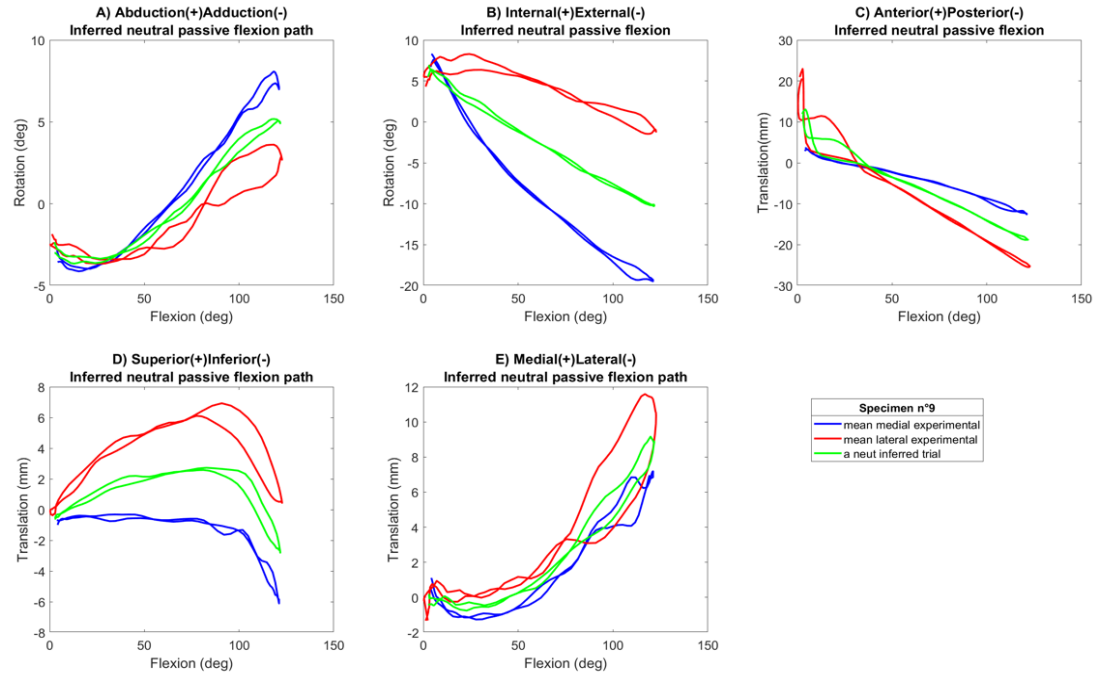

Figure C.1.9.2 *– Specimen9 medial (blue), lateral (red) experimental TF motion and inferred neutral flexion path (green): rotations and translations against FE.*

C.1.10 Specimen 10

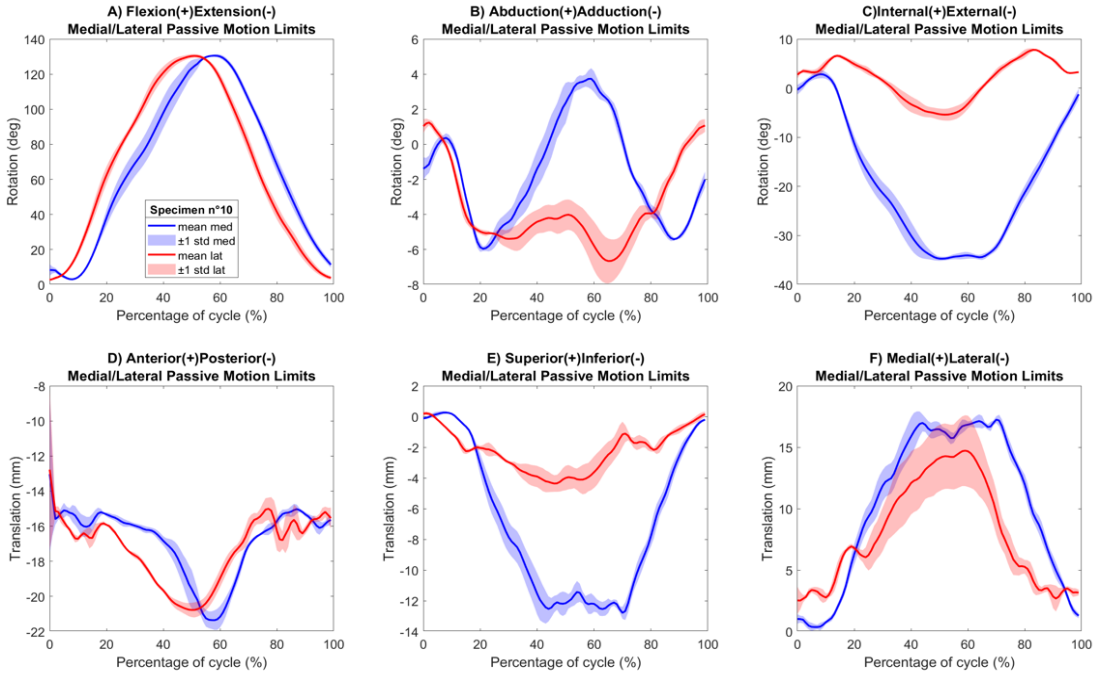

Figure C.1.10.1 *– – Specimen10 medial (blue) and lateral (red) experimental TF motion: FE, AA, IE rotations and AP, SI, and ML translations mean and standard deviation.*

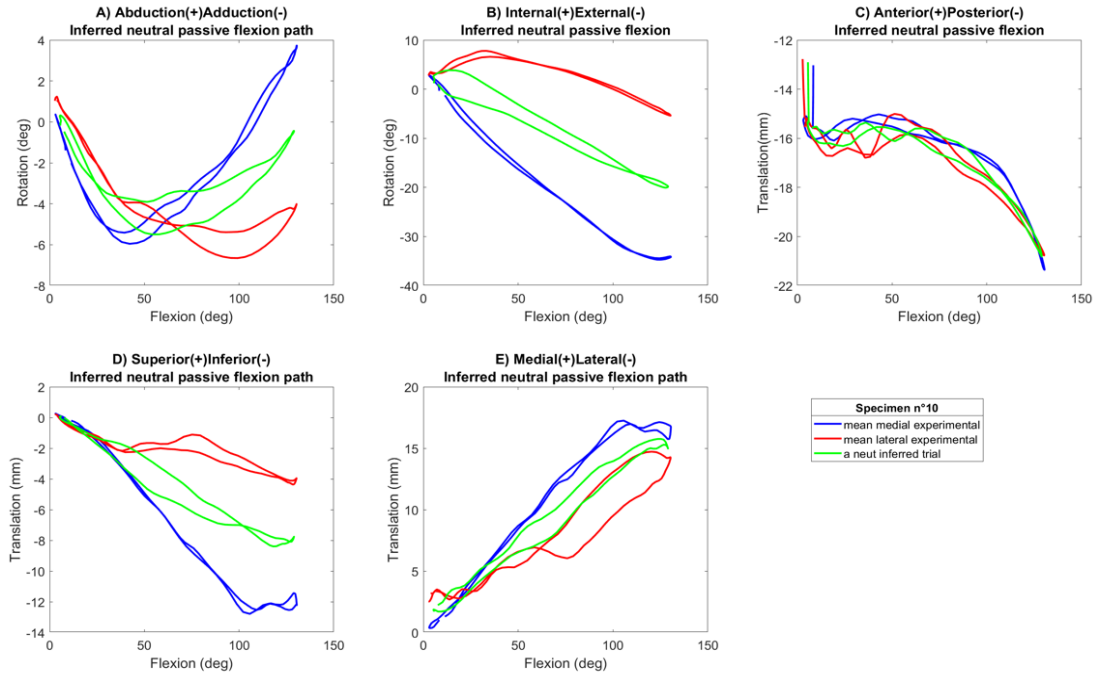

Figure C.1.10.2 *– Specimen10 medial (blue), lateral (red) experimental TF motion and inferred neutral flexion path (green): rotations and translations against FE.*

C.1.11 Specimen 11

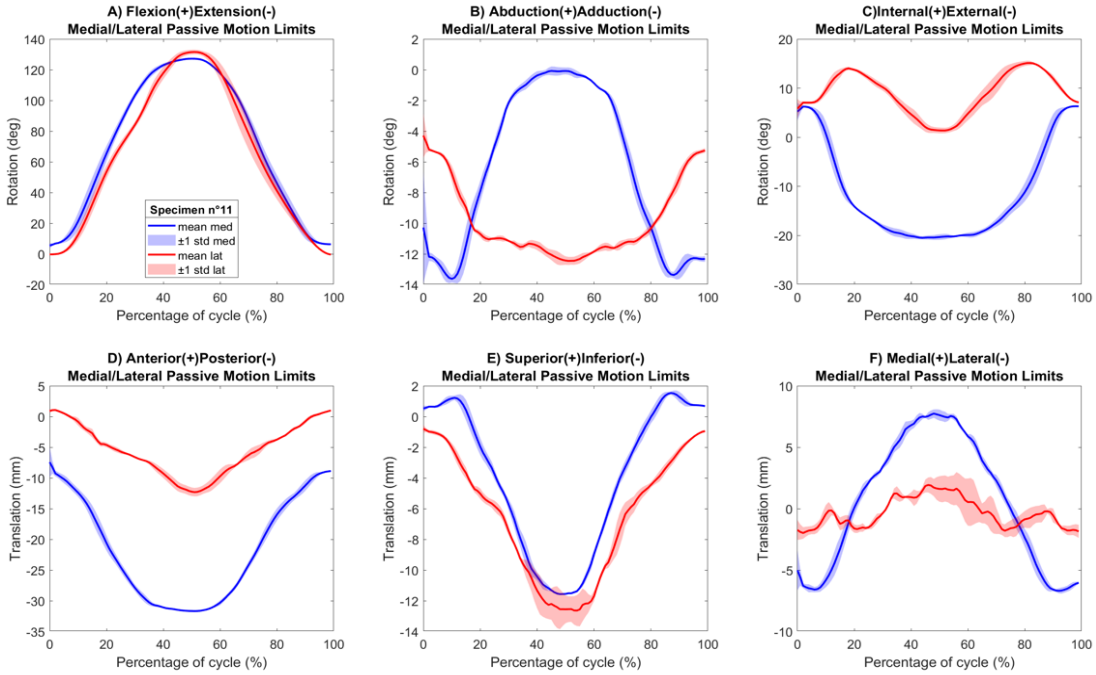

Figure C.1.11.1 *– Specimen11 medial (blue) and lateral (red) experimental TF motion: FE, AA, IE rotations and AP, SI, and ML translations mean and standard deviation.*

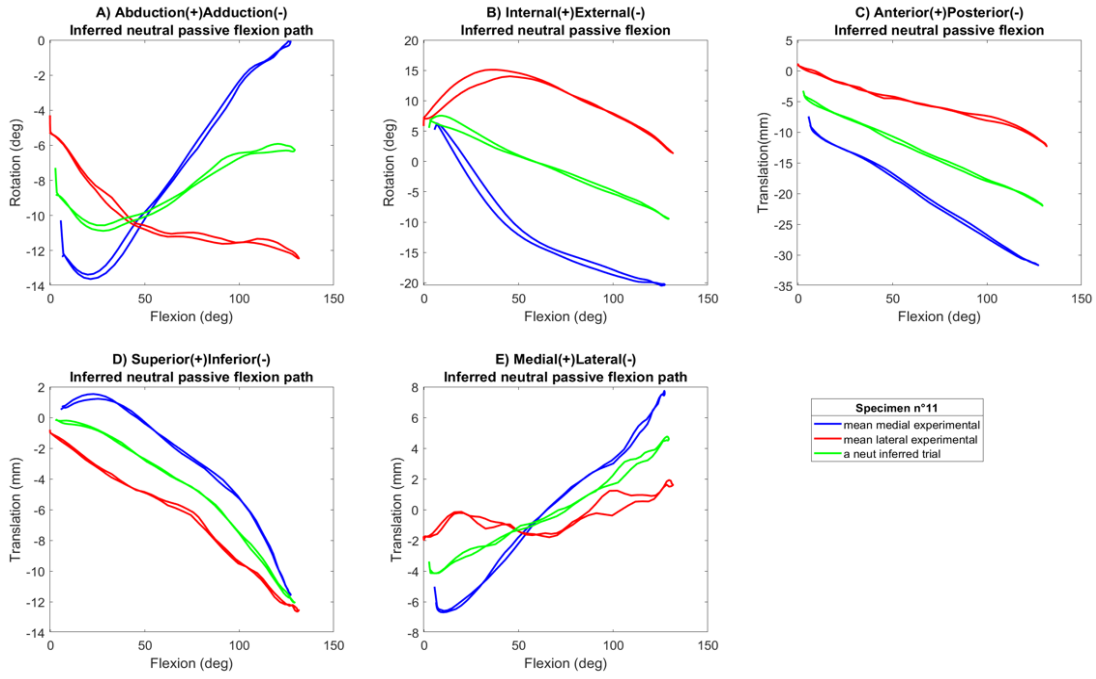

Figure C.1.11.2 *– Specimen11 medial (blue), lateral (red) experimental TF motion and inferred neutral flexion path (green): rotations and translations against FE.*

C.1.12 Specimen 12

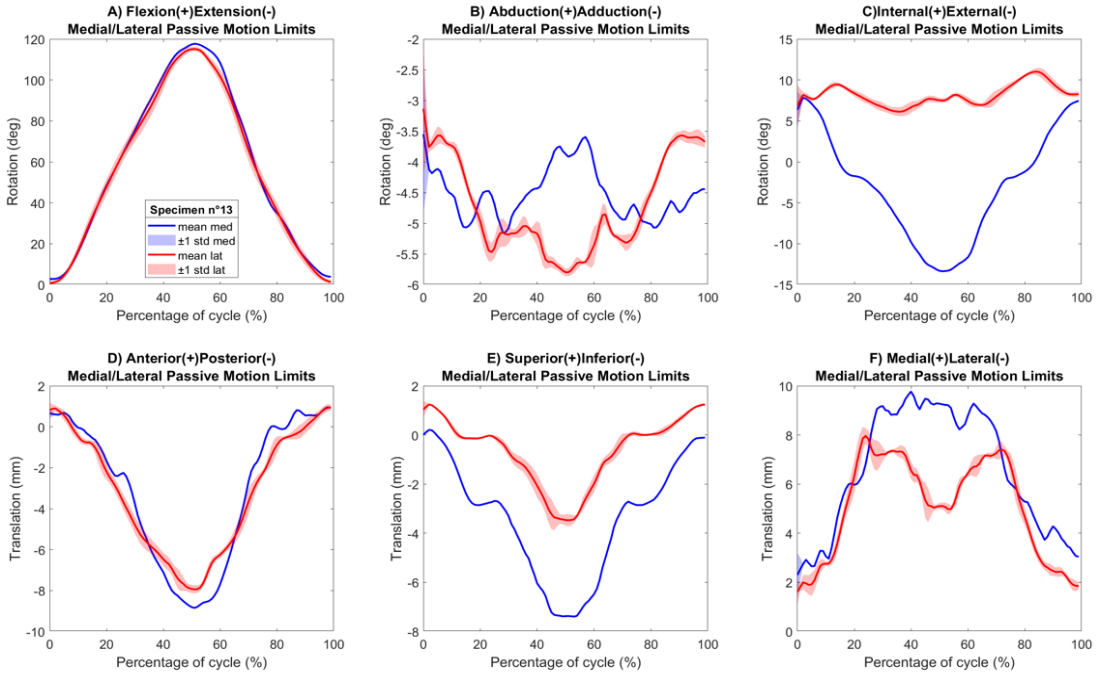

Figure C.1.12.1 *– Specimen12 medial (blue) and lateral (red) experimental TF motion: FE, AA, IE rotations and AP, SI, and ML translations mean and standard deviation.*

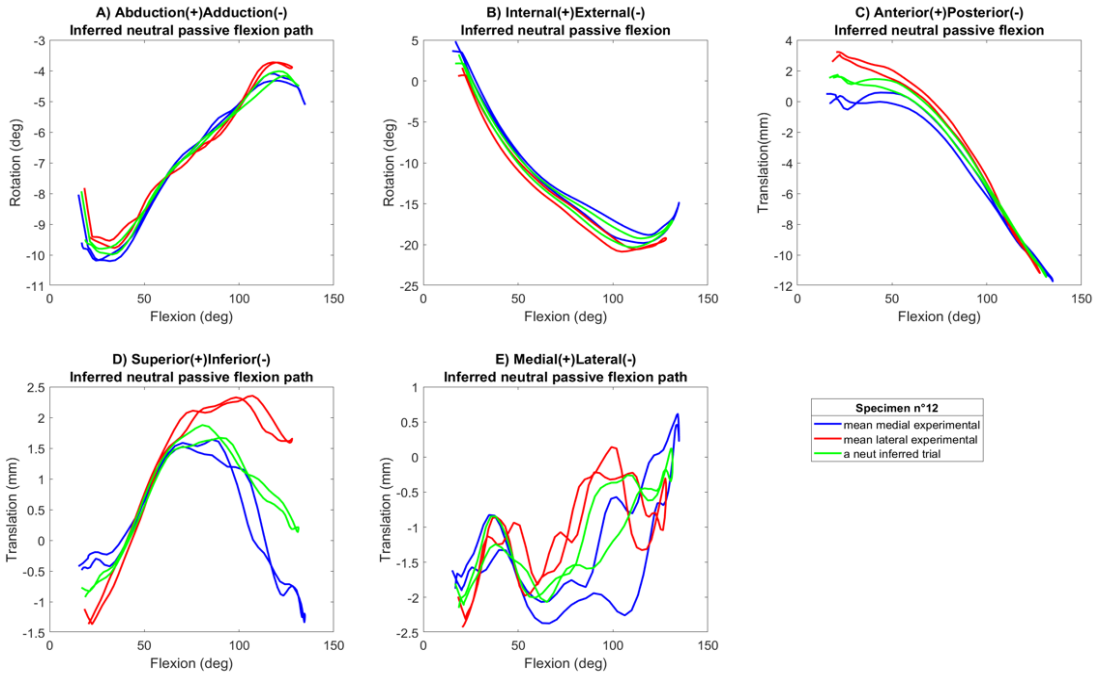

Figure C.1.12.2 *– Specimen12 medial (blue), lateral (red) experimental TF motion and inferred neutral flexion path (green): rotations and translations against FE.*

C.1.13 Specimen 13

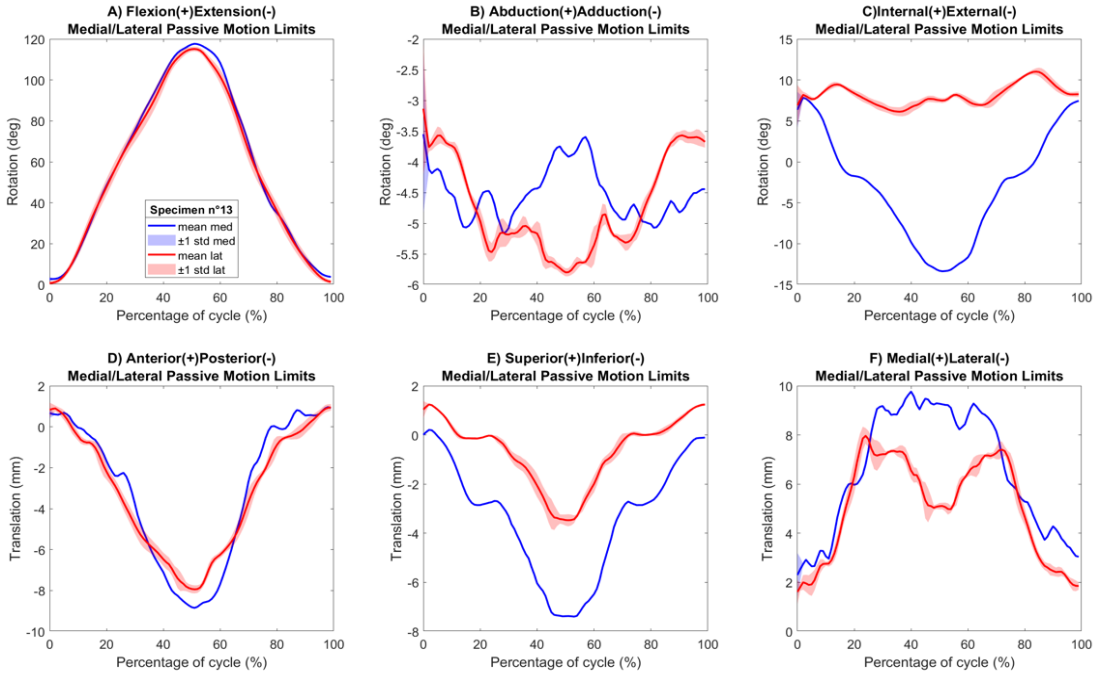

Figure C.1.13.1 *– Specimen13 medial (blue) and lateral (red) experimental TF motion: FE, AA, IE rotations and AP, SI, and ML translations mean and standard deviation.*

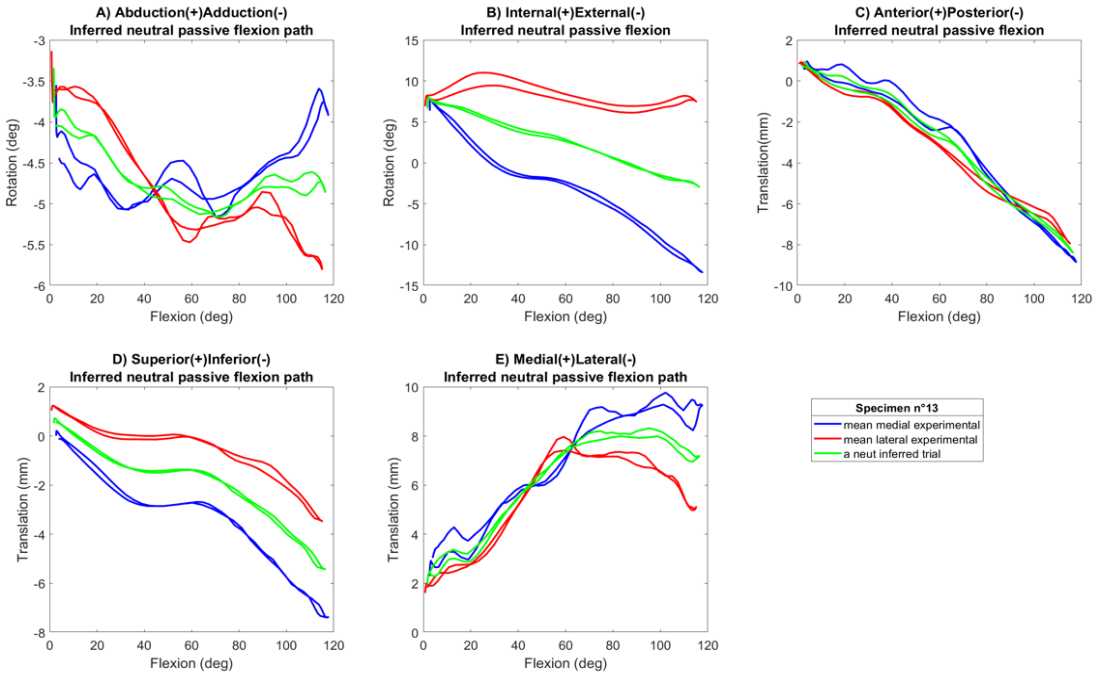

Figure C.1.13.2 *– Specimen13 medial (blue), lateral (red) experimental TF motion and inferred neutral flexion path (green): rotations and translations against FE.*

C.1.14 Specimen 14

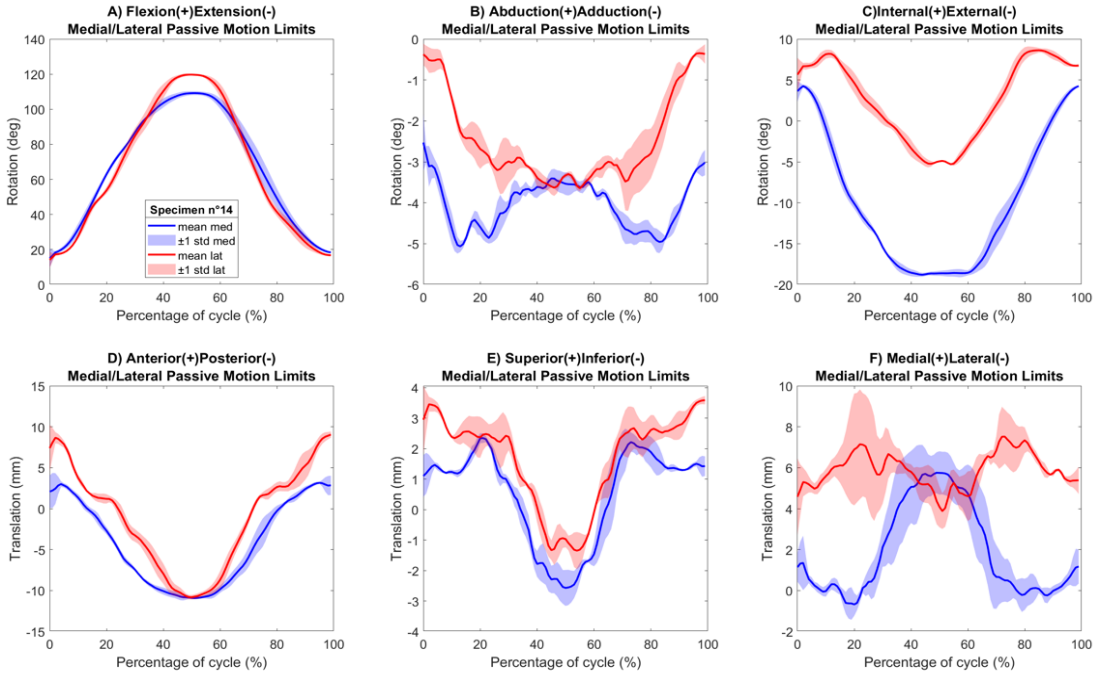

Figure C.1.14.1 *– Specimen14 medial (blue) and lateral (red) experimental TF motion: FE, AA, IE rotations and AP, SI, and ML translations mean and standard deviation.*

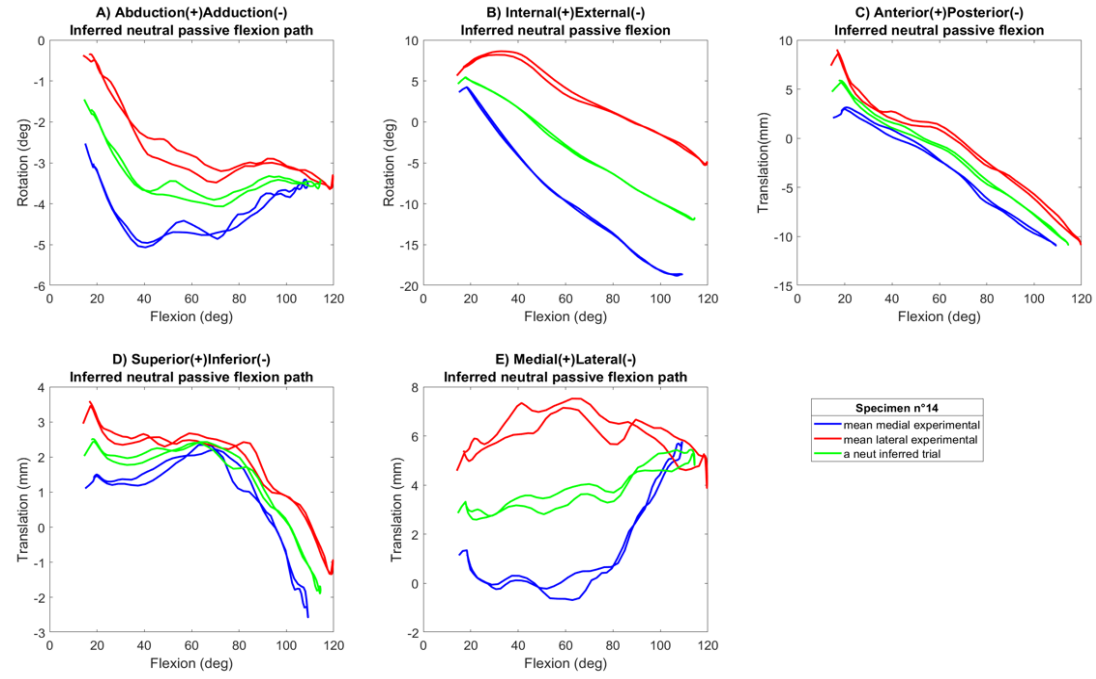

Figure C.1.14.2 *– Specimen14 medial (blue), lateral (red) experimental TF motion and inferred neutral flexion path (green): rotations and translations against FE.*

C.1.15 Specimen 15

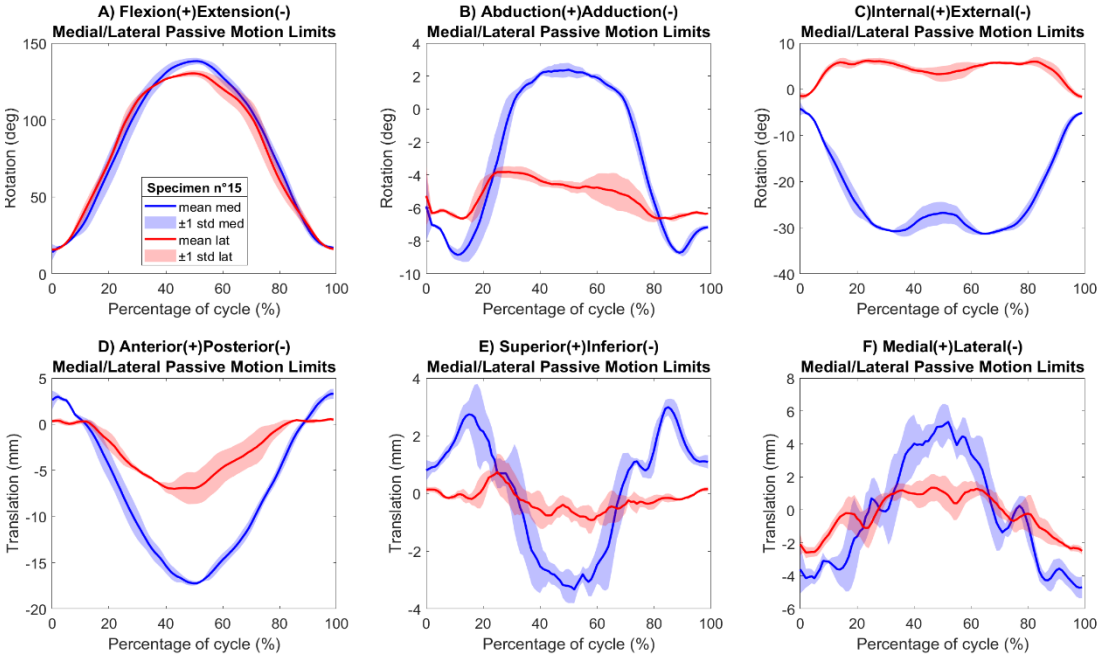

Figure C.1.15.1 *– Specimen15 medial (blue) and lateral (red) experimental TF motion: FE, AA, IE rotations and AP, SI, and ML translations mean and standard deviation.*

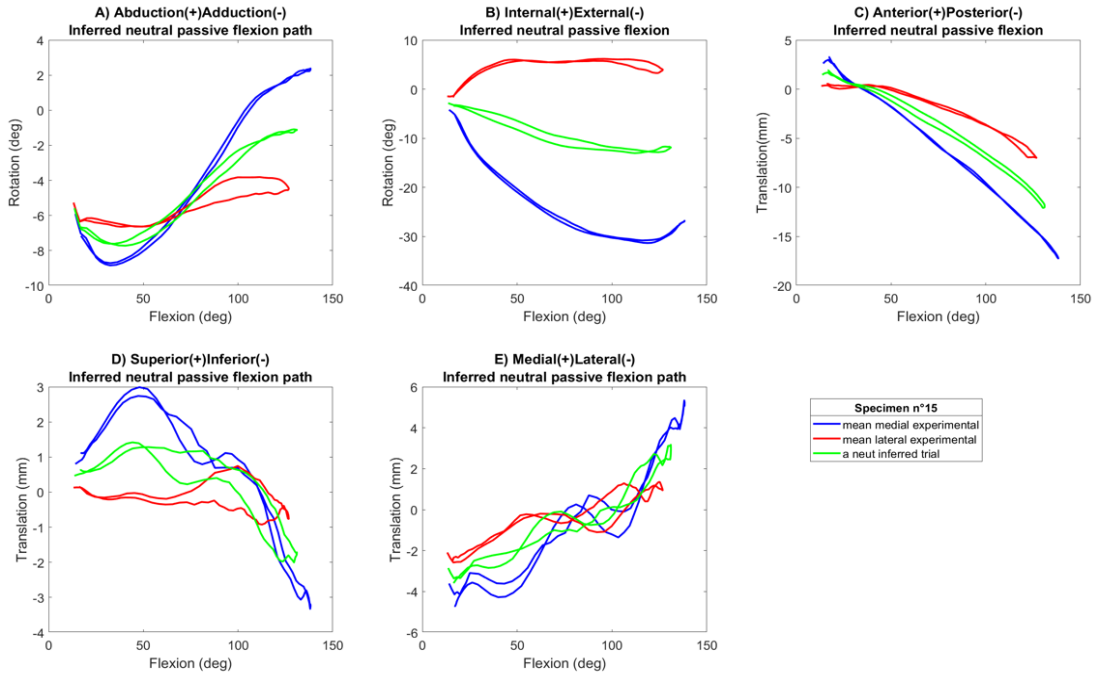

Figure C.1.15.2 *– Specimen15 medial (blue), lateral (red) experimental TF motion and inferred neutral flexion path (green): rotations and translations against FE.*

C.1.16 Specimen 16

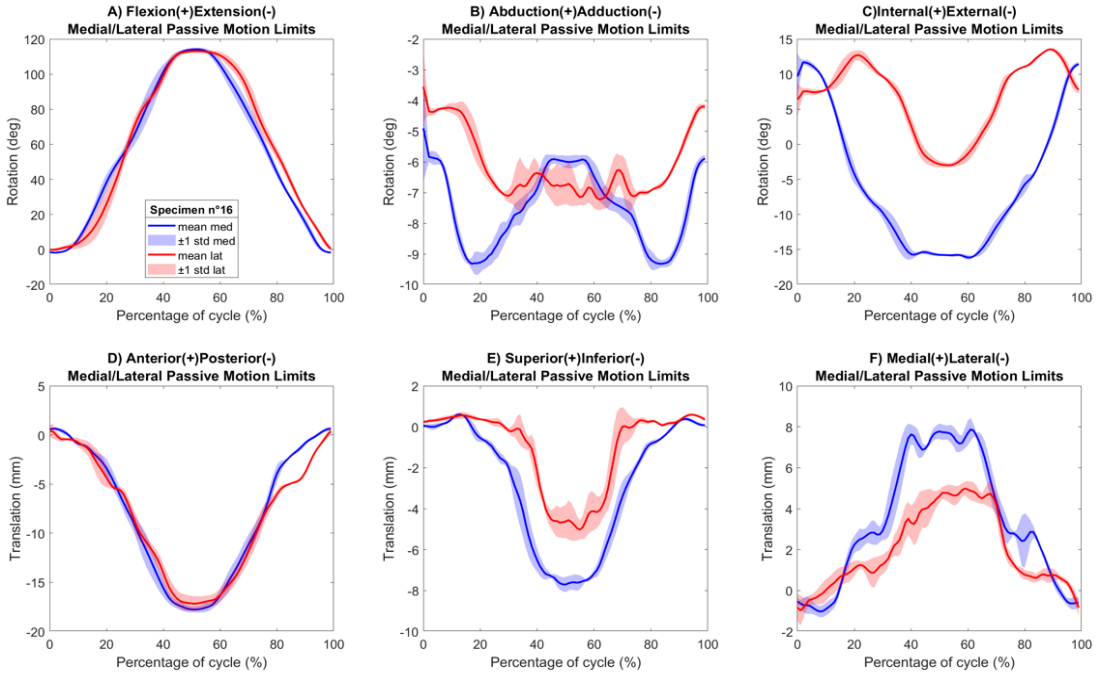

Figure C.1.16.1 *– Specimen16 medial (blue) and lateral (red) experimental TF motion: FE, AA, IE rotations and AP, SI, and ML translations mean and standard deviation.*

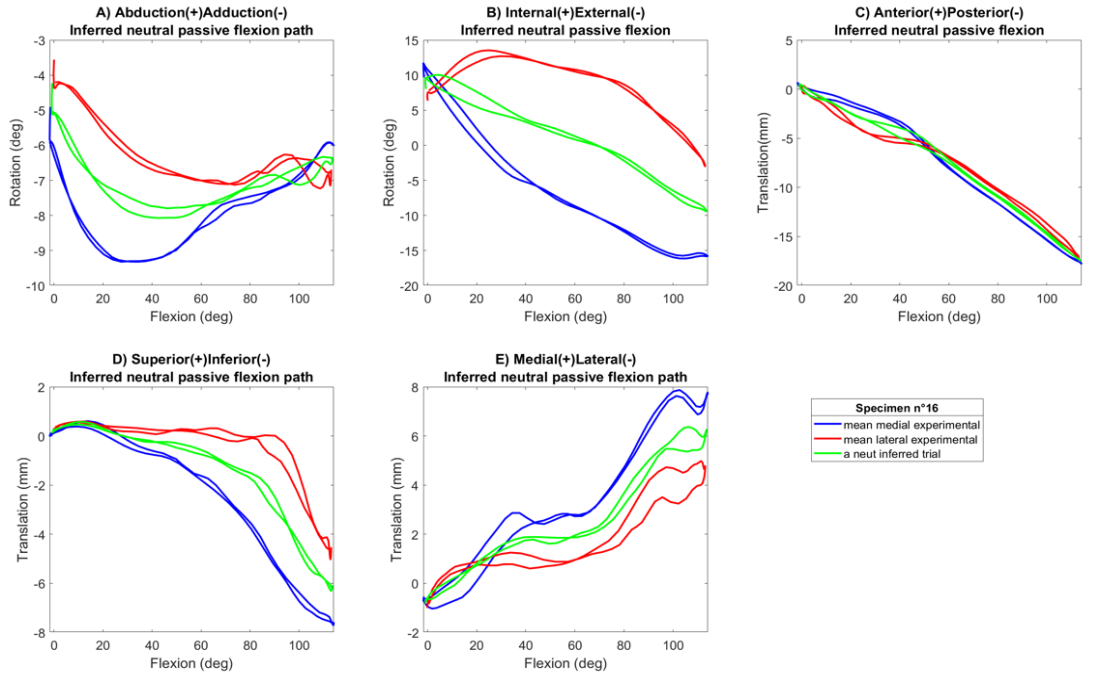

Figure C.1.16.2 *– Specimen16 medial (blue), lateral (red) experimental TF motion and inferred neutral flexion path (green): rotations and translations against FE.*

C.1.17 Specimen 17

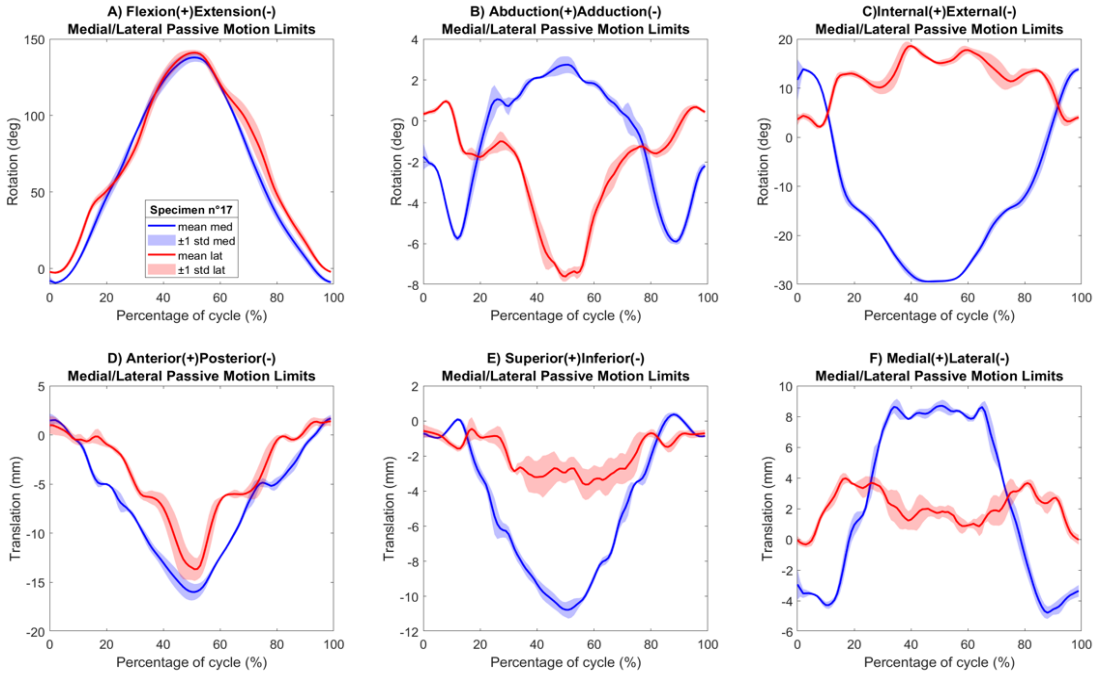

Figure C.1.17.1 *– Specimen17 medial (blue) and lateral (red) experimental TF motion: FE, AA, IE rotations and AP, SI, and ML translations mean and standard deviation.*

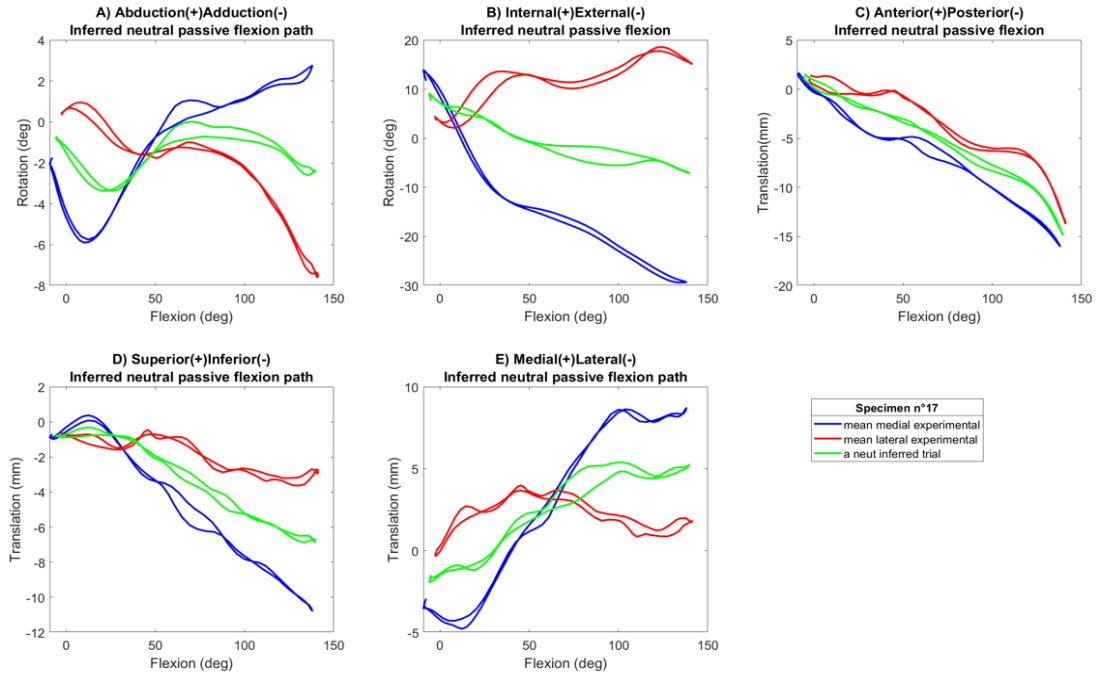

Figure C.1.17.2 *– Specimen17 medial (blue), lateral (red) experimental TF motion and inferred neutral flexion path (green): rotations and translations against FE.*

C.1.18 Specimen 18

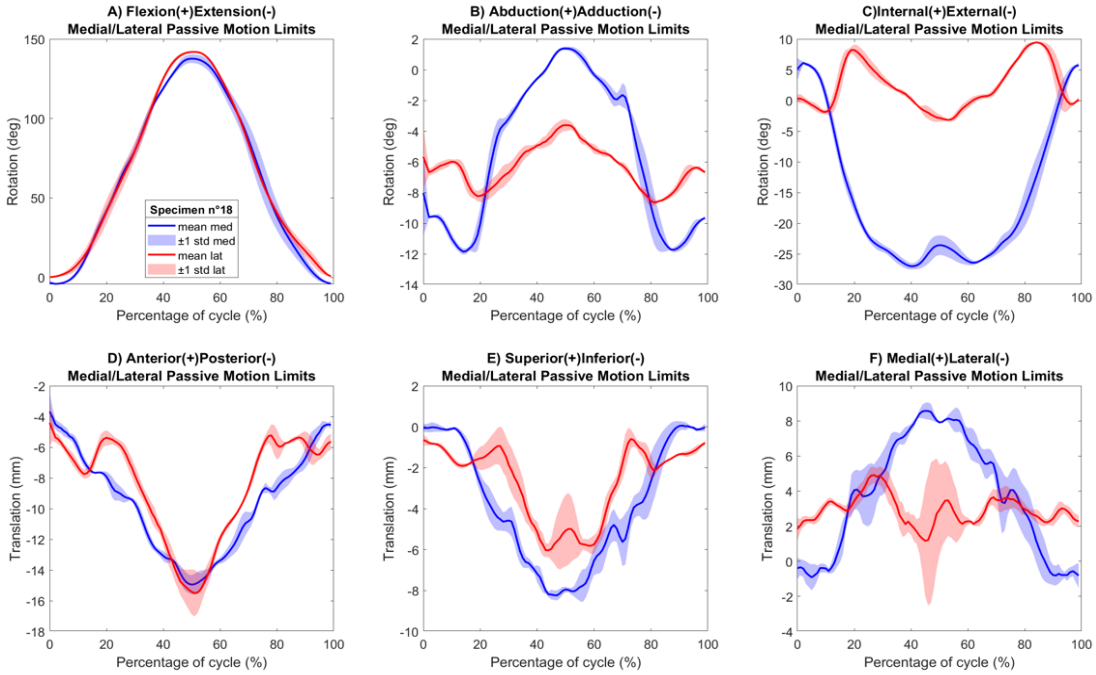

Figure C.1.18.1 *– Specimen18 medial (blue) and lateral (red) experimental TF motion: FE, AA, IE rotations and AP, SI, and ML translations mean and standard deviation.*

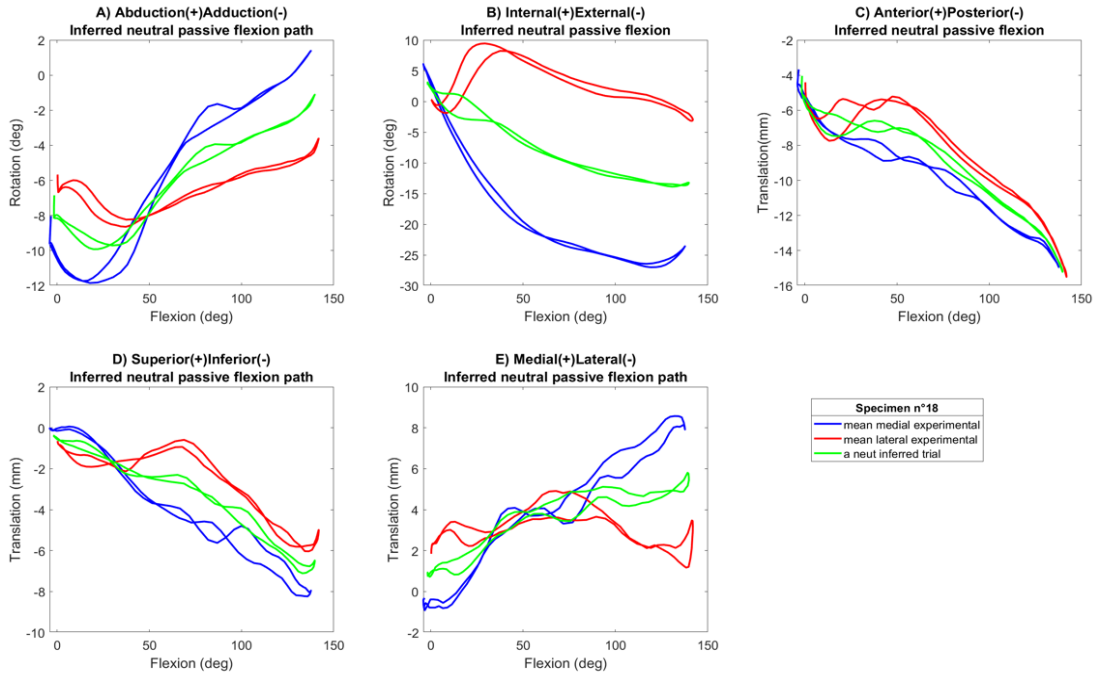

Figure C.1.18.2 *– Specimen18 medial (blue), lateral (red) experimental TF motion and inferred neutral flexion path (green): rotations and translations against FE.*

C.1.19 Specimen 19

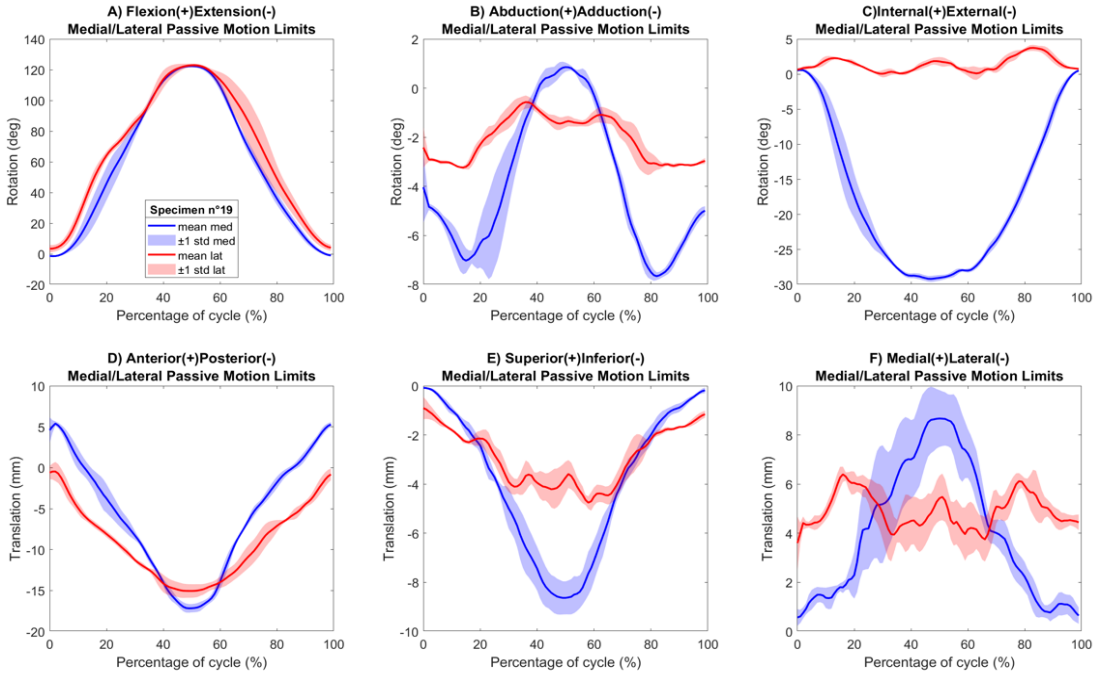

Figure C.1.19.1 *– Specimen19 medial (blue) and lateral (red) experimental TF motion: FE, AA, IE rotations and AP, SI, and ML translations mean and standard deviation.*

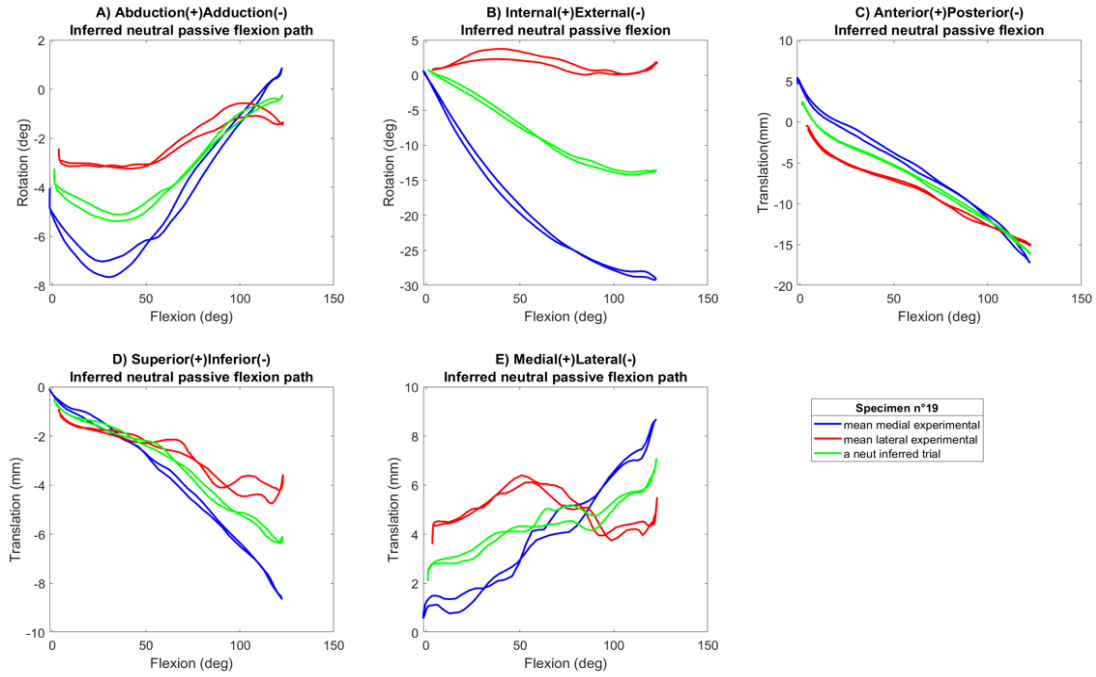

Figure C.1.19.2 *– Specimen19 medial (blue), lateral (red) experimental TF motion and inferred neutral flexion path (green): rotations and translations against FE.*

C.1.20 Specimen 20

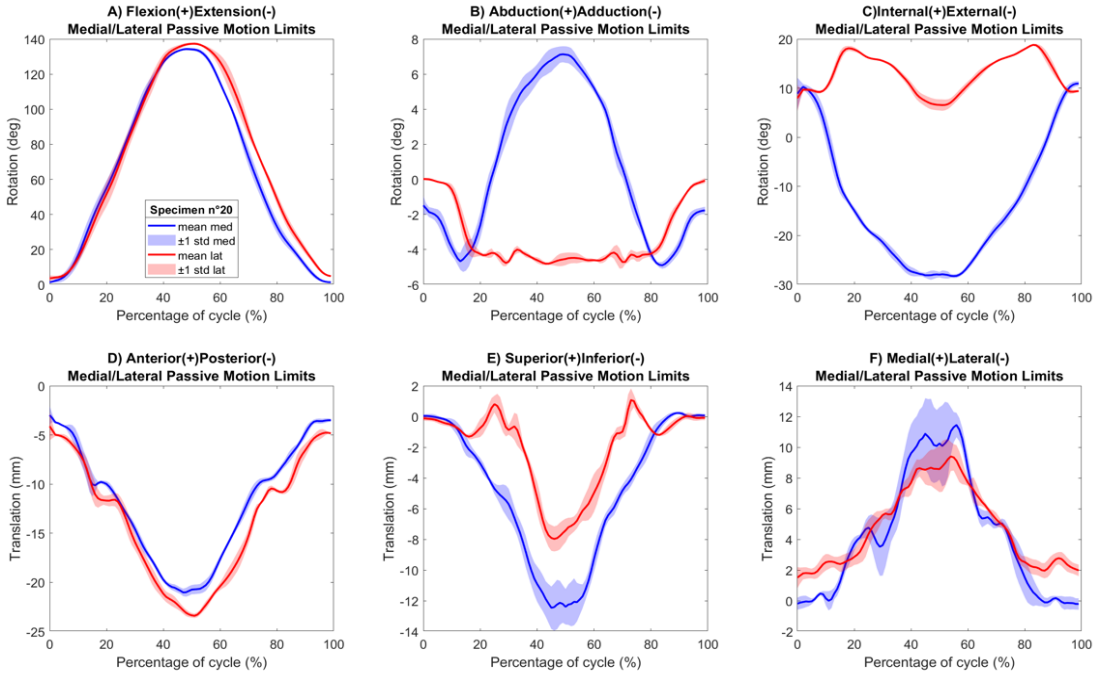

Figure C.1.20.1 *– Specimen20 medial (blue) and lateral (red) experimental TF motion: FE, AA, IE rotations and AP, SI, and ML translations mean and standard deviation.*

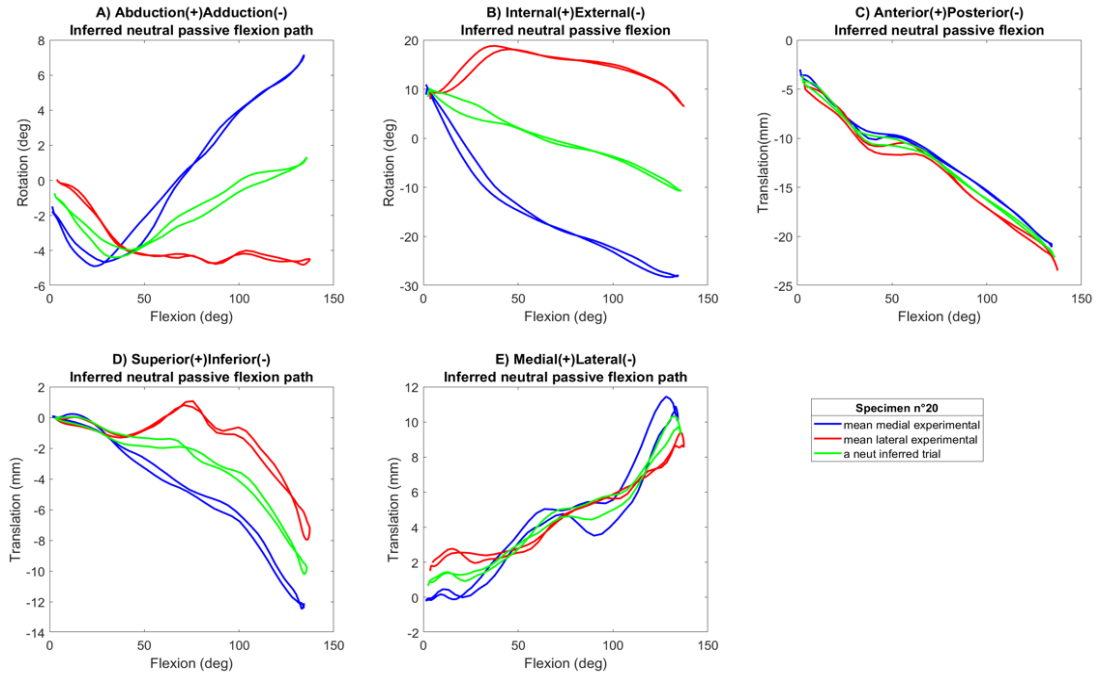

Figure C.1.20.2 *– Specimen20 medial (blue), lateral (red) experimental TF motion and inferred neutral flexion path (green): rotations and translations against FE.*

C.1.21 Specimen 21

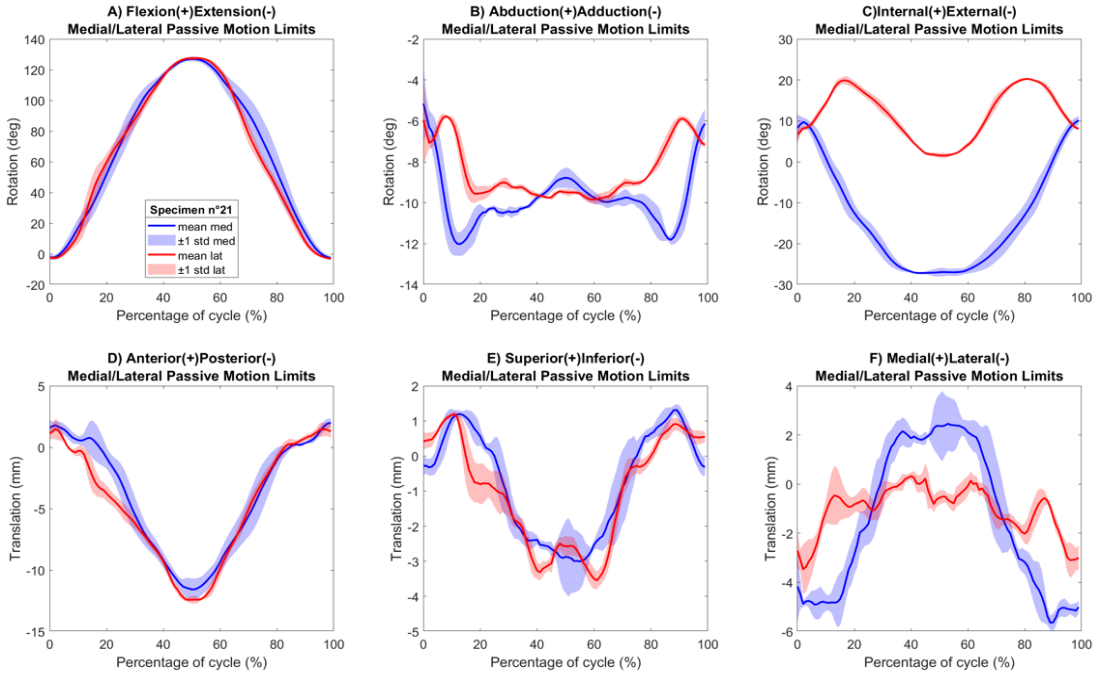

Figure C.1.21.1 *– Specimen21 medial (blue) and lateral (red) experimental TF motion: FE, AA, IE rotations and AP, SI, and ML translations mean and standard deviation.*

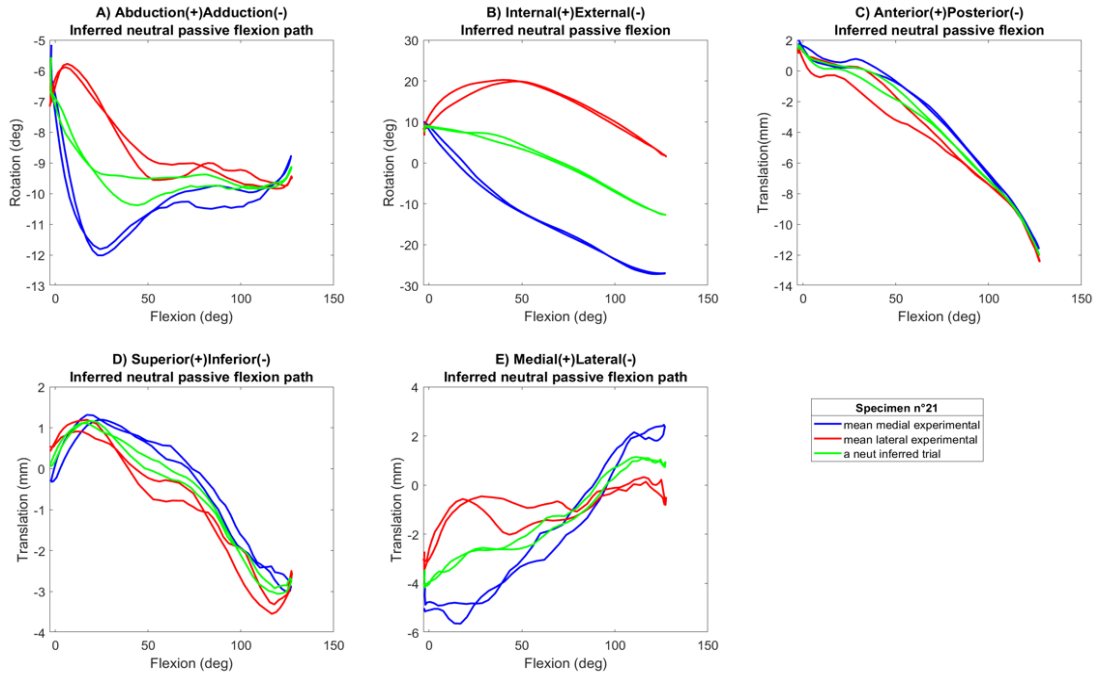

Figure C.1.21.2 *– Specimen21 medial (blue), lateral (red) experimental TF motion and inferred neutral flexion path (green): rotations and translations against FE.*

C.1.22Specimen 22

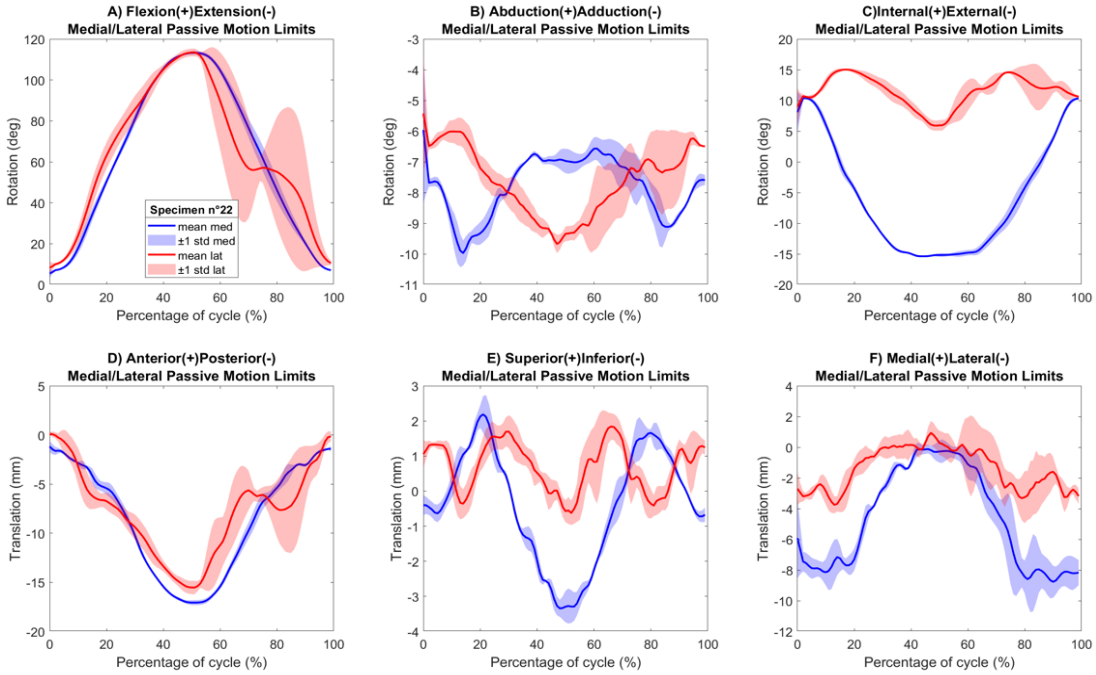

Figure C.1.22.1 *– Specimen22 medial (blue) and lateral (red) experimental TF motion: FE, AA, IE rotations and AP, SI, and ML translations mean and standard deviation.*

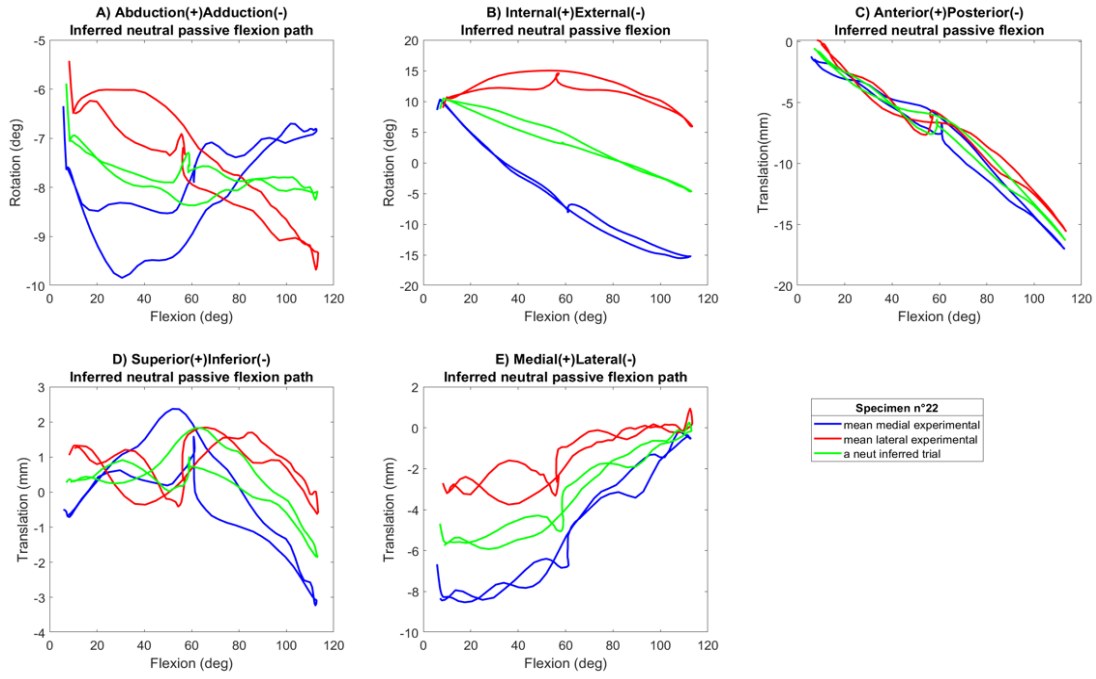

Figure C.1.22.2 *– Specimen22 medial (blue), lateral (red) experimental TF motion and inferred neutral flexion path (green): rotations and translations against FE.*

C.1.23Specimen 23

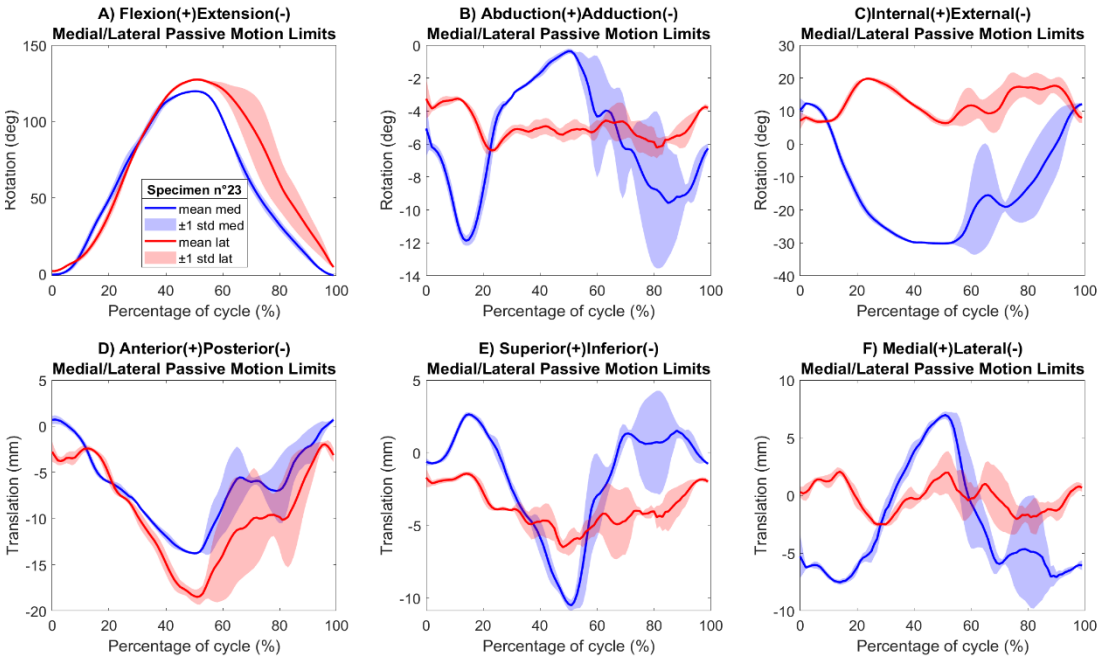

Figure C.1.23.1 *– Specimen23 medial (blue) and lateral (red) experimental TF motion: FE, AA, IE rotations and AP, SI, and ML translations mean and standard deviation.*

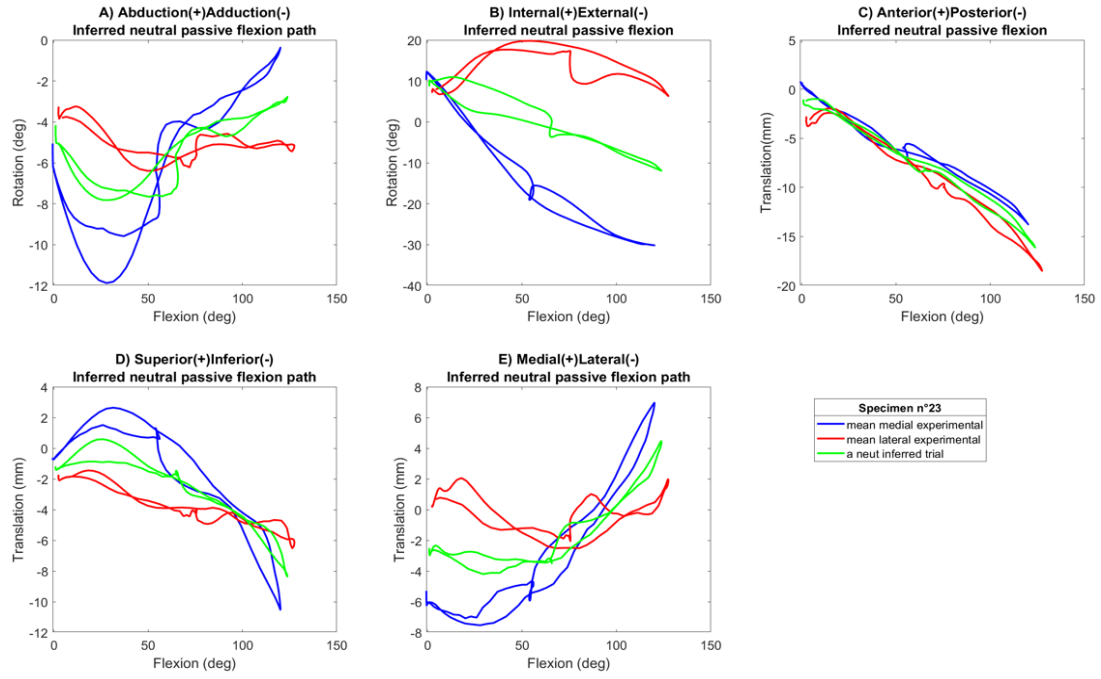

Figure C.1.23.2 *– Specimen23 medial (blue), lateral (red) experimental TF motion and inferred neutral flexion path (green): rotations and translations against FE.*

C.1.24Specimen 24

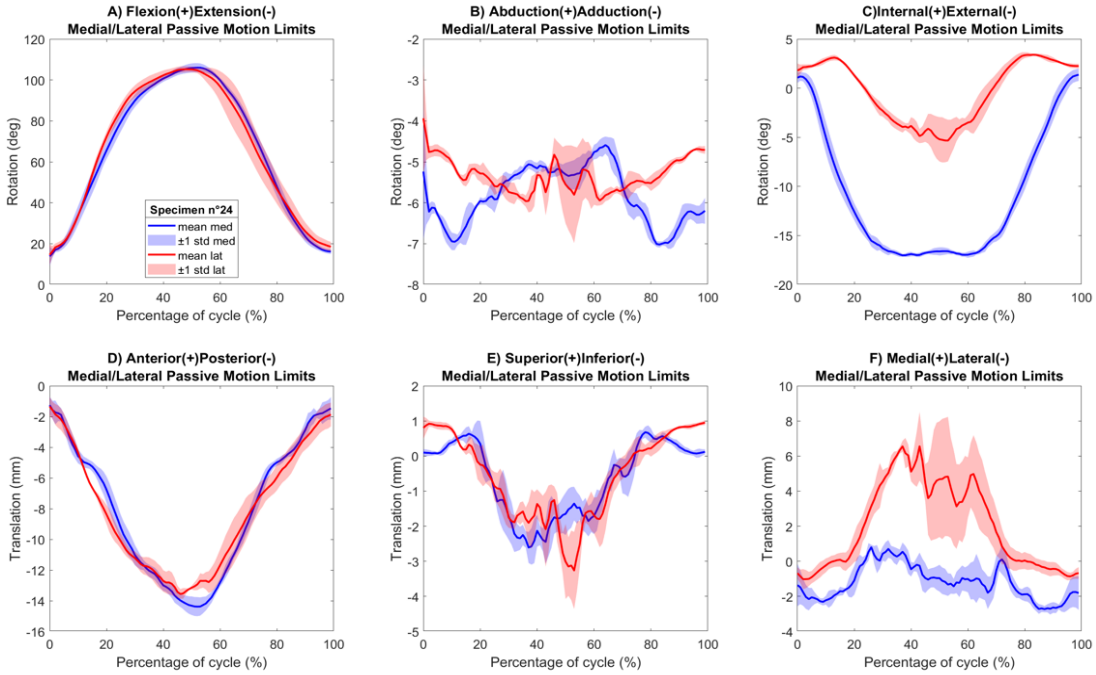

Figure C.1.24.1 *– Specimen24 medial (blue) and lateral (red) experimental TF motion: FE, AA, IE rotations and AP, SI, and ML translations mean and standard deviation.*

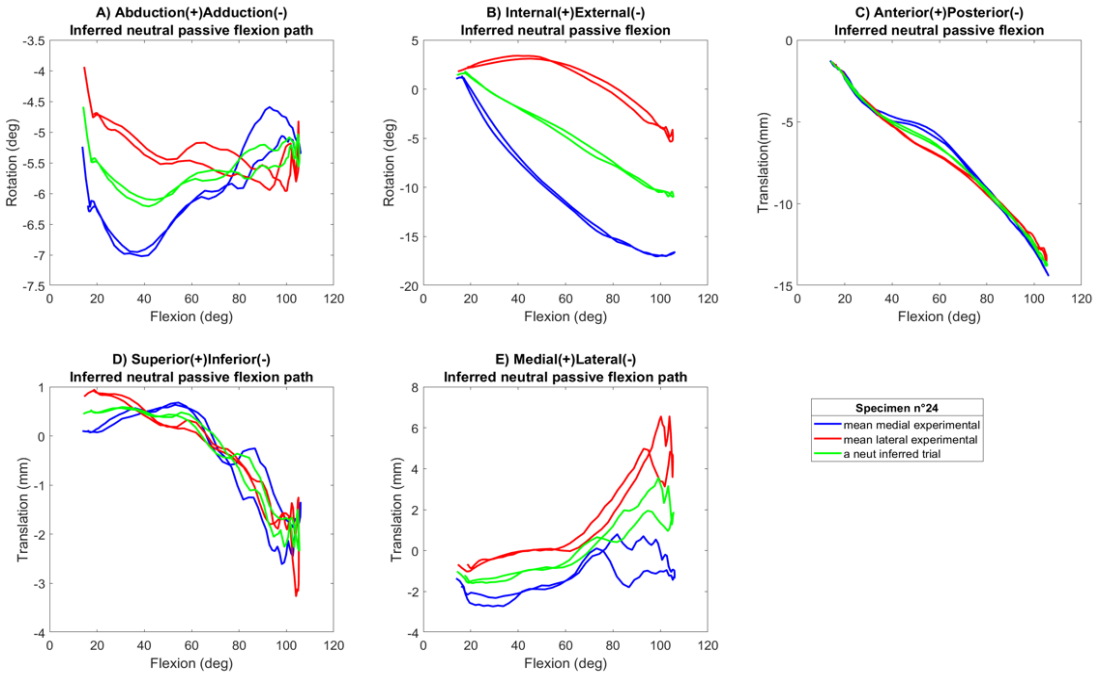

Figure C.1.24.2 *– Specimen24 medial (blue), lateral (red) experimental TF motion and inferred neutral flexion path (green): rotations and translations against FE.*

C.1.25 Specimen 25

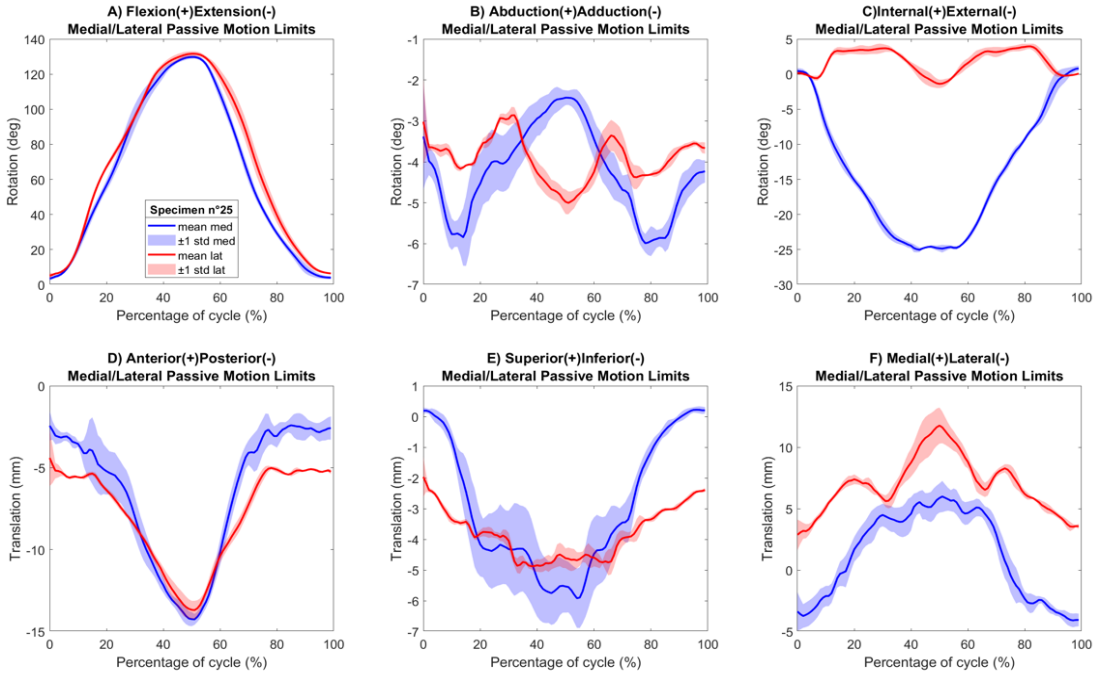

Figure C.1.25.1 *– Specimen25 medial (blue) and lateral (red) experimental TF motion: FE, AA, IE rotations and AP, SI, and ML translations mean and standard deviation.*

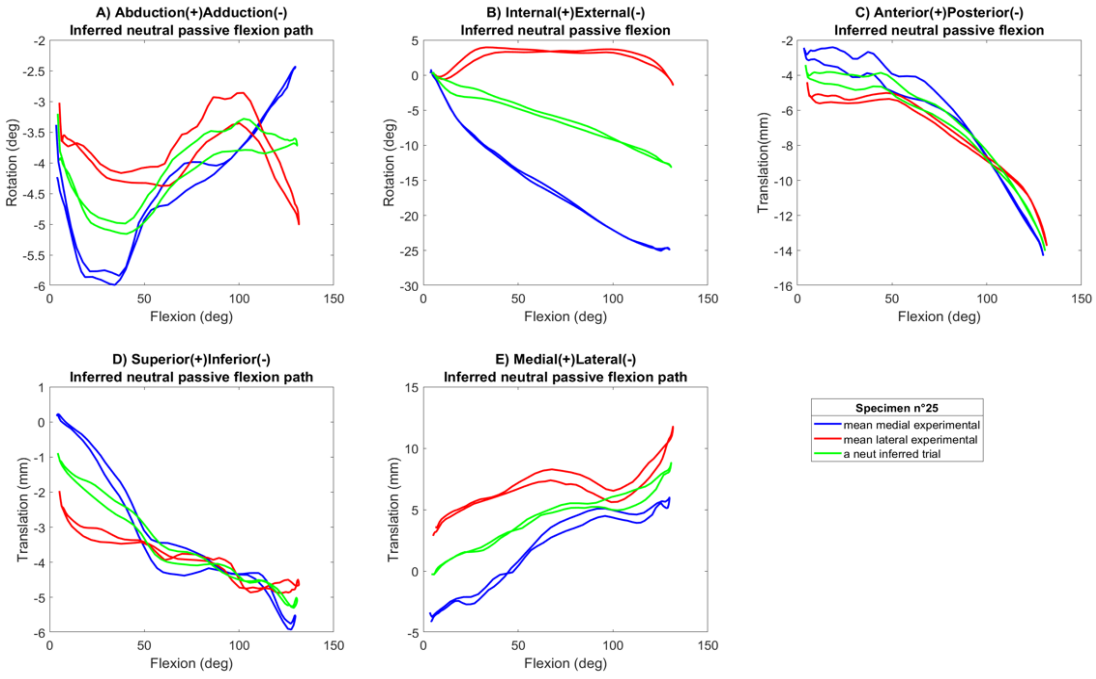

Figure C.1.25.2 *– Specimen25 medial (blue), lateral (red) experimental TF motion and inferred neutral flexion path (green): rotations and translations against FE.*

C.1.26Specimen 26

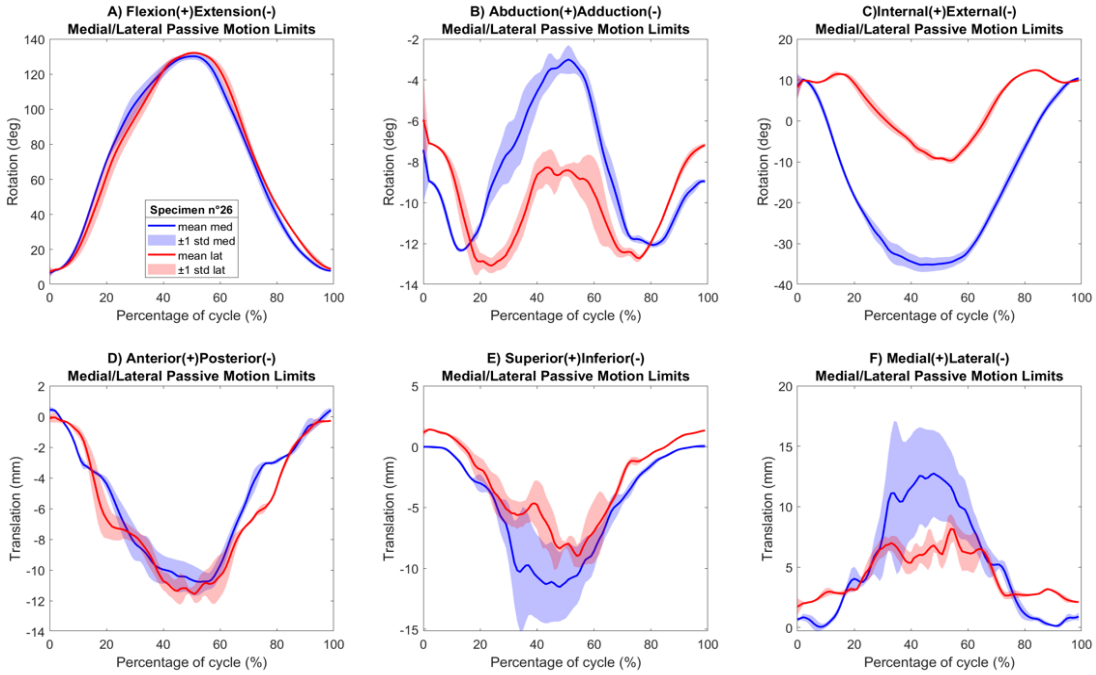

Figure C.1.26.1 *– Specimen26 medial (blue) and lateral (red) experimental TF motion: FE, AA, IE rotations and AP, SI, and ML translations mean and standard deviation.*

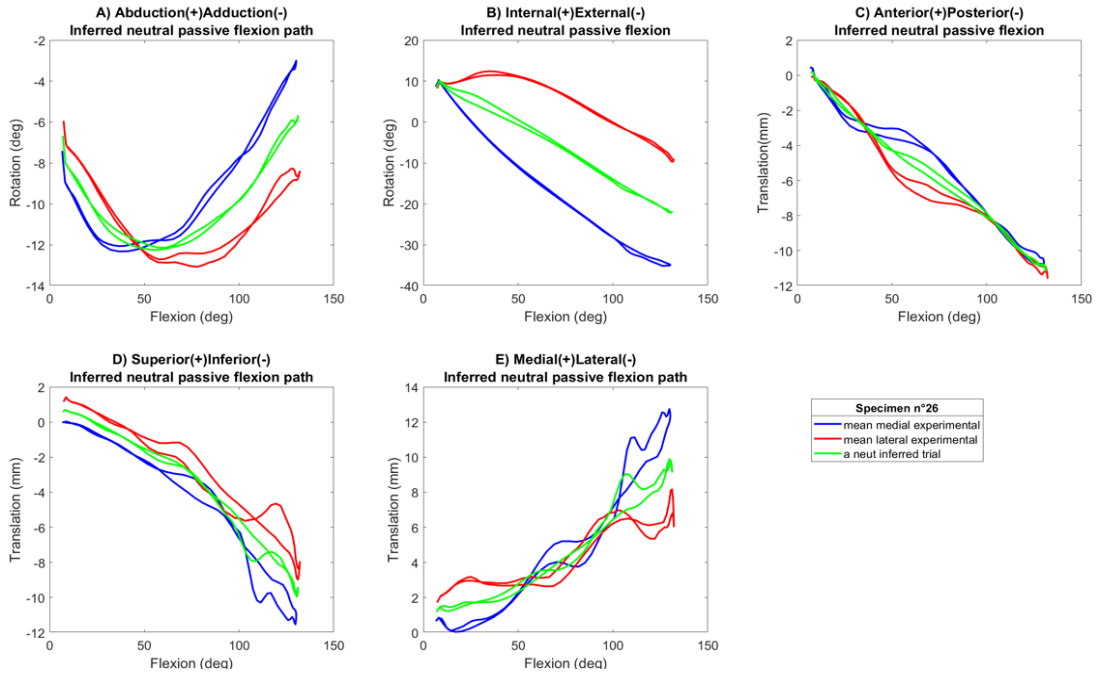

Figure C.1.26.2 *– Specimen26 medial (blue), lateral (red) experimental TF motion and inferred neutral flexion path (green): rotations and translations against FE.*

C.1.27 Specimen 27

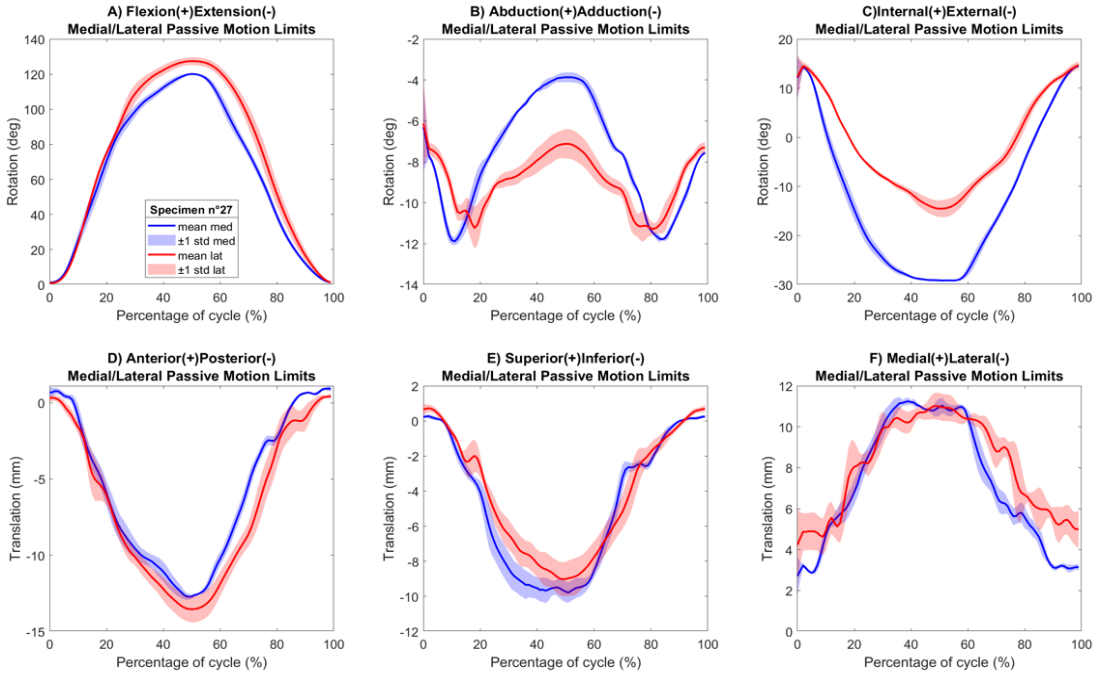

Figure C.1.27.1 *– Specimen27 medial (blue) and lateral (red) experimental TF motion: FE, AA, IE rotations and AP, SI, and ML translations mean and standard deviation.*

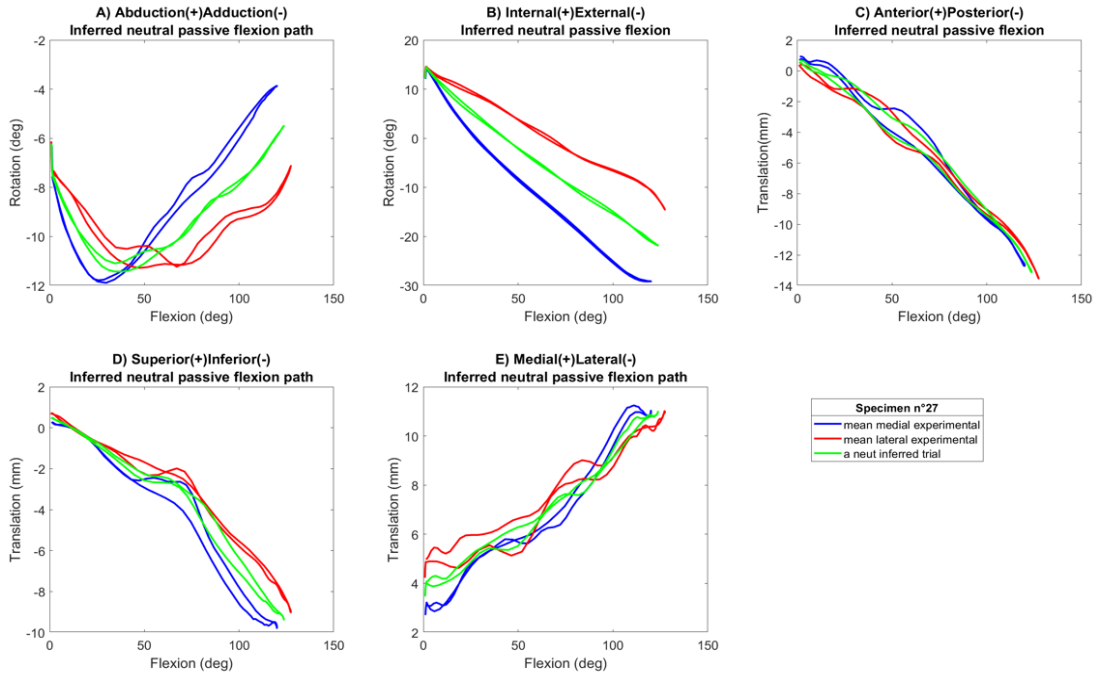

Figure C.1.27.2 *– Specimen27 medial (blue), lateral (red) experimental TF motion and inferred neutral flexion path (green): rotations and translations against FE.*

C.1.28 Specimen 28

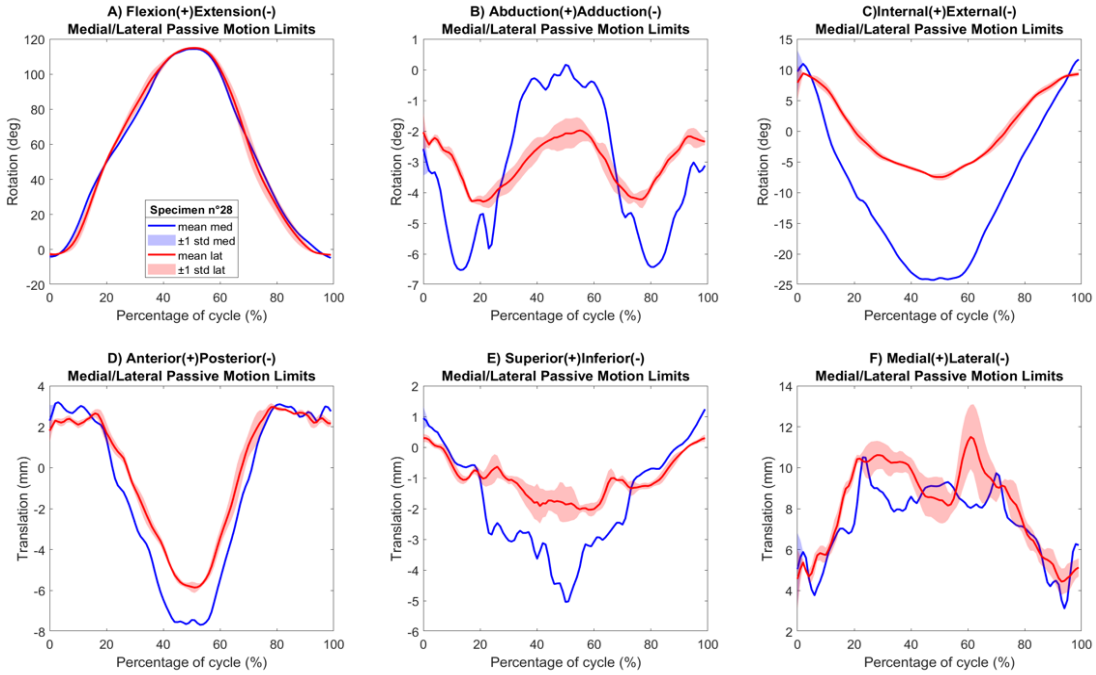

Figure C.1.28.1 – *Specimen28 medial (blue) and lateral (red) experimental TF motion: FE, AA, IE rotations and AP, SI, and ML translations mean and standard deviation.*

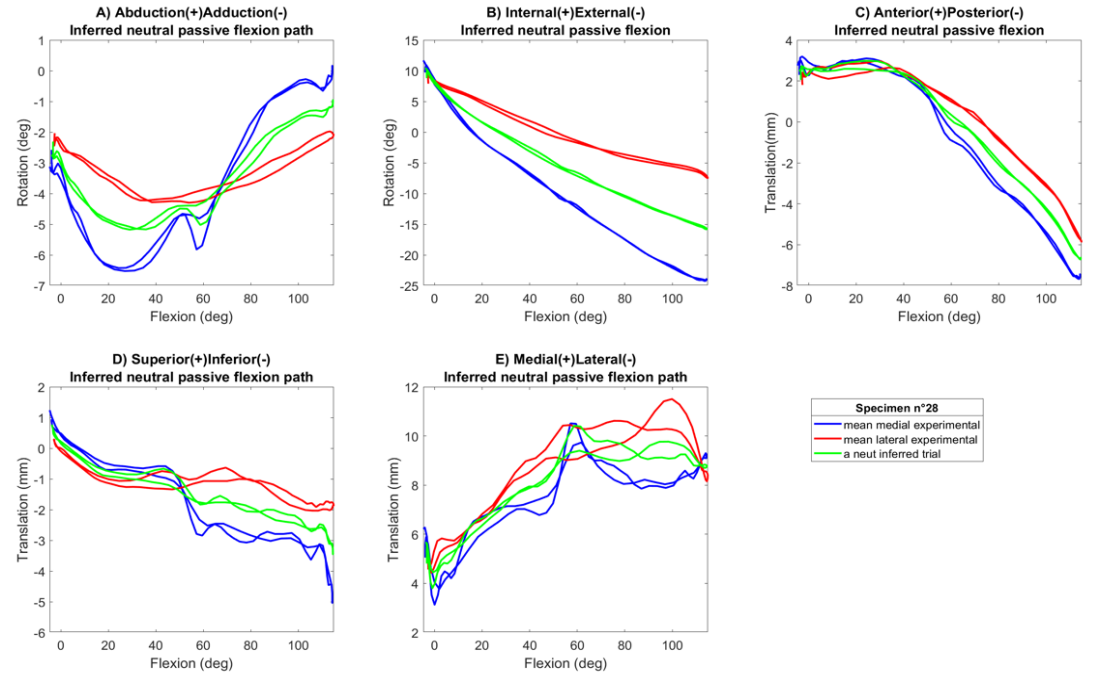

Figure C.1.28.2 *– Specimen28 medial (blue), lateral (red) experimental TF motion and inferred neutral flexion path (green): rotations and translations against FE.*

C.1.29Specimen 29

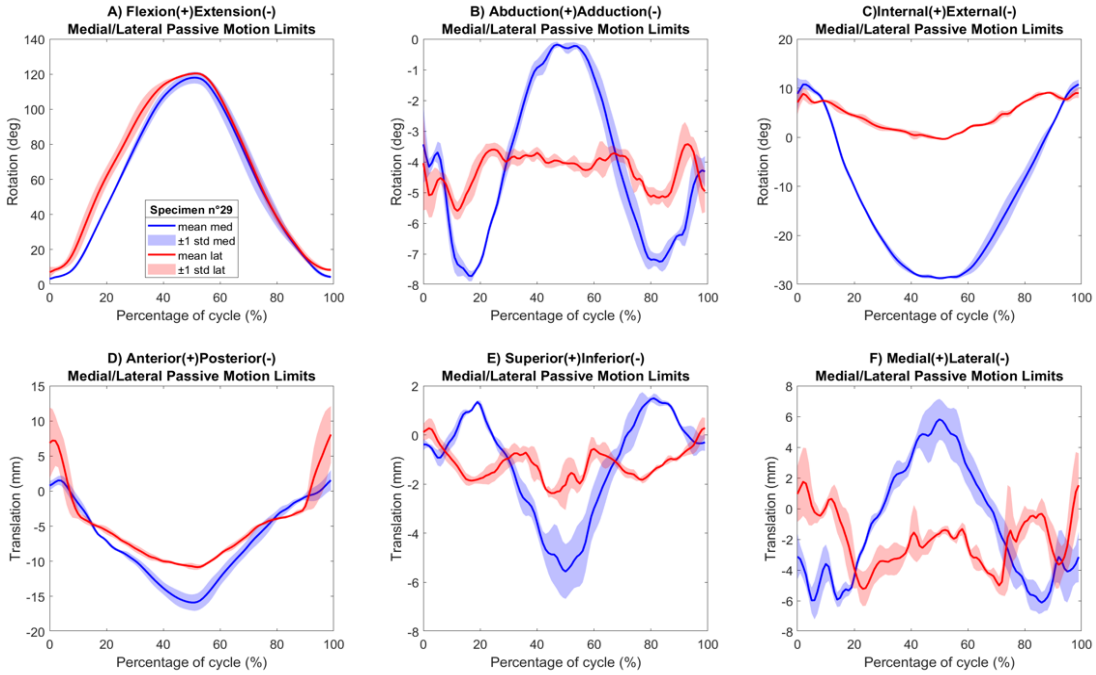

Figure C.1.29.1 *– Specimen29 medial (blue) and lateral (red) experimental TF motion: FE, AA, IE rotations and AP, SI, and ML translations mean and standard deviation.*

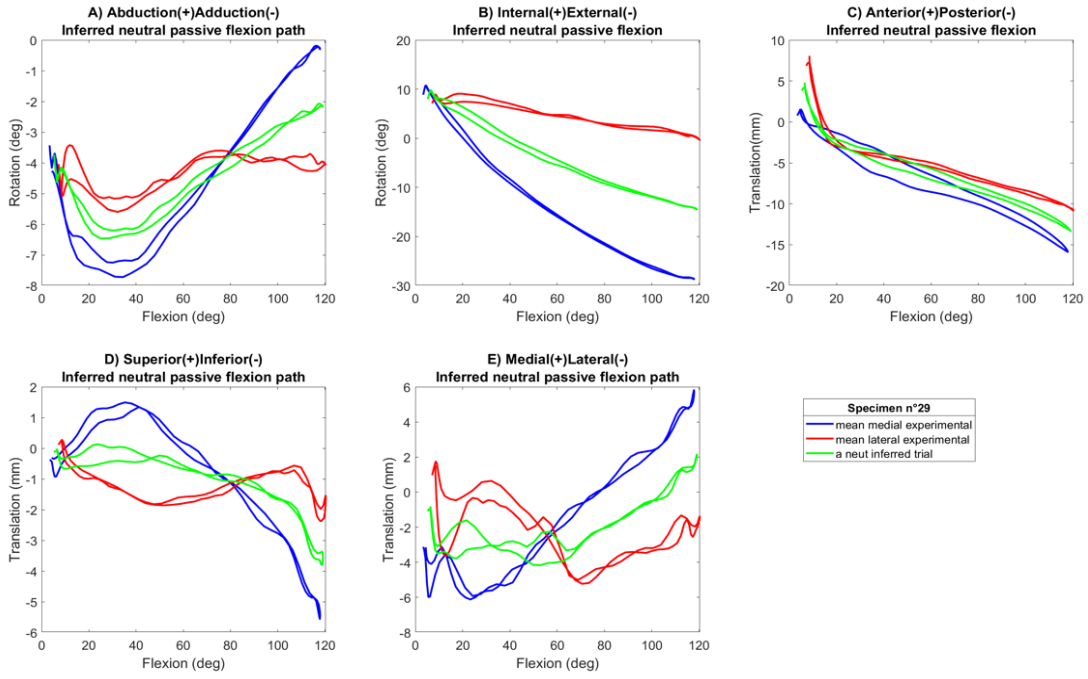

Figure C.1.29.2 *– Specimen29 medial (blue), lateral (red) experimental TF motion and inferred neutral flexion path (green): rotations and translations against FE.*

C.1.30 Specimen 30

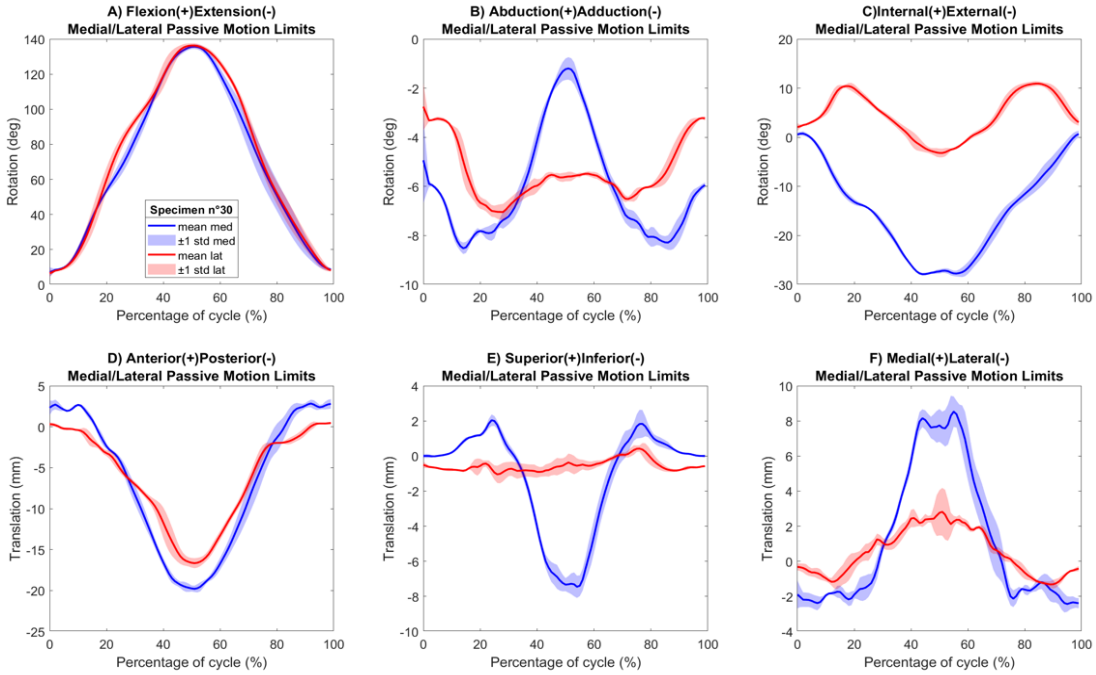

Figure C.1.30.1 *– Specimen30 medial (blue) and lateral (red) experimental TF motion: FE, AA, IE rotations and AP, SI, and ML translations mean and standard deviation.*

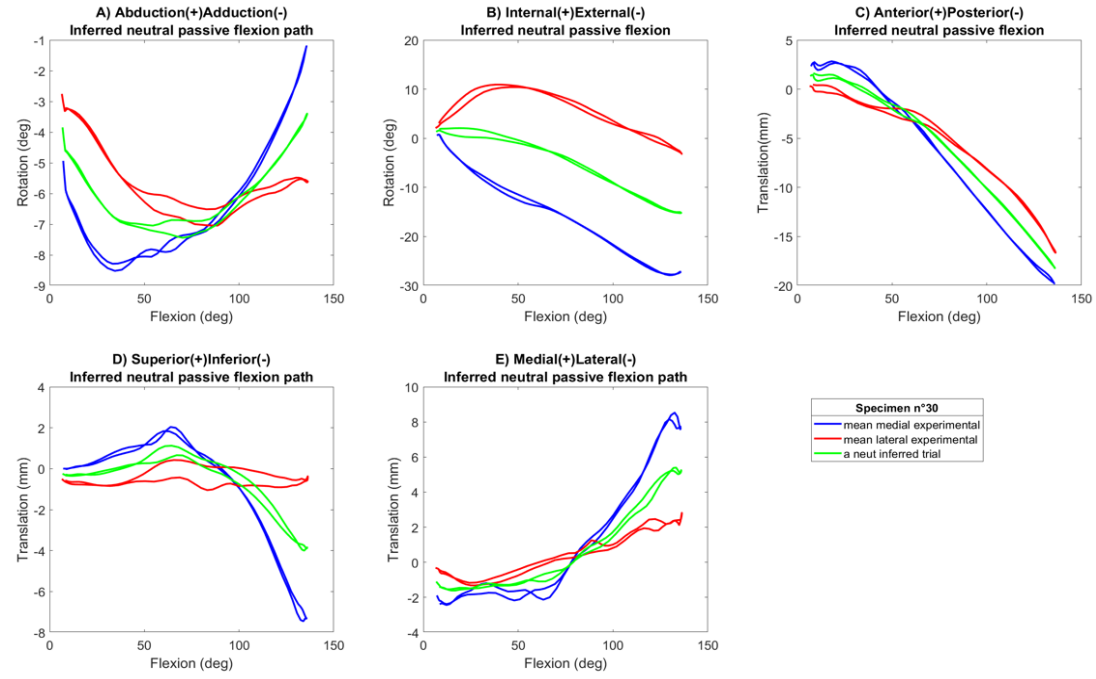

Figure C.1.30.2 *– Specimen30 medial (blue), lateral (red) experimental TF motion and inferred neutral flexion path (green): rotations and translations against FE.*

Appendix D

STUDY

The Relationship Between Knee Articular Shape And Passive Motion With PLS, And The Influence Of Sex

CONTENTS

D. O'Rourke, **F. Bucci**, M. Taylor, R. Al-Dirini, S. Martelli (2023) – Determining the relationship between tibiofemoral geometry and passive motion with partial least squares regression. Journal of Orthopaedic Research. Journal Article. https://doi.org/10.1002/jor.25526. *Manuscript Published.*

Please refer to the appendices at the end of this thesis for a detailed outline of the author's contribution to this study (Appendix A).

D.1 Abstract

Tibiofemoral geometry influences knee passive motion and understanding their relationship can provide insight into knee function and the mechanisms of injury. However, the complexity of the geometric constraints has made the characterising the relationship challenging. The aim of this study was to determine the tibiofemoral bone geometries that explain the variation in passive motion using a partial least squares regression (PLSR) model. The PLSR model was developed for 29 healthy cadaver specimens (10 female, 19 male) with femur and tibia geometries retrieved from MRI images and 6-DOF tibiofemoral kinematics determined during a flexion cycle with minimal medial force. The first 13 PLS components explained 90% of the variation in the kinematics and accounted for 89% of the variation in geometry. The first three PLS components which shared geometric changes to articular surface congruency of the tibial and femoral condyles explained the most amount of variation in the kinematics, primarily in anterior-posterior translation. Meanwhile, variations in femoral condyle width and the intercondylar space, tibia plateau size and conformity, and tibia eminences heights in PLS 2 and PLS 4 explained the greatest amount of variation in internal-external rotation. PLS 4 exhibiting variation in overall size of the knee accounted for greatest amount of variation in geometry (50%) and had the greatest influence on the abduction-adduction motion and some on internal-external rotation but, overall, explained only a small proportion of the kinematics (10%). There remains a complex relationship between the geometric constraints of the tibiofemoral joint and the passive motion.

D.2 Introduction

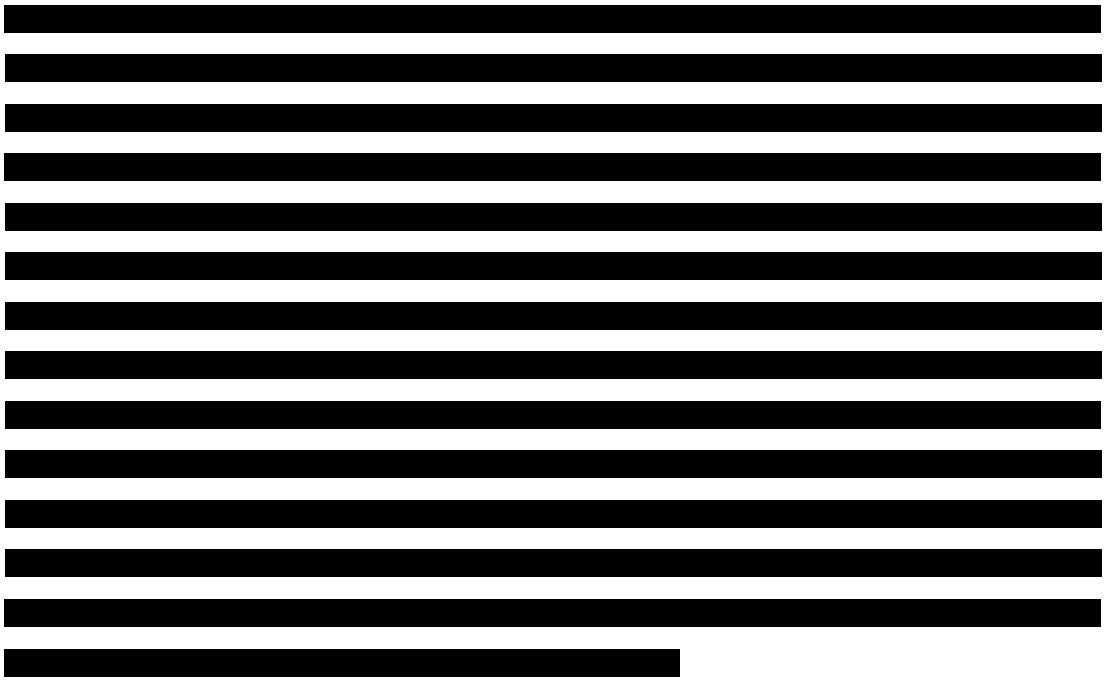

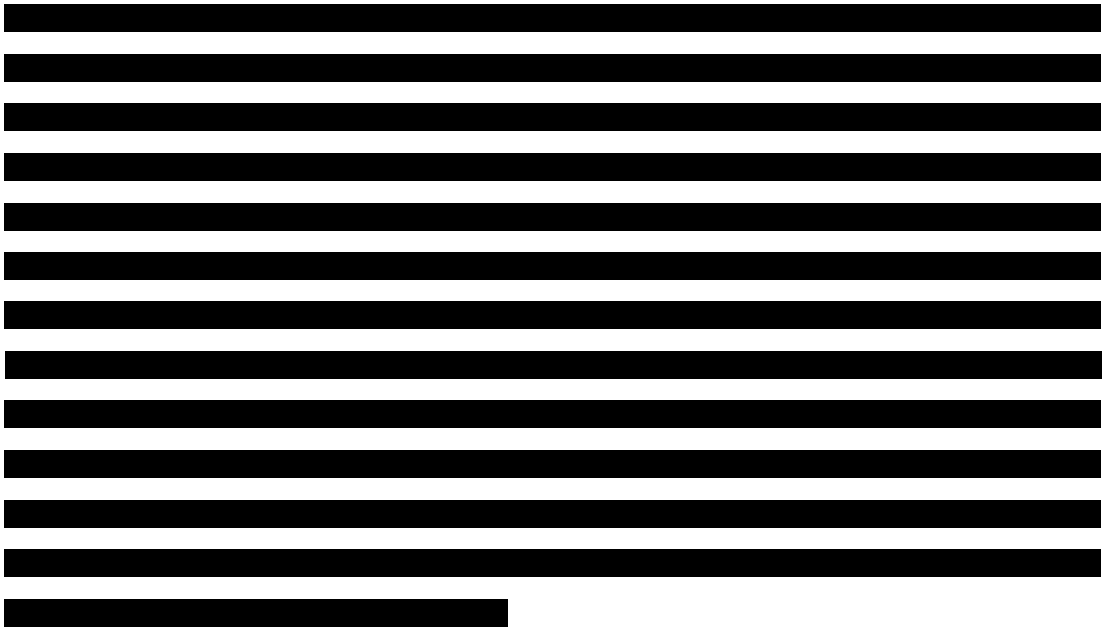

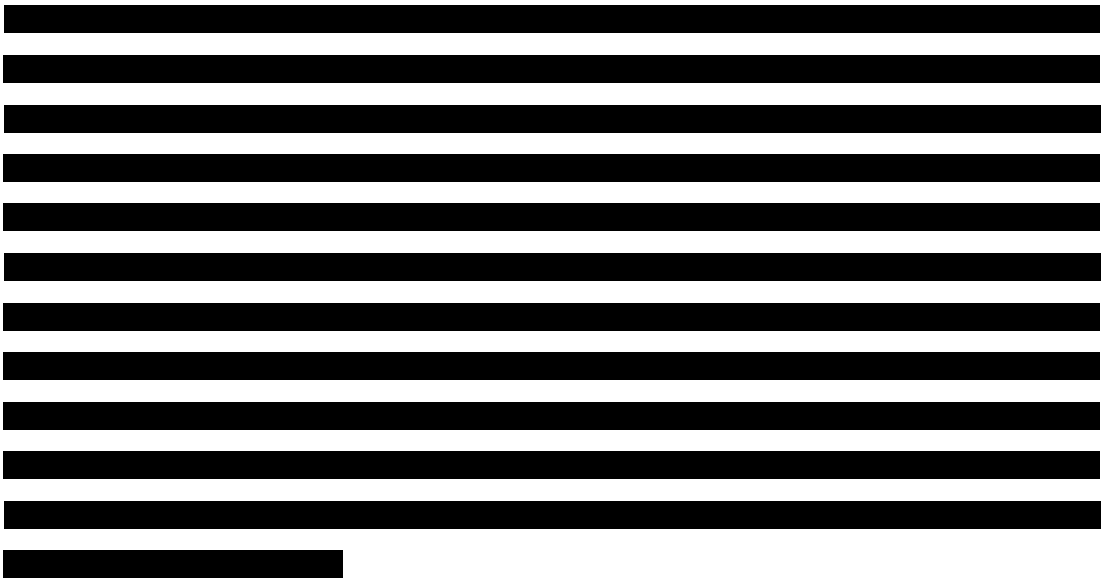

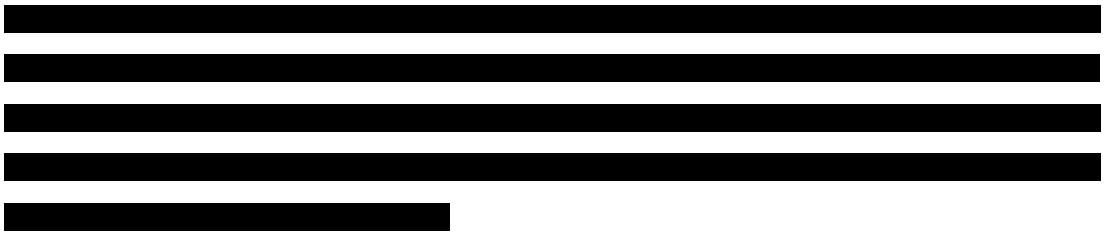

[redacted]

[redacted]

[redacted]

[redacted]

[redacted]

[redacted]

[redacted]

[redacted]

[redacted]

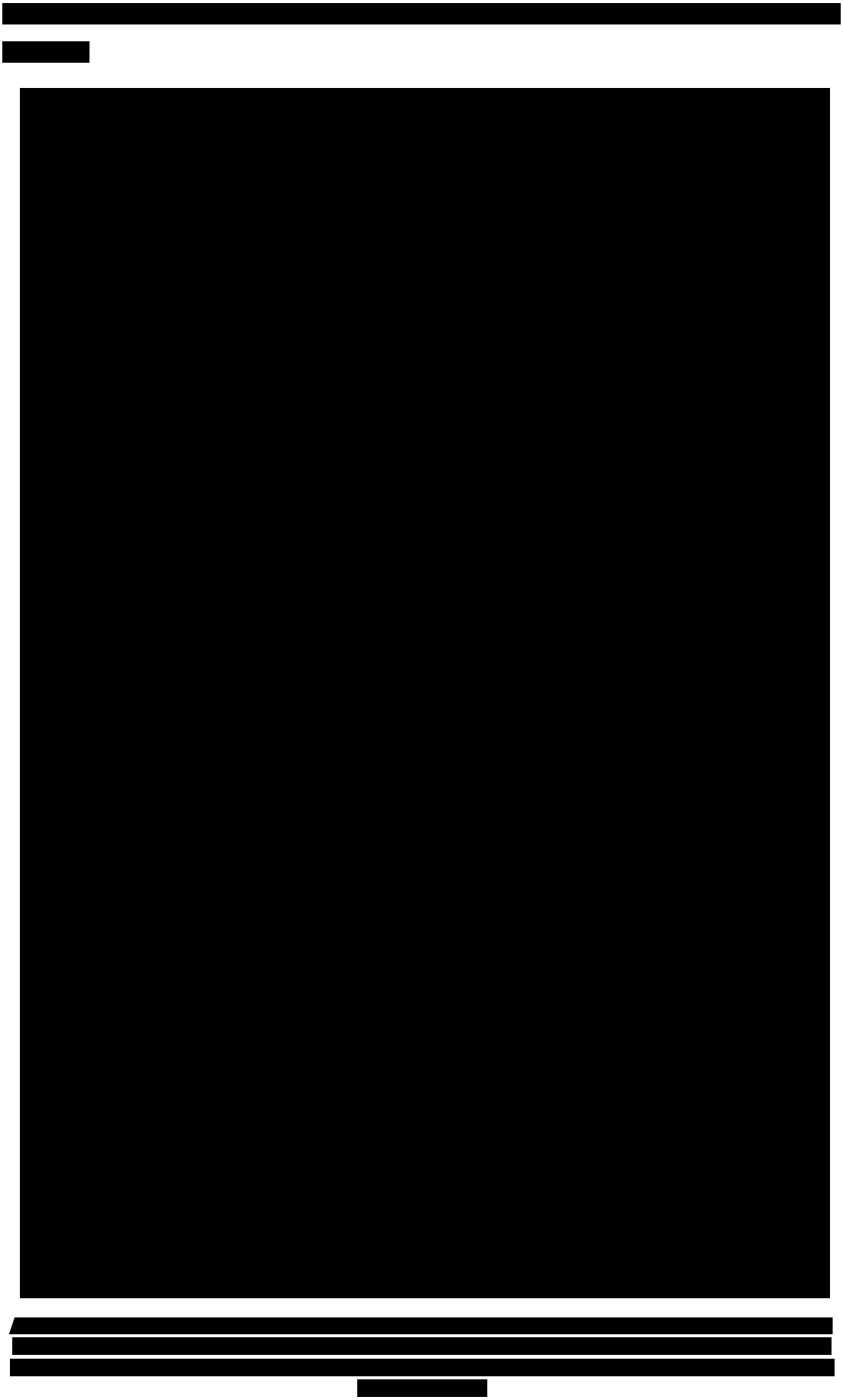

[redacted]

[redacted]

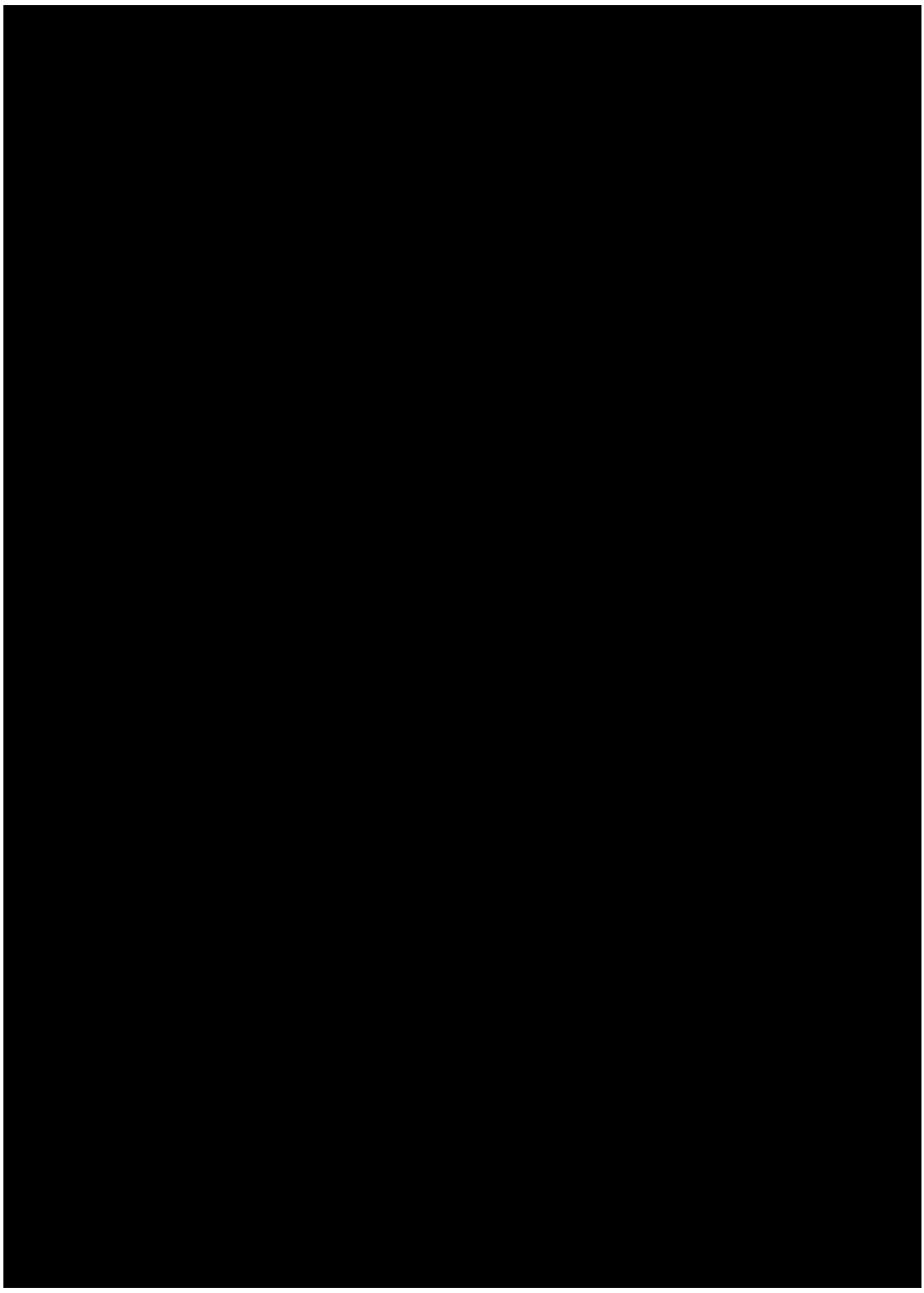

[redacted]

[redacted]

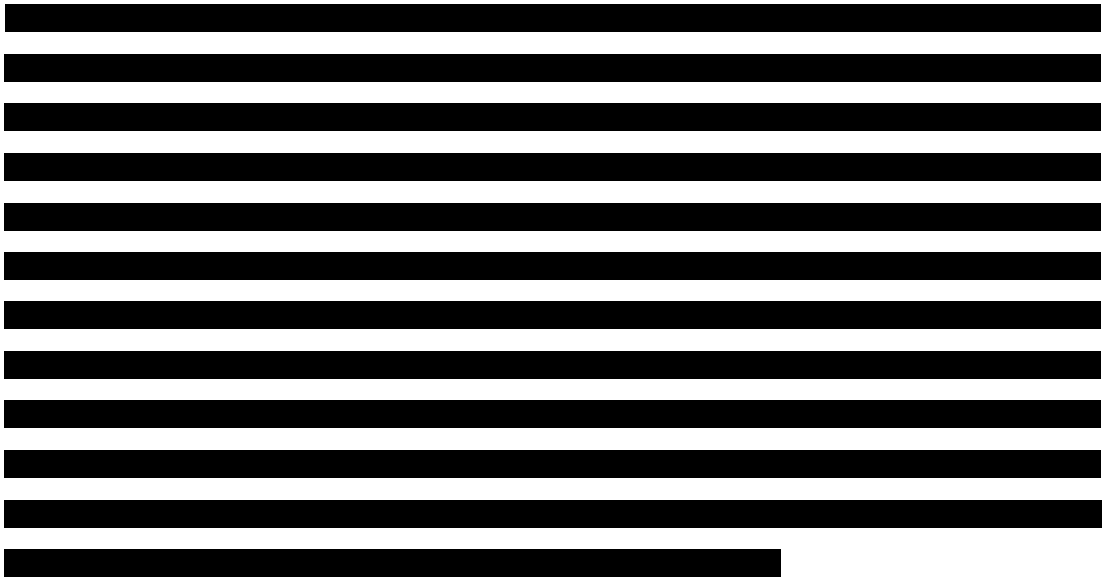

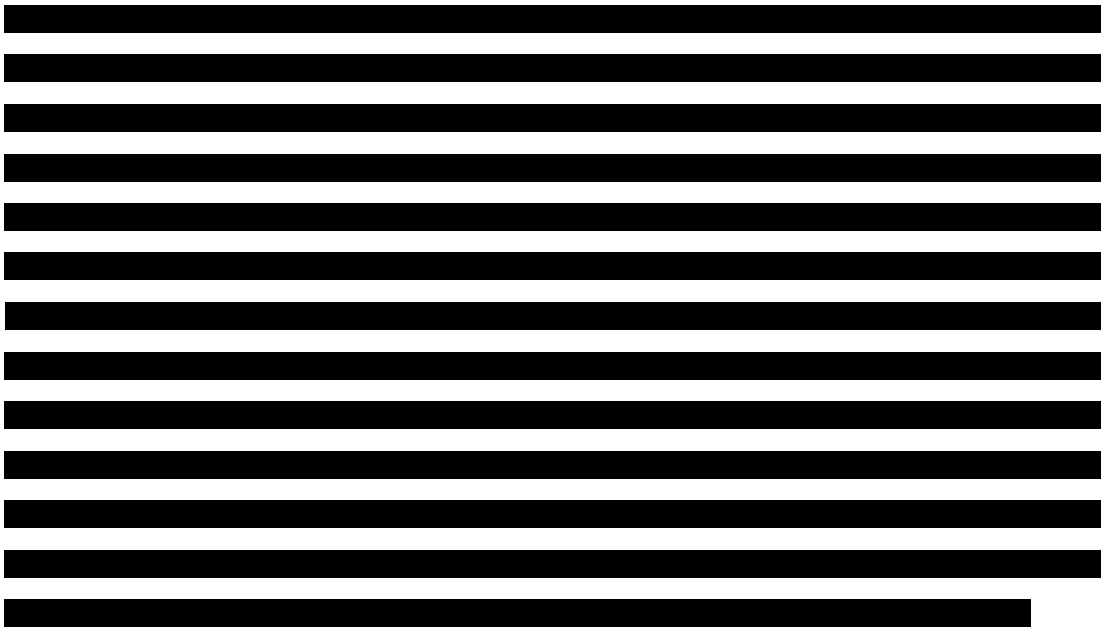

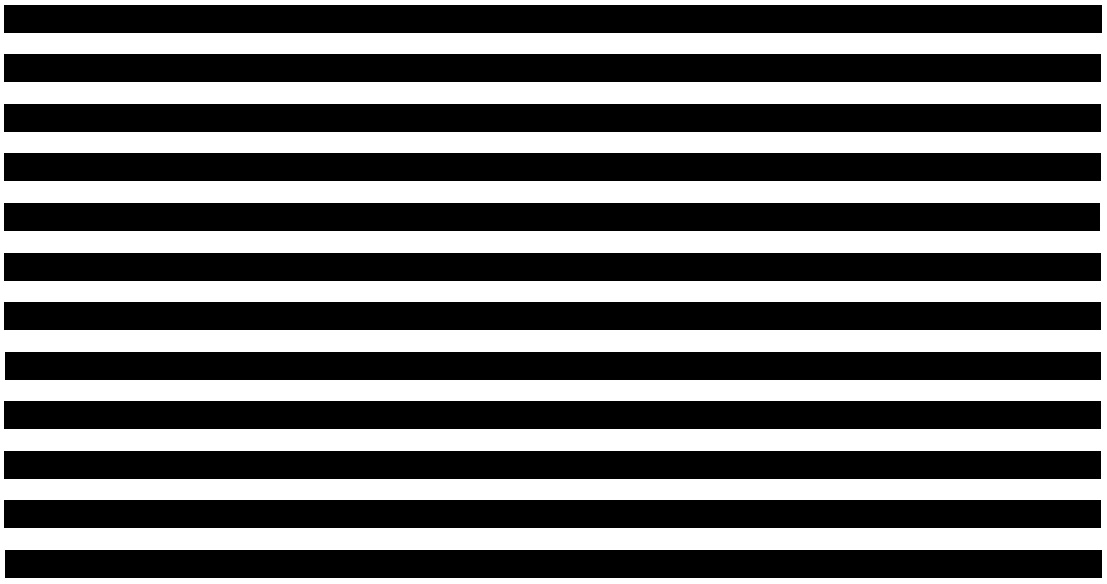

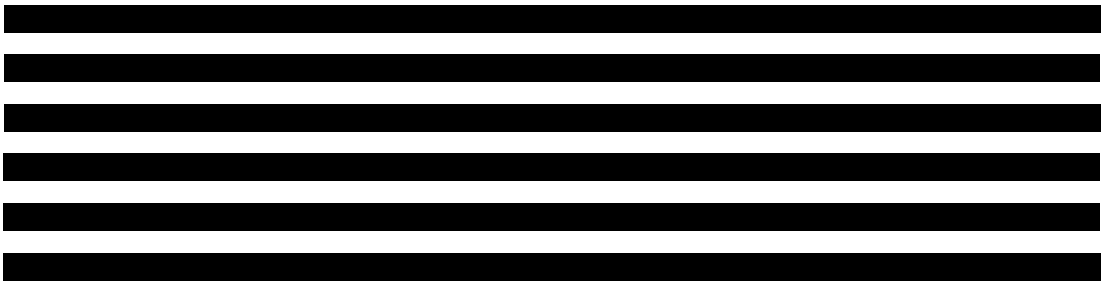

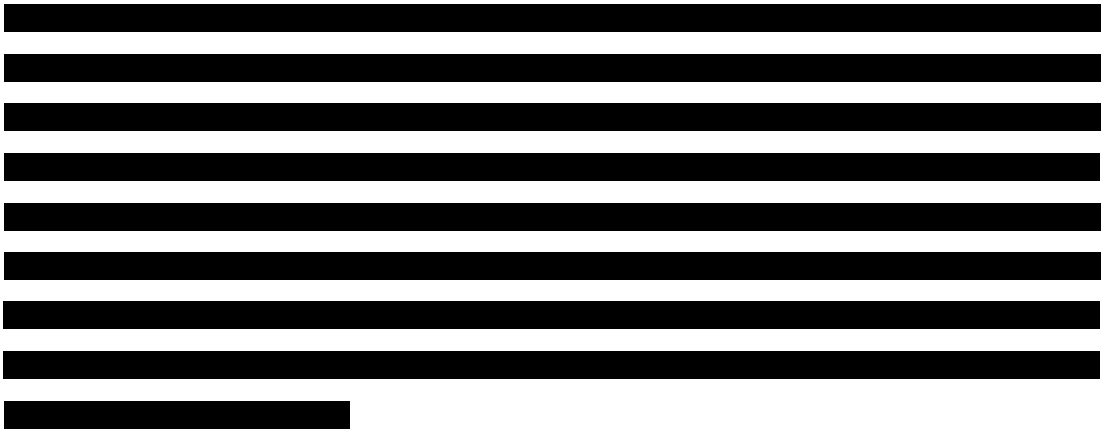

D.6 References

Simon TD, Bublitz C, Hambidge SJ. 2006. Emergency department visits among pediatric patients for sports-related injury: Basic epidemiology and impact of race/ethnicity and insurance status. Pediatric Emergency Care 22:309-315.

Gage BE, McIlvain NM, Collins CL, et al. 2012. Epidemiology of 6.6 million knee injuries presenting to United States emergency departments from 1999 through 2008. Academic Emergency Medicine 19:378-385.

Gianotti SM, Marshall SW, Hume PA, et al. 2009. Incidence of anterior cruciate ligament injury and other knee ligament injuries: A national population-based study. Journal of Science and Medicine in Sport 12:622-627.

Blagojevic M, Jinks C, Jeffery A, et al. 2010. Risk factors for onset of osteoarthritis of the knee in older adults: a systematic review and meta-analysis. Osteoarthritis and Cartilage 18:24-33.

Felson DT. 2013. Osteoarthritis as a disease of mechanics. Osteoarthritis and Cartilage 21:10-15.

Blankevoort L, Huiskes R, De Lange A. 1988. The envelope of passive knee joint motion. Journal of biomechanics 21:705-720.

Rahnemai-Azar AA, Yaseen Z, Van Eck CF, et al. 2016. Increased lateral tibial plateau slope predisposes male college football players to anterior cruciate ligament injury.Journal of Bone and Joint Surgery - American Volume 98:1001-1006.

Kakarlapudi TK, Bickerstaff DR. 2000. Knee instability: Isolated and complex. British Journal of Sports Medicine 34:395-400.

Neogi T, Bowes MA, Niu J, et al. 2013. Magnetic resonance imaging-based three- dimensional bone shape of the knee predicts onset of knee osteoarthritis: Data from the osteoarthritis initiative. Arthritis and Rheumatism 65:2048-2058.

Fitzpatrick CK, Baldwin MA, Laz PJ, et al. 2011. Development of a statistical shape model of the patellofemoral joint for investigating relationships between shape and function. Journal of biomechanics 44:2446-2452.

Rao C, Fitzpatrick CK, Rullkoetter PJ, et al. 2013. A statistical finite element model of the knee accounting for shape and alignment variability. Medical Engineering and Physics; pp. 1450-1456.

Smoger LM, Fitzpatrick CK, Clary CW, et al. 2015. Statistical modelling to characterize relationships between knee anatomy and kinematics. Journal of Orthopaedic Research; pp. 1620-1630.

Shalhoub S, Cyr A, Maletsky LP. Correlation between knee anatomy and joint laxity using principal component analysis. Journal of Orthopaedic Research [Epub ahead of print].

Clouthier AL, Smith CR, Vignos MF, et al. 2019. The effect of articular geometry features identified using statistical shape modelling on knee biomechanics. Medical Engineering & Physics 66:47-55.

Lynch JT, Perriman DM, Scarvell JM, et al. 2020. Shape is only a weak predictor of deep knee flexion kinematics in healthy and osteoarthritic knees. Journal of Orthopaedic Research 38:2250-2261.

Wold S, Trygg J, Berglund A, et al. 2001. Some recent developments in PLS modelling. Chemometrics and Intelligent Laboratory Systems 58:131-150.

De Roeck J, Duquesne K, Van Houcke J, et al. 2021. Statistical-Shape Prediction of Lower Limb Kinematics During Cycling, Squatting, Lunging, and Stepping-Are Bone Geometry Predictors Helpful? Front Bioeng Biotechnol 9:696360-696360.

Reijman M, Pols HAP, Bergink AP, et al. 2007. Body mass index associated with onset and progression of osteoarthritis of the knee but not of the hip: The Rotterdam Study. Annals of the Rheumatic Diseases 66:158-162.

Burton W, Myers C, Rullkoetter P. 2020. Semi-supervised learning for automatic segmentation of the knee from MRI with convolutional neural networks. Computer Methods and Programs in Biomedicine 189:105328.

Audenaert EA, Pattyn C, Steenackers G, et al. 2019. Statistical Shape Modelling of Skeletal Anatomy for Sex Discrimination: Their Training Size, Sexual Dimorphism, and Asymmetry. Front Bioeng Biotechnol 7.

Gray HA, Guan S, Thomeer LT, et al. 2019. Three-dimensional motion of the knee- joint complex during normal walking revealed by mobile biplane x-ray imaging. Journal of Orthopaedic Research 37:615-630.

Appendix E

STUDY

A New Algorithm For Automatic CT Segmentation Of Knee Bones

CONTENTS

M. How M. Howes, M. Bajger, G. Lee, **F. Bucci**, S. Martelli (2021) – Texture enhanced Statistical Region Merging with application to automatic knee bones segmentation from CT. In 2021 Digital Image Computing: Techniques and Applications (DICTA) (pp. 01-08). IEEE. https://doi.org/10.1109/DICTA52665.2021.9647224. *Manuscript Published.*

Please refer to the appendices at the end of this thesis for a detailed outline of the author's contribution to this study (Appendix A).

E.1 Abstract

Statistical Region Merging technique belongs to the portfolio of very successful image segmentation methods across diverse domains and applications. The method is based on a solid probabilistic principle and was extended in various directions to suit specific applications, including those from medical domains. In its basic implementation the technique is based on a merging criterion relying on image pixel intensities. Sufficient to segment well some natural scene images, it often deteriorates dramatically when challenging medical images are segmented. In this study we introduce a new merging criterion into the method which utilizes texture characteristic of the image. We demonstrate that the enhanced criterion allows segmentation of knee bones in CT comparable to state-of-the-art outcomes found in literature while preserving the desirable properties of the original technique.

Index Terms — statistical region merging, knee segmentation, super pixels, texture classification, CT.

E.2 Introduction

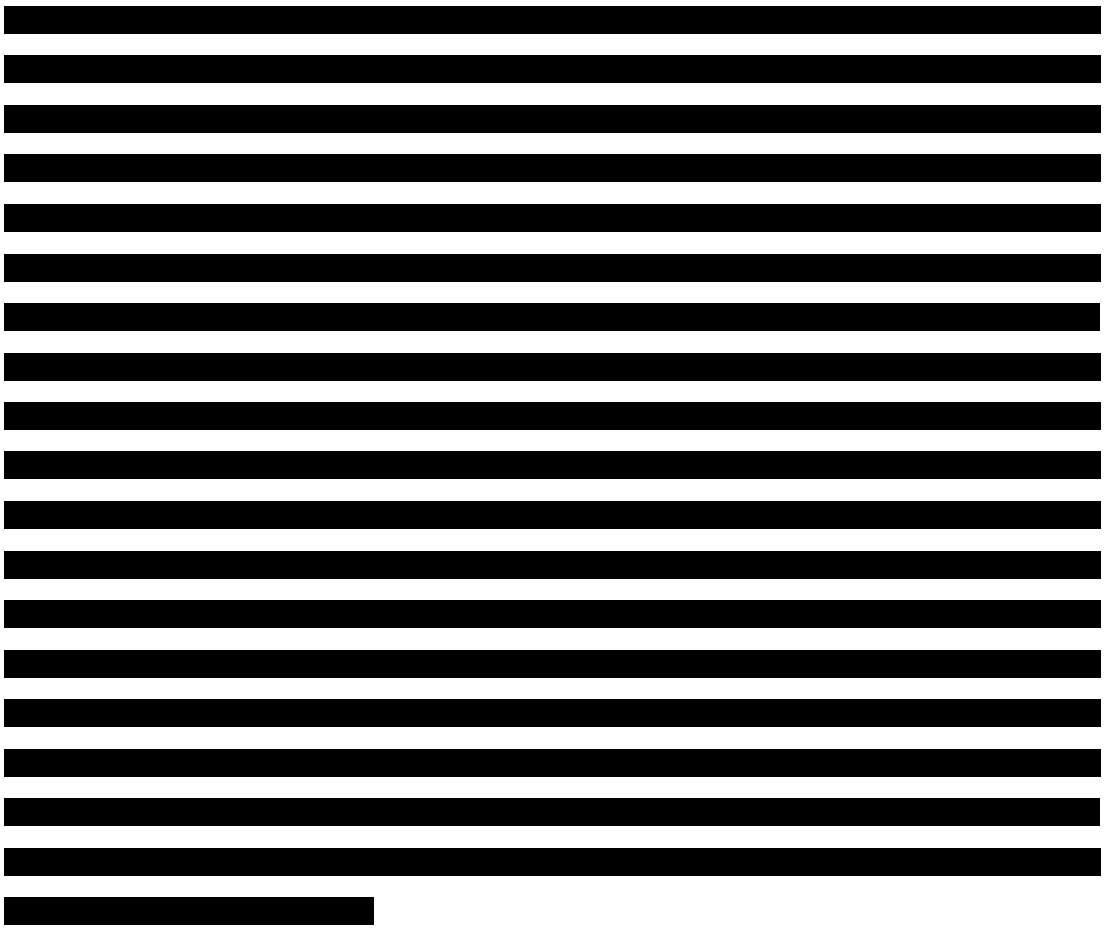

[redacted]

[redacted]

[redacted] , (3)

[redacted]

$\frac{1}{6\,|I|^2}$ [redacted]

[redacted]

[redacted]

[redacted]

[redacted] (4)

[redacted] (5)

[redacted] (6)

[redacted] (7)

[redacted]

[redacted]

[redacted]

[redacted]

[redacted] $\frac{\square}{\sum_{i=1}^{K} s_i}$. (8)

[redacted]

[redacted]

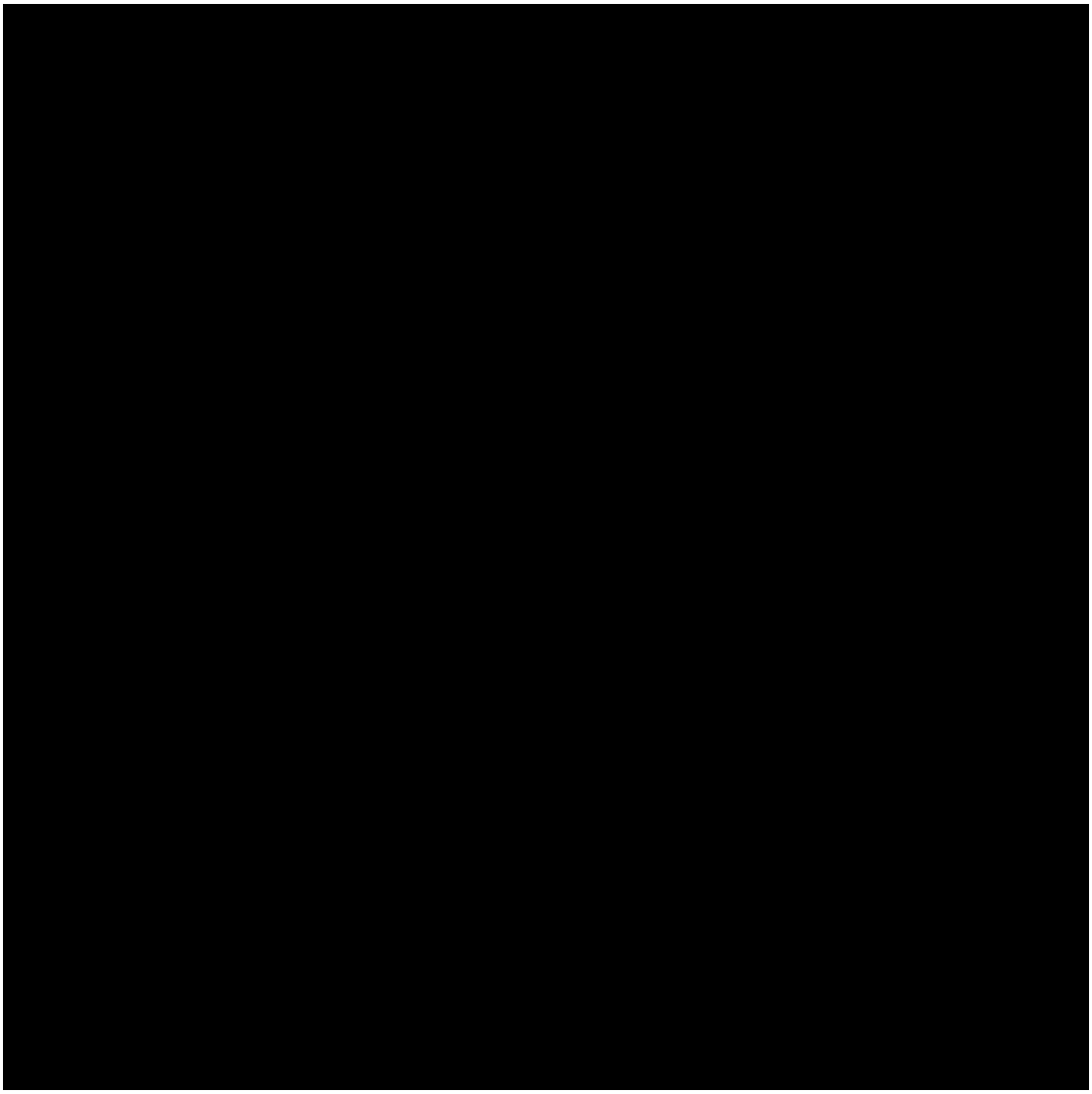

[redacted]

[redacted]

[redacted]

[redacted] $\Big)\Big] - 1,$ (9)

[redacted]

[redacted] , (12)

[redacted] , (13)

[redacted]

[redacted] (14)

[redacted]

[redacted] $\Big) \ln\frac{2}{\delta}.$ (15)

[redacted]

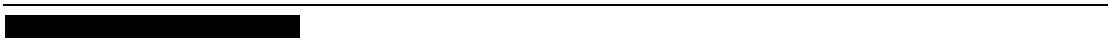

[redacted]

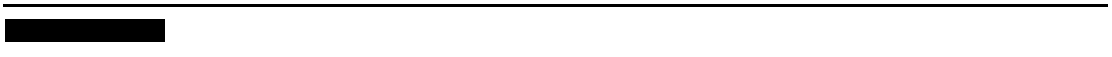

[redacted]

[redacted]

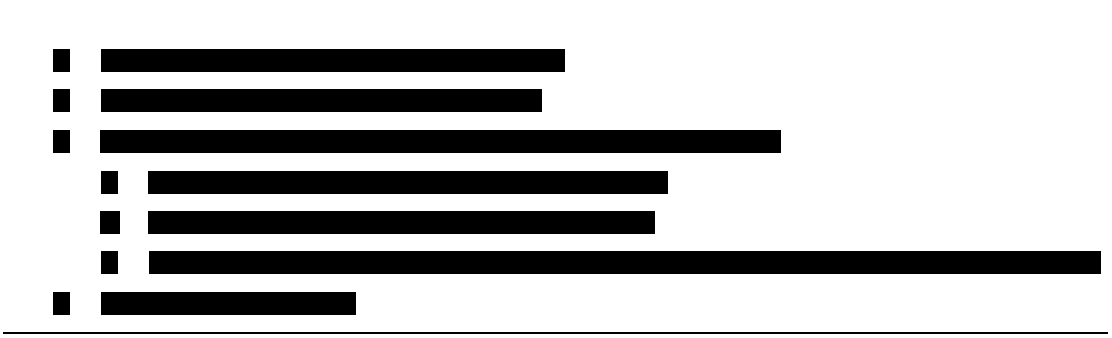

[redacted]

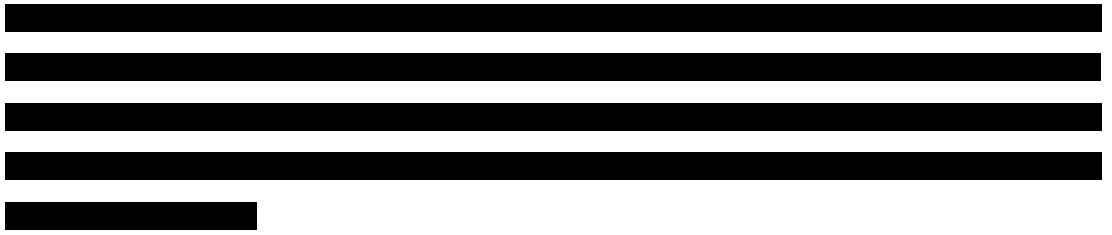

[redacted]

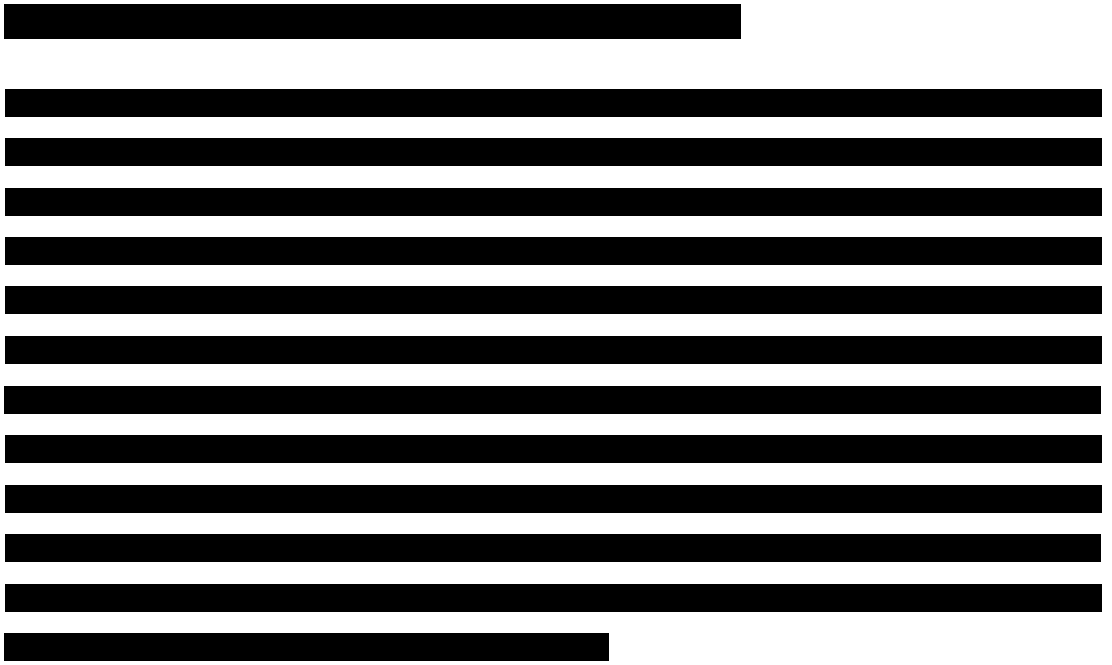

(16)

(17)

(18)

E.4 Results And Discussion

[redacted]

[redacted]

[redacted]

[redacted]

(a) [redacted] (b) [redacted] (c) [redacted]

[redacted]

[redacted]

[redacted]

[redacted]

[redacted]

[redacted]

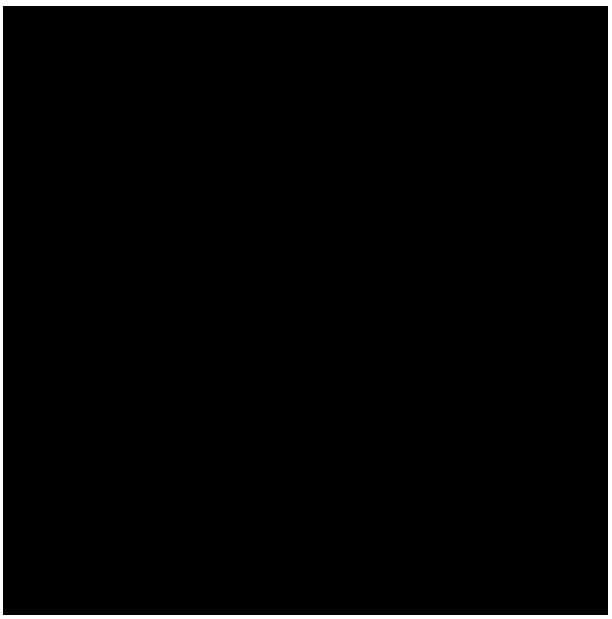

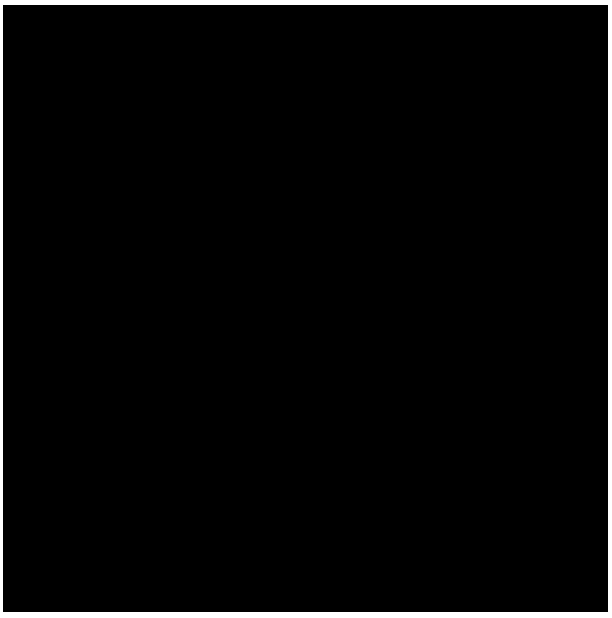

[redacted]

E.5 References

F. Renard, S. Guedria, N. De Palma, and N. Vuillerme, "Variability and reproducibility in deep learning for medical image segmentation," Sci Rep, vol. 10, no. 13724, 2020.

A. Stupple, D. Singerman, and L. Celi, "The reproducibility crisis in the age of digital medicine." npj Digit. Med., vol. 2, no. 2, 2019.

O. Fink, Q. Wang, M. Svens´en, P. Dersin, W.-J. Lee, and M. Ducoffe, "Potential, challenges and future directions for deep learning in prognostics and health management applications," Engineering Applications of Artificial Intelligence, vol. 92, p. 103678, 2020.

T. J. Sejnowski, "The unreasonable effectiveness of deep learning in artificial intelligence," Proceedings of the National Academy of Sciences, vol. 117, no. 48, pp. 30 033–30 038, 2020.

R. Nock and F. Nielsen, "Statistical region merging," IEEE Trans. Pattern Anal. Mach. Intell., vol. 26, no. 11, pp. 1452–1458, 2004.

M. E. Celebi, H. A. Kingravi, H. Iyatomi, Y. A. Aslandogan, W. Van Stoecker, R. Moss, J. M. Malters, J. M. Grichnik, A. A.

Marghoob, H. Rabinovitz, and S. W. Menzies, "Border detection in dermoscopy images using Statistical Region Merging," Skin Research and Technology, pp. 347–353, 2008.

M. Bajger, F. Ma, S. Williams, and M. Bottema, "Mammographic mass detection with Statistical Region Merging," in Digital Image Computing: Techniques and Applications, Proc. of DICTA 2010, Sydney, Australia, 2010, pp. 27–32.

S. Sajeev, M. Bajger, and G. Lee, "Improving breast mass segmentation in local dense background: an entropy based optimization of Statistical Region Merging method," in Breast Imaging - 13th International Workshop, IWDM 2016, Proceedings, ser. Lecture Notes in Computer Science,

A. Tingberg, K. Lang, and P. Timberg, Eds., no. 9699. Springer, Jan. 2016, pp. 635–642.

G. Lee, M. Bajger, and M. Caon, "Multi-organ segmentation of CT images using Statistical Region Merging," in Proceedings of the 9th IASTED International Conference on Biomedical Engineering, BioMed 2012, ser. Proceedings of the 9th IASTED International Conference on Biomedical Engineering, BioMed 2012, Jul. 2012, pp. 199–206.

M. Bajger, G. Lee, and M. Caon, "Full-body CT segmentation using 3D extension of two graph-based methods: a feasibility study," in Proceedings of the IASTED International Conference on Signal Processing, Pattern Recognition and Applications, SPPRA 2012, Aug. 2012, pp. 43–50.

—, "3D segmentation for multi-organs in CT images," Electronic Letters on Computer Vision and Image Analysis, vol. 12, no. 2, pp. 13–27, 2013

M. Caon, J. Sedl´aˇr, M. Bajger, and G. Lee, "Computer-assisted segmentation of CT images by statistical region merging for the production of voxel models of anatomy for CT dosimetry," Australasian Physical and Engineering Sciences in Medicine, vol. 37, no. 2, pp. 393–403, 2014.

J. Sedl´aˇr, M. Bajger, M. Caon, and G. Lee, "Model-guided segmentation of liver in CT and PET-CT images of child patients based on Statistical Region Merging," in 2016 International Conference on Digital Image Computing: Techniques and Applications, DICTA 2016, A. Wee-Chung,

B. Lovell, C. Fookes, J. Zhou, Y. Gao, M. Blumenstein, and Z. Wang, Eds., Dec. 2016.

R. Saha, M. Bajger, and G. Lee, "SRM superpixel merging framework for precise segmentation of cervical nucleus," in 2019 Digital Image Computing, ser. 2019 Digital Image Computing: Techniques and Applications,DICTA 2019, Dec. 2019.

N. Jegou, F. Desaize, G. Lee, M. Bajger, O. Acosta, J. Leseur, R. De Crevoisier, and M. Caon, "Organs-at-risk contouring on head CT for RT planning using 3D slicer-a preliminary study," in Proceedings - 2019 IEEE 19th International Conference on Bioinformatics and Bioengineering, BIBE 2019, Oct. 2019, pp. 503–506.

F. Lang, J. Yang, D. Li, L. Zhao, and L. Shi, "Polarimetric SAR image segmentation using Statistical Region Merging," IEEE Geoscience and Remote Sensing Letters, vol. 11, no. 2, pp. 509–513, 2014.

D. Xiang, W. Wang, T. Tang, D. Guan, S. Quan, T. Liu, and Y. Su, "Adaptive statistical superpixel merging with edge penalty for PolSAR image segmentation," IEEE Transactions on Geoscience and Remote Sensing, vol. 58, pp. 2412–2429, 2020.

F. Ambellan, A. Tack, M. Ehlke, and S. Zachow, "Automated segmentation of knee bone and cartilage combining statistical shape knowledge and convolutional neural networks: Data from the Osteoarthritis Initiative." Med. Image Anal., vol. 02, no. 52, pp. 109–118, 2019.

Ridhma, M. Kaur, S. Sofat, and D. K. Chouhan, "Review of automated segmentation approaches for knee images," IET Image Processing, vol. 15, no. 2, pp. 302–324, 2021.

McDiarmid C., "Concentration," in Probabilistic Methods for AlgorithmicDiscrete Mathematics. Algorithms and Combinatorics, Habib M.and McDiarmid C. and Ramirez-Alfonsin J. and Reed B, Ed., vol. 16,1998.

Z. Li and J. Chen, "Superpixel segmentation using Linear Spectral Clustering," in 2015 IEEE Conference on Computer Vision and Pattern Recognition (CVPR), 2015, pp. 1356–1363.

S. Selvan and S. Ramakrishnan, "SVD-based modelling for image texture classification using wavelet transformation," IEEE Transactions on Image Processing, vol. 16, no. 11, pp. 2688–2696, 2007.

A. Taha and A. Hanbury, "Metrics for evaluating 3D medical image segmentation: analysis, selection, and tool." BMC Med Imaging, vol. 15, no. 29, 2015.

O. Kubassova, R. D. Boyle, and A. Radjenovic, "A novel method for quantitative evaluation of segmentation outputs for dynamic contrastenhanced MRI data in RA studies," in Proceedings of the Joint Disease Workshop, 9th International Conference on Medical Image Computing and Compter Assisted Intervention, vol. 1, 2006, pp. 72–79.

M. ˇSonka, V. Hlav´aˇc, and R. Boyle, Image Processing, Analysis, and Machine Vision. Thomson, 2008.

Y. Jonmohamadi, Y. Takeda, F. Liu, F. Sasazawa, G. Maicas, R. Crawford, J. Roberts, A. K. Pandey, and G. Carneiro, "Automatic segmentation of multiple structures in knee arthroscopy using deep learning," IEEE Access, vol. 8, pp. 51 853–51 861, March 2020.

W. Shen, W. Xu, H. Zhang, Z. Sun, J. Ma, X. Ma, S. Zhou, S. Guo, and Y. Wang, "Automatic segmentation of the femur and tibia bones from X-ray images based on pure dilated residual U-Net," Inverse Problems and Imaging, vol. 0, pp. –, 2020.

D. Wu, M. Sofka, N. Birkbeck, and S. K. Zhou, "Segmentation of multiple knee bones from CT for orthopedic knee surgery planning," in Medical Image Computing and Computer-Assisted Intervention – MICCAI 2014, P. Golland, N. Hata, C. Barillot, J. Hornegger, and R. Howe, Eds. Cham: Springer International Publishing, 2014, pp.372–380.

Appendix F

ADDITIONAL MATERIAL

Scoring Tables for Knee Joint Models

	TITLE	Effect of Posterior Tibial Slope on Knee Biomechanics during Functional Activity.	An EMG-driven musculoskeletal model to estimate muscle forces and knee joint moments in vivo	Prediction of In Vivo Knee Joint Loads Using a Global Probabilistic Analysis	Muscle, Ligament, and Joint-Contact Forces at the Knee during Walking	Subject-specific knee joint geometry improves predictions of medial tibiofemoral contact forces	Dependence of Muscle Moment Arms on In Vivo Three-Dimensional Kinematics of the Knee	Determinants of crucitae-ligament loading during rehabilitation exercise	A Dynamic Model of the Knee and Lower Limb for Simulating Rising Movements	An improved OpenSim gait model with multiple degrees of freedom knee joint and knee ligaments	Neuromuscular Biomechanical Modeling to Understand Knee Ligament Loading
	AUTHORS	Shelburne, Kim, Sterett, Pandy	Lloyd, Besier	Navacchia, Myers, Rullkoetter, Shelburne	Shelburne, Torry, Pandy	Gerus, Sartori, Besier, Fregly, Delp, Banks, Pandy, D'Lima, Lloyd	Navacchia, Kefala, Shelburne	Shelburne, Panty	Shelburne, Pandy	Xu, Bloswick, Merryweather	Lloyd, Buchanan, Besier
	LABEL	Shelburne et al. 2010	Lloyd et al. 2002	Navacchia et al. 2016	Shelburne et al. 2005	Gerus et al. 2013	Navacchia et al. 2016 (2)	Shelburne et al. 1998	Shelburne et al. 2010	Xu et al. 2015	Lloyd et al. 2005
CATEGORY											
OFFSET	OFFSET X - COST	0,00	0,00	0,00	0,00	0,00	0,00	0,00	0,00	0,00	0,00
	OFFSET Y - COMPLEXITY	-1,00	-1,00	-1,00	-1,00	-1,00	-1,00	-1,00	-1,00	-1,00	-1,00
COMPLEXITY	OTHER COMPLEXITY	1,00	1,00	0,00	0,00	1,00	0,00	1,00	1,00	0,00	1,00
	BONES	1,00	1,00	1,00	1,00	1,00	1,00	1,00	1,00	1,00	1,00
	CARTILAGES	1,00	0,00	0,00	0,00	0,00	0,00	0,00	0,00	0,00	0,00
	MENISCI	0,00	0,00	0,00	0,00	0,00	0,00	0,00	0,00	0,00	0,00
	LIGAMENTS	1,00	0,00	1,00	1,00	0,00	0,00	1,00	1,00	1,00	0,00
	OTHER LIGAMENTS AND STRUCTURES	1,00	0,00	0,00	1,00	0,00	0,00	0,00	1,00	0,00	0,00
	INTEGRATION MULTIPLE MODELS	0,00	0,00	0,00	1,00	0,00	0,00	0,00	1,00	0,00	0,00
	COMPLEXITY OF THE MECHANISM USED TO MODEL THE JOINT	1,00	0,00	0,00	1,00	1,00	1,00	0,00	1,00	0,00	0,00
COST	OTHER COST (FOR TASKS PERFORMED or particolar tecnique used)	1,00	1,00	0,00	1,00	1,00	0,00	0,00	1,00	0,00	1,00
	DATA SORCES	1,00	1,00	1,00	3,00	4,00	1,00	1,00	3,00	0,00	1,00
	VALIDATION	1,00	1,00	0,00	1,00	1,00	0,00	0,00	1,00	0,00	1,00
	COMPUTATIONAL COST OF THE MODEL	0,00	0,00	0,00	0,00	1,00	0,00	0,00	0,00	1,00	0,00
	CLINICAL APPLICATION ADAPTABILITY	☑	_	_	_	_	☑	_	_	_	_
ADJUSTMENT CONTRIBUTES	MSK ANALISYS (PERFORMED SO, JR or also CMC, FD)	1,00	1,00	0,00	1,00	1,00	0,00	0,00	1,00	0,00	0,00
	MSK COMPLEXITY OF SCALING	0,00	0,00	0,00	0,00	0,00	0,00	0,00	0,00	0,00	0,00
	FE TISSUE MODELS USED	1 model, 1 detailed, distribution of the force measured and stiffness of ligaments, ligaments as multi bundles (1 subjects)	1 for complexity of muscle model used - hill type modified, 1 other cost for 1 subject (1 subjects)		1 other cost related to the previous model creation and validation for muscle contribution , Dynamic optimization performed (1 subjects)	Implementation with splines of subject specific kinematics and torugh fluoroscopy of the geometry (1subject)	(7subjects)				
	FE BOUNDARY CONDITIONS AND CONTACTS										
	SS Number of variables accounted e.g. shape, alignment, Kinematics, material properties models										
	SS NUMBER OF SUBJECTS FOR BUILDING THE MODEL										
	ANALITICAL OVERAL COMPLEXITY										
	ACCURACY	HIGH	MEDIUM-LOW			HIGH	MEDIUM-LOW				
TOTAL	TOTAL COMPLEXITY Y	9	2	1	5	3	1	2	6	1	1
	TOTAL COST - UTILITY X	3	3	1	6	7	1	1	6	1	3
TOTAL	COST - UTILITY X	42,86	42,86	14,29	85,71	100,00	14,29	14,29	85,71	14,29	42,86
	COMPLEXITY Y	75,00	16,67	8,33	41,67	25,00	8,33	16,67	50,00	8,33	8,33

	TITLE	Computation of the role of kinetics, kinematics, posterior tibial slope and muscle cocontraction on the stability of ACL-deficient knee joint at heel strike – Towards identification of copers from non-copers	Computational stability of human knee joint at early stance in Gait: Effects of muscle coactivity and anterior cruciate ligament deficiency	A lower extremity model for muscle-driven simulation of activity using explicit finite element modelling	A computationally efficient strategy to estimate muscle forces in a finite element musculoskeletal model of the lower limb	The interaction of muscle moment arm, knee laxity, and torque in a multi-scale musculoskeletal model of the lower limb	Combined measurement and modelling of specimen-specific knee mechanics for healthy and acl-deficient conditions	Contributions of Muscles, Ligaments, and the Ground-Reaction Force to Tibiofemoral Joint Loading During Normal Gait
	AUTHORS	Sharifi, Shirazi-Adl, Marouane	Sharifi, Shirazi-Adl, Marouane	Hume, Navacchia, Rullkoetter, Shelburne	Navacchia, Hume, Rullkoetter, Shelburne	Hume, Navacchia, Ali, Shelburne	Ali, Harris, Shalhoub, Maletsky, Rullkoetter, Shelburne	Shelburne, Torry, Pandy
	LABEL	Sharifi et al. 2018	Sharifi et al. 2017	Hume et al. 2018	Navacchia et al. 2018	Hume et al. 2018	Ali et al. 2017	Shelburne et al. 2006
CATEGORY								
OFFSET	OFFSET X	1.00	1.00	1.00	1.00	1.00	1.00	1.00
	OFFSET Y	-1.00	-1.00	-1.00	-1.00	-1.00	-1.00	-1.00
	OTHER COMPLEXITY	1.00	1.00	0.00	0.00	2.00	1.00	1.00
COMPLEXITY	BONES	1.00	1.00	1.00	1.00	1.00	1.00	1.00
	CARTILAGES	1.00	1.00	1.00	1.00	1.00	1.00	0.00
	MENISCI	1.00	1.00	0.00	0.00	0.00	1.00	0.00
	LIGAMENTS	1.00	1.00	1.00	1.00	1.00	1.00	1.00
	OTHER LIGAMENTS AND STRUCTURES	1.00	1.00	1.00	1.00	1.00	1.00	1.00
	INTEGRATION MULTIPLE MODELS	1.00	1.00	1.00	1.00	1.00	1.00	1.00
	COMPLEXITY OF THE MECHANISM USED TO MODEL THE JOINT	1.00	1.00	0.00	0.00	0.00	1.00	1.00
	OTHER COST (FOR TASKS PERFORMED)	1.00	1.00	1.00	1.00	0.00	1.00	1.00
COST	DATA SORCES	1.00	1.00	1.00	1.00	1.00	1.00	1.00
	VALIDATION	0.00	0.00	0.00	0.00	0.00	1.00	1.00
	COMPUTATIONAL COST OF THE MODEL	1.00	1.00	0.00	0.00	0.00	0.00	0.00
	CLINICAL APPLICATION ADAPTABILITY					_		_
ADJUSTMENT CONTRIBUTES	MSK ANALISYS (PERFORMED SO, JR or also CMC, FD)	1.00	1.00	1.00	1.00	0.00	1.00	1.00
	MSK COMPLEXITY OF SCALING	1.00	1.00	1.00	1.00	0.00	1.00	0.00
	FE TISSUE MODELS USED	1.00	1.00	1.00	1.00	1.00	1.00	0.00
	FE BOUNDARY CONDITIONS AND CONTACTS	1.00	1.00	1.00	1.00	0.00	1.00	1.00
	SS Number of variables accounted e.g. shape, alignment, Kinematics, material properties models					1 other for complexity muscle-tendon model with attachments and 1 for deformable model of the knee (11 subjects)		
	SS NUMBER OF SUBJECTS FOR BUILDING THE MODEL							
	ANALITICAL OVERAL COMPLEXITY							
	ACCURACY					HIGH		
TOTAL	TOTAL COST - UTILITY X	4	4	3	3	2	4	6
	TOTAL COMPLEXITY Y	11	11	8	8	7	11	7
TOTAL	COST - UTILITY X	57.14	57.14	42.86	42.86	28.57	57.14	85.71
	COMPLEXITY Y	91.67	91.67	66.67	66.67	58.33	91.67	58.33

	TITLE	Open Knee: Open Source Modeling & Simulation to Enable Scientific Discovery and Clinical Care in Knee Biomechanics	Biomechanics of the human knee joint in compression: reconstruction, mesh generation and finite element analysis	A Combined Experimental and Computational Approach to Subject-Specific Analysis of Knee Joint Laxity	Cruciate coupling and screw-home mechanism in passive knee joint during extension–flexi on	A three-dimensional finite element analysis of the combined behavior of ligaments and menisci in the healthy human knee joint	Comparison between kinetic and kinetic-kinematic driven knee joint finite element models	Subject-specific finite element analysis of the human medial collateral ligament during valgus knee loading	A viscoelastic poromechanica l model of the knee joint in large compression	The effect of constitutive representation s and structural constituents of ligaments on knee joint mechanics
	AUTHORS	Erdemir	Bendjaballah, Shirazi-Adl, Zukor	Harris, Cyr, Ali, Fitzpatrick,Rullk oetter, Maletsky, Shelburne	Moglo, Shirazi-Adl	Pena, Calvo, Martinez, Doblaré	Bolcos, Mononen, Mohammadi, Ebrahimi, Tanaka, Samaan, Souza, Li, Suomalainen, Jurvelin, Toyras, Korhonen	Gardiner, Weiss	Kazemi, Li	Orozco, Tanska, Mononen, Halonen, Korhonen
	LABEL	Erdemir et al. 2016	Bendjaballah et al. 1995	Harris et al. 2016	Moglo et al. 2004	Pena et al. 2006	Bolcos et al. 2018	Gardiner et al. 2003	Kazemi et al. 2014	Orozco et al. 2018
CATEGORY										
OFFSET	OFFSET X	1.00	1.00	1.00	1.00	1.00	1.00	1.00	1.00	1.00
	OFFSET Y	0.00	0.00	0.00	0.00	0.00	0.00	0.00	0.00	0.00
	OTHER COMPLEXITY	1.00	0.00	1.00	1.00	1.00	1.00	1.00		1.00
COMPLEXITY	BONES	1.00	1.00	1.00	1.00	1.00	1.00	1.00	1.00	1.00
	CARTILAGES	1.00	0.00	1.00	0.00	1.00	1.00	1.00	0.00	1.00
	MENISCI	1.00	1.00	0.00	1.00	0.00	0.00	1.00	0.00	1.00
	LIGAMENTS	1.00	0.00	1.00	1.00	1.00	1.00	1.00	0.00	1.00
	OTHER LIGAMENTS AND STRUCTURES	0.00	0.00	0.00	0.00	1.00	0.00	0.00	0.00	1.00
	INTEGRATION MULTIPLE MODELS : e.g. FE+MSK	0.00	0.00	0.00	0.00	0.00	0.00	0.00	0.00	0.00
	COMPLEXITY OF THE MECHANISM USED TO MODEL THE JOINT	1.00	0.00	1.00	1.00	1.00	1.00	1.00	0.00	1.00
	OTHER COST (FOR TASKS PERFORMED)	1.00	0.00	1.00	0.00	1.00	1.00	1.00	0.00	1.00
COST	DATA SORCES	1.00	1.00	1.00	1.00	1.00	1.00	1.00	1.00	1.00
	VALIDATION	1.00	0.00	1.00	0.00	1.00	1.00	0.00	0.00	1.00
	COMPUTATIONAL COST OF THE MODEL	1.00	0.00	0.00	0.00	0.00	0.00	0.00	0.00	1.00
	CLINICAL APPLICATION ADAPTABILITY									
ADJUSTMENT CONTRIBUTES	MSK ANALISYS PERFORMED (IK, ID, SO, JR or also CMC, FD)									
	MSK COMPLEXITY OF SCALING									
	FE TISSUE MODELS USED	1.00	0.00	1.00	0.00	1.00	1.00	0.00		1.00
	FE BOUNDARY CONDITIONS AND CONTACTS	1.00	0.00	0.00	0.00	0.00	0.00	0.00		0.00
	SS Number of variables accounted e.g. shape, alignment, Kinematics, material properties models									
	SS NUMBER OF SUBJECTS FOR BUILDING THE MODEL									
	ANALITICAL OVERAL COMPLEXITY									
	ACCURACY									
TOTAL	TOTAL COST - UTILITY X	5	2	4	2	4	4	3	2	5
	TOTAL COMPLEXITY Y	8	2	6	5	7	6	6	1	8
TOTAL	COST - UTILITY X	71.43	28.57	57.14	28.57	57.14	57.14	42.86	28.57	71.43
	COMPLEXITY Y	66.67	16.67	50.00	41.67	58.33	50.00	50.00	8.33	66.67

	TITLE	A three-dimensional mathematical model of the knee-joint	A global verification study of a quasi-static knee model with multi-bundle ligaments	An analytical model of the knee	Dependence of cruciate-ligament loading on muscle forces and external load	Articular surface approximation in equivalent spatial parallel mechanism models of the human knee joint: an experiment-based assessment	Articular contact in a three-dimensional model of the knee	Orientation of the cruciate ligament in the sagittal plane.	Biomechanical analysis of knee flexion and extension. Journal of Biomechanics.	A planar model of the knee joint to characterize the knee extensor mechanism.	Three-Body Segment Dynamic Model of the Human Knee.
	AUTHORS	Wismans, Veldpaus, Janssen	Mommersteeg, Huiskes, Blankevoort, Kooloos, Kauer, Maathuis	Crowninshield, Pope, Johnson	Pandy, Shelburne	Ottoboni, Parenti-Castelli, Sancisi, Belvedere, Leardini	Blankevoort, Kuiper, Huiskes, Grootenboer	Bradley, Fitzpatrick, Daniel, Shercliff, O'Connor	Smidt	Yamaguchi, Zajac	Tumer, Engin
	LABEL	Wismans et al. 1980	Mommersteeg et al. 1996	Crowninshield et al. 1976	Pandy et al. 1997	Ottoboni et al. 2009	Blankevoort et al. 1991	Bradley et al. 1988	1973	1989	1993
CATEGORY											
OFFSET	OFFSET X	-1,00	-1,00	-1,00	-1,00	-1,00	-1,00	-1,00	-1,00	-1,00	-1,00
	OFFSET Y	-1,00	-1,00	-1,00	-1,00	-1,00	-1,00	-1,00	-1,00	-1,00	-1,00
COMPLEXITY	BONES	1,00	1,00	1,00	1,00	1,00	1,00	1,00	1,00	1,00	1,00
	CARTILAGES	0,00	0,00	0,00	0,00	0,00	1,00	0,00	0,00	0,00	0,00
	MENISCI	0,00	0,00	0,00	0,00	0,00	0,00	0,00	0,00	0,00	0,00
	LIGAMENTS	1,00	1,00	1,00	1,00	1,00	1,00	1,00	1,00	0,00	1,00
	OTHER LIGAMENTS AND STRUCTURES	1,00	0,00	1,00	1,00	0,00	0,00	0,00	1,00	1,00	1,00
	INTEGRATION MULTIPLE MODELS : e.g. FE+MSK	0,00	0,00	0,00	0,00	0,00	0,00	0,00	0,00	0,00	0,00
	COMPLEXITY OF THE MECHANISM USED TO MODEL THE JOINT	1,00	0,00	1,00	0,00	1,00	1,00	0,00	1,00	0,00	1,00
	OTHER COST (FOR TASKS PERFORMED)	1,00	0,00	0,00	0,00	0,00	0,00	1,00	1,00	0,00	0,00
COST	DATA SORCES	0,00	1,00	1,00	1,00	1,00	1,00	0,00	1,00	1,00	0,00
	VALIDATION	0,00	0,00	1,00	0,00	1,00	1,00	0,00	1,00	1,00	0,00
	COMPUTATIONAL COST OF THE MODEL	0,00	0,00	0,00	0,00	1,00	0,00	0,00	0,00	1,00	1,00
	CLINICAL APPLICATION ADAPTABILITY	0,00	0,00	0,00	0,00	0,00	0,00	0,00	0,00	0,00	0,00
ADJUSTMENT CONTRIBUTES	MSK ANALISYS PERFORMED (IK, ID, SO, JR, CMC, FD)	capsule too, geometry surfaces, material properties (from lit), ligaments non spring elements, polynomial approximation surfaces, forces in the joint and laxity, device used for measuring geometry surfaces		capsule ligam add, experimental in vivo and in vitro for attachments and dimensions, provide strains	sagittal model, relationship forces-muscles,11 musc linear, main lig + post. capsule, geometry from cadaver data, tf,pf	passive, one degree on freedom, isometr lig, rigid surface, computer simulation, geometry accuracy spectrum, ex vivo valutation	rigid and deformable contacts, non linear elastic ligaments (litter.), kinematics included to compare results of the model, attachments from specimen, passive	passive behvaiour	roentegem system, with load cell, 11 partecipants, isometric contraction	planar model, same results of more complex models, patella and patellar tendon included and muscle (quad) include, tibiofemoral geometries from a specimen,	tf -pf joints, 1d, 1 segment, muscles, computed, dynamic conditions, complex analytical model, easily extended to lower limb one, ligaments included, kinematic, active
	MSK COMPLEXITY OF SCALING										
	FE TISSUE MODELS USED										
	FE BOUNDARY CONDITIONS AND CONTACTS										
	SS Number of variables accounted e.g. shape, alignment, Kinematics, material properties models										
	SS NUMBER OF SUBJECTS FOR BUILDING THE MODEL										
	ANALITICAL OVERAL COMPLEXITY	1,00	0,00	1,00	0,00	1,00	1,00	0,00		0,00	1,00
	ACCURACY	MEDIUM	LOW	MEDIUM	LOW		MEDIUM	LOW		LOW	
TOTAL	TOTAL COST - UTILITY X	0	0	1	0	2	1	0	2	2	0
TOTAL	TOTAL COMPLEXITY Y	4	1	4	2	3	4	1	3	1	4
	COST - UTILITY X	0,00	0,00	14,29	0,00	28,57	14,29	0,00	28,57	28,57	0,00
	COMPLEXITY Y	33,33	8,33	33,33	16,67	25,00	33,33	8,33	25,00	8,33	33,33

	TITLE	Statistical Modeling to Characterize Relationships between Knee Anatomy and Kinematics	Femur, tibia and fibula bone templates to estimate subject-specific knee ligament attachment site locations	Development of subject-specific and statistical shape models of the knee using an efficient segmentation and mesh-morphing approach	Development of a statistical model of knee kinetics for applications in pre-clinical testing	Statistical Shape Model-Based Femur Kinematics From Biplane Fluoroscopy	A statistical finite element model of the knee accounting for shape and alignment variability	Development of a Statistical Shape-function Model of the Implanted Knee for Real-time Prediction of Joint Mechanics	The effect of articular geometry features identified using statistical shape modelling on knee biomechanics	Three-dimensional MRI-based statistical shape model and application to a cohort of knees with acute ACL injury	Principal component analysis in construction of 3D human knee joint models using a statistical shape model method	Incorporating a statistically based shape model into a system for computer-assisted anterior cruciate ligament surgery
	AUTHORS	Smoger, Fitzpatrick, Clary, Cyr, Maletsky, Rullkoetter, Laz	Pillet, Bergamini, Rochcongar, Camomilla, Thoreux, Rouch, Capozzo, Skalli	Baldwin, Langenderfer, Rullkoetter, Laz	Galloway, Worsley, Stokes, Nair, Taylor	Bruijne, Walsum, Kaptein, Giphart, Schaap, Niessen, Lelieveldt	Rao, Fitzpatrick, Rullkoetter, Maletsky, Kim, Laz	Gibbons, Clary, Rullkoetter, Fitzpatrick	Clouthier, Smith, Vignos, Thelen, Deluzio, Rainbow	Pedoia, Lansdown, Zaid, McCulloch, Souza, Ma, Li	Tsai, Li, Wang, Li, Kwon, Li	Fleute, Lavallee, Julliard
	LABEL	Smoger et al. 2016	Pillet et al. 2016	Baldwin et al. 2010	Galloway et al. 2012	Bruijne et al. 2012	Rao et al. 2012	Gibbons et al. 2019	Clouthier et al. 2019	Pedoia et al. 2015	Tsai et al. 2013	Fleute et al. 1999
CATEGORY												
OFFSET	OFFSET X	0.00	0.00	0.00	0.00	0.00	0.00	0.00	0.00	0.00	0.00	0.00
	OFFSET Y	1.00	1.00	1.00	1.00	1.00	1.00	1.00	1.00	1.00	1.00	1.00
	OTHER COMPLEXITY	0.00	0.00	1.00	1.00	0.00	1.00	1.00	1.00	0.00	0.00	0.00
COMPLEXITY	BONES	1.00	1.00	1.00	1.00	1.00	1.00	1.00	1.00	1.00	1.00	1.00
	CARTILAGES	1.00	0.00	1.00	0.00	0.00	1.00	0.00	1.00	0.00	1.00	0.00
	MENISCI	0.00	0.00	0.00	0.00	0.00	0.00	0.00	0.00	0.00	0.00	0.00
	LIGAMENTS	0.00	0.00	1.00	0.00	0.00	0.00	0.00	1.00	0.00	0.00	0.00
	OTHER LIGAMENTS AND STRUCTURES	0.00	0.00	0.00	0.00	0.00	1.00	1.00	0.00	0.00	0.00	0.00
	INTEGRATION MULTIPLE MODELS : e.g. FE+MSK	0.00	0.00	1.00	0.00	0.00	0.00	0.00	0.00	0.00	0.00	0.00
	COMPLEXITY OF THE MECHANISM USED TO MODEL THE JOINT	0.00	0.00	0.00	0.00	0.00	0.00	0.00	0.00	0.00	0.00	0.00
	OTHER COST (FOR TASKS PERFORMED)	1.00	1.00	1.00	1.00	1.00	1.00	1.00	1.00	1.00	1.00	1.00
COST	DATA SORCES	1.00	1.00	1.00	1.00	1.00	1.00	1.00	1.00	1.00	1.00	1.00
	VALIDATION	0.00	0.00	0.00	0.00	0.00	0.00	0.00	0.00	0.00	0.00	0.00
	COMPUTATIONAL COST OF THE MODEL	1.00	1.00	1.00	1.00	1.00	1.00	1.00	1.00	1.00	1.00	1.00
	CLINICAL APPLICATION ADAPTABILITY											☑
	MSK ANALISYS PERFORMED (IK, ID,											
ADJUSTMENT CONTRIBUTES	SO, JR or also CMC, FD)											
	MSK COMPLEXITY OF SCALING											
	FE TISSUE MODELS USED											
	FE BOUNDARY CONDITIONS AND CONTACTS											
	SS Number of variables accounted e.g. shape, alignment, Kinematics, material properties models	1.00	1.00	1.00	1.00	1.00	1.00	1.00	1.00	1.00	1.00	1.00
	SS NUMBER OF SUBJECTS FOR BUILDING THE MODEL	1.00	1.00	1.00	1.00	1.00	1.00	1.00	1.00	1.00	1.00	1.00
	ANALITICAL OVERAL COMPLEXITY ACCURACY											
	TOTAL COST - UTILITY X	4	4	4	4	4	4	4	4	4	4	4
TOTAL	TOTAL COMPLEXITY Y	4	3	7	4	3	6	5	6	3	4	3
TOTAL	COST - UTILITY X	57,14	57,14	57,14	57,14	57,14	57,14	57,14	57,14	57,14	57,14	57,14
	COMPLEXITY Y	33,33	25,00	58,33	33,33	25,00	50,00	41,67	50,00	25,00	33,33	25,00